KATHOLIEKE UNIVERSITEIT LEUVEN

Faculteit Wetenschappen

Departement Biologie
Laboratorium voor Moleculaire Celbiologie
Kasteelpark Arenberg 31
3001 Heverlee-Leuven

Signaling mechanisms for nutrient activation of protein kinases and phosphatases in yeast

Proefschrift voorgedragen tot
het behalen van de graad van
Doctor in de Wetenschappen,
Groep Biochemie door

Johan Kriel

Leden van de jury:
Prof. Dr. J.M. Thevelein, promotor
Prof. Dr. P. Van Dijck
Prof. Dr. E. Martegani
Prof. Dr. F. Rolland
Prof. Dr. V. Janssens
Dr. D. Castermans

27 mei 2010

ISBN 978-90-8649-343-2
Wettelijk depot D/2010/10.705/36

THANK YOU

As I am reaching the closing stages of what can only be described as an amazing journey, I would like to take this opportunity to sincerely thank those people who have made all of this possible.

First and foremost, my supervisor, Prof. Thevelein, whose passion and enthusiasm for the subject were both inspiring and contagious. Meetings with you changed seemingly negative results into new opportunities, and laid the bases for many constructive discussions. Your constant support and positive outlook made things just that much easier. Thank you for granting me the opportunity of a lifetime to work in your laboratory; I thoroughly enjoyed it.

I am also grateful to the members of the jury: Prof. Johan Thevelein, Prof. Patrick van Dijck, Prof. Enzo Martegani, Prof. Filip Rolland, Prof. Veerle Janssens and Dr. Dries Castermans for their critical evaluation of the manuscript. Thank you for your constructive comments and suggestions.

I also want to express my gratitude to the KU Leuven and VIB for their financial support.

Doing a PhD requires teamwork. Fortunately for me, the MCB laboratory is blessed with some of the greatest players any team can hope for: the dynamic duo of Hilde and Leni who took excellent care of all the tricky administration, the computer genius that is Nico, the set of experienced technicians comprising of Willy, Catherina, Evy, Renata, Paul, Martine and Jan who assisted me whenever I needed their help. A special ‘dikke merci’ also goes out to all my colleagues, past and present, who made working at MCB a truly enjoyable experience: Ole, Wendy, Patrick VDo, Griet, Kim, Wim, Stijn, Steve, Karin, Marlies, Ben, Bram, Yudi, Yutaka-sun, Harish, Mekonnen, Georg, Klaus, Lucie, Thiago, Frederik, et al. The various contributions of the post-docs Griet, Dries, Alessandro and Tine to the positive outcome of my study should also not go unmentioned.

Life outside of the laboratory was never dull with the likes of André, Maria AV, Linh, Lisa and Gabriella.

En dan natuurlik die kontingent Suid-Afrikaners, hier in België maar ook tuis, sonder wie se volgehoue ondersteuning, gebede en motivering alles hier in die vreemde soveel moeiliker sou wees. ’n Hartelike dank aan al my vriende en familie, in besonder Arno, Chris, Jan, William, my Pa, my susters, tante Rea en my wonderlike Ma. Hierdie Ph.D. is soveel méér Ma s’n as myne, en daarom dra ek dit volledig aan jou op. Dankie uit die bodem van my hart.

Johan Kriel, Leuven, Belgium

TABLE OF CONTENTS

LIST OF ABBREVIATIONS

AGC	homologs of protein kinases A, G and C
AKAP	A-kinase anchoring protein
AMPK	AMP-activated protein kinase
AMTEM	artificial marker track exclusion mapping
ASI	amino acid sensor independent
ATP	adenosine-5'-triphosphate
bp	basepair
cAMP	3', 5'-cyclic adenosine monophosphate
CDK	cyclin-dependent kinase
COPI/II	coat protein complex I/II
CR	calorie restriction
DNA	deoxyribonucleic acid
DRM	detergent-resistant membrane
eIF2	eukaryotic translation initiation factor 2
ER	endoplasmic reticulum
ERAD	ER-associated degradation
ESCRT	endosomal sorting complex required for transport
FBPase	fructose-1,6-bisphosphate
FGM	fermentable growth medium-induced
GAAC	general amino acid control
GAP	GTPase activating protein
GEF	Guanine nucleotide exchange factor
GDP	guanosine 5'-diphosphate
GPCR	G protein coupled receptor
GSE	GTPase-containing complex for Gap1 sorting in the endosome
GTP	guanosine 5'-triphosphate
HA	hemagglutinin
HisRS	histidyl-tRNA synthetase
Hsp	heat shock protein

mM	millimolar
μM	micromolar
mRNA	messenger ribo-nucleic acid
MVE	multivesicular endosome
NCR	nitrogen catabolite repression
NLS	nuclear localization sequence
NM	nuclear membrane
OD	optical density
PAGE	polyacryl amide gel electrophoresis
PCR	polymerase chain reaction
PDK	phosphoinositide-dependent kinase
pH	*pondus Hydrogenii*
PKA/B	protein kinase A/B
PM	plasma membrane
PP1	protein phosphatase type 1
PP2A	protein phosphatase type 2A
SCAM	substituted cysteine accessibility method
SCF	Skp1/Cul1/F-box
SDS	sodium dodecyl sulphate
SEG1	suppressor of ER-exit deficient Gap1
(i/t/v)-SNARE	(inhibitory/target/vesicle)- soluble *N*-ethylmaleimide sensitive factor attachment protein receptor
SPS	Ssy1-Ptr3-Ssy5
STRE	stress responsive element
TBS(T)	tris-buffered saline (tween)
TGN	*trans*-Golgi network
TOR	target of rapamycin
TORC1	target of rapamycin complex 1
TRAPP1	transport protein particle I
tRNA	transfer ribo-nucleic acid
UAS	upstream activating sequences
UDP	uridine-5'-diphosphate

LIST OF YEAST GENES

AGP1	low-affinity amino acid permease with broad substrate specificity
ARG1	arginosuccinate synthase
ASI1, *ASI2*, *ASI3*	involved in ubiquitin-dependent protein catabolism
ATH1	acid trehalase
AVO1, *AVO2*, *AVO3*	subunits of TORC2
BAP2, *BAP3*	branched-chain amino acid permease
BAT1	mitochondrial branched-chain amino acid aminotransferase
BCY1	regulatory subunit of PKA
BET1	v-SNARE involved in fusion of COPII vesicles with the Golgi
BIT61	subunit of TORC2
BNI4	regulatory subunit of PP1
BOS1	v-SNARE involved in fusion of COPII vesicles with the Golgi
BUD14	regulatory subunit of PP1
BUL1, *BUL2*	two redundant ubiquitin ligase adapters; binds Rsp5
CAN1	arginine permease
CDC4	ubiquitin ligase
CDC25, *SDC25*	guanine nucleotide exchange factors of Ras
CDC28	cyclin-dependent protein kinase
CDC34	ubiquitin conjugating enzyme
CDC55	PP2A regulatory subunit
CRM1	nuclear export factor
CYR1/CDC35	adenylate cyclase
DAL5	allantoate permease
DAL80/UGA43	transcriptional GATA family repressor involved in NCR
DALG81/UGA35	transcription factor involved in GAAC

DIP5	dicarboxylic amino acid permease
DOA4	ubiquitin hydrolase
GAC1	PP1 regulatory subunit in glycogen metabolism
GAP1	general amino acid permease
GCN1	involved in activation of Gcn2 by uncharged tRNA
GCN2	eukaryotic initiation factor 2 alpha (eIF2-α) kinase
GCN4	transcriptional activator involved in amino acid biosynthesis
GCN20	involved in activation of Gcn2 by uncharged tRNA
GDB1	glycogen debranching enzyme
GGA1, *GGA2*	Golgi-localized proteins with homology to gamma-adaptin, facilitate traffic through the late Golgi
GIP1	meiosis-specific regulatory subunit of Glc7
GIP2	putative regulatory subunit of Glc7
GLC3	glycogen debranching enzyme
GLC7	catalytic subunit of PP1
GLC8	PP1 regulatory subunit, homologue of mammalian inhibitor-2
GLK1	glucokinase
GLN1	glutamine synthetase
GLN3	GATA transcription factor involved in NCR
GOS1	v-SNARE protein involved in Golgi transport
GPA2	Gα-protein involved in cAMP signaling
GPH1	glycogen phosphorylase
GPR1	cognate P-protein coupled receptor of Gpa2
GSE1, *GSE2*	component of the GSE complex, which is required for proper sorting of Gap1
GSY1, *GSY2*	glycogen synthase
GTR1, *GTR2*	component of the GSE complex, which is required for proper sorting of Gap1
HSP60	heat shock protein of MW 60

HXK1, HXK2	hexokinases, phosphorylate hexose sugars
ILV5	mitochondrial protein involved in branched-chain amino acid biosynthesis
IRA1, IRA2	GTPase activating proteins of Ras
KAR2	ATPase involved in protein import into the ER, also acts as a chaperone to mediate protein folding in the ER
KRH1, KRH2	kelch repeat homologs; interact with Gpr1
KOG1	subunit of TORC1
LST4, *LST7*	required for the transport of Gap1 from the Golgi to the cell surface
LST8	subunit of TORC1 and TORC2
LTV1	component of the GSE complex, which is required for proper sorting of Gap1
MEP1, *MEP2*	high affinity ammonium permease
MSN2, *MSN4*	transcription factors for STRE-controlled genes
NIL1/GAT1	GATA transcription factor involved in NCR
NIL2/DEH1/GZF3	GATA transcription factor involved in NCR
NPR1	protein kinase that stabilizes plasma membrane transporters
NPR2	component of a conserved Npr2/3 complex that mediates downregulation of TORC1 activity in response to amino acid limitation
NTH1, NTH2	neutral trehalase
PCL5	specific Pho85 cyclin
PDE1	low-affinity phosphodiesterase
PDE2	high-affinity phosphodiesterase
PEP3	membrane protein that promotes vesicular docking and fusion reactions in conjunction with SNARE proteins
PEP5	membrane protein required for protein trafficking
PHO84, *PHO87*	inorganic phosphate transceptors
PHO85	multifunctional cyclin-dependent kinase
PIG1, *PIG2*	PP1 regulatory subunits in glycogen metabolism

PKH1, *PKH2*, *PKH3*	serine/threonine kinases, yeast orthologs of PDK1
PMR1	high affinity Ca^{2+}/Mn^{2+} ATPase required for Ca^{2+} and Mn^{2+} transport into Golgi
PPE1	methylesterase
PPG1	PP2A-like catalytic subunit
PPH3	PP2A-like catalytic subunit
PPH21, *PPH22*	PP2A catalytic subunits
PPM1, *PPM2*	protein methyltransferase
PTR3	core component of the SPS sensing complex
PUT4	proline permease
RAS1, *RAS2*	small G-proteins, positive regulators of adenylate cyclase
RED1	PP1 regulatory subunit in meiosis
REG1, *REG2*	regulatory subunits of Glc7
RGT2	glucose sensor
RRD1, *RRD2*	peptidyl-prolyl cis/trans-isomerase, activator of the phosphotyrosyl phosphatase activity of PP2A
RSP5/NPI1	ubiquitin ligase
RTS1	PP2A regulatory subunit
SAR1	involved in formation of ER transport vesicles
SCH9	serine/threonine protein kinase involved in FGM signaling
SDS22	PP1 regulatory subunit in cell division
SEC12	ER membrane protein involved in formation of ER transport vesicles
SEC13	involved in formation of ER transport vesicles
SEC16	ER membrane protein involved in formation of ER transport vesicles
SEC22	SNARE involved in fusion of COPII vesicles with the Golgi
SEC23	involved in formation of ER transport vesicles

SEC24	involved in formation of ER transport vesicles
SED4	ER protein involved in formation of ER transport vesicles
SED5	SNARE involved in fusion of COPII vesicles with the Golgi
SFT1	v-SNARE, required for transport of proteins between an early and a later Golgi compartment
SHP1	ubiquitin regulatory X domain-containing protein that regulates Glc7
SHR3	ER-resident chaperone required for the packaging of amino acid permeases into ER-derived transport vesicles
SIT4	protein with serine/threonine phosphatase activity
SNF1	protein kinase, involved in glucose repression
SNF3	glucose sensor
SRP1	nuclear import factor
SSY1	amino acid sensor
SSY5	essential component of the SPS amino acid sensing complex
STP1, STP2	transcription factors involved in SPS induced transcription
STT4	type III phosphoinositide 4-kinase
TAP42	essential protein involved in TOR signaling
TOR1, *TOR2*	serine/threonine protein kinases, target of rapamycin
TPD3	PP2A scaffolding subunit
TPK1, *TPK2*, *TPK3*	catalytic subunits of PKA
TPS1	trehalose-6 phosphate synthase
TPS2	trehalose-6 phosphate phosphatase
TPS3	trehalose synthase complex regulatory subunit
TSL1	trehalose synthase complex regulatory subunit
URE2	co-repressor involved in NCR
USO1	tethering factor involved in fusion of ER transport vesicles with the Golgi

VPS16, VPS33, VPS41	part of the Class C VPS complex essential for membrane docking and fusion at Golgi-to-endosome and endosome-to-vacuole protein transport stages
VPS39	vacuolar protein that plays a critical role in the tethering steps of vacuolar membrane fusion
YCK1, YCK2	casein kinase I proteins
YKT6	SNARE involved in fusion of COPII vesicles with the Golgi
YPT1	Rab GTPase involved in fusion of ER transport vesicles with the Golgi
ZDS1	involved in localizing Bcy1

NOMENCLATURE

Yeast genes and proteins

GAP1	wild-type allele
Gap1	wild-type protein
Gap1ΔC6$_{(14aa)}$	protein with the indicated C-terminal truncation
*gap1*Δ	deletion mutant
*gap1*Δ*::KanMX*	deletion mutant where *GAP1* is replaced with the *KanMX* gene

Chapter I

LITERATURE OVERVIEW

1.1. INTRODUCTION

Yeasts are truly fascinating organisms. Their diverse activities impinge on a variety of commercially important sectors, including the food, beverage and pharmaceutical industry. The brewing of beer might just be the oldest biotechnological application of yeast! While most of their activities are beneficial to human life, some yeasts have been implicated in processes of spoilage and as agents of human disease. Not surprising then that the opportunistic pathogen *Candida albicans* has emerged as the major cause of morbidity and mortality in immunocompromised patients.

In recent years, however, the importance of yeasts, in particular *Saccharomyces cerevisiae*, has extended far beyond traditional industrial applications to the ever-increasing role it plays in furthering our fundamental understanding of microorganisms. The relative ease and rapidity of growth, combined with a well-defined genetic system, and most important, a highly versatile DNA transformation system, has made yeast the preferred research system of most molecular biologists.

The success of *S. cerevisiae* as model system is also in part due to the extent in which basic biological structures and processes have been conserved throughout eukaryotic life (Broach et al., 1991). Comparative genomics studies have shown that up to 40% of yeast proteins share an amino acid sequence similarity with at least one human protein, and 30% of genes with a proven involvement in human disease have an ortholog in yeast (Foury, 1997; Parsons et al., 2003). With a fully-sequenced- and defined genome, which allows the expression of the entire yeast proteome *in vitro*, *S. cerevisiae* permits, for the first time ever, the possibility of a comprehensive proteome-wide screen of drug function in higher eukaryotes (Martzen et al., 1999; Sturgeon et al., 2006). *S. cerevisiae*'s role at the forefront of biomedical research is thus firmly entrenched.

1.2. NUTRIENT-SENSING IN YEAST

The unicellular eukaryote *S. cerevisiae* has a limited ability to store nutrients, and are consequently, completely dependent on the availability of nutrients in its immediate surrounding. To maximize survival in a constantly changing environment, yeast has evolved numerous metabolic pathways that ensure the optimal use of all available nutrients. The yeast cell is therefore able to assess the amount of nutrient available (sensing), transmit this information to the nucleus (signaling) and adjust its growth and developmental programs accordingly (transcriptional regulation) (Zaman et al., 2008).

Concerted research efforts have revealed a complicated network of sensing mechanisms and signaling pathways that governs the cell's responses to the nutritional environment. For the purpose of this review, however, we will focus on the three most prominent nutrient-sensing pathways in *S. cerevisiae*: the cAMP-Protein Kinase A (PKA) pathway, the Fermentable Growth Medium-induced (FGM) pathway and the Target Of Rapamycin (TOR) pathway.

1.2.1. cAMP-PKA pathway

Glucose is the most abundant monosaccharide in nature, and as the preferred energy source of most microorganisms, it elicits profound changes in the cell's metabolism. More than 40% of the *S. cerevisiae* genes rapidly alter their expression levels after the addition of glucose to cells growing on a non-fermentable carbon source (Schneper et al., 2004). These transcriptional changes allow the cell to use glucose exclusively before switching to less favourable carbon sources like galactose and mannose. The cAMP-PKA pathway plays an intricate part in regulating these responses to glucose.

The addition of glucose to non-fermenting or stationary phase cells results in a rapid, albeit transient, increase in cellular cAMP (Thevelein et al., 1987; Broach, 1991; Thevelein, 1994). An increased cAMP level activates PKA, which in turn initiates a PKA-dependent phosphorylation cascade during the cell's transition from respiratory to fermentative growth (Kraakman et al., 1999; Portela and Moreno, 2006). High

intracellular levels of cAMP therefore correlate with growth in a nutrient-rich environment, whereas low cAMP levels indicate growth in a nutrient-limited environment.

cAMP is synthesized from ATP by the *CYR1*/*CDC35*-encoded adenylate cyclase (reviewed in Broach, 1991) (Figure 1.1). Similarly to higher eukaryotes, the yeast adenylate cyclase is activated by two small guanine nucleotide-binding proteins (G proteins), Ras1 and Ras2. Both these proteins are active in the GTP-bound state while the hydrolysis of GTP to GDP inactivates it. The GDP/GTP exchange is catalyzed by Cdc25, and possibly Sdc25 (Camus et al., 1994), and the GTP hydrolysis is stimulated by Ira1 and Ira2. Intracellular acidification accomplishes the activation of the cAMP-PKA pathway by inhibiting both Ira1 and Ira2, thus increasing the GTP/GDP ratio bound to Ras.

Cellular cAMP levels are regulated by two cAMP phosphodiesterases, Pde1 and Pde2. The low-affinity phosphodiesterase Pde1 was identified as a PKA target that specifically downregulates cAMP signaling through a method of feedback inhibition (Ma et al., 1999), whereas the high-affinity phosphodiesterase Pde2 regulates the basal level of cellular cAMP.

1.2.1.1. Glucose signaling: a dual sensing system

The preference which *S. cerevisiae* has for glucose as its main source of carbon is reflected in the complexity of the sensing systems. Glucose is detected by two sensing systems and both systems are required for activation of the cAMP-PKA pathway (Rolland et al., 2000).

Extracellular D-glucose and sucrose are sensed by a G protein-coupled receptor (GPCR) system that comprises the receptor Gpr1 and its G protein Gpa2 (Colombo et al., 1998; Kraakman et al., 1999). By analogy to other GPCRs, it was demonstrated that Gpa2 functions as a classic Gα subunit by coupling extracellular ligand activation of Gpr1 to an intracellular signaling event (Zaman et al., 2008). There is currently no evidence for the binding of glucose to Gpr1. However, the fact that mutants of Gpr1 have been obtained in which glucose-induced, but not sucrose-induced, activation of

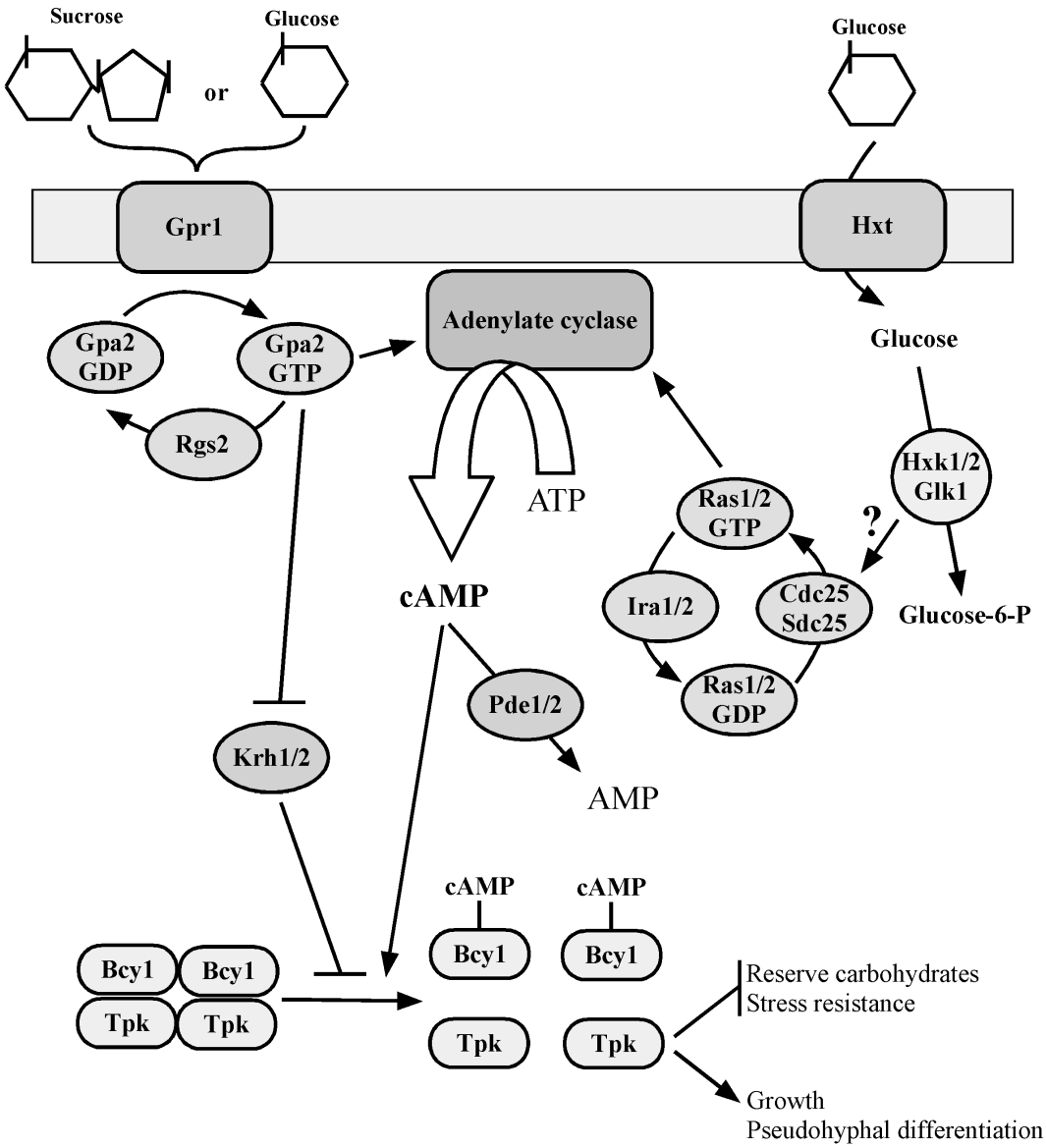

Figure 1.1: The cAMP-PKA pathway in yeast.

The addition of glucose to cells growing on non-fermentable carbon sources or to stationary phase cells results in a rapid increase in cellular cAMP. An increased cAMP level activates PKA, which in turn activates a PKA-dependent phosphorylation cascade. Glucose is detected by two sensing systems, and both are required for full activation of the cAMP-PKA pathway.

the cAMP-PKA pathway are abolished, strongly suggests that there is a binding site for glucose in Gpr1 (Lemaire et al., 2004). In *C. albicans*, Gpr1 functions as a putative amino acid sensor and mediates the yeast-to-hypha morphogenetic transition (Maidan et al., 2005). This attribute makes *Ca*Gpr1 an attractive target for a novel range of antifungals (Van Dijck, 2009).

Upon ligand binding, Gpr1 activates Gpa2, which is, similar to the Ras proteins, active in the GTP-bound state and inactive when GDP is bound. A member of a family of regulators of G protein signaling, Rgs2; promotes the intrinsic GTPase activity of Gpa2, hereby inhibiting glucose-induced cAMP synthesis (Versele et al., 1999). In contrast to other canonical Gα subunits, Gpa2 is unable to form a heterotrimeric G protein with the known Gβ and Gγ subunits in yeast, Ste4 and Ste18 (Harashima et al., 2006). Instead, Gpa2 associates with two kelch-repeat proteins Krh1 (Gpb2) and Krh2 (Gpb1) (Batlle et al., 2003; Peeters et al., 2006; Niranjan et al., 2007). Both Krh1 and Krh2 (Krh1/2) contain seven kelch-repeat domains that fold into a β propeller structure and mediate protein-protein interactions. Cells containing *krh1*Δ *krh2*Δ mutations display phenotypes that are typical of high PKA activity: low levels of storage carbohydrates, decreased stress resistance and increased pseudohyphal growth. Consistent with this, increased phosphorylation of PKA substrates was observed in *krh1*Δ *krh2*Δ mutants, confirming that Krh1/2 negatively regulate the cAMP-PKA pathway (Lu and Hirsch, 2005). The precise mechanism by which this is achieved, is still subject to debate. Two different mechanisms have been proposed, one in which Krh1/2 enable the association between the regulatory and catalytic subunits of PKA, as shown in a two-hybrid assay (Peeters et al., 2006). Contrary to this, Harashima et al. (2006) found that Krh1/2 bind to a conserved C-terminal domain in Ira1 and Ira2, stabilizing them. Without this stabilization, Ira1 and Ira2 are more easily degraded and the resulting elevated levels of GTP-bound Ras lead to increased cAMP synthesis.

A second, intracellular sensing mechanism requires sugar uptake and phosphorylation but no further metabolism of the sugar. Glucose phosphorylation in yeast is apparently stimulated by transport of the sugar, and catalyzed by the hexose kinases Hxk1 and Hxk2 and glucokinase Glk1 (Rolland et al., 2000; Rolland et al., 2001). How glucose phosphorylation is coupled to the Gpr1-Gpa2-dependent activation of the pathway remains unclear.

The subsequent section deals with the target of the Ras-cAMP pathway in yeast, PKA.

1.2.1.2. PKA as central regulator of metabolism

As in all eukaryotes, yeast PKA is an inactive tetramer composed of two regulatory subunits bound to two catalytic subunits. The regulatory subunits are encoded by a single gene, *BCY1*, and the three partially redundant catalytic subunits are encoded by the *TPK1*, *TPK2* and *TPK3* genes respectively. The three Tpk proteins are remarkably similar in amino acid sequence and structure and the C-termini are highly conserved over a region of 300 residues. The shorter N-terminal domains are, however, distinct (Gagiano et al., 2002).

Triple mutants lacking all three *TPK* genes are inviable, but the expression of any one of the catalytic subunits in such a strain restores viability (Toda et al., 1987b). The three catalytic subunits, however, play very different roles in respect to other metabolic phenotypes. The deletion of *TPK2*, for example, abolishes the filamentous growth phenotype observed in yeast cells of the Σ1278b genetic background, whereas the deletion of *TPK3* causes enhanced pseudohyphal differentiation of these cells (Robertson and Fink, 1998). *TPK1*, on the other hand, is required for the derepression of both the *BAT1* and *ILV5* genes involved in branched chain amino acid biosynthesis, which in effect allows the cell to exit the stationary phase (Robertson et al., 2000).

The Bcy1 subunit acts as pseudo substrate for the catalytic subunits by binding and inhibiting their activity. cAMP binding to Bcy1 alleviates this inhibitory activity by causing conformational changes in the regulatory subunits that decrease their affinity for the catalytic subunits. The activated catalytic subunits are capable of phosphorylating a whole range of substrates, including proteins involved in the breakdown of storage carbohydrates, in stress resistance and in glycolysis and gluconeogenesis (Thevelein et al., 2000; Ptacek et al., 2005). Hydrolysis of cAMP by the phosphodiesterases restores PKA to the inactive state.

In addition to being regulated by cellular cAMP levels, PKA activity is also strictly controlled by the subcellular compartmentalization of the individual subunits (Griffioen et al., 2000). In actively-growing cells, Bcy1 and Tpk1 reside almost exclusively in the nucleus. However, in respiring or stationary-phase cells, both Bcy1 and Tpk1 are distributed equally over the nucleus and cytosol. Localization studies on

the subunits revealed that the subcellular localization of Tpk1 depends on cAMP, for the addition of cAMP to yeast cells causes the majority of nuclear Tpk1 to translocate to the cytosol (Griffioen et al., 2000; Griffioen et al., 2001). The proper cytoplasmic localization of Bcy1, on the other hand, requires both the Yak1-dependent phosphorylation of the N-terminus of Bcy1, as well as interaction with the yeast homologue of the mammalian A-kinase anchoring protein (AKAP), Zds1 (Griffioen et al., 2003). The deletion of *ZDS1* was shown to decrease the levels of Bcy1 in the cytoplasm, whereas the overexpression of *ZDS1* resulted in the opposite phenotype.

Although cAMP plays a determining role in activation of PKA, a novel, cAMP-independent activation of PKA has been proposed. In the presence of a fermentable carbon source, the re-addition of a missing nutrient, such as nitrogen, sulphate or phosphate, causes an activation of PKA that is independent of cAMP, but dependent on the free catalytic subunits. The signaling pathway responsible for the sustained activation of PKA is the FGM pathway (Thevelein, 1994; Thevelein et al., 2005) (see section 1.2.2.).

1.2.1.3. Downstream targets

As mentioned in the previous section, activated PKA can phosphorylate various proteins involved in growth and metabolism. The phosphorylating activity of active PKA is for example required to ensure the successful progression from the G_1 to the S phase of the cell cycle (Tokiwa et al., 1994).

The downstream target that I have used extensively to quantify PKA activity is the metabolism of storage carbohydrates trehalose and glycogen.

Storage carbohydrates

When fermentable carbon source levels start to wane, *S. cerevisiae* diverts the remaining hexose carbon into storage carbohydrates trehalose and glycogen. Both storage carbohydrates serve as a storehouse of glucose when extracellular sources are scarce. Trehalose, however, is more than simply a storage compound. It has the unique ability to exclude water from the surface of proteins and hence protect proteins

from denaturation in dehydrated cells (Simola et al., 2000). Trehalose's function as stress protectant is further highlighted by its ability to suppress the aggregation of proteins that already have been denatured (Elbein et al., 2003).

Trehalose is a nonreducing disaccharide of glucose that occurs naturally in insects, plants fungi and bacteria. It does not occur in mammalian cells, although trehalase, the enzyme responsible for the breakdown of trehalose, is found in humans and other mammals at the brush border of the intestinal mucosa, as well as in the kidney, liver, and blood plasma (Ouyang et al., 2009).

The synthesis of trehalose in *S. cerevisiae* necessitates the participation of four different enzymes. *TPS1* and *TPS2* encode the trehalose-6-phosphate synthase and trehalose-6-phosphate phosphatase, respectively, and *TPS3* and *TSL1* code for two regulatory subunits of the TPS complex (Jules et al., 2008; Mahmud et al., 2010). Synthesis of trehalose occurs in two successive steps; trehalose-6-phosphate (T6P) is synthesized using UDP-glucose and glucose-6-phosphate as substrates, and then directly converted to trehalose (Elbein et al., 2003). The concentration of trehalose in the yeast cell is the sum of the synthetic activity of the TPS complex and the degradative activity of trehalase. Under optimal conditions, i.e. decreasing glucose levels, trehalose levels may reach 15% of cellular dry weight (De Silva-Udawatta and Cannon, 2001).

The hydrolysis of trehalose generates two glucose molecules. Yeast carries two types of trehalose-degrading enzymes: the neutral trehalases (Nth1) localized in the cytoplasm and the acidic trehalase (Ath1) found predominantly in the vacuole. Recently, a third gene, *NTH2*, was shown to encode a functional neutral trehalase with a measurable, if somewhat reduced, activity during stationary phase (Jules et al., 2008). Nth1 constitutes the main source of trehalase activity in stationary phase cells, but also in proliferating and germinating cells. Ath1 is mainly required for growth on trehalose, which accounts for its enhanced activity at the cell surface (Jules et al., 2008).

In contrast to trehalose, glycogen is a typical reserve carbohydrate that is synthesized during exponential growth and utilized throughout periods of starvation. Biosynthesis

of glycogen is mediated by the *GSY1*/*GSY2*-encoding glycogen synthase which catalyzes the formation of the α -1,4-glycosidic linkages of the polymer, and branching enzyme Glc3 which forms the α-1,6-glycosidic branchpoints (Farkas et al., 1991; Rowen et al., 1992). Degradation of glycogen depends on the activities of glycogen phosphorylase (Gph1) and the debranching enzyme Gdb1 (François and Parrou, 2001).

Glycogen synthase is controlled by multisite phosphorylation. Dephosphorylation by protein phosphatase Glc7 activates the enzyme, whereas protein phosphatase 2A (PP2A) indirectly regulates glycogen metabolism by controlling cell growth (Stark, 1996; Ramaswamy et al., 1998) (see section 1.5.).

Transcriptional control

Yeast cells exposed to stresses develop within minutes metabolic responses that ultimately lead to the acquisition of a so-called 'stress resistance' state (Ruis and Schuller, 1995). A general characteristic of these stress conditions is the induction of a large number of genes which share a common promoter sequence, the *cis*-acting stress responsive element (STRE) (Martinez-Pastor et al., 1996; Schmitt and McEntee, 1996). Msn2 and Msn4, the two Zn-finger transcription factors, bind to the CCCCT core sequence of the STREs to initiate transcription and, consequently, trigger a general stress response (Thevelein et al., 2000). STREs have been identified in the promoter regions of over 180 stress-associated genes, including *TPS1*, *TPS2* and *NTH1* (Moskvina et al., 1998) (see previous section).

Subcellular localization of Msn2 and Msn4 is regulated by both PKA and stress conditions. PKA directly phosphorylates the Msn2 nuclear localization signal (NLS) which inhibits its function by restricting it to the cytoplasm. As a result, Msn2, and to a lesser extent Msn4, resides in the cytoplasm when PKA is active and, conversely, is found in the nucleus when PKA activity is low (Gorner et al., 2002; Rolland et al., 2002).

Stress conditions, in particular nitrogen starvation, heat shock and osmotic shock, control Msn2 subcellular localization through modification of the N-terminal nuclear

export signal (NES) instead of the NLS (Zaman et al., 2008). In this case, PP2A dephosphorylates the NES to retain the protein in the nucleus (see section 1.5.1.). Interesting to note, is that the deletion of *MSN2* and *MSN4* suppresses the lethality of a PKA deficient strain, placing both transcription activators downstream of PKA (Smith et al., 1998).

1.2.2. FGM pathway

The sustained activation of PKA requires a fermentable carbon source and a complete growth medium in which nitrogen, sulphur and phosphate are present in adequate amounts.

Cells growing in these optimal conditions display characteristics typically associated with the so-called 'high PKA phenotype'; low levels of trehalose and glycogen, decreased expression of STRE-regulated genes and an overall upregulation of ribosomal protein gene expression (Thevelein et al., 2005). Starving it for one of the nutrients, even in the presence of glucose, causes the cell to enter the G_0 state in which it acquires stationary phase characteristics.

This observation points to the existence of an additional signaling network, one that integrates information from different nutrient sensing systems into a common response that modifies PKA activity accordingly. This alternate pathway for the maintenance of PKA activity is known as the FGM pathway (Thevelein and de Winde, 1999; Thevelein et al., 2005) (Figure 1.2).

The most compelling evidence for the existence of an additional pathway for PKA activation, as opposed to the classic Ras-cAMP signaling cascade, is that the maintenance of the high PKA phenotype is not mediated by an increase in cellular cAMP. Moreover, transport and phosphorylation of the sugar, a prerequisite for Ras-cAMP-dependent activation of PKA, is no longer required as demonstrated in *hxk1*Δ *hxk2*Δ *glk1*Δ triple mutants lacking the sugar phosphorylating enzymes. The FGM pathway detects the presence of sugar through either the extracellular Gpr1-Gpa2 sensing system, or the intracellular sugar kinase-dependent system (Giots et al., 2003; Van Nuland et al., 2006).

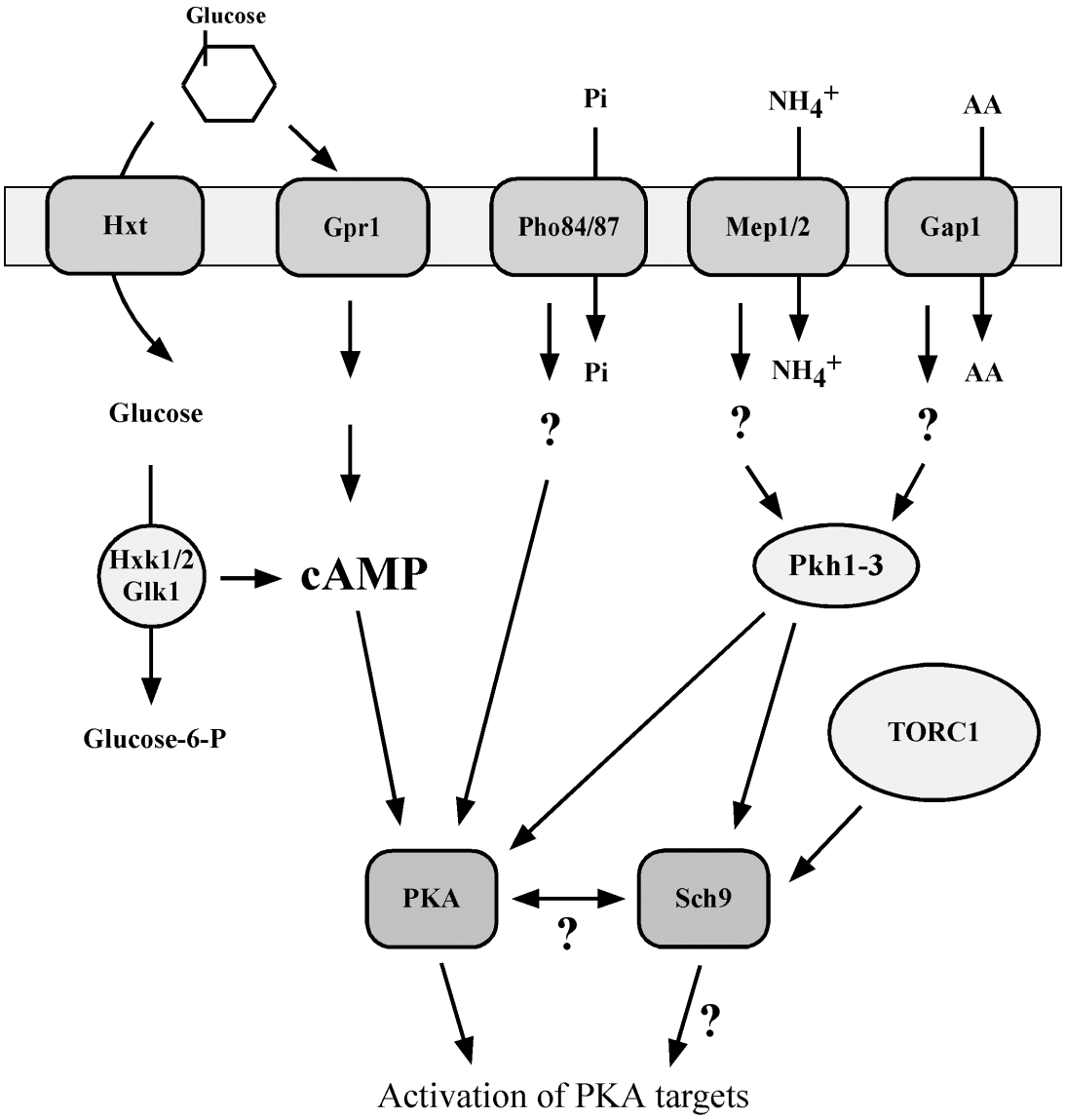

Figure 1.2: The FGM pathway in yeast.

Re-addition of phosphate to cells starved for it or ammonium/amino acids to nitrogen-depleted cells, triggers a rapid activation of PKA targets. In addition to the missing nutrient, FGM signaling also requires the presence of a readily-fermentable carbon source.

Several transporter-related nutrient sensors, or transceptors, that mediate nutrient-induced activation of the FGM pathway through the plasma membrane, have been identified: the general amino acid permease (Gap1) senses amino acids, inorganic phosphate is sensed by Pho84 and Pho87, and Mep1 and Mep2 sense ammonium (Donaton et al., 2003; Giots et al., 2003; Van Nuland et al., 2006; Van Zeebroeck et al., 2009). Interestingly, the activation of the FGM pathway does not

require the metabolization of the transported nutrient. However, the intracellular part of the pathway that connects the signal generated by the transceptor to its downstream effector PKA, remains as-yet elusive. Strong experimental evidence suggest that the serine/threonine kinase Sch9 may act downstream of the nitrogen sensors (Crauwels et al., 1997).

The next section details the two components of the FGM pathway most important to my own research, Sch9 and Gap1.

1.2.2.1. Sch9

The protein kinase Sch9 is an AGC family kinase and the closest yeast homolog to the mammalian pro-survival Protein Kinase B (PKB)/Akt as well as the TOR-regulated S6 kinase (Yorimitsu et al., 2007). Originally identified as a multi-copy suppressor of a *cdc25*^{ts} conditional mutant, overexpression of *SCH9* can also suppress the lethality caused by *cyr1*Δ, *ras1*Δ *ras2*Δ, and *tpk1*Δ *tpk2*Δ *tpk3*Δ mutants. Conversely, overactivation of the Ras-cAMP pathway suppresses the slow growth phenotype observed in a deletion strain of *SCH9*. The ability of Sch9 to compensate for mutations in the Ras-cAMP pathway likely results from the fact that Sch9 regulates similar targets as Ras-cAMP.

Recent biochemical data places Sch9 in both nutrient- and stress signaling pathways (Fabrizio et al., 2001; Kaeberlein et al., 2005b; Smets et al., 2008). Stressing the yeast cell through rapamycin treatment, starving it for carbon or nitrogen, or shifting the nitrogen source from ammonium to less-favourable urea leads to the rapid dephosphorylation of Sch9. Re-addition of the missing nutrient quickly restores the phosphorylation. *In vivo* studies have shown that the TOR complex 1 (TORC1) directly regulates Sch9 by phosphorylating six conserved serine/threonine residues on its C-terminal tail (see section 1.2.3.). Elimination of these phosphorylation sites on Sch9 diminishes the kinase activity (Jacinto and Lorberg, 2008). Pkh1 and Pkh2, the yeast homologues of mammalian 3-phosphoinositide-dependent kinase-1 (PDK1) also phosphorylate Sch9. In contrast to TORC1 though, Pkh1 and Pkh2 phosphorylates a specific threonine^{570} residue in the activation loop. Both the phosphorylation of the activation loop and the C-terminus are required for activation of Sch9.

Mounting evidence suggests that Sch9 may also regulate longevity in yeast. Calorie restriction (CR) in yeast, whereby cells are grown on a low glucose concentration, is a well-established method to increase chronological life span. The molecular mechanism underlying this has always been vague, until it was recently demonstrated that *sch9*Δ mutants, as well as *tor1*Δ cells have an increased life span (Kaeberlain et al., 2005a). CR of *sch9*Δ or *tor1*Δ cells had no significant influence on the lifespan, indicating that Sch9 and Tor1 are putative targets of CR in yeast. The longevity-promoting role of Sch9 and Tor1 has apparently been evolutionary conserved – the deletion of the Sch9 and TOR orthologs in the nematode worm *Caenorhabditis elegans* and the fruit-fly *Drosophila melanogaster* increased the lifespan as well (Hansen et al., 2007; Honjoh et al., 2009).

As noted before, Sch9 forms an important part of the FGM pathway. The deletion of *SCH9* in glucose-grown, nitrogen starved cells abolishes the nitrogen-induced activation of the PKA targets. Crauwels et al. (1997) reported on the absence of both nitrogen-induced trehalase activation and ribosomal protein gene induction in glucose-repressed *sch9*Δ cells. Repression of STRE-regulated genes was also severely impaired. Phosphate-induced activation of the FGM pathway, however, seems to operate independent of Sch9 (Giots et al., 2003).

1.2.2.2. Gap1

S. cerevisiae import amino acids from the extracellular environment to serve either as alternative nitrogen source or directly in protein synthesis. Gap1 and the proline utilization permease Put4 constitute the main route by which the cell is provided with amino acids as a source of nitrogen. Whereas Put4 can only transport proline, Gap1 transports a wide variety of amino acids, including D-amino acids, toxic amino acid analogues and L-citrulline (Jauniaux and Grenson, 1990). The activity of Gap1 is tightly regulated through mechanisms that sense the availability, and quality, of amino acids in the environment. In yeast cells grown on a poor nitrogen source, like proline, or in the absence of nitrogen, Gap1 is transported to the plasma membrane to increase the cell's uptake of amino acids. In nitrogen-rich conditions, Gap1 is downregulated and sorted to the vacuole for degradation (Magasanik and Kaiser, 2002; Seaman,

2006) (for a comprehensive overview of the transcriptional and post-translational regulation of Gap1, see section 1.4.).

In addition to its well-documented function as an amino acid transporter, it was shown that Gap1 also acts as a receptor, signaling the availability of its substrate to the interior of the cell. The dual function of Gap1 as amino acid transporter/receptor (transceptor) was supported by the isolation of constitutively activating alleles (Donaton et al., 2003). These Gap1 mutants contain short truncations of the extreme C-terminus of the protein, resulting in a high PKA phenotype that affected all the downstream targets investigated, even in the absence of a nitrogen source (see "Chapter II", section 2.3.).

Further evidence highlighting Gap1's dual role is observed in *gap1*Δ cells where both amino acid transport and signaling are absent, suggesting that *S. cerevisiae* lacks a transport-independent receptor for sensing extracellular amino acids. Moreover, metabolization of the transported nutrient as possible activator of the FGM pathway can be excluded since non-metabolizable analogues are still able to trigger a rapid activation of the pathway (Holsbeeks et al., 2004; Thevelein et al., 2008). Taking advantage of Gap1's ability to transport L-citrulline at low concentrations, Donaton et al. (2003) determined PKA activity in nitrogen-starved wild-type cells, supplemented with 2 mM L-citrulline, and nitrogen-starved *gap1*Δ cells to which 50 mM L-citrulline were added. In both cases citrulline uptake was detected; activation of the FGM pathway however was only observed in the wild-type strain. These findings prompted a model whereby Gap1 acts as sensor and the amino acids activate the innate receptor function of the protein, in similar fashion as a ligand activates a receptor.

Recent work by Van Zeebroeck et al. (2009) revealed in part the mechanism by which Gap1 senses amino acids. The authors employed the substituted cysteine accessibility method (SCAM) to identify two amino acid residues in transmembrane domain VIII, serine^{388} and valine^{389}, which are exposed into the amino acid binding domain of Gap1. Blocking the binding site with MTSEA, they could demonstrate that Gap1 uses the same amino acid binding site for both transport and signaling. A large collection

of amino acid analogs was also screened for its ability to inhibit transport and trigger signaling. Various compounds were isolated that act as competitive and non-competitive inhibitors of transport, either with or without agonist function. Of particular relevance was the isolation of non-transported agonists that modulated Gap1's activity to that of a non-transporting transceptor, i.e. signaling without transport. The results suggest that the Gap1-dependent signaling event apparently requires only the binding of the signaling agonist and partial conformational change of the transceptor, but not the completion of the transport cycle (Van Zeebroeck et al., 2009).

As Gap1 provides the cell with nutrients required for its growth, and the Ras-cAMP - and FGM pathways regulate growth according to nutrient availability, it is not surprising that particular connections have been identified between these pathways. Amitrano and colleagues (1997), for example, demonstrated an increase in L-citrulline uptake in *cyr1-1* mutants as the exogenously-added cAMP levels were increased from 0.25 to 1.0 mM. The authors, however, did not determine Gap1 activity at higher cAMP levels, which would have ruled out the probability that cells grown at such low cAMP levels may have a decreased viability and as a consequence, low permease activity. A more physiologically-pleasing link between cAMP concentration and Gap1 activity was recently offered (Garrett, 2008). It was shown that an increase in cAMP, either through an elevated Ras2 or the addition of cAMP, results in a decrease in Gap1 transport activity. A drop in cAMP levels or the loss of Ras2, in turn, results in an increase in Gap1 activity, even in the presence of a preferred nitrogen source. The downregulation of the permease is proposed to occur through a Ras2-dependent ubiquitination event, which explains the high Gap1 activity observed in ammonia-grown *ras2*Δ cells (see section 1.4.4.).

1.2.3. TOR pathway

The control of cell growth and proliferation in all eukaryotic cells studied so far is largely directed by the evolutionary-conserved Tor kinases. The Tor proteins were first identified in *S. cerevisiae* cells as the target of the toxic complex formed between the immunosuppressive drug rapamycin and a conserved proline-isomerase FKBP12 (Heitman et al., 1991). Exposing yeast to rapamycin results in profound physiological

changes that include reserve carbohydrate accumulation, downregulation of amino acid permeases, inhibition of protein synthesis and eventual entry into a G_0-like state; all phenotypes generally associated with nutrient-starved cells (De Virgilio and Loewith, 2006; Zurita-Martinez et al., 2007). These findings support the notion that Tor couples nutrient cues to the cell's developmental program (Figure 1.3).

While most eukaryotes express only one Tor protein, *S. cerevisiae* has two distinct Tor kinases, encoded by *TOR1* and *TOR2*. The Tor proteins associate with two multiprotein complexes to form what is known as TORC1 and TORC2. TORC1 comprises of Tor1, or Tor2 in *tor1*Δ mutants, bound to Kontroller of Growth (Kog1), Lst8 and Tco89, whereas TORC2 is formed by a separate pool of Tor2 bound to Avo1, Avo2, Avo3, Lst8 and Bit61 (Adami et al., 2007; Sturgill et al., 2008). Rapamycin-sensitive TORC1 promotes cell growth and G_1 phase progression through the phosphatase regulatory network composed of the type 2A phosphatases Pph21 and Pph22, the related type 2A phosphatase Sit4, and the two regulators encoded by *TAP42* and *TIP41* (Urban et al., 2007). TORC2, which is insensitive to rapamycin, serves a unique role by controlling polarization of the cell's actin cytoskeleton (Rohde et al., 2008).

Recent studies, however, suggest that the exclusivity in function of TORC1 and TORC2 may not be as stringent as previously thought. It has been reported that Kog1, restricted to TORC1, regulates both actin polarization and cell wall integrity. Rapamycin treatment and inhibition of Tap42 or Sit4 also induced unexpected changes in actin organization (Araki et al., 2005). These data lend support to a proposed overlap in function between TORC1 and TORC2.

1.2.3.1. Targets of TOR

Most of the TORC1 functions are mediated through its downstream target Tap42. In nutrient-rich conditions, TORC1 directly phosphorylates Tap42 to stimulate its inhibitory binding to the catalytic subunits of PP2A and PP2A-like phosphatases - Pph21, Pph22, and Sit4. Upon nitrogen starvation or treatment with rapamycin, i.e. inhibition of TORC1, Tap42 becomes dephosphorylated and released from the catalytic subunits.

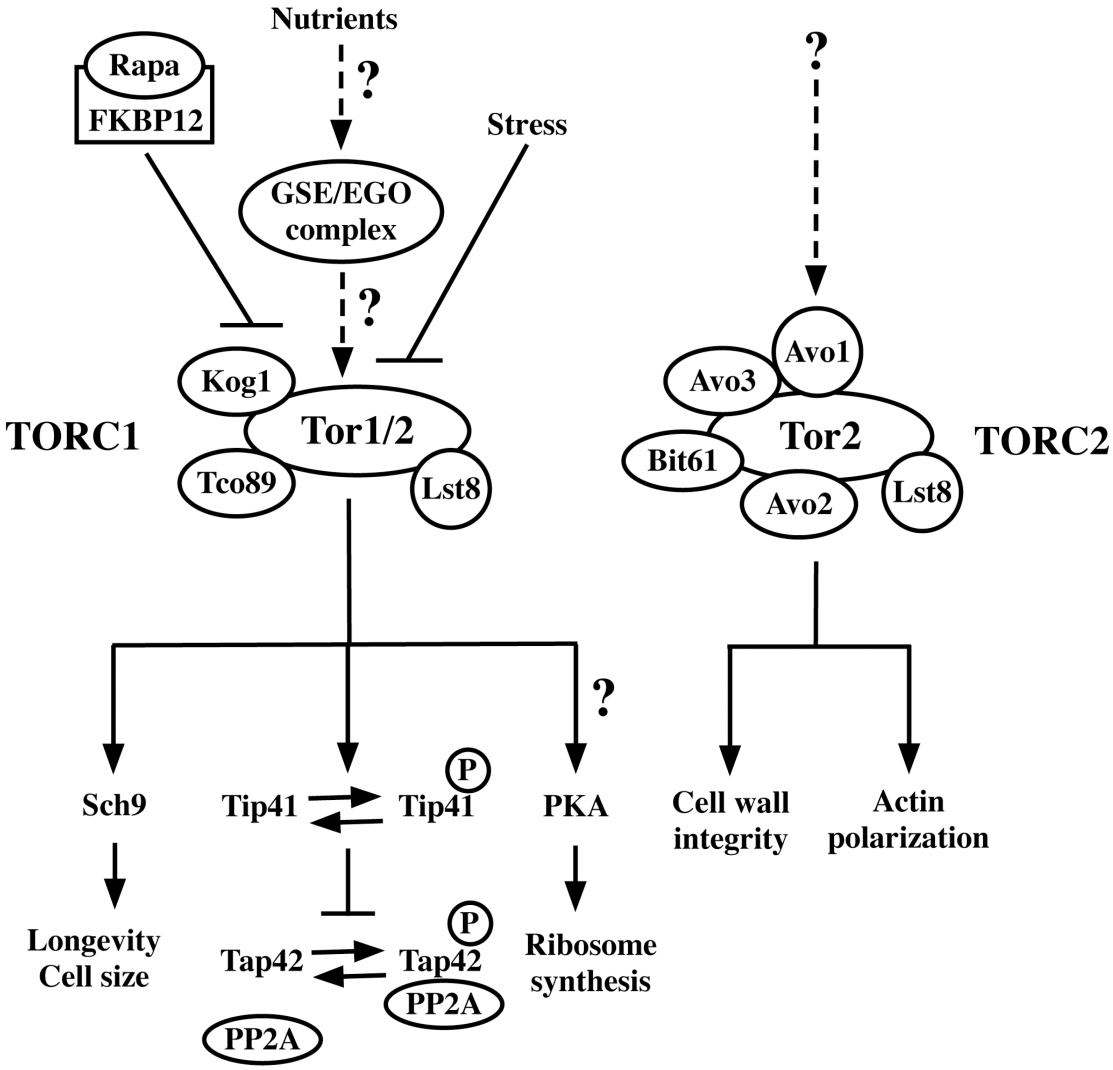

Figure 1.3: The TOR pathway in yeast.

The rapamycin-sensitive yeast TORC1 and rapamycin-insensitive TORC2 couples nutrient and environmental cues to cellular metabolism. The two protein complexes reside in separate signaling pathways and regulate different facets of growth. Circles containing the letter P denote phosphorylated amino acid residues.

Liberated and activated Sit4 in turn dephosphorylates and activates targets such as the transcriptional activator Gln3 and the protein kinase Npr1. The ensuing nuclear translocation of Gln3 induces the expression of a range of nitrogen-repressed genes, e.g. Gap1, Mep2 and Dal5, which allows the cell to utilize less-favored nitrogen sources (De Virgilio and Loewith, 2006; see section 1.3.1.).

Based on these observations, it is tempting to formulate a model in which phosphorylated Tap42 bolsters growth by inhibiting PP2A activity, while rapamycin treatment and poor growth conditions cause growth arrest through the release of PP2A. Such a model, however, can not explain the discrepancy in time observed for rapamycin-induced gene expression to take effect compared to the much slower dissociation of the Tap42-PP2A complex.

Furthermore, since the cell contains up to tenfold less Tap42 than PP2A catalytic subunits, the majority of PP2A protein in the cell are found in the unbound, active form. A more plausible explanation of Tap42 activity was recently offered by Yan et al. (2006). This group showed that the Tap42-PP2A complex is localized to detergent-resistant membranous fractions in the cell in close association with TORC1. In response to TORC1 inactivation, the Tap42-PP2A complex is released to the cytosol, where it slowly dissociates, probably due to the dephosphorylation of Tap42. The Yan model is particularly attractive as it not only accounts for the difference in kinetics of rapamycin action but also sheds light on the previously unknown mechanism by which mutations in Tap42, e.g. the *tap42-11* allele, renders the cell rapamycin resistant (Di Como and Arndt, 1996). Yan et al. (2006) demonstrated a modification in the binding of the *tap42-11*-PP2A complex to TORC1, which is insensitive to rapamycin-induced dissociation.

Once active, TORC1 functions as a key regulator of the general amino acid control (GAAC) system through the control it exerts on the GAAC transcriptional activator Gcn4. Upon amino acid starvation, the protein kinase Gcn2 induces the enhanced translation of *GCN4* mRNA to upregulate the expression of most amino acid biosynthesis genes. Gcn2, in turn, is stimulated by the binding of uncharged tRNAs. Active Gcn2 phosphorylates the α subunit of eukaryotic translation initiation factor 2 (eIF2) and in doing so, Gcn2 ensures priority to the translation of specifically *GCN4* mRNA while general protein synthesis is downregulated (Hinnebusch, 2005; Mascarenhas et al., 2008) (see section 1.3.2. for a more detailed overview).

Recent biochemical studies suggest that Gcn2 activation may also occur in response to rapamycin treatment. Rapamycin apparently induces dephosphorylation of a specific residue on Gcn2, serine^{577}, which results in an increased phosphorylation of

eIF2α and an eventual increase in Gcn4. Conversely, TORC1 represses Gcn4 expression by boosting the phosphorylation of serine^{577} through the Tap42-dependent inhibition of the PP2A-like phosphatase Sit4. These findings were further supported in *sit4*Δ mutants or cells carrying the rapamycin-resistant *tap42-11* allele; in both cases a decreased rapamycin-induced dephosphorylation of serine^{577}, coupled to a diminished induction of eIF2α, were observed. Together, these data indicate a potential cross-talk mechanism in the cell where the availability of nutrients is linked to the synthesis of proteins (Cherkasova and Hinnebusch, 2003; Magazinnik et al., 2005).

As noted before, TORC1 has been localized, among other places, to intracellular membranous structures that are near, but still distinct from, the plasma membrane. Novel research has suggested that the relevance of TORC1 localization is not only physical, but, more importantly, functional as demonstrated by the Golgi-localized ATPase Pmr1 (Devasahayam et al., 2006; Devasahayam et al., 2007). Pmr1 transports Ca^{2+} and Mn^{2+} ions from the cytosol into the Golgi, and is as such part of the secretory pathway also used by permeases. Remarkably, deletion of *PMR1* caused resistance to rapamycin, with wild-type sensitivity restored to the *pmr1*Δ cells through the addition of Mn^{2+} to the growth medium. Epistasis analysis positions Pmr1 upstream and as a negative regulator of TORC1 activity. The mechanism by which Pmr1 achieves TORC1 inhibition is thought to involve the regulation of Mn^{2+} homeostasis. Tor, like most phosphatidylinositol 3-kinase-related kinases, requires Mn^{2+} as cofactor for maximal activity and may be partly localized to the Golgi, as suggested for mammalian Tor, where there is access to Mn^{2+} within the secretory pathway (Liu and Zheng, 2007).

The prevailing theory of a prominent link between TORC1 activity and vacuolar function was further underscored by two recent studies. First, cells lacking any of the five proteins of the 'Gap1 sorting in the endosome' (GSE) complex, also known as the EGO complex, fail to recover from rapamycin treatment. The GSE/EGO complex is required for the delivery of Gap1 to the plasma membrane and colocalizes to the vacuolar and pre-vacuolar membranes (Gao and Kaiser, 2006) (see section 1.4.4.). Mutants of the GSE/EGO complex are also deficient in reversing rapamycin-induced

phenotypes like eIF2α phosphorylation, which would indicate that it functions upstream of TORC1 signaling. Together with TORC1, the GSE/EGO complex initiates recovery from rapamycin inhibition by recycling of vacuolar membranes, a process termed microautophagy. These results argue for a role of the GSE/EGO complex in relaying nutrient signals from the vacuole to TORC1 (Figure 1.3). Bearing in mind that the vacuole serves as an amino acid store, this seems a likely scenario (Gao and Kaiser, 2006; Rohde et al., 2008).

Second, a genome-wide screen by Zurita-Martinez et al. (2007) identified the class C vacuolar protein sorting (VPS) complex, consisting of the Pep3, Pep5, Vps16, Vps33, Vps39 and Vps41 proteins, as another vacuole-bound complex essential in maintaining TORC1 signaling. The VPS complex plays a determining role in protein sorting, mainly by regulating the key processes of vesicle docking and fusion at the endosome. Deleting any component of the VPS complex, results in mutant cells that are unable to recover from either rapamycin-induced growth inhibition or nitrogen starvation. In addition, these mutants exhibit low levels of internal amino acids, in particular glutamate and glutamine. Combining the *vps*Δ with a *tor1*Δ is synthetically lethal but interestingly, growth is restored to the double deletion strain by supplementing the media with glutamate or glutamine, and to a lesser degree arginine. These findings propose a model whereby TORC1's localization to membranes places it in an ideal position to receive nutrient signals generated by the components of the secretory pathway, i.e. TORC1's localization allows for its diverse function.

1.3. AMINO ACID SIGNALING IN YEAST

Yeast can utilize a wide range of organic and inorganic sources of nitrogen, but as with carbon sources, not all of these are utilized with the same efficiency. In order to use non-preferred nitrogen sources, like proline, allantoin or ornithine, *S. cerevisiae* first has to convert it into either glutamine or glutamate. Both serve as sole nitrogen donors for the synthesis of all nitrogenous substances found in the cell.

As with carbon sources, yeast has evolved a variety of physiological processes that allow the selective use of the more-favored nitrogen sources before switching to the poor ones. The regulatory mechanism encompassing this phenomenon is known as nitrogen catabolite repression or nitrogen discrimination pathway (Magasanik and Kaiser, 2002; Wong et al., 2008).

1.3.1. Nitrogen Catabolite Repression (NCR)

The expression of nearly all NCR genes studied so far is under direct control of GATA-type transcription factors. These transcription factors share a very distinct Zn-finger region (Cys-X_2-Cys-X_{17}-Cys-X_2-Cys) that recognizes and binds to a 5'- GATA-3' sequence upstream of genes subject to NCR. *S. cerevisiae* has two positively-acting GATA factors, Gln3 and Gat1 (Nil1), and two repressors of transcription, Dal80 (Uga43) and Gzf3 (Nil2 or Deh1). Given the high sequence similarity between the four proteins, it is not surprising that the difference in structure between activator and repressor is limited to its N- and C-termini respectively. Gln3 and Gat1 differ from Dal80 and Gzf3 by having an asparagine-rich region located 200 residues from its N-terminus, whereas Dal80 and Gzf3 share a unique leucine zipper in its C-terminal domain not present in the positive transcription factors (Stanborough et al., 1995; Magasanik and Kaiser, 2002).

Regulation of the GATA transcription factors is exerted at the level of subcellular localization. In the presence of poor nitrogen sources, Gln3 and Gat1 localize to the nucleus where they induce the expression of genes encoding permeases and enzymes required for transport and degradation of poor nitrogen sources. On the contrary, when cells are grown on good nitrogen sources, Gln3 and Gat1 are found predominantly in the cytosol. The anchor protein, Ure2, is proposed to control the nuclear localization of Gln3 by sequestering it in the cytoplasm under nitrogen repressing conditions - a Gln3-Ure2 complex can be isolated from cells in which NCR transcription is repressed and deletion of *URE2* results in an increased expression of Gln3-sensitive genes, even in the presence of a preferred nitrogen source (Beck and Hall, 1999; Bertram et al., 2000; Tate et al., 2006a) (Figure 1.4). A similar cytoplasmic anchor for Gat1 remains to be identified.

Although the quality of the nitrogen source begins to explain the localization of the GATA factors, it does not address the molecular events behind the process. Earlier studies with rapamycin, however, provided the first clue to the underlying mechanism. Treatment of actively-growing cells with the immunosuppressive drug, results in the release of phosphorylated Gln3 from Ure2, its dephosphorylation and eventual translocation to the nucleus. Moreover, the addition of rapamycin also increases the rate of Gln3 electrophoretic migration, similar to that observed in cell extracts treated with protein phosphatases (Beck and Hall, 1999; Cooper, 2002). Based on these results, a simple model was formulated in which a nitrogen-rich environment activates the Tor proteins, which in turn boosts Gln3 phosphorylation. According to this model, inhibition of Tor1 through rapamycin prevents, or alters, Gln3 phosphorylation, and allows non-phosphorylated Gln3 to enter the nucleus. Further evidence in support of such a model came from the observation that in cells lacking the type 2A-related protein phosphatase Sit4, Gln3 remains in the cytosol despite rapamycin treatment. Sit4's role in regulating the phosphorylation status of Gln3 was thus established.

The significance of the phosphorylation status of Gln3 in determining its subcellular localization was extended by the finding that the nuclear transport protein Srp1 only binds non-phosphorylated Gln3. The Gln3-Srp1 complex translocates to the nucleus, allowing Gln3 to promote GATA-mediated transcription and Srp1, in association with Cse1, to recycle back to the cytosol. Gln3 exits the nucleus in complex with the nuclear export factor Crm1 (Carvalho et al., 2001). The directionality of nuclear transport is ensured by the Ran proteins, present either in its GTP-bound form in the nucleus or as GDP-bound in the cytosol (Moy and Silver, 1999).

However, recent data on Gln3 phosphorylation and cellular localization has been difficult to reconcile with the model described previously. These results include the observation that, although methionine sulfoximine (MSX), a potent inhibitor of glutamine synthesis, and rapamycin treatment both elicit Gln3 nuclear localization, they generate the opposite phosphorylation profile - MSX increases Gln3 phosphorylation whereas rapamycin decreases it. Similarly, a lack in correlation between dephosphorylation and localization was also demonstrated for growth on rich *vs*. poor nitrogen sources, during nitrogen starvation and after prolonged rapamycin

treatment, i.e. more than 30 minutes. The only time a clear correlation was observed, was within 10 to 20 minutes after rapamycin treatment (Tate and Cooper, 2007; Georis et al., 2008; Tate et al., 2009).

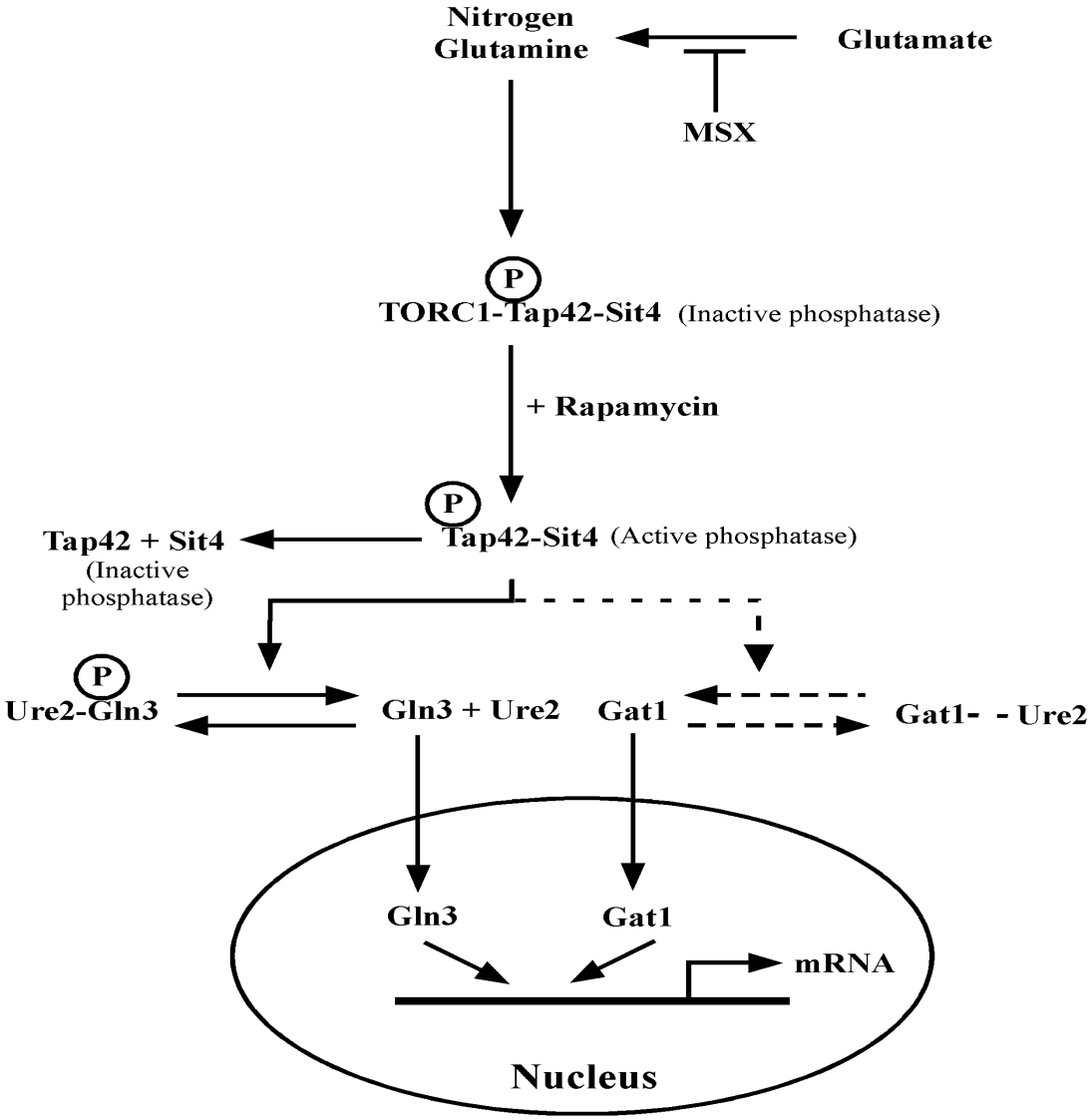

Figure 1.4: Nitrogen catabolite repression (NCR) in yeast.

The current model describing TORC1-dependent regulation of Gln3's phosphorylation status, subcellular localization, and activation of NCR-sensitive transcription. Circles containing the letter P denote phosphorylated amino acid residues (adapted from Tate et al., 2009).

Significant advances made in recent years on the mechanism of Tor signaling, also changed our understanding of the role it plays in Gln3 regulation. It appears that

Tap42, in its phosphorylated form, is required for Sit4 activity; the phosphorylated Tap42-Sit4 complex released from TORC1 in response to rapamycin exposure or nitrogen limitation, is active for as long as Tap42 is bound to Sit4. More importantly, was the unexpected discovery of the involvement of PP2A phosphatases in Gln3 control. PP2A, like Sit4, dephosphorylates Gln3 in response to nitrogen sources; their respective activities, however, depend largely on the nitrogen source present. In cells grown on favored sources, Gln3 dephosphorylation occurs mainly through Sit4 activity with Pph21 and Pph22 contributing very little to the overall process, whereas growth on poor nitrogen sources results in the opposite phenotype.

This inverse in regulation may well be due to Gln3's cellular localization during these growth conditions. On good nitrogen sources, Gln3 is found predominantly in the cytosol and is as such not available to the nuclear-restricted PP2A for modification. Once present in the nucleus, Gln3 phosphorylation status is under control of PP2A and immune to the cytoplasmic Sit4-dependent dephosphorylation (Tate et al., 2009).

In contrast to Gln3, much less is known about the regulation of Gat1 activity. Modifications in Gat1 phosphorylation levels in response to nitrogen source quality and/or rapamycin treatment have not been demonstrated, although the Snf1-dependent phosphorylation of Gat1 in carbon-starved cells was easily identified. In addition, MSX-treatment also resulted in the opposite effects on Gln3 and Gat1 localization. In nearly all the cells exposed to the inhibitor, Gln3 was present in the nucleus whereas Gat1 concentrated in the cytoplasm. As with rapamycin, MSX-treatment had no influence on Gat1 phosphorylation. It is this lack of a general response of Gln3 and Gat1 localization to the inhibitors that supports the notion that these two transcriptional activators represent the branches of parallel pathways for the positive regulation of NCR transcription (Georis et al., 2008; Wong et al., 2008; Georis et al., 2009). Finally, transcriptional control of *GAT1* is Gln3- and Gat1-dependent, i.e. auto-activation of its own transcription, and demonstrates particular sensitivity to Dal80 inhibition.

As noted before, the two negative regulators of NCR-sensitive transcription, Dal80 and Gzf3, contain leucine-zipper motifs near their C-termini, allowing them to self-associate. The strength with which Dal80 and Gzf3 bind DNA is, in fact, believed to

originate from their ability to do so as a dimer. In contrast to Gln3, which binds a single GATA, the Dal80 homodimer requires two GATA sequences, positioned either head to tail or tail to tail, but not head to head, spaced 15 to 40 bp apart, for binding. Gzf3, on the other hand, functions via a single GATA sequence and forms homodimers or heterodimers with Dal80 (Svetlov and Cooper, 1998; Distler et al., 2001). The expression of Dal80 and Gzf3 are nitrogen source-dependent, with Gzf3 functioning as the major inhibitor in the presence of rich sources. Therefore, when cells are shifted from favorable, i.e. conditions where Dal80 levels are very low, to poor nitrogen sources, Dal80 does not initially antagonize NCR transcription. It is only through the upregulation in expression, brought about by Gln3 and Gat1's nuclear localization in poor nitrogen conditions that Gal80 levels are sufficient to regulate NCR-sensitive genes. One of the targets Gal80 downregulates is its own activator, Gat1, in a process commonly referred to as autogenous regulation (Cunningham et al., 2000; Magasanik and Kaiser, 2002). By regulating its own expression, Gal80 provides a negative feedback loop that allows the cell to fine-tune its response to the prevailing conditions. Such a mechanism is proposed to be most advantageous to the cell in the intermediate period when adjusting its metabolism to being shifted from a good to a poor nitrogen source.

A recent genome-wide study identified 44 additional genes subject to NCR. The new targets include the GAAC transcriptional activator Gcn4, the membrane peptide transporter Ptr2 and the regulator of nitrogen permeases Npr2 (Godard et al., 2007). Interestingly, the screen also identified the anabolic glutamate dehydrogenase Gdh1 and glutamate synthase Glt1 as NCR-sensitive. These two proteins, together with Gln1 (glutamine synthetase) and Gdh2 (catabolic glutamate dehydrogenase) constitute the main route of nitrogen utilization in *S. cerevisiae*. With Gln1 and Gdh2 both well-established targets of NCR, the new data suggest that the complete set of enzymes forming the core of nitrogen metabolism in yeast is in fact NCR regulated.

1.3.2. General Amino Acid Control (GAAC)

As described in the previous section, most amino acids can serve as a source of nitrogen or as building blocks during protein synthesis. Intracellular amino acid concentrations are constantly monitored by the GAAC system. Starving cells for any

amino acid induces the activator protein Gcn4 which in turn activates the transcription of a large number of genes, many of which are involved in amino acid biosynthesis. Gcn4 activity is regulated at the level of translation initiation through the presence of four small open reading frames (ORFs) upstream of the main mRNA coding sequence. These upstream ORFs function as a translational barrier in nonstarvation conditions by preventing scanning ribosomes from reaching the *GCN4* start codon. However, during amino acid starvation, uncharged tRNA molecules bind and activate the Gcn2 kinase, which in turn phosphorylates the translation initiation factor eIF2α. Active eIF2 inhibits the guanine nucleotide exchange factor (GEF), eIF2B, from recycling inactive eIF2-GDP to active eIF2-GTP. Since only the GTP-bound form of eIF2 can deliver charged methionyl initiator tRNA (Met-$tRNA_i^{Met}$) to the 40S ribosome in the first step of translation initiation, inhibition of eIF2B results in a severely reduced level of active eIF2-GTP. Under these circumstances, initiation at the upstream ORFs is abolished with ribosomes scanning further downstream to the *GCN4* ORF instead (Hinnebusch and Natarajan, 2002; Wilson and Roach, 2002; Gárriz et al., 2009) (see Figure 1.5).

Because eIF2α functions by inhibiting translation, its activity is tightly regulated to prevent any inhibitory effect on translation during favorable conditions. The protein kinase Gcn2 is at the heart of this regulation. Gcn2 itself is essentially inactive and depends on the binding of uncharged tRNAs to its regulatory domain for activation. The regulatory domain is a 500 residue region, C-terminal to the Gcn2 kinase domain, whose sequence resembles that of histidyl-tRNA synthetase (HisRS). Binding of any uncharged tRNA to HisRS permits a short N-terminal segment of the HisRS motif to interact with a part of the kinase domain that contains the hinge that connects the N- and C-terminal lobes, resulting in a conformational change that is thought to stimulate Gcn2 kinase activity (Hinnebusch, 2005). Similar to other kinases, autophosphorylation of the activation loop is a prerequisite for Gcn2 activity. Gcn2 autophosphorylates a threonine^{882} and a threonine^{887} in the so-called activation loop of which the latter is essential for proper function. There is also evidence that Gcn2 activation requires interaction between the N-terminus of Gcn2 with the Gcn1-Gcn20 complex. The Gcn1-Gcn20 complex promotes the binding of tRNAs to the translating ribosome's decoding site, or its transfer from the decoding site to the HisRS domain of Gcn2.

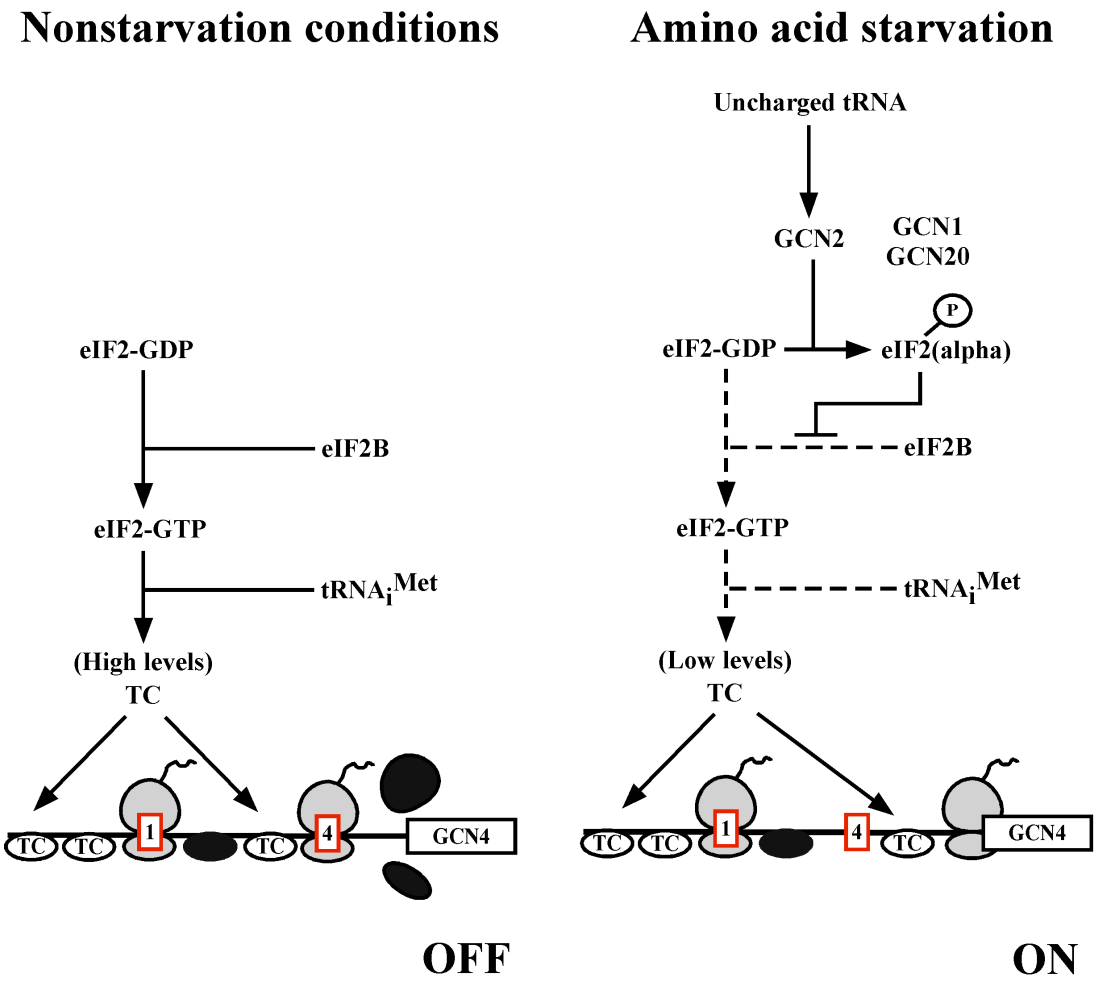

Figure 1.5: General amino acid control in yeast.

The current model for *GCN4* translational control. Starving cells for any amino acid induces Gcn4 which in turn activates the transcription of various genes involved in amino acid biogenesis. Gcn4 activity is regulated at the level of translation initiation through the presence of four small ORFs upstream of the main coding sequence. The circle containing the letter P denotes a phosphorylated amino acid residue.

The domain structure and function of Gcn2 appears to be evolutionary conserved in other fungi and higher eukaryotes. The *Drosophila* and mouse Gcn2 proteins restore viability to yeast *gcn2*Δ mutants starved for amino acids. Furthermore, eIF2α phosphorylation in starved mammalian cells induces the translation of *ATF4* mRNA in a similar fashion as yeast Gcn4. What makes this remarkable is that Atf4 is a transcriptional activator belonging to the same family as Gcn4 (Santoyo et al., 1997;

Sood et al., 2000; Vattem and Wek, 2004). The core elements of this nutritional control are thus highly conserved (see section 1.2.3.).

Besides amino acid deprivation, the Gcn2-mediated synthesis of Gcn4 is also induced during starvation for purines, glucose limitation or growth on the non-fermentable carbon source ethanol, high salinity in the growth media, exposure to methyl methanesulfonate (MMS) and treatment with rapamycin. The requirement of Gcn2 kinase activity in such diverse environmental stress conditions is probably due to an impaired synthesis of amino acids in these conditions. This results in the accumulation of uncharged tRNAs and the activation of Gcn2 in the same manner that functions in amino acid-depleted cells. New experimental evidence, however, demonstrated this not to be the case for purine starvation, MMS and rapamycin treatment or high salt concentrations (Hinnebusch, 2005). For glucose limitation, Yang et al. (2000b) showed that cytosolic amino acid levels dropped as cells stored amino acids in vacuoles instead. The levels of amino acids accumulated in the vacuole during glucose limitation exceeded by far the net loss measured in the cytosol; the difference being attributed to Gcn4 activity. It was rationalized that by vacuolar storage of amino acids and the accompanying translation of *GCN4* mRNA during glucose limitation, cells would have immediate access to nitrogen once glucose levels are replenished.

Apart from the Gcn2-mediated regulation of *GCN4* translation, a Gcn2-independent mechanism also exists that operates as cells are shifted from amino acid-rich to minimal media. It requires activation of PKA and is absent in constitutively low PKA mutants. Accordingly, mutants with overactive PKA activity, e.g. *bcy1*Δ or *RAS2*^{G19V} cells, display a constitutively derepressed translation of *GCN4* that is partly independent of Gcn2 (Marbach et al., 2001). The role PKA activity plays in *GCN4* translation is poorly understood.

In addition to stimulating its synthesis, amino acid starvation also stabilizes Gcn4. In a nutrient-rich environment, Gcn4 is quickly degraded, with a half-live of typically 2 to 3 minutes, whereas degradation occurs four to five times slower in amino acid-deprived conditions. Degradation of Gcn4 is a complex process and requires the phosphorylation of both threonine^{105} and threonine^{165} in the activation loop, as well as

ubiquitination by the ubiquitin-conjugating enzyme Cdc34 and the associated ubiquitin ligase complex SCF^{CDC4}. Phosphorylation of the threonines by the two multifunctional cyclin-dependent kinases (CDKs), Pho85 and Srb10, enhances ubiquitination. As with all CDKs, substrate specificity is ensured through the binding of a specific cyclin, and in the case of Pho85-mediated phosphorylation of Gcn4, the cyclin is Pcl5 (Shemer et al., 2002; Aviram et al., 2008). Pcl5 itself is under transcriptional control of Gcn4 and the negative feedback loop created ensures Gcn4 activity is regulated according to the nutritional situation. A similar Pho85-Pcl5 regulatory loop seems to operate in *C. albicans* as well (Gildor et al., 2005).

A novel study employing an analog sensitive version of the Snf1 kinase, the *snf1-as* allele, identified Snf1 as a repressor of *GCN4* translation in amino acid-rich media. Shirra et al. (2008) demonstrated *snf1*Δ cells to have elevated levels of Gcn4 protein and that the phenomenon is dependent on both Gcn2 and Gcn20, suggesting that Snf1 regulates the translation of *GCN4* and not the stability of the protein. The exact mechanism by which it is achieved remains unknown. An unexpected consequence of the research is the finding that Snf1 exhibited activity, although severely reduced, in the presence of high glucose, a condition normally associated with its inhibition. Similar contradictions for Snf1 were observed for pseudohyphal growth (Van de Velde and Thevelein, 2008).

1.3.3. SPS amino acid-sensing

Nutrients have the capacity to regulate cell function beyond their crucial role in metabolism. In *S. cerevisiae*, the sensing of extracellular amino acids is dependent on the amino acid permease homologue Ssy1. It is the largest member of the amino acid permease family and also the only member that has lost its transport capability. A striking feature of Ssy1 is an extended N-terminus, 276 residues in length, which makes it significantly larger than any of the other amino acid permeases (Andréasson and Ljungdahl, 2002; Kodama et al., 2002). These are characteristics similar to those that distinguish the glucose sensors, Rgt2 and Snf3, from the rest of the hexose transporter family.

Ssy1, together with the intracellular peripheral membrane proteins Ptr3 and Ssy5, form the core components of the SPS sensing pathway. Binding of amino acids to Ssy1 generates a signal that is transduced to Ptr3 and Ssy5 (Andréasson and Ljungdahl, 2004; Poulsen et al., 2005). Ssy5 is synthesized as an inactive chymotrypsin-like protease, consisting of an inhibitory N-terminal pro-domain and a C-terminal catalytic domain. In receiving the Ssy1-Ptr3-relayed signal, Ssy5 is autolyticly processed and consequently activated. Active Ssy5, in turn, stimulates the proteolytic cleavage of two related transcription factors, Stp1 and Stp2. That Ssy1, Ptr3 and Ssy5 function in a highly interdependent, conformationally coordinated fashion is supported by two important findings. First, in two-hybrid assays Ptr3 was shown to interact with itself and with Ssy5, while Ssy1 was found to interact with Ptr3 (Eckert-Boulet et al., 2004). Second, mutants containing the constitutive signaling forms of Ptr3 and Ssy5 are only active in the presence of the complete SPS sensor. Thus, in *ssy1*Δ or *ssy5*Δ cells carrying the *PTR3-5* allele as well as *ssy1*Δ or *ptr3*Δ cells carrying the *SSY5-6* allele, activation of downstream reporters were completely abolished (Poulsen et al., 2005). These results are consistent with the notion that the three proteins are not only functionally but also physically associated.

The SPS-mediated processing of the transcription activators Stp1 and Stp2 (Stp1/2) also requires the SCF^{Grr1} E3 ubiquitin ligase complex and the activity of either of the two yeast casein kinases Yck1 or Yck2. As positive regulators of the SPS pathway, Yck1/2 and Grr1 were shown to hyperphosphorylate Ptr3 during conditions of amino acid availability. The conformational change that occurs in the Ptr3-Ssy5 complex due to Ptr3 hyperphosphorylation results in Ssy5 activation and the processing of Stp1/2 (Zaman et al., 2008). Conversely, in the absence of external amino acids, a phosphatase complex encompassing the PP2A regulatory subunit Rts1 dephosphorylates Ptr3, and the SPS pathway is as a consequence inactivated. A role as negative regulator of the SPS pathway was confirmed for Rts1; *rts1*Δ cells exhibit an increased phosphorylation of Ptr3 that coincides with the constitutive expression of SPS-responsive genes. It is important to note that the constitutive signaling by mutants of the SPS complex always requires the presence of the wild-type copies of the two other components of the sensor (Ljungdahl, 2009). This suggests that the

presence of extracellular amino acids causes a conformational change in the SPS sensor from a non-signaling to a signaling conformation.

Stp1/2 is synthesized as latent precursor forms that are excluded from entering the nucleus under non-inducing conditions. In response to amino acids, active Ssy5 removes a 10-kDA N-terminal inhibitory fragment from Stp1/2 in a process known as receptor-activated proteolysis (Boban and Ljungdahl, 2007). The truncated form of the transcription factors enters the nucleus and activates transcription of relevant amino acid permeases by binding to specific upstream activating sequences (UAS_{aa}) within SPS-sensitive promoters. Single deletions of either *STP1* or *STP2* has no significant effect on SPS signaling, whereas in a *stp1*Δ *stp2*Δ double mutant signaling is completely abolished.

Several eukaryotic transcription factors involved in signal transduction are synthesized as latent, inactive precursors restricted to the cytosol. Well-documented examples include *Drosophila*'s Cubitus interruptus transcription activator, involved in the Hedgehog signaling pathway, and the NF-κB family of transcription factors that regulate cell division and apoptosis according to nutrient cues (Wang and Price, 2008; Graff et al., 2009). The subcellular relocalization of activated transcription factors therefore provide a novel means by which nutrient-induced signals generated at the plasma membrane are physically transferred from the cytosol to the nucleus.

The negative regulation of full-length Stp1/2 is not restricted to cytoplasmic retention alone. A backup system, consisting of the three amino acid sensor independent (ASI) proteins, Asi1, Asi2 and Asi3, prevents full-length Stp1 and Stp2 that 'leaks' into the nucleus from activating transcription. Asi1 was originally identified in a genetic screen designed to isolate mutations that restore leucine uptake in SPS-deficient strains (Forsberg et al., 2001). Cells carrying the *ssy1*Δ *asi1*Δ double mutations displayed constitutive activation of SPS-regulated genes and restored amino acid uptake to wild-type levels. Remarkably, Stp1/2 did not accumulate in the nucleus of *ssy1*Δ *asi1*Δ mutants as expected; the low levels of full-length Stp1/2 that enter the nucleus are sufficient to induce expression of SPS-responsive genes. This latter result clearly indicates that the Asi proteins confer their inhibitory effect on unprocessed

Stp1/2 in an additional, i.e. cytoplasmic retention-independent, manner. A novel study by Zargari et al. (2007) shed some light on the mechanism involved. The authors proposed a simple model whereby the Asi proteins function as a complex localized within the inner nuclear membrane (Figure 1.6).

The model is based on the following observations. First, deletions of *ASI1*, *ASI2* or *ASI3* result in comparable levels of SPS gene expression. Moreover, all deletion mutants display the same, if not identical amino acid uptake-related phenotypes. Second, Asi1 and Asi3 are structurally related, but not redundant, proteins. Both proteins contain a C-terminal localized RING domain characteristic of ubiquitin ligases. Third, all three Asi proteins function to inhibit the activity of full-length Stp1/2 in the absence of inducing amino acids. Finally, the Asi proteins co-fractionate to membranes of similar density (Forsberg et al., 2001; Boban et al., 2006).

The fact that the low levels of unprocessed Stp1/2 induce SPS-regulated gene expression in *ssy1*Δ *asi1*Δ cells to levels undistinguishable from wild-type cells, did not escape the attention of Boban and Ljungdahl (2007). The authors identified an additional layer of control exerted on SPS gene expression by the *AGP1* transcription factor, Dal81 (Uga35) (Abdel-Sater et al., 2004). Dal81 acts as an amplifier of expression by facilitating the binding of Stp1/2 to the UAS_{aa} promoter region of amino acid permeases. It does, however, not discriminate between full-length or processed Stp1/2, which explains the apparent contradiction observed in *ssy1*Δ *asi1*Δ cells. Although important, Dal81 activity is not an absolute requirement for amino acid-induced SPS gene expression. During these conditions the truncated forms of Stp1/2 accumulate in the nucleus at levels high enough to stimulate expression independent of Dal81. In line with its role as an amplifier, Dal81 does not affect the nuclear targeting of processed Stp1/2; neither does it activate expression of SPS-regulated genes by itself (Ljungdahl, 2009).

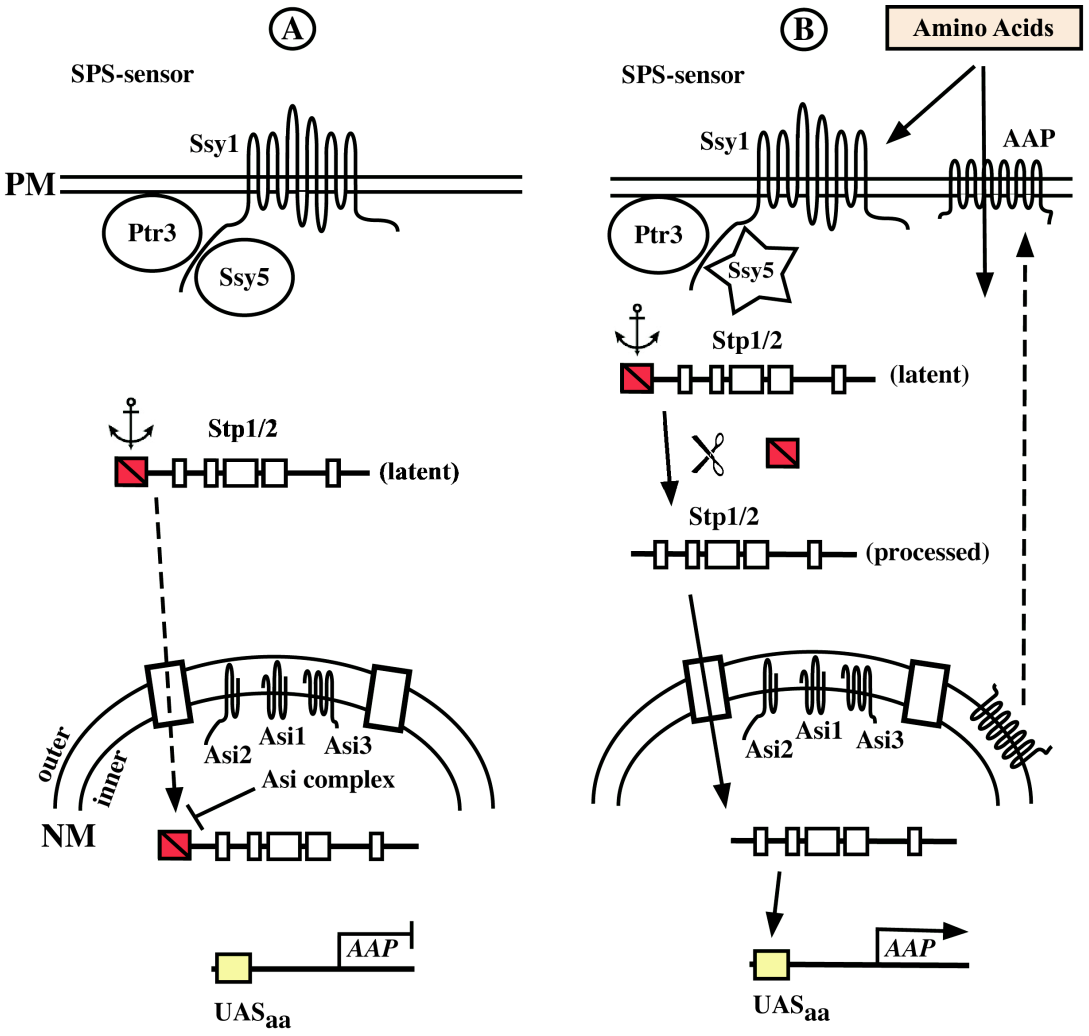

Figure 1.6: The SPS amino acid-sensing pathway.

Amino acid sensing is initiated by its binding to Ssy1, which relays signals through Ptr3 and Ssy5 to the two transcription factors Stp1 and Stp2. Once in the nucleus, Stp1 and Stp2 activate the expression of genes encoding amino acid permeases. **(A).** The non-induced state in the absence of amino acids. **(B).** The induced state in the presence of amino acids (adapted from Ljungdahl, 2009).

SPS regulates the transcription of several amino acid permeases in response to the presence of all the amino acids, except proline. These include genes that code for *AGP1*, *BAP2*, *BAP3*, *GNP1*, *DIP5*, *TAT1*, *TAT2*, the arginase *CAR1* and the peptide transporter *PTR2*. SPS also negatively regulates *CAN1*, *PUT4* and *GAP1* in amino acid-rich media. In addition to these direct effects on the amino acid permease genes, two independent transcription profile studies have indicated that it only represents a part of the full spectrum of SPS-regulated gene expression (Kodama et al., 2002;

Eckert-Boulet et al., 2004). For example, *ssy1*Δ and *stp1*Δ *stp2*Δ mutants display an overall upregulation of NCR-sensitive and stress-responsive gene expression.

1.4. REGULATED TRAFFICKING OF GAP1

The transport of proteins between intracellular membrane-bound compartments, or organelles, is common to all eukaryotic cells. It involves the selective packaging of newly synthesized proteins into the budding region formed of the donor compartment. These regions bud off as transport vesicles and are targeted to specific acceptor compartments to which they deliver their cargo. The general mechanism and the main proteins involved in these reactions appear to be conserved from yeast to humans (Salama and Schekman, 1995; Lupashin et al., 1996). Major stages in protein secretion in yeast includes: (i) synthesis of proteins on endoplasmic reticulum (ER)-associated polysomes, (ii) release of newly synthesized proteins into the lumen of the ER, (iii) chaperone-assisted protein folding and glycosylation in the ER, (iv) vesicle-mediated transport of proteins from the ER to the *cis*-Golgi apparatus, (v) further modification of the protein's carbohydrate side-chain in the Golgi, (vi) secretory vesicles derived from budding of the *trans*-Golgi deliver proteins to the cell surface, which in the case of membrane proteins, are inserted into the lipid bilayer.

The *S. cerevisiae* general amino acid permease Gap1 has long proved to be an extremely useful system to unravel the complex genetic and molecular events underpinning protein trafficking. Particularly in recent years, it has provided a wealth of information about new gene products and mechanisms involved in the transport and regulation of membrane proteins. The transcriptional regulation of Gap1 is absolutely intertwined with the presence of nitrogen in the extracellular environment - the GATA transcriptional activator Gln3 induces *GAP1* transcription under nitrogen-deplete conditions whereas the presence of extracellular amino acids results in its SPS-dependent repression. The following section, however, deals with the post-translational control Gap1 encounters on its movement through the secretory pathway.

Earlier work on Gap1 regulation in the Σ1278b and S288c genetic backgrounds highlighted a crucial difference in their response to the addition of ammonia to starved cells. For Σ1278b strains, ammonia is a repressing nitrogen source and causes the rapid downregulation of Gap1; a process known as ammonium inactivation (Magasanik and Kaiser, 2002). The S288c strains, on the other hand, do not suffer from ammonia inactivation. For the sake of this section, we will refer to nitrogen-rich conditions in the context of a rapid decline in Gap1 activity.

1.4.1. ER quality control

The ER plays a critical role in the folding of newly-synthesized proteins. Although the proper conformation of proteins lies encoded in their amino acid sequence, the ER provides the optimal environment for folding. It is packed with folding enzymes and molecular chaperones, like Lhs1, Pbn1 and the essential Kar2, that actively monitor the folding state of the new protein. Misfolded or incompletely assembled proteins are recognized by these chaperones and retained in the ER until they are correctly folded, in a process known as 'ER quality control' (Watanabe and Riezman, 2004; Pety de Thozée and Ghislain, 2006). Failure to do so results in protein aggregation, which was shown to be the root cause of human diseases like cystic fibrosis, Alzheimer's and Huntington's. The ER quality control system also ensures proteins that are persistently misfolded are targeted for ER-associated degradation (ERAD) (Spear and Ng, 2003; Kleizen and Braakman, 2004). The ERAD pathway re-translocates the misfolded protein back into the cytosol where proteasomal degradation takes place.

1.4.2. ER exit

Once fully folded, proteins destined for secretion are segregated from ER-resident proteins and taken up into transport vesicles, the so-called coat protein complex II (COPII) vesicles. Proteins may enter the COPII vesicles at the concentration present in the ER, a process termed bulk-flow, or at concentrations substantially higher than that in the ER. The bulk-flow model is an extremely inefficient mode of transport and accounts for only a small volume of total protein transport. Most of the transmembrane proteins are specifically enriched in COPII vesicles. The selective

enrichment is achieved by the presence of an ER exit signal located on the exposed region of the cargo protein that binds directly to COPII components. Gap1, for example, is enriched threefold in COPII vesicles compared to membrane phospholipids (Watanabe et al., 2008).

The ER exit signal of Gap1 was elucidated in a study by Malkus et al. (2002). The authors identified a short di-acidic sequence (-DxD-; residues 564-566) within the C-terminal cytosolic domain of Gap1 essential for the concentrative sorting of the permease. Interestingly, this region was shown to be highly conserved among yeast amino acid permeases (Figure 1.7).

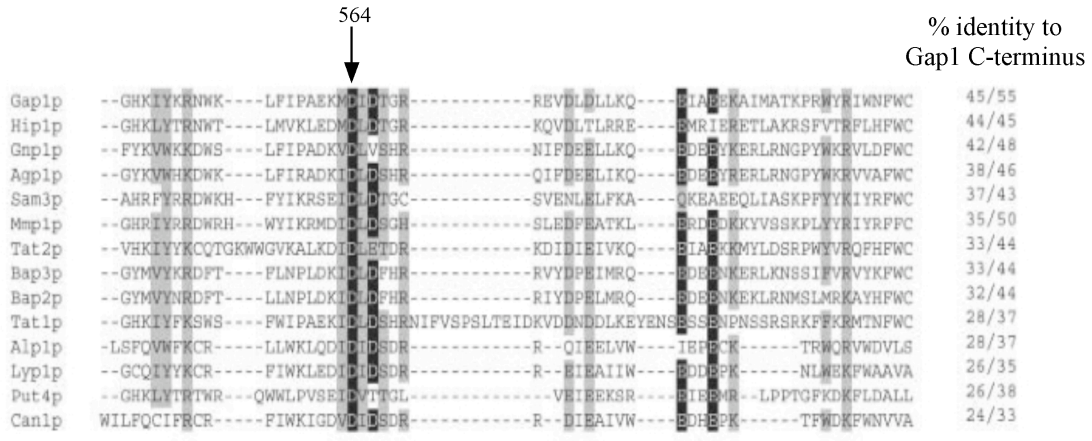

Figure 1.7: The C-terminal domain of Gap1.

A ClustalW alignment of Gap1 and 13 other *S. cerevisiae* amino acid permeases. Residues shaded black are identical in more than 80% of the aligned sequences and residues shaded grey are similar in more than 80% of the aligned sequences.

Mutations within this region severely reduced packing of the mutant Gap1 into COPII vesicles without affecting its folding, as demonstrated by the mutant protein's stability and functionality; aspartic acid[564] and isoleucine[565] are apparently the most sensitive to amino acid substitutions.

Moreover, the authors demonstrated the universality of the Gap1 ER export signal. In an experimental approach similar to an earlier study (Ma et al., 2001), Malkus and co-workers constructed an arginine permease Can1 chimeric protein in which its

native C-terminal localized export signal is replaced with that of Gap1. Strikingly, the chimeric Can1 was concentrated in COPII vesicles more efficiently than the wild-type. This suggests that Can1 make use of an additional export signal(s) located outside the C-terminal domain that may have an accumulative affect with the Gap1 exit signal.

COPII assembly on the ER membrane starts with activation of the small GTPase Sar1 by its ER-restricted GEF Sec12. Activated Sar1-GTP binds to the ER membrane by inserting an N-terminal α-helix into the lipid bilayer. Once anchored to the membrane, Sar1-GTP recruits the cytosolic Sec23/24 heterodimer. The Sec23 subunit functions as the GTPase activating protein (GAP) for Sar1 whereas Sec24 is responsible for the majority of cargo binding. Together with cargo, the Sec23/24-Sar1 complex forms the inner shell of the vesicle, also known as the prebudding complex (Bi et al., 2002; Fath et al., 2007; Kirchausen, 2007). Finally, the prebudding complex recruits the Sec13/31 complex that acts as a scaffold for the outer layer of the COPII vesicle (Figure 1.8).

A screen for secretory pathway mutants in yeast identified two additional proteins involved in COPII assembly, Sec16 and Sed4. Sec16 is a large hydrophobic protein that physically interacts with all of the COPII components, except Sec13. Deletion of *SEC16* blocks ER to Golgi transport and is lethal in *sec13*Δ or *sec23*Δ cells; an indication that Sec16 probably serves as a scaffold onto which the coat subunits assemble. A similar function was assigned to Sed4 (Sato and Nakano, 2007). Isolated as a multi-copy suppressor of *sec16*Δ mutations, *SED4* was shown to encode an important, but not essential, factor of the coat assembling machinery. Cells lacking Sed4 display a reduced rate in ER-Golgi transport and results in an exacerbated phenotype in combination with deletions in *SEC16*, *SEC12*, *SEC13*, *SEC23* and *SAR1*.

Accumulating evidence indicates that all amino acid permeases, including Gap1, depend on the membrane protein Shr3 to exit the ER. In *shr3*Δ mutants, amino acid permeases accumulate as large molecular weight complexes within the ER, and as a

consequence fail to enter COPII vesicles (Gilstring et al., 1999; Kota and Ljungdahl, 2005).

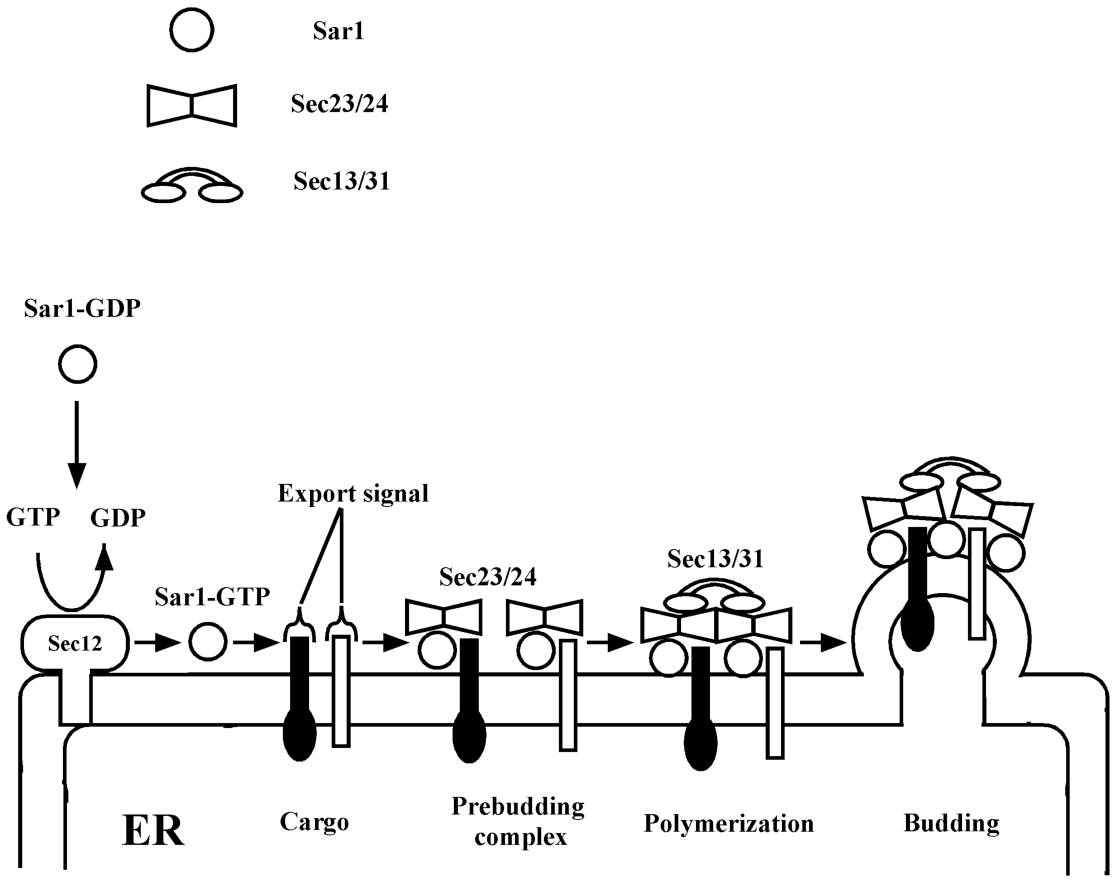

Figure 1.8: COPII vesicle formation and uptake of cargo protein.

COPII assembly on the ER membrane starts with activation of the GTPase Sar1 by its ER-bound guanine nucleotide exchange factor Sec12. Sar1-GTP binds to the ER and recruits the Sec23/24 complex. Together with cargo, the Sec23/24-Sar1 complex forms the "prebudding complex". These prebudding complexes are clustered by the Sec13/31 complexes, giving rise to COPII-coated vesicles.

These cells typically exhibit poor growth on amino acids due to the low levels of functional amino acid permeases present at the plasma membrane. The molecular mechanism underlying Shr3-dependent regulation of amino acid permease traffic was only recently determined (Kota et al., 2007). Using 'split' Gap1 constructs, it was demonstrated that Shr3 physically binds to the charged amino acid residues within the

transmembrane domains of the unfolded protein. It is believed that these charged, or polar, residues are the trigger for targeting misfolded proteins for ERAD. Therefore, by covering up the charged residues in the transmembrane domains, Shr3 prevents incompletely folded Gap1 from being degraded prematurely, i.e. the protein is allowed sufficient time for proper folding. Not surprising then, that deletions within the ERAD pathway partially restore amino acid uptake in *shr3*Δ cells. Protein folding and degradation are thus tightly connected processes.

In a related study, Kota et al. (2007) identified additional factors that regulate the passage of amino acid permeases through the secretory pathway. Exploiting the *shr3*Δ mutant's inability to import amino acids, the authors isolated three high-copy suppressors of the phenotype, *SSH4*, *RCR2* and *RCR1*. When overexpressed, *SSH4*, *RCR2* and *RCR1* restores amino acid uptake to near wild-type levels in *shr3*Δ, *ssy1*Δ and *stp1*Δ *stp2*Δ mutant strains. Analogously, overexpression of *SSH4*, *RCR2* and *RCR1* in wild-type strains resulted in a threefold increase in plasma membrane-bound Gap1. In contrast to the ER-restricted Shr3, the suppressor proteins have been localized to the endosome-vacuole pathway, from where they determine the plasma membrane protein's fate only after it has left the ER.

1.4.3. Delivery of vesicles: Tethering and Fusion

The journey of the COPII vesicle ensues with its pinching-off from the ER and delivery to the next compartment in the secretory pathway. Two independent processes ensure proper targeting of the vesicle to, and fusion with, the acceptor compartment: tethering and SNARE (soluble *N*-ethylmaleimide-sensitive factor attachment protein receptor) assembly.

Vesicle tethering marks the first interaction between a transport vesicle and its acceptor compartment (Lee et al., 2004). Tethers are either long coiled-coil proteins, e.g. Uso1, or large multi-subunit complexes, like the transport protein particle I (TRAPPI) complex. In yeast, TRAPPI is thought to serve as the recognizable feature on the Golgi that attracts the COPII vesicles. More importantly, TRAPPI also

functions as a GEF for the small Rab GTPase Ypt1, facilitating its conversion from the inactive GDP-bound form to the active GTP-bound state.

In a series of groundbreaking studies, the mechanistic detail of the process was recently resolved. It was shown that tethering depends on the direct interaction between the TRAPPI subunit Bet3 and its binding partner Sec23, a component of the COPII inner coat complex (Cai et al., 2007; Fromme et al., 2008; Spang, 2009). This initial binding activates Ypt1 to recruit Uso1, whose binding stabilizes the vesicle on the Golgi membrane and also promotes the formation of SNAREs on the membrane. These findings refute the long-held believe that tethering only occurs after the vesicle uncoats; instead it reveals an additional role for COPII coats in determining its own binding to the target membranes.

The final phase of vesicular transport involves fusion of the vesicle with the acceptor compartment. This process is mediated by a highly conserved family of membrane-associated proteins called SNAREs. Generally, this family is classified in two categories: the v-SNAREs that reside on vesicles and t-SNAREs that are found on target membranes. Both v-SNAREs and t-SNAREs self-assemble into extremely stable four helix-bundles; three α helixes contributed by the t-SNAREs and the fourth by the v-SNARE (Volchuk et al., 2004; Weinberger et al., 2005). Crucially, the three t-SNARE helixes are always composed of one member of the syntaxin heavy chain family and two non-syntaxin light chains.

In yeast, the *cis*-Golgi-localized syntaxin Sed5 plays an essential role in ER-Golgi and intra-Golgi transport. It forms functional SNARE complexes with Bet1, Sec22, Ykt6, Bos1, Sft1 and Gos1. This apparent promiscuity in binding partners has been difficult to reconcile with the ordered fashion in which vesicle fusion proceeds. However, Parlati et al. (2002) have shown that there are actually two distinct SNARE complexes operating in tandem in the Golgi; one, consisting of Sed5 as the heavy chain, Bos1 and Sec22 as the light chains and Bet1 as the v-SNARE, is required for entry into the Golgi, whereas Sed5, in combination with Gos1 and Ykt6 as the two light chains and Sft1 as the v-SNARE, is required for transport within the Golgi.

Gos1 is an atypical v-SNARE in that it participates in more than one transport step. In addition to its role in intra-Golgi transport, Gos1 is also proposed to direct vesicular transport from the ER to the Golgi (McNew et al., 1997). Accordingly, disruption of *GOS1* causes clear secretory defects. The ER-restricted chaperone, Kar2 (see section 1.4.1.), is secreted five-fold more in *gos1*Δ cells compared to wild-type cells, suggesting that *gos1*Δ cells display an ER-retention defective (*erd*) phenotype. The proteolytic processing of carboxypeptidase Y (CPY) also notably decreased such that both the p1CPY and p2CPY precursors accumulated in *gos1*Δ mutants (McNew et al., 1998).

1.4.4. *trans*-Golgi network: Finding yourself at the cross-roads

The *trans*-Golgi network (TGN) has a central role in protein sorting. The transport of newly synthesized proteins along the ER and Golgi stack occurs with basically no diversion to alternative routes. However, once proteins reach the TGN they face numerous possible subcellular destinations, including the plasma membrane, secretory vesicles or endosomes. The TGN sorts proteins to each of these destinations by segregating them from Golgi complex-resident proteins, before being packaged into specific membrane-coated vesicles. The role of the TGN as a sorting station is not limited to forward-transport; it also receives protein for recycling from the late endosome (Seaman, 2008).

Movement of Gap1 through the late secretory pathway is for the greater part regulated by the quality of the available nitrogen source. As mentioned before, in cells grown on proline or urea, i.e. poor nitrogen sources, Gap1 is directly sorted to the plasma membrane where it is active for amino acid uptake. In de-repressing growth conditions, however, newly synthesized Gap1 is sorted from the TGN to the vacuole without ever being delivered to the cell surface (Soetens et al., 2001; Horák, 2003). Ubiquitination is essential to this nitrogen source-dependent downregulation of Gap1.

The mechanism of ubiquitination involves the attachment of a highly conserved, 76 amino acid protein, ubiquitin, to specific lysine residues of the target protein. Ubiquitin itself contains seven lysines that can be used for the attachment of another

ubiquitin moiety. Hence, substrate proteins can either be monoubiquitinated (one ubiquitin molecule on a single lysine), multiubiquitinated (several lysines modified with just one ubiquitin molecule) or polyubiquitinated (several ubiquitin molecules in a chain on a single lysine residue) (Staub and Rotin, 2006).

Previous work has shown that Gap1 is ubiquitinated on two N-terminal lysine residues, lysine^{9} and lysine^{16}. Mutational analysis of the events leading to the loss of both plasma membrane-bound Gap1 and newly synthesized, TGN-localized Gap1 revealed that both groups share the same elements: (i) Gap1 must be ubiquitinated on at least one of the two lysines, (ii) ubiquitination requires the essential E3 ubiquitin ligase Rsp5 and at least one of the two redundant ubiquitin ligase adapters, Bul1 and Bul2, and finally, (iii) a functional, full-length C-terminal tail of Gap1. There are, however, two schools of thought on the exact role of ubiquitination in the regulation of Gap1 trafficking.

Helliwell et al. (2001) have reported that sorting of Gap1 at the TGN can be regulated by polyubiquitination. Therefore, overexpression of either *BUL1* or *BUL2* results in the polyubiquitination of Gap1 and sorting of it to the vacuole, irrespective of the nitrogen source. Conversely, in the *bul1*Δ *bul2*Δ double mutant, polyubiquitination of Gap1 is abolished and Gap1, in its monoubiquitinated form, reaches the plasma membrane more efficiently than in wild-type cells. Moreover, an *rsp5-1* allele lacking Rsp5 catalytic activity, displays the same sorting defect for Gap1 as observed in *bul1*Δ *bul2*Δ cells. These observations suggest that polyubiquitination is the main determinant for Gap1 sorting from the TGN to the vacuole. In contrast, Soetens et al. (2001) observed no increase in the monoubiquitinated form of Gap1 in *bul1*Δ *bul2*Δ cells, neither in the polyubiquitinated form of Gap1 in response to the overexpression of the *BUL* genes. Instead, polyubiquitination of the transporter was only detected in proline-grown cells supplemented with ammonium. In addition, the authors failed to demonstrate an essential role of polyubiquitin in sorting of Gap1 to the vacuole. These experiments were, however, performed in cells lacking Doa4, the deubiquitinating enzyme, which could perhaps explain the requirement of polyubiquitination of Gap1 for TGN - vacuole sorting in *DOA4* cells.

Mutations that influence Gap1 sorting can be divided into two general classes: mutations that cause constitutive sorting of Gap1 to the vacuole, or mutations that constitutively sort Gap1 to the plasma membrane. The first group includes mutations in *SEC13*, one of the components constituting the outer coat of the COPII vesicle, as well as *LST4*, *LST7* and *LST8*; the latter being isolated on the basis of their synthetic lethality with *sec13-1* (Roberg et al., 1997; Magasanik and Kaiser, 2002). Genetic analysis of *sec13-1* mutants reveals no apparent defect in ER-Golgi transport, indicating that Sec13's proposed function at the TGN is independent of its role in ER-Golgi traffic. Lst8, a subunit of TORC1, negatively regulates the GATA transcription factor Gln3, limiting the synthesis of α-ketoglutarate, glutamate and glutamine in the cell. Mutations inactivating *LST8* therefore results in an increase in intracellular levels of glutamate and glutamine, which acts as a signal for Gap1 sorting to the vacuole (Chen and Kaiser, 2003). The functions of Lst4 and Lst7 remain to be determined.

The second group of mutations is mainly found in the genes involved in ubiquitination of Gap1, namely Rsp5, Bul1, Bul2, and Doa4. As polyubiquitination of Gap1 is required for its sorting to the vacuole, mutations that interfere with this process cause high Gap1 activity and increased missorting of Gap1 to the plasma membrane. Importantly, combining a mutation that inhibits ubiquitination and causes constitutive sorting of the transporter to the plasma membrane, with a mutation that causes constitutive sorting to the vacuole, results in a double mutant in which Gap1 is constitutively sorted to the cell surface, i.e. in *rsp5-1 lst4*Δ cells Gap1 is constitutively targeted to the plasma membrane (Helliwell et al., 2001). This implies that ubiquitination of Gap1 occurs before its sorting to the vacuole.

The degradation of plasma membrane proteins in the vacuolar/lysosomal lumen requires its prior sorting into the multivesicular endosome (MVE) pathway. MVEs originate from early endosomes, as the protein-laden endosomal membrane buds off into the endosome to form an internal vesicle. Proteins are eventually delivered to the vacuole/lysosome when the MVE fuses with it (Bowers and Stevens, 2005; Nikko and André, 2007a; Nikko and André, 2007b). Formation of the MVE requires the sequential participation of three different protein complexes: ESCRT-I is required for the recognition of ubiquitinated proteins targeted to the pathway and ESCRT-II and

ESCRT-III assist in the sorting of proteins into the MVE vesicles. ESCRT-III also recruits Doa4 to deubiquitinate proteins before they are sorted to the vesicles, thus replenishing the intracellular pools of ubiquitin. ESCRTs are encoded by the class E *VPS* genes.

The endosome is, however, more than just a pit stop for plasma membrane proteins on the road to degradation. A study by Rubio-Texeira and Kaiser (2006) highlighted the importance of the bi-directional traffic between the endosome and the TGN. In a genome-wide screen designed to isolate novel genes involved in the intracellular sorting of Gap1, the authors reported that mutations in all of the class E *VPS* genes resulted in the missorting of Gap1 to the plasma membrane, possibly via the TGN. Thus, in conditions where the formation of inwardly budding MVE vesicles is compromised, e.g. dysfunctional ESCRTs, Gap1 is recycled to the plasma membrane. More importantly, the authors demonstrated that this recycling step is inhibited by high levels of internal amino acids or deletion of *LST4*. The vacuolar sorting of Gap1 also occurs independently of the ubiquitin-binding GGA (Golgi-associated, γ-adaptin homologues, ARF-binding) proteins, as an *lst4*Δ *gga1*Δ *gga2*Δ triple mutant still exhibits constitutive sorting of the permease to the vacuole (Babst, 2004). The recycling of Gap1 between the endosome and plasma membrane allows for a quick and effective response to changes in the cell's nutritional environment.

The same group also elucidated the mechanism by which the recycling of Gap1 between the two organelles is achieved (Gao and Kaiser, 2006). In a screen for mutants that display constitutively low Gap1 activity, a conserved multi-protein complex was identified. It consists of five different proteins, Gse1, Gse2, Ltv1, Gtr1 and Gtr2, and was dubbed the GSE/EGO complex. Two of the components, Gtr1 and Gtr2, are small GTPases, and control the formation of the complex according to their nucleotide-bound state. Gtr2, only active in the GDP-bound state, directly interacts with a di-aromatic sequence KPRWYR in the C-terminal tail of Gap1; a prerequisite for its sorting from the endosome to the plasma membrane (Seaman, 2006).

In addition to regulating transcription and intracellular sorting of Gap1, nitrogen source quality and quantity have been implicated in a third mechanism of regulation: the activity-dependent inactivation of plasma membrane-localized Gap1. In utilizing

the Gap1^{K9R,K16R} mutant's inability to be ubiquitinated, it was shown that the permease loses its transport activity upon the addition of amino acids while remaining localized in the plasma membrane. Moreover, this inactivation of Gap1 seems to be reversible, because the removal of exogenously-added amino acids restores transport activity in the Gap1^{K9R,K16R} mutant (Risinger et al., 2006). Gap1 inactivation at the plasma membrane also requires active transport of the amino acids by the protein, indicating that the amino acid-induced inactivation of Gap1 probably involves a reversible conformational change that occurs during the transport cycle. The advantage of an additional layer of control lies in the nutritional efficiency it affords the cell. When internal amino acid levels are low, *GAP1* expression and trafficking to the plasma membrane is upregulated. As internal amino acid stores are replenished, transport of amino acids by Gap1 causes both its inactivation at the plasma membrane and sorting of the newly synthesized form of the transporter to the vacuole. In the meantime, the cell continues making use of the nitrogen-rich conditions by inducing the expression of specialized, Ssy1-regulated amino acid permeases, i.e. general amino acid transport by Gap1 satisfies the cell's immediate need for nitrogen after which it is replaced by a more controlled transport of the available nitrogen source.

1.4.5. Endocytosis and degradation

The loss of Gap1 activity at the plasma membrane is the result of its endocytosis and subsequent targeting to and degradation in the vacuole. Although is has been ascertained that direct sorting of Gap1 at the TGN is independent from its endocytosis at the plasma membrane, it is unclear what role ubiquitin-mediated endocytosis plays in targeting Gap1 to the vacuole. With all the available mutants affecting both sorting steps, it was assumed that the same *cis*- and *trans*-acting ubiquitin elements participate in both sorting steps of Gap1. However, a recent study has revealed interesting differences in the ubiquitination events occurring at the two cellular locations (Risinger and Kaiser, 2008) (Figure 1.9). It was demonstrated that direct sorting from the TGN to the MVE requires the Rsp5-Bul1-Bul2-dependent polyubiquitination of Gap1 on either lysine^{9} or lysine^{16}; the level of polyubiquitination is not influenced by a single mutation of either lysine residue.

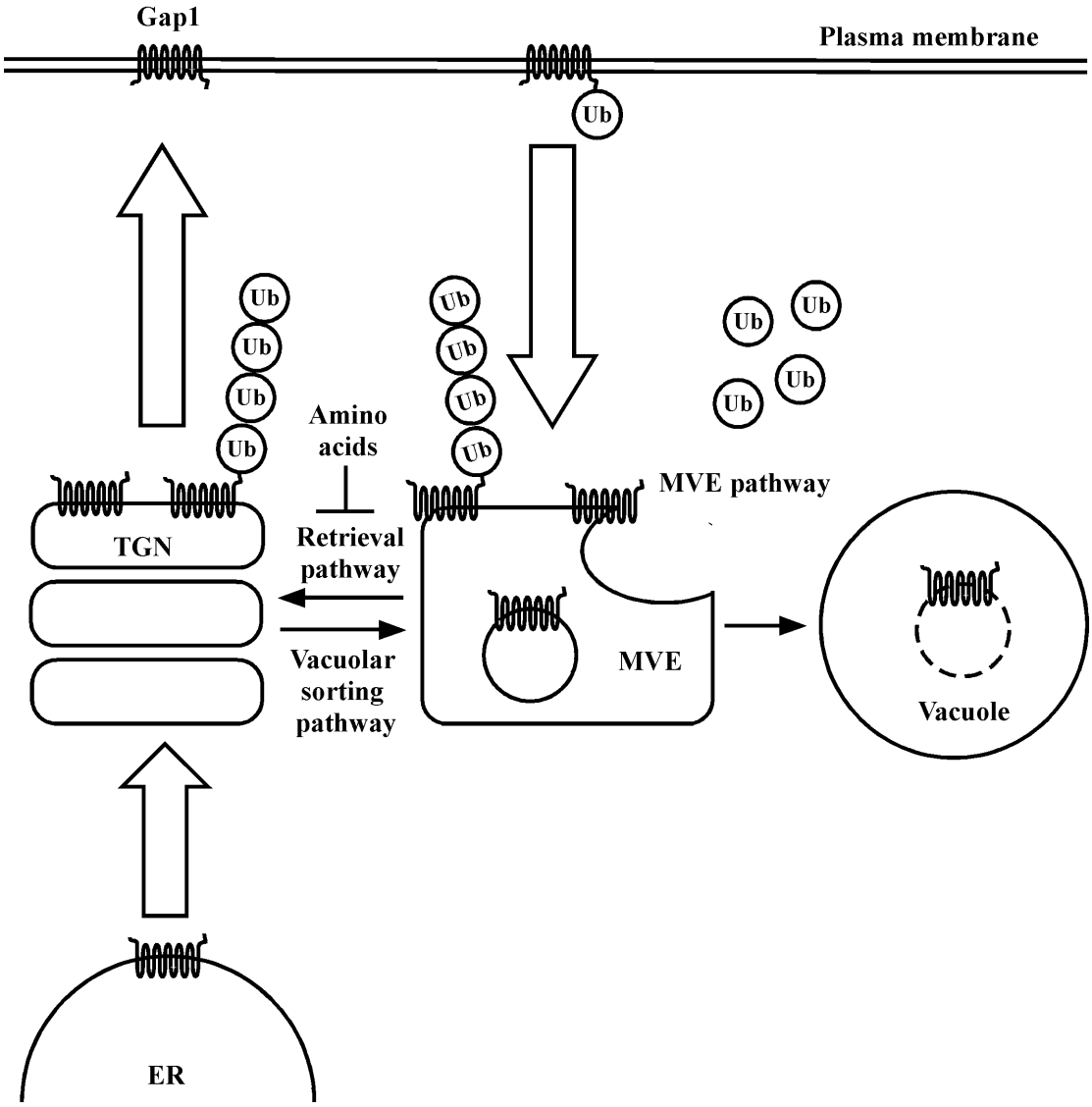

Figure 1.9: Proposed model for the sorting of Gap1 at the *trans*-Golgi network.

Neosynthesized Gap1 reaching the TGN has two possible fates: sorting to the plasma membrane where it is active for amino acid transport, or to the vacuole for eventual degradation. Its fate is decided by the nutritional situation both intracellularly and intracellularly (see text for details).

In addition to the N-terminal lysines, the extreme C-terminus of Gap1 also aids in the identification of the transporter by the ubiquitin ligase complex, as confirmed by a point mutation in the C-terminal domain, Gap1^{E583D}, that abolishes both the polyubiquitination of Gap1, and as a result, the direct targeting of newly synthesized Gap1 to the MVE.

Endocytosis, on the other hand, occurs through either the Rsp5-Bul1-Bul2-dependent monoubiquitination of lysine^{9} or lysine^{16}, or by the Rsp5-dependent, Bul1-Bul2-independent monoubiquitination of specifically lysine^{16}. These findings indicate a formerly unrecognized level of specificity in the ubiquitin-mediated trafficking of Gap1. Elaborating on their work, Lauwers et al. (2009) demonstrated the necessity of lysine^{63}-inked polyubiquitination of Gap1 as a specific signal for its sorting into the MVE pathway. Once internalized by the monoubiquitination of either lysine^{9} or lysine^{16}, Gap1 must undergo lysine^{63}-linked polyubiquitination on at least one of the acceptor lysines. Failure to do so, e.g. in an ubiquitin^{K63R} mutant, causes the recycling of internalized Gap1 to the plasma membrane via the TGN, with a small amount of the permease accumulating at the vacuole. The mechanism by which lysine^{63}-linked ubiquitination of Gap1 bolsters its MVE sorting remains poorly understood. It has been proposed that the GGA proteins may recognize the lysine^{63}-inked chains, since deletion of the ubiquitin-binding GAT domain of GGA proteins display a similar phenotype as ubiquitin^{K63R} cells, i.e. recycling of Gap1 to the plasma membrane.

The role of the C-terminus of Gap1 in determining its ubiquitin-mediated internalization and downregulation is well-established. Previous work has identified a di-leucine motif (residues 575-576) and a glutamate (residue 582) critical to the ammonium-induced inactivation of Gap1 in proline-grown cells. Replacing the di-leucine with di-alanine, or substituting the glutamate for a lysine, results in a mutant Gap1 allele fairly resistant to ammonium-induced degradation. The two motifs are located in a region predicted to form an α-helix (residues 571-588) (Hein and André, 1997; Springael and André, 1998). Deleting the 11 amino acid tail following the α-helix causes the same resistance to ammonium-induced downregulation as observed in the di-alanine and lysine^{582} mutants. Other then containing a high proportion of aromatic amino acids and ending in a highly conserved tripeptide, the 11 amino acid tail lacks any distinct features. The exact role of the C-terminus in Gap1 trafficking requires further study. The assembly of the N- and C-termini of Gap1 into a signaling complex that is recognized by the Rsp5-Bul1-Bul2 ubiquitin ligase complex, as predicted by Risinger and Kaiser (2008), seems very likely (for an overview of the known interactions and functions of the C-terminal portion of Gap1 in determining its fate, see Table 1.1).

Table 1.1: Role and function of specific residues within the C-terminal portion of Gap1.

C-terminal position:	Required for:	Interacting partner(s):
Residues 564-566 (DxD)	ER exit and concentrative sorting into COPII vesicles	Sec23-Sec24-Sar1
Residue 583	Polyubiquitination of Gap1 on the N-terminal lysines	Rsp5-Bul1-Bul2
Residues 590-595 (KPRWYR)	Sorting of Gap1 from the endosome to the plasma membrane	Gtr2
Residues 575-576, 582, 589-599	NH_4^+-induced inactivation of Gap1	Rsp5-Bul1-Bul2

The serine/threonine kinase Npr1 is another key determinant in the nitrogen-regulated sorting of Gap1. The main function of Npr1 involves the stabilization of Gap1 at the plasma membrane. Thus, loss of Npr1 activity triggers both the rapid internalization of membrane-bound Gap1 and targeting of newly synthesized Gap1 from the TGN to the vacuole; phenotypes reminiscent of those observed in nitrogen-starved cells supplemented with a good nitrogen source. Intriguingly, the C-terminal mutations described above restore wild-type Gap1 activity to *npr1*Δ cells. The reduced levels of Gap1 phosphorylation detected in proline-grown, *npr1*Δ cells led to the notion that Gap1 stability at the plasma membrane is acquired through the Npr1-dependent phosphorylation of the permease (De Craene et al., 2001).

However, the high levels of phosphorylation seen in *npr1*Δ *rsp5-1* mutants suggest that the target of Npr1 may not be Gap1 itself. Instead, it seems more probable that the high levels of Gap1 phosphorylation in wild-type cells is due to the transporter localizing to the plasma membrane. Npr1's own phosphorylation status, and therefore activity, is regulated by TORC1 in response to the nutritional conditions: it is phosphorylated in ammonia-grown cells and dephosphorylated in rapamycin-treated or nitrogen-starved cells (Tate et al., 2006b).

1.4.6. Role of sphingolipids in Gap1 trafficking

Newly synthesized Gap1 attains detergent insolubility at the TGN, and as a consequence, is associated with detergent-resistant membranes (DRMs) when present at the cell surface. DRMs are usually enriched in sphingolipids and to some extent, in ergosterols, the structural component of the yeast plasma membrane (Lauwers and André, 2006; Pineau et al., 2008). Gap1 synthesized in the absence of *de novo* sphingolipid biosynthesis displays various anomalies. In addition to being immediately downregulated at the plasma membrane, the permease synthesized under these conditions is also completely inactive and exhibits both an increased sensitivity to proteolytic breakdown and an inability to fractionate with DRMs. These observations are consistent with a model where sphingolipids associate with newly synthesized Gap1 to assist the folding of the protein into a functionally active conformation. Furthermore, the rapid downregulation of Gap1 observed in the absence of sphingolipid synthesis involves the uncontrolled ubiquitination of the protein on lysines other than the typical lysine^{9} and lysine^{16}. Lauwers et al. (2007) reported the Rsp5-mediated ubiquitination of N-terminal lysines at positions 76, 87 and 91. Under wild-type conditions, i.e. conditions where Gap1 is correctly folded, these lysines are close to the plasma membrane and are as such protected from ubiquitination. This result suggests that sphingolipids, in addition to their chaperone activity, may also regulate the ubiquitination of Gap1.

1.5. PROTEIN PHOSPHATASES IN NUTRIENT-INDUCED SIGNALING

Protein phosphorylation and dephosphorylation are essential regulatory mechanisms in multiple, if not all, cellular processes. The importance of the phosphorylation networks in eukaryotic biology is emphasized by the estimated one-third of proteins that are reversibly phosphorylated. The phosphorylation status, and potentially, the activity, of any given protein is determined by both the enzymes performing the phosphorylation reaction, serine/threonine kinases, and the enzymes performing the dephosphorylation reaction, the serine/threonine phosphatases. The *S. cerevisiae*

genome is reported to contain 139 protein kinases and, in contrast, only 32 protein phosphatases, implying that protein phosphatases are generally promiscuous in their activity. However, these phosphatases are required multi-subunit enzymes, constructed from a limited number of catalytic subunits (C subunits) associating with literally hundreds of regulatory subunits (Garcia et al., 2003; Gallego and Virshup, 2005). As a consequence, the C subunits of the main protein phosphatases are synthesized in excess; the C subunit of protein phosphatase 2A (PP2A), for example, constitutes nearly 1% of total cellular protein (Fellner et al., 2003a). It is this versatility of the combinatorial subunit arrangement that lends specificity and accuracy to the activity of protein phosphatases.

Based on sequence similarities and crystal structures, the protein phosphatases can be divided into the PPP family, PPM family and PTP family (Table 1.2). The serine/threonine PPP family includes the protein phosphatase 1 (PP1), PP2A and PP2B (also known as calcineurin). The PPM family consists of Mg^{2+}-dependent phosphatases such as PP2C and pyruvate dehydrogenase phosphatase, whereas the PTP family comprises both phosphotyrosine-specific and dual-specific phosphatases, like Cdc14, that can dephosphorylate all three phosphoresidues (Yigong, 2009).

Table 1.2: Protein phosphatases from *S. cerevisiae* (adapted from Stark, 1996).

Class	Specificity	Function/Gene
PPP family	serine/threonine	PP1: Glc7 PP2A: Pph21, Pph22 PP2B: Cna1 (Cmp1), Cna2 (Cmp2) PP2A-like: Ppg1, Sit4, Pph3
PPM family	serine/threonine	Ptc1, Ptc2, Ptc3, Ptc4, Ptc5, Ptc7, ycr079w
PTP family	serine/threonine tyrosine	Cdc14, Ptp1, Ptp2, Ltp1, Msg5, Yvh1, Sdp1

PP2A and PP1 are the two most thoroughly studied protein phosphatases, and account for more than 80% of the total cellular serine/threonine phosphatase activity. Deregulation of these two phosphatases has been linked to several crippling

conditions such as cancer and Alzheimer's disease. Furthermore, several viruses, e.g. SV40 tumor virus and polyomavirus, employ PP2A to deregulate the metabolic pathways in the host, highlighting the importance of phosphatases in general signal transduction (Janssens et al., 2005; Xing et al., 2008).

1.5.1. PP2A: structure and function

The yeast PP2A, like its equivalent in higher eukaryotes, is a multimeric protein complex consisting of three different subunits, namely the A, B and C subunit. The structural A subunit serves as a scaffold to receive the other two subunits. The C subunit, in association with the A subunits, forms the heterodimeric core enzyme. The B subunit is the regulatory subunit that confers substrate specificity and subcellular localization to the A-C core enzyme (Figure 1.10). In *S. cerevisiae*, the C subunit is encoded by two related genes, *PPH21* and *PPH22*. Deletion of either gene has no observable effect on cell growth; deletion of both genes, however, eliminates 90% of total PP2A activity and results in mutant cells displaying a severely impaired growth- and temperature-sensitive phenotype, as well as cell wall and polarity defects (Stark, 1996; Janssens and Goris, 2001; Zabrocki et al., 2002a). The remaining phosphatase activity in *pph21*Δ *pph22*Δ cells is thought to originate from the PP2A-related *PPH3* gene product. Deletion of *PPH3* does not affect growth but is lethal in a *pph21*Δ *pph22*Δ background. Curiously, there is no evidence of Pph3 in association with either A or B subunit. Moreover, the Pph3 phosphatase exhibits enzymatic activities and subunit composition very different to that of the classic PP2A phosphatase.

A distinguishing feature of the *S. cerevisiae* C subunit is the presence of an acidic stretch of 70 amino acids in the N-terminal regions of both Pph21 and Pph22. The relevance of the N-terminal extensions remains to be determined, but a report by Zabrocki et al. (2002a) offered a possible role for these regions in regulating the C subunit's catalytic activity. Removal of the N-terminus results in a mutant Pph22 protein responding notably different than the wild-type to protamine, polylysine and various reducing agents. The N-terminus of Pph22 also influences the enzyme's binding of specific phospholipids and membranes. Intriguingly, the N-termini of

Pph21 and Pph22 show only 45% amino acid sequence identity, compared to the 87% overall identity of the two enzymes (Zabrocki et al., 2002b). This suggests that the N-terminal regions of Pph21 and Pph22 may have unique functions.

In line with a role in signal transduction, overexpression of *PPH22* was shown to trigger the induction of the cAMP-PKA pathway, even in the absence of nutrients. Modest overexpression of *PPH22* affected all the PKA targets investigated, with *PPH22*-overexpression cells demonstrating a constitutive repression of STRE-regulated genes, heat sensitivity, low trehalose levels and high trehalase activity. A similar high PKA phenotype is observed in *sch9*Δ cells, and since the *PPH22*-overexpression results are dependent on the presence of a functional Sch9, it was proposed that Sch9 represents a novel Pph22 substrate (Sugajska et al., 2001).

The A subunit in yeast is encoded by a single gene, *TPD3*. Like its mammalian homologue, Tpd3 mainly consists of 15 tandem repeats of a 39 amino acid sequence, termed a HEAT (Huntington/Elongation/A subunit/TOR) domain (Janssens and Goris, 2001). Deletion of *TPD3* is not lethal, but confers both temperature sensitive and cold sensitive phenotypes.

The B subunits of *S. cerevisiae* PP2A are encoded by two distinct genes, *CDC55* and *RTS1*. Inactivation of *CDC55* results in highly elongated, multiply budded and multinucleated cells, indicative of delayed cytokinesis. Deletion of *CDC55* also allows sister chromatid segregation in the absence of a fully constructed spindle, which normally blocks G2/M cell cycle progression by activating the spindle checkpoint. The spindle assembly checkpoint ensures the accuracy of mitosis by hindering the onset of anaphase until the spindle has been completely assembled and each pair of sister chromatids are attached to it (Jiang, 2006; Pal et al., 2008). The morphological and cytokinetic defects of *cdc55*Δ mutants are largely suppressed by the expression of a mutant form of the *S. cerevisiae* cyclin-dependent kinase, $Cdc28^{Y19F}$. Rts1 was isolated in two independent genetic screens: as a multicopy suppressor of the $hsp60^{ts}$ mutant allele, and later as a Rox three suppressor. Disruption of *RTS1* diminishes the mRNA levels of the Hsp60 chaperone, thus impairing the deletion mutant's overall stress response. Consequently, *rts1*Δ cells display severe

temperature and osmotic sensitivity. Similar to Cdc55, Rts1 is also required for the proper regulation of the cell cycle; the two B subunits are, however, not functionally interchangeable. In a screen aimed to identify downregulating components of the SPS amino acid-sensing pathway, Rts1 was isolated as a negative regulator of the pathway (Eckert-Boulet et al., 2006). Deletion of *RTS1* results in the constitutive transcription of both Agp1 and Bap2. These results indicate that PP2A is involved in the SPS-dependent pathway and suggest that a dephosphorylation step is required to downregulate signaling in the absence of extracellular amino acids (see section 1.3.3.).

1.5.1.1. PP2A-like phosphatases

Budding yeast also contains a group of phosphatases known as PP2A-like phosphatases, so called because they share more sequence similarity with PP2A than with PP1. Three different PP2A-like catalytic subunits have been identified in yeast: Ppg1, Sit4 and Pph3. The function of Ppg1 is unclear as inactivation of the protein causes a decrease in glycogen accumulation without affecting cell growth. Deletion of *SIT4* diminishes cell growth and, depending on the strain background, is lethal. In *ssd1-d* strains such as W303, *sit4*Δ is lethal; in *SSD1-v* strains such as BY and S288c *sit4*Δ is viable, resulting in a slow-growth phenotype (Wang et al., 2003). Sit4 normally exists in complex with the Sit4-associated proteins (Saps) Sap155, Sap185, Sap190, and possibly Sap4.

1.5.1.2. Alternative PP2A complexes: Variety of forms and functions

Most cellular PP2A corresponds to an A-C heterodimer core enzyme, able to complex with a variety of B subunits. A much smaller fraction of C subunit, not associated with the A subunit, instead exists as a complex with another yeast protein, Tap42 (Figure 1.10). The first clue to the existence of an alternative PP2A structure came from higher eukaryotes. Alpha4, the mammalian homologue of Tap42, binds directly to the C subunit, at the exclusion of both the A and B subunits. Similar observations were later noted in yeast, where the deletion of *TPD3* and *CDC55* enhanced the association of Tap42 with Pph21 and Pph22. Since then, homologues of Tap42 in

various organisms have been found to associate with PP2A, indicating that the Tap42-PP2A complex is conserved during evolution. Contrary to the A subunit that binds only to the PP2A C subunits, Tap42 was shown to be also a binding partner of the PP2A-like phosphatases Sit4 and Pph3 (Di Como and Arndt, 1996; Yang et al., 2007; Janssens et al., 2008). Nevertheless, the amount of C subunit that associates with Tap42 represents only about 10% of the total cellular phosphatase.

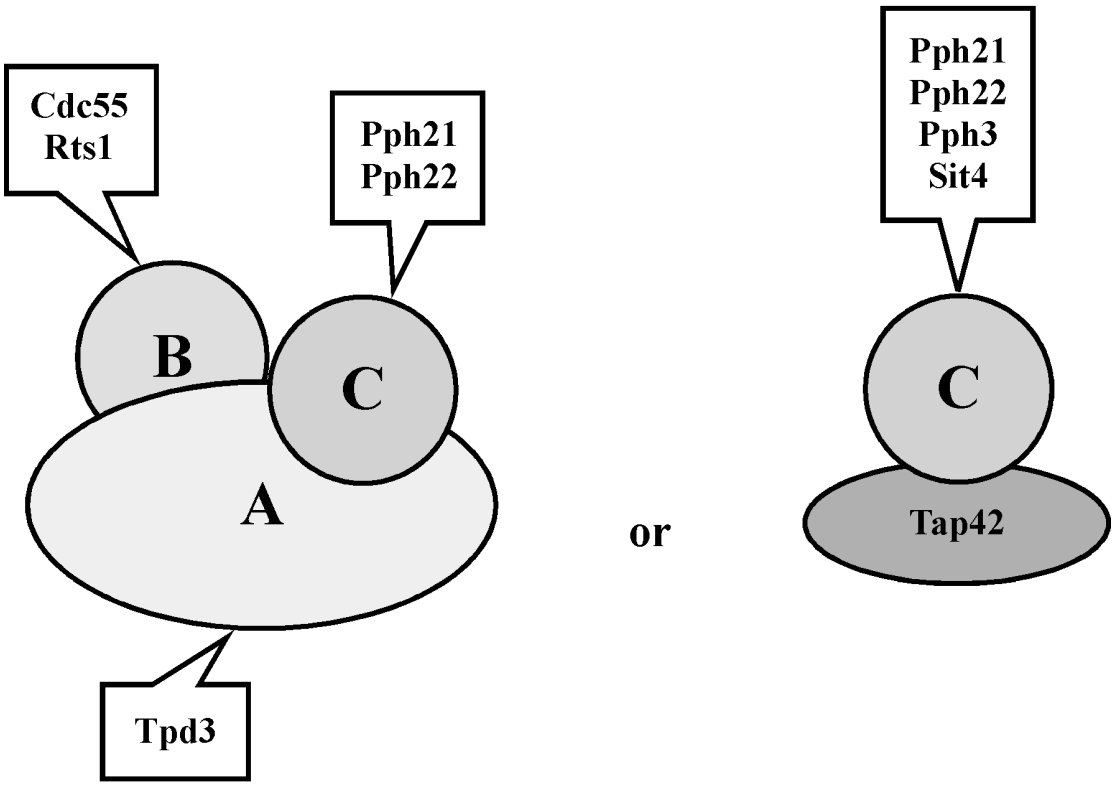

Figure 1.10: Multiple forms of PP2A in yeast.

The A subunit is the structural subunit that serves as a scaffold to accommodate the regulatory (B) and catalytic (C) subunits. In addition to the association with the A and B subunits, the C subunits can also complex with Tap42.

Tap42 is an essential protein, probably due to its participation in the TOR signaling pathway. Inhibition of TORC1 by rapamycin, or nutrient deprivation, causes dissociation of Tap42 from the PP2A C subunit and subsequently inactivates the complex. Rapamycin, however, has no effect on the association of Tpd3 and Cdc55 with Pph21. These findings have led to the notion that Tor elicits its function by inhibiting phosphatase activity via a Tap42-dependent mechanism, suggesting that

Tap42 functions as a phosphatase inhibitor by binding to, and restricting, phosphatase activity in response to signaling cues from Tor. Despite this, deletion of either *SIT4* or the C subunits, the two Tap42-associating proteins, does not result in rapamycin resistance, and in the case of *sit4*Δ, it actually renders the cells more sensitive to the macrolide drug (Zheng and Jiang, 2005). Earlier work by Wang and Jiang (2003), however, clarified the seemingly contradictory data on the role of Tap42 in the regulation of phosphatase activity. The authors demonstrated that the Tap42-C subunit complex, rather than the PP2A heterodimer, is involved in the organization of the actin cytoskeleton during the cell cycle. These results were further substantiated by the observation that deletions of both *PPH21* and *PPH22* had no effect on cytoskeleton organization. Tap42's essential role in this process was further underscored by the finding that rapamycin-resistant *tap42-11*-carrying cells exhibit an incorrectly polarized distribution of the actin cytoskeleton, a consequence of a modified binding between *tap42-11* and the C subunit (see section 1.2.3.1.).

Taken together, these findings suggest that Tap42 fulfills a function similar to that of the conventional regulatory subunits, i.e. by binding to the C subunit of the PP2A and PP2A-like phosphatases, Tap42 modifies their substrate specificity and cellular localization (Yang et al., 2007).

1.5.1.3. Post-translational control of PP2A

The essential role of PP2A in various cellular processes requires an exact and dynamic regulation of PP2A activity, localization, and substrate specificity. Although several factors, such as interacting proteins and reversible phosphorylation, have been linked to the regulation of PP2A activity, reversible methylation appears to be the main regulator of PP2A assembly. Comprehensive *in vitro* and *in vivo* studies have identified the target of methylation as a specific leucine, leucine^{369}, present in a highly conserved C-terminal region within the catalytic subunits.

In yeast, methylation of the PP2A C subunits is catalyzed by two enzymes, Ppm1 and Ppm2. Subsequent work showed that Ppm1 is the major methyltransferase acting on PP2A; methylated forms of Pph21 and Pph22 decreased from about 60% in wild-type

cells to less than 10% in *ppm1*Δ cells and to about 1% in *ppm1*Δ *ppm2*Δ mutants. *PPM1* codes for a 37-kDa protein that displays an overall weak sequence similarity to other eukaryotic methyltransferases, other than the trademark *S*-adenosylmethionine domain. Removal of the methyl group is catalyzed by the PP2A-specific methylesterase, Ppe1 (Wei et al., 2001; Leulliot et al., 2004). Interestingly, overexpression of *PPE1* yields phenotypes similar to those observed in *ppm1*Δ cells or cells lacking either B subunit. To date, no clear phenotype has been identified following deletion of *PPE1* in yeast.

Methylation of PP2A has been shown to affect the affinity of the A-C core enzyme for the various B subunits. The regulatory machinery, however, appears to be quite complex, as some regulatory subunits bind more efficiently to an A-C core when the C subunit has been methylated, while other regulatory subunits are not influenced by the C subunit methylation state.

PP2A activity is also regulated by a set of evolutionary-conserved proteins known as Rrd1 and Rrd2 (Rrd1/2), the yeast homologs of the mammalian phosphotyrosyl phosphatase activator (PTPA) (Van Hoof et al., 2001; Van Hoof et al., 2005). Deletion of both *RRD* genes causes resistance to rapamycin and an increased sensitivity to spindle depolymerizing drugs. Both are phenotypes normally associated with strains lacking the B subunits of PP2A and, more importantly, are indicative of a functional relationship between PP2A and Rrd1/2. Detailed analysis of the *rrd1*Δ *rrd2*Δ double deletion mutants indeed revealed a previously unknown role for Rrd1/2 in the generation of catalytically active PP2A. Cells deficient for Rrd1/2 typically produce C subunits with conformationally altered active sites, as substantiated by its severely reduced catalytic activity towards phosphoserine/phosphothreonine residues and its metal dependence. The lack of Rrd1/2, however, did not influence the assembly of the PP2A complex, as the mutant C subunit can still associate with the A en B subunits (Fellner et al., 2003a; Douville et al., 2006).

Recent work by Hombauer et al. (2007) has uncovered a novel mechanism of PP2A assembly in which a highly-regulated series of events protect the cell from unspecific

dephosphorylation reactions. It was demonstrated that the A subunit, Tpd3, physically associates with Rrd2 and that this Tpd3-Rrd2 interaction is an essential prerequisite for optimal binding of the C subunit. The Tpd3-Rrd2 complex interacts exclusively with the demethylated, i.e. inactive, form of the C subunit, by specifically targeting the Pph21/Pph22-Ppe1 complex. By monitoring the Tpd3-Rrd2 association and ensuing targeting of the demethylated C subunit, Ppe1 prevents the premature methylation and concomitant activation of the C subunits in the absence of the scaffolding subunit.

1.5.2. PP1

S. cerevisiae is unique in that it has only one PP1 gene, *GLC7*, compared to the multiple forms found in all other eukaryotes. As in mammalian cells, Glc7 regulates numerous processes in yeast, including glucose and glycogen metabolism, sporulation, transcriptional responses and amino acid biosynthesis. The catalytic activity of Glc7 is controlled by its association with a broad range of regulatory subunits, some of which have been identified in a recent two-hybrid screen (Walsh et al., 2002). These include proteins like Reg1 and Reg2, Gac1, Pig1 (and possibly Pig2), and Sds22; all of which will be discussed in further detail. In an attempt to isolate additional interacting partners of Glc7, Logan et al. (2008) identified 245 genes in a synthetic suppressor screen required for viability of yeast cells carrying a *glc7* mutant. The majority of these genes are implicated in nutrient-sensing, stress response and mitochondrial activity, suggesting additional, previously unknown, functions for the catalytic subunit of PP1 (Virshup and Shenolikar, 2009).

1.5.2.1. Regulation of Snf1 activity: Reg1 and Reg2

The Snf1 protein kinase of *S. cerevisiae* is the founding member of a family of serine/threonine protein kinases that include the mammalian AMP-activated protein kinase (AMPK). Like its mammalian counterpart, yeast Snf1 is required for metabolic control and energy homeostasis. In glucose-grown cells, the Snf1 kinase complex exists primarily in an inactive conformation. When glucose is depleted, Snf1 is rapidly activated through the phosphorylation of a conserved threonine, threonine^{210}, in the activation loop segment of the protein (Hong and Carlson, 2007). Three highly

similar and redundant upstream kinases, Sak1, Elm1, and Tos3 carry out the phosphorylation.

The Reg1-Glc7 phosphatase complex counteracts Snf1's activation by the upstream kinases. Reg1 interacts with activated Snf1 and directs Glc7 to the activation loop of the kinase, resulting in Snf1's dephosphorylation and subsequent inactivation. Snf1, in turn, phosphorylates and restricts Reg1-Glc7 activity, thereby creating a positive feedback loop governing its own activity. Consistent with its role as a targeting protein, *reg1*Δ cells exhibit both a constitutive activation of Snf1 and a hyperphosphorylation of its activation loop (Orlova et al., 2008; Hedbacker and Carlson, 2009). Localization and expression of Reg1, as well as its association with Glc7, do not appear to be regulated by the carbon source, but the activity of the Reg1-Glc7 complex may be regulated by a posttranslational phosphorylation event; direct biochemical evidence of such a mechanism is, however, still lacking.

Recent work by Rubenstein et al. (2008) has uncovered part of the mechanistic detail of the Snf1 dephosphorylation event. It was shown that both the upstream kinases and Glc7 are catalytically active, in spite of glucose availability. However, under conditions of glucose limitation, the phosphorylated activation loop of Snf1 is protected from Reg1-Glc7-dependent dephosphorylation by an as-yet unknown protein, allowing the accumulation of phosphorylated and active Snf1. The identity of the protein shielding threonine^{210} from dephosphorylation remains to be determined, but a likely candidate is Reg1. It is an important component of the Snf1 complex and requires direct interaction with the activation loop threonine, an interaction which is stronger in low glucose. Reg1 may therefore have a dual function in regulating Snf1 activity: as a recruiter of Glc7 phosphatase activity during high glucose levels or safeguarding the Snf1 activation loop during glucose-depleted conditions.

In line with its role in maintaining energy homeostasis, the Reg1-Glc7 complex also participates in the downregulation and degradation of certain gluconeogenic enzymes, like fructose-1,6-bisphosphate (FBPase), when they are no longer required. These enzymes are essential when cells are grown on non-fermentable carbon sources, but as cells are replenished with glucose, they necessitate rapid inactivation to prevent any unnecessary loss of energy (Cui et al., 2004; Gancedo, 2008). The Reg1-Glc7

complex ensures validity of the degradation process by promoting the import of FBPase into intermediate transport vesicles, before it is delivered to the vacuole for degradation. Hence, conditions that affect the binding of Glc7 to Reg1 also negatively affect FBPase degradation, e.g. *reg1*Δ mutants or cells carrying the *glc7*^{T152K} point mutation that decreases the interaction between Glc7 and Reg1 display a severely impaired degradation of FBPase.

REG2 encodes a homologue of Reg1 that, like Reg1, also associates with Glc7. While deletion of *REG2* is without a clear phenotype, deletion of both *REG1* and *REG2* results in a strong growth defect. This defect is suppressed either by the loss of Snf1 or the overexpression of *REG2*, suggesting that Reg1 and Reg2 are also functionally related (Frederick and Tatchell, 1996; Jiang et al., 2000). Reg2 is, however, not involved in glucose repression, as concluded from a fully-functional, Snf1-dependent glucose repression pathway operating in *reg2*Δ cells. Instead, the Reg2-Glc7 phosphatase complex is involved in stimulating the glucose-induced proteolytic breakdown of the maltose permease.

1.5.2.2. Glycogen synthesis: Gac1, Pig 1 and Pig2

In *S. cerevisiae*, as in higher eukaryotes, Glc7 is thought to dephosphorylate, and as a result, activate, glycogen synthase. Glc7 activity towards glycogen synthase is controlled by the regulatory subunit Gac1. Yeast cells deficient for Gac1 fail to accumulate glycogen and glycogen synthase in these strains remains in a hyperphoshorylated, inactive form. Similarly, cells harboring the *glc7*^{R73C} mutation that is unable to bind Gac1, also fails to accumulate normal levels of glycogen (François and Parrou, 2001; Williams-Hart et al., 2002). The glycogen deficiencies of both mutant strains can, however, be alleviated by either mutating the three putative C-terminally-located phosphorylation sites of Gsy2, the main glycogen synthase in yeast, or by truncation of the C-terminal tail of the enzyme.

GAC1 encodes an 88-kDa protein that shares 30% identity with its mammalian equivalent R_{GL}. It contains two separate functional domains required for binding Glc7 and Gsy2: an N-terminally-located valine^{71}-X-phenylalanine^{73} motif (where X

denotes any amino acid), also known as the VXF motif, is crucial for Glc7 binding, whereas asparagine[356] and tyrosine[357] are the essential residues for Gsy2 binding. Two additional Gac1-related genes, *PIG1* and *PIG2*, were identified in a two-hybrid screen with Gsy2 as bait. Disruption of *PIG1* causes a minor reduction in glycogen levels; combining it with a *gac1*Δ mutation, however, results in a severe glycogen accumulation defect, even stronger than that of the *gac1*Δ single mutant (Cheng et al., 1997; Wu et al., 2001). Together, these data suggest that Gac1 and Pig1 are functionally redundant glycogen targeting subunits for Glc7. The role of Pig2 in glycogen metabolism remains unknown. One intriguing characteristic of these three proteins is that they share a common 25 residue region, designated 'GVNK'. The yeast genome encodes only four examples of the GVNK motif; the fourth being the product of *YER054*. The GVNK motif is also present in mammalian R_{GL} and may regulate its interaction with either PP1 catalytic subunits or glycogen molecules.

1.5.2.3. Cell division: Sds22

Accurate chromosome segregation is at the core of mitosis – failure causes both genetic disorders and cancer in mammals. An essential innovation that makes chromosome segregation possible is the kinetochore, a protein-like structure on the chromosome that binds to spindle microtubules. Once both kinetochores of an individual chromosome have secured a proper microtubular attachment, anaphase is initiated. The identification of a mitotic requirement for Glc7 in yeast came from the observation that the temperature-sensitive *glc7-12* mutant displays the so-called 'dumb-bell' phenotype at the nonpermissive temperature – large-budded cells with the nucleus stretched across the bud neck (Hong et al., 2000; Peggie et al., 2002).

In *S. cerevisiae*, the mitosis-specific functions of Glc7 are regulated by the nuclear targeting subunit Sds22. The essential gene *SDS22* encodes a 40-kDa protein found mainly in the nucleus, despite lacking a NLS. Sds22 also lacks the VXF motif found in other Glc7 targeting subunits. Rather, interaction between Sds22 and Glc7 seems to be mediated by the 11 imperfect leucine-rich repeats present in Sds22's central domain, and occurs at a site in Glc7 distinct from the one used to bind the VXF motif (Pedelini et al., 2007). Overexpression of *SDS22* suppresses the 'dumb-bell'

phenotype of a *glc7-12* mutant; extra copies of *GLC7* can in turn suppress the deletion of *SDS22*. Sds22 also plays a role in ensuring the typical nuclear localization of Glc7, as evident from the accelerated loss of nuclear Glc7 in *sds22* mutant cells (Stark, 1996).

A recent study by Pedelini et al. (2007) identified the first inhibitory subunit of Glc7 in *S. cerevisiae*. The 155 amino acid, heat-stable protein was dubbed Ypi1, for yeast phosphatase inhibitor 1. Absence of *YPI1* results in phenotypes similar to those observed in *sds22*Δ cells, i.e. mislocalization of nuclear Glc7 and a mitotic arrest of all mutant cells. This suggests that Sds22 and Ypi1 may be functionally related. In support of this notion, it was shown that overexpression of *YPI1* increases the interaction between Sds22 and Glc7, while overexpression of *SDS22* increases the interaction between Ypi1 and Glc7 (Bharucha et al., 2008). These effects may be due to the stabilization of the interaction between two components, which is brought about by the overexpression of the third component. Curiously, the combination of equal amounts of Ypi1 and Sds22 leads to a nearly complete inactivation of Glc7.

AIM OF THIS STUDY

Adaptation to a constantly-changing nutritional environment is of critical importance to the survival of all organisms. The unicellular fungus *S. cerevisiae* has evolved numerous signaling pathways that ensure the optimal use of all available nutrients, thus maximizing the yeast cell's potential for survival under the existing conditions. Depriving yeast cells of an essential nutrient, like nitrogen, phosphor or sulfur, causes growth arrest and entry into the G_0 state of the cell cycle. The latter is characterized by an increase in levels of the storage carbohydrates trehalose and glycogen, and the transcriptional repression of ribosomal protein genes.

The general amino acid permease Gap1 was recently shown to act as a nutrient receptor, signaling the availability of its substrate to the interior of the cell. The dual function of Gap1 as amino acid transporter/receptor, or transceptor, was supported by the isolation of constitutively signaling alleles. These Gap1 mutants contain short truncations of the extreme C-terminus of the protein, with their expression resulting in a high PKA phenotype that affected all the downstream targets investigated, even in the absence of any nitrogen source. The high PKA phenotype was shown to be independent of the carbon source in the growth medium, and is also observed in the presence of ammonium as sole nitrogen source.

In Chapter II and Chapter III, we further characterized the underlying mechanism involved in the constitutive signaling of truncated Gap1 alleles. To determine the (possible) contribution of known nutrient signaling pathways to the overactive PKA phenotype observed in these mutants, we studied the effect that blocking of these pathways may have on PKA activity. We also evaluated different C-terminal truncations of Gap1 for their influence on the PKA phenotype.

Chapter IV deals with the molecular underpinnings of the mechanism by which glucose addition to carbon-deprived cells cause rapid activation of the serine/threonine-specific protein phosphatases PP2A and PP1. We assessed the roles that the different regulatory, catalytic and structural subunits of the respective

phosphatase enzymes may play in the process. We also studied the effect glucose addition may have on methylation of the PP2A catalytic subunits.

Chapter II

CHARACTERIZATION OF CONSTITUTIVELY SIGNALING ALLELES OF GAP1

2.1. ABSTRACT

The cAMP-PKA pathway in budding yeast controls an array of characteristics that depend on the nutrient composition of the growth medium. Rapid activation of the pathway by amino acids is triggered by the general amino acid permease Gap1. Expression of short, C-terminal truncations of the transporter results in cells that display a constitutively high PKA phenotype, even when starved for nitrogen. We show here that this phenomenon is not caused by the overactivation of either Tor1 or Stt4, or by the inhibition of the protein kinase Sch9. We provide evidence that the mutant alleles mediate the overactive PKA phenotype in a cAMP-independent, but PKA-dependent manner. Our results also show that the PKA phenotype is dependent on a background mutation in the specific *gap1*Δ strain used. The *seg1-1* mutation, an acronym for "Suppressor of ER exit-deficient Gap1", causes the secretion of truncated Gap1 alleles that would otherwise be retained in the ER by the organelle's quality control system. Finally, we show that the overactive Gap1ΔC6$_{(14aa)}$ phenotype is synergistically dependent on both the truncated allele and the *seg1-1* mutation.

2.2. INTRODUCTION

Yeast contains a series of transport proteins entrusted with the uptake of nitrogenous compounds from the medium, some of which also acts as receptors signaling the availability of their substrate to the interior of the cell. The first indication of such a dual function for some transporters came from the observation that low levels of L-citrulline, exclusively transported by Gap1, can activate the PKA pathway *in vivo*. In contrast, higher levels of L-citrulline, transported by additional amino acid permeases, were unable to activate the pathway. Further evidence highlighting Gap1's additional regulatory function is observed in *gap1*Δ cells where both amino acid transport and signaling are absent, suggesting that *S. cerevisiae* lacks a transport-independent receptor for sensing extracellular amino acids (Thevelein et al., 2008). Moreover, metabolization of the transported amino acid as possible activator of the PKA pathway can be excluded, as deletion of *ARG1*, the gene encoding

arginosuccinate synthase, had no affect on the rapid L-citrulline-induced activation of the PKA pathway through Gap1.

The dual function of Gap1 as an amino acid transporter/receptor (transceptor) is further supported by the isolation of constitutively active alleles. These Gap1 mutants contain short truncations of the extreme C-terminus of the protein, resulting in a high PKA phenotype that affects all the downstream targets investigated, even in the absence of a nitrogen source (Donaton et al., 2003) (Figure 2.1). The high PKA phenotype is independent of the carbon source in the growth medium and is also observed in the presence of ammonium as sole nitrogen source. Cells carrying these Gap1 alleles typically have a low trehalose and glycogen content, while expression of STRE-regulated genes is severely reduced, causing very high stress sensitivity. Amino acid-induced trehalase activation, however, is slightly reduced compared to the wild-type, probably due to an increased feedback inhibition of the enzyme. Transport activity of Gap1 is unaffected by the short truncations. These mutants represent the first case of an active nutrient transporter that causes permanent activation of a signaling pathway in eukaryotic cells.

Figure 2.1: Amino acid sequence of the C-terminal region of Gap1 (amino acids 533 – 602) and the various truncations thereof.

Residues shaded green represent the last transmembrane domain; those in brown constitute the predicted α-helix. The ER exit signal of Gap1 is shaded in red. Underlined sequences are involved in NH_4^+-induced inactivation and degradation of Gap1. The names of the various Gap1 truncated alleles do not refer to the actual number of amino acids removed, but rather to the order in which they were constructed.

The role of the C-terminus of Gap1 in determining the transporter's fate is well-established. The ubiquitin-mediated internalization and downregulation of Gap1, as well as its concentrative sorting into COPII vesicles, are both dependent on the presence of a complete and functional C-terminal tail. Previous work has identified a di-leucine motif and a glutamate residue essential for ammonium-induced inactivation of Gap1 in proline-grown cells. Moreover, deleting the 11 amino acid tail following the predicted α -helix causes complete resistance to ammonium-induced downregulation (Springael and André, 1998; Malkus et al., 2002).

In this chapter, we have further characterized the underlying mechanism involved in the constitutive signaling of truncated Gap1 alleles. To determine the possible contribution of known nutrient signaling pathways to the high PKA phenotype observed in these mutants, we studied the effect of blocking these pathways, either through the inactivation of an activating protein or through the use of specific inhibitors.

2.3. RESULTS AND DISCUSSION

2.3.1. Role of components known to be involved in nutrient signaling

2.3.1.1. Gap1ΔC6$_{(14aa)}$ does not genetically interact with Sch9

The serine/threonine protein kinase Sch9 is a functional yeast homologue of mammalian PKB/Akt, both of which are involved in the regulation of growth in response to nutrient availability. More recently, Sch9 has been assigned to the FGM pathway as a nitrogen- and glucose-sensitive regulator that acts independently of cellular cAMP to control PKA targets (Crauwels et al., 1997; Thevelein and de Winde, 1999). Moreover, the authors also demonstrated that deletion of *SCH9* results in a partial increase in PKA activity and, as a consequence, *sch9*Δ cells display an inability to properly enter stationary phase when starved for nitrogen. These are all phenotypic properties it shares with the Gap1ΔC6$_{(14aa)}$-carrying cells.

We checked whether the overexpression of *SCH9* can suppress the overactive signaling phenotype of Gap1ΔC6$_{(14aa)}$. Cloned under transcriptional control of its native promoter and on a multicopy plasmid, various *SCH9*-overexpression strains were monitored for their L-citrulline-induced mobilization of trehalose. The overexpression of *SCH9*, however, had no influence on the phenotype of Gap1ΔC6$_{(14aa)}$-carrying cells, as evident from the levels of trehalose accumulated by the various overexpression strains during nitrogen starvation (Figure 2.2). Similar unchanged phenotypes were observed for the wild-type and *gap1*Δ strains carrying the *SCH9*-overexpression constructs, i.e. PKA status is apparently unaffected.

The efficacy of our overexpression construct was determined by examining growth of a wild-type strain in the presence of the potent immunosuppressive drug, wortmannin. The overexpression of *SCH9* was previously shown to restore growth of cells exposed to this toxic compound (Geyskens, 2004; see section 2.3.1.5.). Similar results were obtained with our constructs, indicating functionality (data not shown).

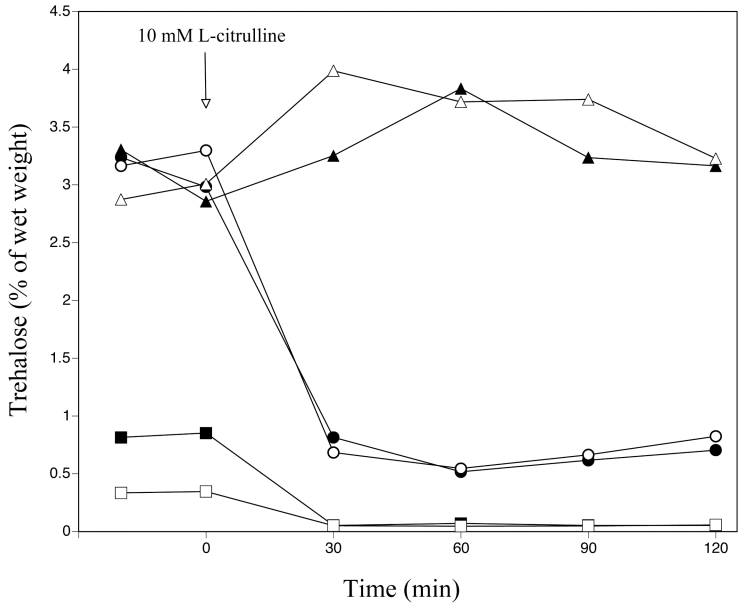

Figure 2.2: Overexpression of *SCH9* does not suppress the overactive signaling phenotype of Gap1ΔC6$_{(14aa)}$. (In collaboration with Ole Lagatie)
Mobilization of trehalose after the addition of 10 mM L-citrulline to nitrogen-starved cells of the wild-type + pYX212 (●), wild-type + pYX212-*SCH9* (○), *gap1*Δ + pYX212 (▲), *gap1*Δ + pYX212-*SCH9* (△), Gap1ΔC6$_{(14aa)}$ + pYX212 (■), and Gap1ΔC6$_{(14aa)}$ + pYX212-*SCH9* (□).

Consistent with the overexpression studies, deletion of *SCH9* was also shown to be ineffective in reversing the high PKA phenotype of Gap1ΔC6$_{(14aa)}$ cells (Figure 2.3). Deletion strains of *sch9*Δ carrying the wild-type- or Gap1ΔC6$_{(14aa)}$ alleles accumulate similar levels of trehalose when starved for nitrogen on a glucose-containing medium. Although the amount of trehalose accumulated by the *sch9*Δ mutants is somewhat reduced compared to the wild-type, it is still significantly higher than the trehalose levels obtained in the Gap1ΔC6$_{(14aa)}$-carrying cells. The reduction in trehalose levels may be attributed to the higher basal activity of the trehalose-degrading enzyme, trehalase, in the *sch9*Δ cells (Crauwels et al., 1997).

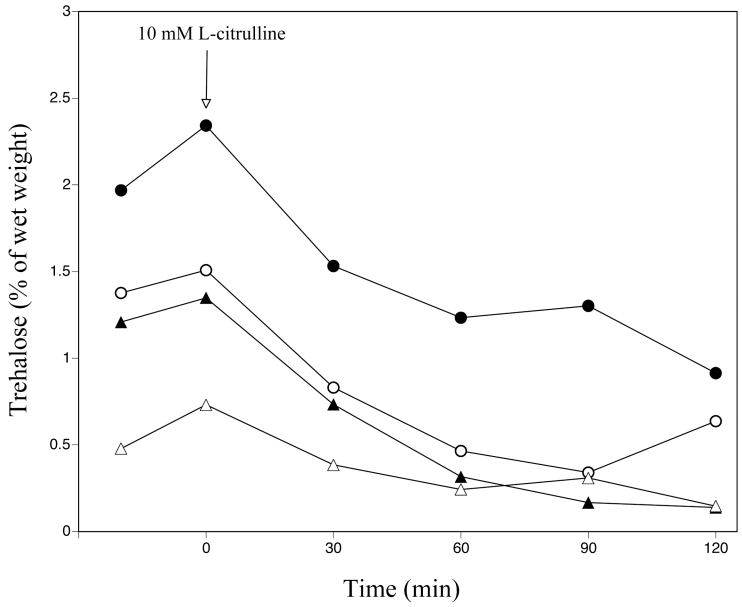

Figure 2.3: The deletion of *SCH9* does not suppress the overactive signaling phenotype of Gap1ΔC6$_{(14aa)}$.

Mobilization of trehalose after the addition of 10 mM L-citrulline to nitrogen-starved cells of the wild-type + pFL38 (●), *sch9*Δ + pFL38-*GAP1* (○), *sch9*Δ + pFL38-*GAP1ΔC6*$_{(14aa)}$ (▲), and Gap1ΔC6$_{(14aa)}$ + pFL38 (△).

2.3.1.2. PKA-dependency of the overactive Gap1ΔC6$_{(14aa)}$ phenotype

Earlier studies have shown that both the glucose- and nitrogen-induced activation of the FGM pathway depends on the activity of the free catalytic subunits of PKA, and that the regulatory subunit, encoded by *BCY1*, is not required and may even be inhibitory to the process. Moreover, the activity levels of individual *TPK* genes differ according to the nutrient used, with glucose-induced activation of trehalase pointing to an order of *TPK2* > *TPK1* > *TPK3*, whereas nitrogen-induced activation of the enzyme is more effective in the order *TPK1* > *TPK2* = *TPK3* (Toda et al., 1987a; Durnez et al., 1994).

To establish if PKA, and more specifically its catalytic subunits, are involved in the constitutive activation of PKA targets in the Gap1ΔC6$_{(14aa)}$ mutant, we investigated whether mutations that alter PKA activity also influenced the overactive phenotype. To this end, we created a PKA mutant with attenuated activity in which both *TPK1* and *TPK3* genes are deleted and cell viability is ensured through the expression of a

temperature-sensitive *tpk2*^{ts} mutant allele. The *tpk1*Δ *tpk2*^{ts} *tpk3*Δ *GAP1*Δ*C6*$_{(14aa)}$ and *tpk1*Δ *tpk2*^{ts} *tpk3*Δ *GAP1* strains were spotted in serial dilutions on nutrient plates and incubated at both the permissive (23°C) and restrictive (35°C) temperatures (Figure 2.4). Strains carrying wild-type *TPK2* were included as a control. As expected, growth at 23°C was unaffected for all the strains evaluated, as the *tpk2*^{ts} allele active at this temperature is sufficient to rescue growth.

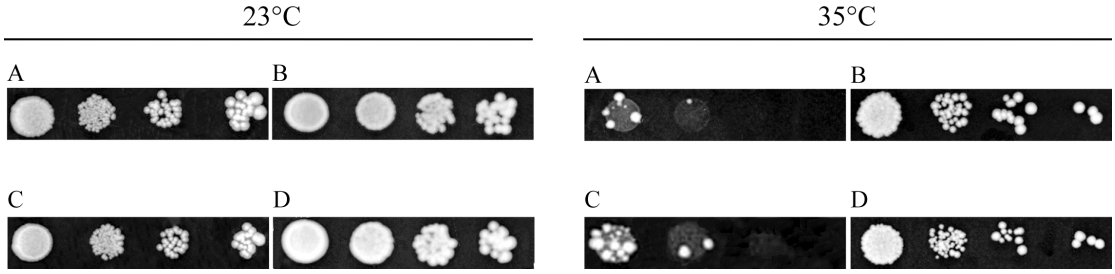

Figure 2.4: The overactive Gap1ΔC6$_{(14aa)}$ allele is unable to rescue a strain with inactive PKA.

The *tpk1*Δ *tpk2*^{ts} *tpk3*Δ *GAP1* (**A**), *tpk1*Δ *TPK2 tpk3*Δ *GAP1* (**B**), *tpk1*Δ *tpk2*^{ts} *tpk3*Δ *GAP1*Δ*C6*$_{(14aa)}$ (**C**), and *tpk1*Δ *TPK2 tpk3*Δ *GAP1*Δ*C6*$_{(14aa)}$ (**D**) strains were serially diluted onto YPD plates and incubated for 3 days at 23°C or 35°C, respectively (The colonies observed in panels A and C at 35°C are likely due to suppressor mutations in *tpk2*^{ts}).

In contrast, at the restrictive temperature both the *tpk1*Δ *tpk2*^{ts} *tpk3*Δ *GAP1*Δ*C6*$_{(14aa)}$ and *tpk1*Δ *tpk2*^{ts} *tpk3*Δ *GAP1* strains displayed a severe growth defect. These data suggest that the overactive Gap1ΔC6$_{(14aa)}$ allele is unable to rescue a strain with inactive PKA; indicative of the fact that the overactive effect on the PKA targets is likely due to an interference with a component(s) upstream of PKA or PKA itself, and not with one or more of the components downstream of the kinase. This is supported by earlier findings which showed that the characteristically low trehalose levels of Gap1ΔC6$_{(14aa)}$ mutants are restored to near wild-type levels in *tpk1*Δ *tpk2*Δ *TPK3 GAP1*Δ*C6*$_{(14aa)}$ cells (Holsbeeks, 2004).

2.3.1.3. Gap1ΔC6$_{(14aa)}$ exerts its effect downstream of *CYR1*-encoded adenylate cyclase

As demonstrated in the previous section, the overactive phenotype of Gap1ΔC6$_{(14aa)}$ depends on the catalytic subunits of PKA. PKA, in turn, is regulated by cAMP which is synthesized from ATP by the *CYR1*/*CDC35*-encoded adenylate cyclase. Deletion of *CYR1* is lethal. Viability of a *cyr1*Δ mutant, however, can be restored by the additional deletion of the high-affinity phosphodiesterase, *PDE2*, and the culturing of the double deletion mutant on medium supplemented with at least 3 mM cAMP (Mitsuzawa, 1993). In addition, earlier work by Matsumoto et al. (1983) demonstrated that if PKA activity is stimulated in an additional, cAMP-independent manner, e.g. through the deletion of *BCY1* in *cyr1*Δ cells, the requirement of exogenously-added cAMP to such cells becomes unnecessary.

To determine the cAMP-dependency nature of the Gap1ΔC6$_{(14aa)}$ phenotype, we evaluated growth of the mutant in the absence of adenylate cyclase. *CYR1* and *PDE2* were deleted in a diploid Gap1ΔC6$_{(14aa)}$ background, and, after sporulation, the progeny was recovered on media enriched with 3 mM cAMP. We selected the *cyr1*Δ *pde2*Δ double deletion spores containing the Gap1ΔC6$_{(14aa)}$ allele, and spotted dilution series of this strain on nutrient plates with decreasing concentrations of cAMP (Figure 2.5). A similar, adenylate cyclase-deficient strain containing wild-type Gap1, was included as experimental control.

Strikingly, the expression of *GAP1ΔC6*$_{(14aa)}$ clearly suppressed the growth deficiency of the *cyr1*Δ *pde2*Δ mutant, even in the complete absence of cAMP, whereas the adenylate cyclase-deficient control strain carrying wild-type Gap1, requires at least 2 mM cAMP for viability. This result convincingly demonstrates that the overactive phenotype of Gap1ΔC6$_{(14aa)}$ does not require the presence of cAMP and as such cannot be caused by either an increase in activity of the adenylate cyclase enzyme itself, or by enhanced stimulation of its enzymatic activity by an upstream activator, such as Cdc25 or Ras.

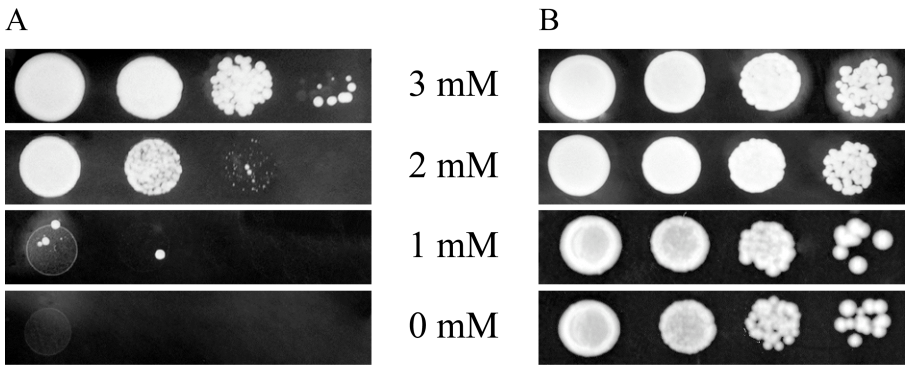

Figure 2.5: The expression of *GAP1ΔC6*$_{(14aa)}$ abolishes the cAMP requirement for growth of an adenylate cyclase mutant.

The *cyr1*Δ *pde2*Δ *GAP1* (**A**) and *cyr1*Δ *pde2*Δ *GAP1ΔC6*$_{(14aa)}$ (**B**) strains were cultured on YPD supplemented with 3 mM cAMP to mid-exponential phase, spotted in serial 10-fold dilutions on YPD plates with the indicated cAMP concentrations, and incubated at 30°C for 3 days.

2.3.1.4. The overactive Gap1ΔC6$_{(14aa)}$ phenotype is not suppressed by inhibition of TORC1

Like Sch9, the serine/threonine TORC1 kinase has been implicated in carbon- and nitrogen source-dependent control of cell growth, mainly through its positive regulation of various anabolic processes, including transcription, translation and nutrient transport. Inhibition of TORC1 by rapamycin elicits many of the cellular responses that are associated with nutrient starvation, such as downregulation of amino acid permeases, inhibition of protein synthesis and a rapid accumulation of storage carbohydrates (Jacinto and Lorberg, 2008).

To gain insight into the molecular mechanisms that underlie the overactive phenotype of Gap1ΔC6, we considered the hypothesis that the mutant allele causes constitutive activation of the TORC1 complex. If this would indeed be the case, then the treatment of GapΔC6 cells with rapamycin should result in abolishment of the high PKA phenotype. We tested this hypothesis by adding rapamycin to both exponentially-growing and nitrogen-starved Gap1ΔC6$_{(14aa)}$ cells (Figure 2.6).

In wild-type cells, exposure to rapamycin or transfer to nitrogen-starvation medium led to rapid accumulation of trehalose; a phenomenon that was more pronounced with the latter treatment. Combination of the two treatments led to faster accumulation of trehalose.

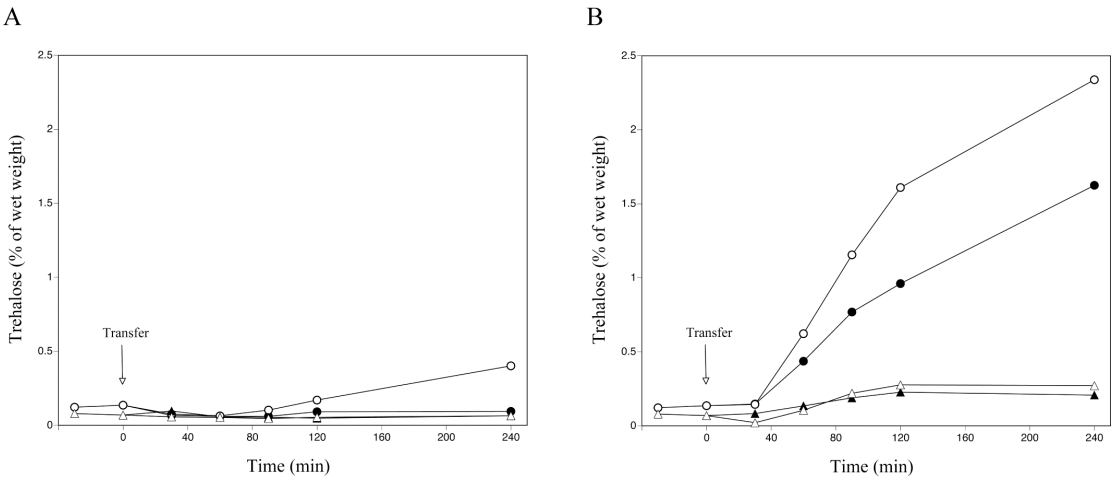

Figure 2.6: Rapamycin treatment, or the transfer to nitrogen-starvation medium, does not interfere with the overactive signaling phenotype of Gap1ΔC6-carrying cells. (In collaboration with Ole Lagatie)

Accumulation of trehalose as measured in wild-type (●, ○) and Gap1ΔC6$_{(14aa)}$ (▲, △) cells, respectively. **(A).** Cells were cultured to mid-exponential phase and at time zero transferred to either synthetic medium containing the drug vehicle alone (●, ▲), or to synthetic medium supplemented with 200 ng/ml rapamycin (○, △). **(B).** Cells were cultured to mid-exponential phase and at time zero transferred to either nitrogen-starvation medium containing the drug vehicle alone (●, ▲), or to nitrogen-starvation medium supplemented with 200 ng/ml rapamycin (○, △).

Similar treatment of the Gap1ΔC6$_{(14aa)}$-carrying cells, however, had no such effect, and trehalose levels remained low throughout the time-course. More intriguing, is the observation that even the addition of rapamycin to nitrogen-starved cells had no influence on the amount of trehalose accumulated. These data suggest that the Gap1ΔC6$_{(14aa)}$ mutant allele functions independently of TORC1, which allows it to overcome the rapamycin-induced inhibition of the complex. We suspect that Gap1ΔC6$_{(14aa)}$ may affect components downstream or parallel of TORC1.

We reasoned that if the mutant allele controls a component downstream (or parallel) of TORC1, the expression of *GAP1*Δ*C6*$_{(14aa)}$ would render cells rapamycin-insensitive, which would correlate with their ability to grow in the presence of rapamycin. We spotted a dilution series of a Gap1ΔC6$_{(14aa)}$-carrying strain on nutrient plates supplemented with 50 ng/ml rapamycin. The expression of *GAP1*Δ*C6*$_{(14aa)}$ could indeed compensate for the growth inhibitory properties of rapamycin (Figure 2.7). The wild-type strain was clearly more inhibited by the rapamycin than the Gap1ΔC6$_{(14aa)}$ mutant. This is in agreement with previous studies which demonstrated that mutants with constitutively high PKA activity, like *RAS2*^{G19V} or *bcy1*Δ cells, can overcome rapamycin sensitivity (Stanhill et al., 1999; Zurita-Martinez and Cardenas, 2005). It is known that under normal growth conditions, the Σ1278b strain has a hyperactive PKA pathway, which may explain, at least in part, why the Σ1278b genetic background is more resistant to rapamycin than for example the W303-1A and BY backgrounds.

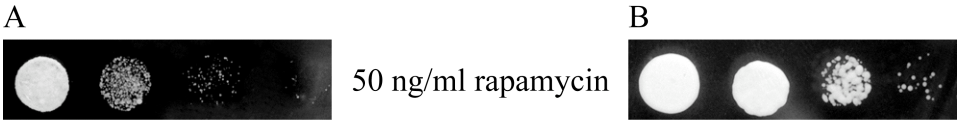

Figure 2.7: The expression of *GAP1*Δ*C6*$_{(14aa)}$ overcomes rapamycin sensitivity.

The ∑1278b wild-type (**A**) and Gap1ΔC6$_{(14aa)}$ (**B**) strains were cultured on YPD to mid-exponential phase, spotted in serial 10-fold dilutions on YPD plates supplemented with rapamycin at the indicated concentration, and incubated at 30°C for 3 days.

We sought to test if this rapamycin-insensitivity of the Σ1278B wild-type strain is indeed linked to its higher PKA activity. Exponentially growing cultures of the *cyr1*Δ *pde2*Δ *GAP1* and *cyr1*Δ *pde2*Δ *GAP1*Δ*C6*$_{(14aa)}$ strains, in which cAMP-dependent PKA activity is severely reduced, were serially diluted and spotted on nutrient plates (see section 2.3.1.3.). When supplemented with cAMP, the *cyr1*Δ *pde2*Δ *GAP1* strain remains viable (Figure 2.8). However, in the absence of exogenously-added cAMP, the *cyr1*Δ *pde2*Δ *GAP1* strain failed to grow, indicating that our previous hypothesis is correct: the hyperactivation of one pathway (PKA pathway) can compensate for the block in another (TORC1 pathway).

In accord with the trehalose accumulation results, the growth of the *cyr1*Δ *pde2*Δ *GAP1*Δ*C6*$_{(14aa)}$ mutant is unaffected by rapamycin. We attribute this apparent rapamycin-insensitivity of the Gap1ΔC6$_{(14aa)}$ strain to its cAMP-independent hyperactivation of the PKA pathway (Figure 2.8). Collectively, these results indicate that TORC1 is dispensable for the overactive phenotype of Gap1ΔC6$_{(14aa)}$, and that the mutant allele, in line with the PKA-dependency results, is acting through PKA.

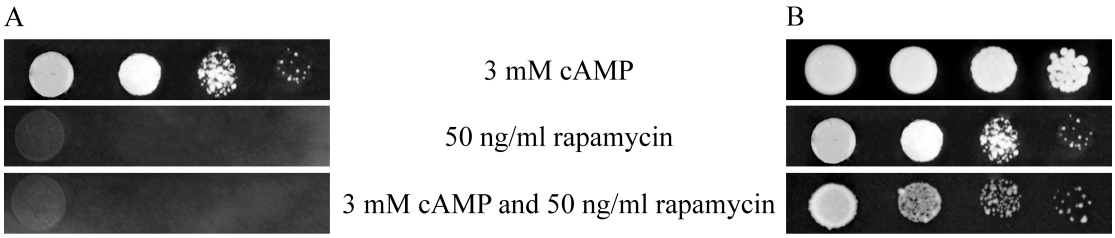

Figure 2.8: TORC1 is dispensable for the overactive signaling phenotype of Gap1ΔC6$_{(14aa)}$.

The *cyr1*Δ *pde2*Δ *GAP1* (**A**) and *cyr1*Δ *pde2*Δ *GAP1*Δ*C6*$_{(14aa)}$ (**B**) strains were cultured on YPD supplemented with 3 mM cAMP to mid-exponential phase, spotted in serial 10-fold dilutions on YPD plates with the indicated cAMP and/or rapamycin concentrations, and incubated at 30°C for 3 days.

2.3.1.5. Gap1ΔC6$_{(14aa)}$ does not genetically interact with Stt4

Phosphoinositide second messengers, generated by the well-conserved type III phosphoinositide 4-kinase Stt4, mediate a variety of signaling pathways through the activation of downstream proteins. Phosphoinositides have been implicated in the regulation of processes as diverse as cell proliferation, membrane trafficking and cytoskeleton organization. The *STT4* gene was originally identified in a screen for mutants that showed increased sensitivity to staurosporine, an inhibitor of protein kinase C (Audhya and Emr, 2002). In addition, work by Bergsma et al. (2001) has defined a unique function for Stt4 in FGM signaling. The authors demonstrated that addition of the Stt4 inhibitor, wortmannin, to nitrogen-starved glucose-repressed cells, inhibited the activation of trehalase and concomitant mobilization of trehalose, which normally occurs in response to the addition of a nitrogen source to such cells. Moreover, wortmannin-treatment also results in cell cycle arrest and the acquisition of

stationary-phase characteristics. The overexpression of *SCH9*, however, can alleviate the growth cessation imposed by the inhibitor, indicating that Stt4 may function as an upstream regulator of Sch9. To address whether Stt4 is involved in the constitutively-active phenotype of the Gap1ΔC6$_{(14aa)}$ mutant, we determined trehalose content of both exponentially-growing and nitrogen-starved cells exposed to 300 ng/ml wortmannin (Figure 2.9).

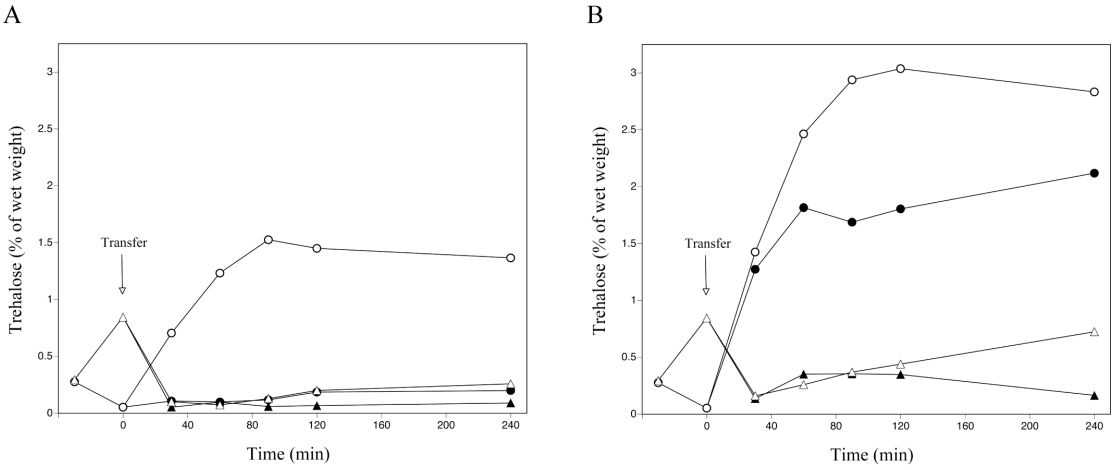

Figure 2.9: Wortmannin-induced inhibition of Stt4 does not block the overactive signaling phenotype of Gap1ΔC6$_{(14aa)}$-carrying cells. (In collaboration with Ole Lagatie)

Accumulation of trehalose as measured in wild-type (●, ○) and Gap1ΔC6$_{(14aa)}$ (▲, △) cells, respectively. **(A).** Cells were cultured to mid-exponential phase and at time zero transferred to either synthetic media containing the drug vehicle alone (●, ▲), or to synthetic media supplemented with 300 ng/ml wortmannin (○, △). **(B).** Cells were cultured to mid-exponential phase and at time zero transferred to either nitrogen-starvation media containing the drug vehicle alone (●, ▲), or to nitrogen-starvation media supplemented with 300 ng/ml wortmannin (○, △).

Similar to the rapamycin data, we found that treating wild-type cells with wortmannin, or transferring it to nitrogen-depleted media, elicit the rapid accumulation of trehalose. The two effects proved to be cumulative. In contrast, the Gap1ΔC6$_{(14aa)}$ cells did not exhibit any change in trehalose levels, which remained consistently low throughout the experiments. Thus, blocking Stt4 activity with

wortmannin has no effect on the constitutive signaling phenotype of Gap1ΔC6$_{(14aa)}$, suggesting that the mutant allele acts independently of Stt4.

2.3.1.6. Possible role of the Krh proteins in the Gap1ΔC6$_{(14aa)}$ phenotype

Concerted research efforts over the last few years have identified an additional mechanism by which the Gα protein Gpa2 activates PKA through two kelch-repeat proteins, bypassing adenylate cyclase stimulation in the process (Lu and Hirsch, 2005; Peeters et al., 2007). The discovery of such a bypass pathway naturally raises the question as to why Gpa2 utilizes both a cAMP-dependent and – independent route for activation of PKA. The authors propose a simple model whereby Krh1/2 serve as integrators of different nutrient cues. As opposed to fermentable sugars that activate PKA by increasing cellular cAMP levels, other nutrients, like nitrogen or phosphate, accomplish activation of the PKA pathway without causing an increase in cAMP. The Krh proteins could therefore integrate nutrient signal(s) with the fermentable sugar-induced cAMP signal for a coordinated activation of PKA.

Cells lacking both *KRH* genes display phenotypes reminiscent of that observed in Gap1ΔC6$_{(14aa)}$ mutants: trehalose and glycogen levels remain low in *krh1*Δ *krh2*Δ mutants, even when starved for an essential nutrient. Moreover, the deletion of *KRH1* and *KRH2* reduces the requirement of cAMP for growth in the absence of *CYR1*, a phenotype that is similar (although not identical) to that seen in Gap1ΔC6$_{(14aa)}$ cells (Peeters et al., 2006).

To investigate the possible functional importance of the Krh proteins in Gap1ΔC6$_{(14aa)}$ signaling, we deleted these genes in both the original *gap1*Δ strain (which contains the *seg1-1* background mutation; see section 2.3.2.), and in a *gap1*Δ strain without the mutation; both *gap1*Δ mutants are in the Σ1278b genetic background. We measured trehalose mobilization in the respective single and double *krh*Δ mutants when starved for nitrogen (Figure 2.10). To our surprise, deletion of the *KRH* genes led to a clear increase in the amount of trehalose accumulated during the starvation period for the Gap1ΔC6$_{(14aa)}$-carrying cells, suggesting a reversal in the PKA phenotype of the constitutive signaling strains. The increase in trehalose levels is most pronounced in

the *krh1*Δ single deletion mutant, whereas the *krh2*Δ mutant shows only a slight increase in the initial level of the storage carbohydrate. This result fits with the data presented by Batlle et al. (2003) that showed the *krh2*Δ mutant to demonstrate PKA phenotypes less pronounced than *krh1*Δ cells. Although there are no differences in initial trehalose levels between similar deletion strains carrying either Gap1 allele, e.g. *krh1*Δ *KRH2 GAP1 vs*. *krh1*Δ *KRH2 GAP1*Δ*C6*$_{(14aa)}$, mobilization of trehalose, however, occurred faster in the strains carrying the wild-type permease than those with the truncated allele. These data indicate that the *krh* deletions counteract the effect of the overactive Gap1ΔC6$_{(14aa)}$ allele, causing it to be even less active than the wild-type allele. As a result, trehalose mobilization by the truncated permease occurs at a slower rate than in the wild-type.

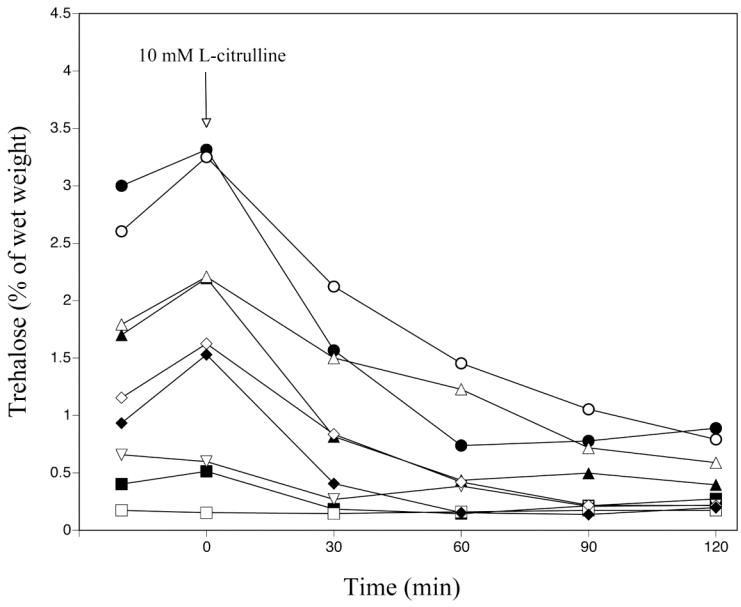

Figure 2.10: Deletion of *KRH1* and/or *KRH2* abrogates the overactive signaling phenotype of Gap1ΔC6$_{(14aa)}$ cells.

Mobilization of trehalose after the addition of 10 mM L-citrulline to nitrogen-starved cells of the ***seg1-1 gap1*Δ background:** *krh1*Δ *KRH2* + pFL38-*GAP1* (●), *krh1*Δ *KRH2* + pFL38-*GAP1*Δ*C6*$_{(14aa)}$ (○), *krh1*Δ *krh2*Δ + pFL38-*GAP1* (▲), *krh1*Δ *krh2*Δ + pFL38-*GAP1*Δ*C6*$_{(14aa)}$ (△), *KRH1 KRH2* + pFL38-*Gap1*Δ*C6*$_{(14aa)}$ (▽), *KRH1 krh2*Δ + pFL38-*GAP1* (◆), and *KRH1 krh2*Δ + pFL38-*GAP1*Δ*C6*$_{(14aa)}$ (◇); and the ***SEG1 gap1*Δ background:** *krh1*Δ *KRH2* + pFL38-*GAP1* (■), and *krh1*Δ *krh2*Δ + pFL38-*GAP1* (□).

Taken together, these results indicate a possible role for the Krh proteins in the overactive signaling phenotype, but require further investigation.

2.3.2. The overactive phenotype of Gap1ΔC6$_{(14aa)}$ is dominant in a specific *gap1*Δ background

As a first step in assessing the dominant or recessive nature of the overactive phenotype, we introduced the Gap1ΔC6$_{(14aa)}$ allele into a wild-type *GAP1* strain. Curiously, the trehalose levels of this hybrid strain after nitrogen starvation was equal to that of the wild-type experimental control, indicating an apparent reversal in the PKA phenotype of the diploid strain. This normally suggests that Gap1ΔC6$_{(14aa)}$ is recessive (Figure 2.11A).

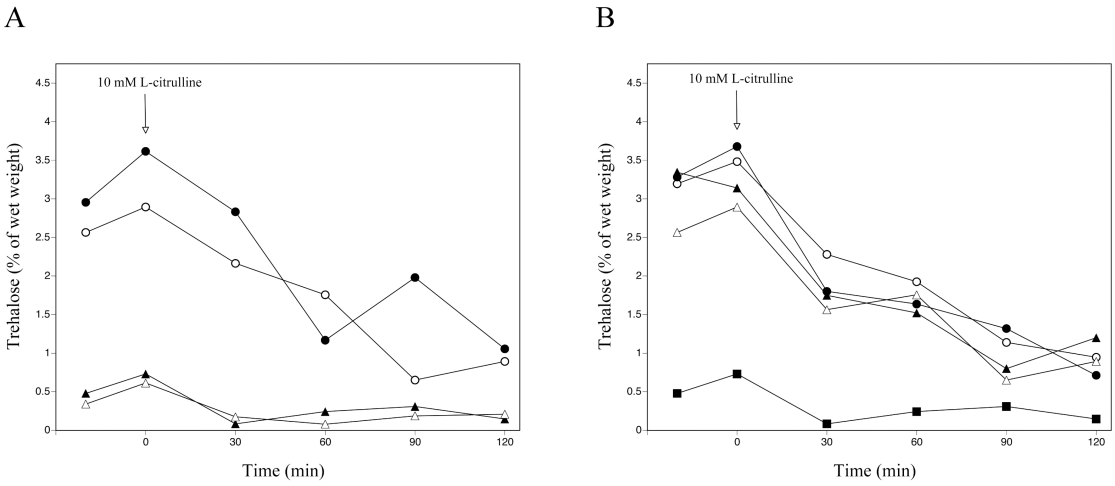

Figure 2.11: The dominant Gap1ΔC6$_{(14aa)}$ phenotype is restricted to a specific background.

Mobilization of trehalose after the addition of 10 mM L-citrulline to nitrogen-starved cells. (**A**). wild-type + pFL38-*GAP1* (●), wild-type + pFL38-*GAP1*Δ*C6*$_{(14aa)}$ (○), Gap1ΔC6$_{(14aa)}$ + pFL38 (▲), and Gap1ΔC6$_{(14aa)}$ + pFL38-*GAP1* (△). (**B**). wild-type + pFL38-*GAP1* (●), BY *gap1*Δ + pFL38-*GAP1*Δ*C6*$_{(14aa)}$ (○), W303-1A *gap1*Δ + pFL38-*GAP1*Δ*C6*$_{(14aa)}$ (▲), ∑1278b *gap1*Δ + pFL38-*GAP1*Δ*C6*$_{(14aa)}$ (△), and Gap1ΔC6$_{(14aa)}$ + pFL38 (■).

In a similar approach, we introduced wild-type *GAP1* into a Gap1ΔC6$_{(14aa)}$ (genomically-integrated) strain. However, contrary to the previous results, the latter strain did show the low trehalose levels that have become the hallmark of the overactive phenotype (Figure 2.11A). This indicates that Gap1ΔC6$_{(14aa)}$ is dominant.

These findings are significant as they demonstrate that the Gap1ΔC6$_{(14aa)}$ allele is only dominant in a specific *gap1*Δ strain in the Σ1278b genetic background. The *gap1*Δ strain concerned was employed in all our characterization experiments (section 2.3.1.) and is the same strain used by Donaton et al. (2003). It was originally a gift from B. André (Brussels).

These results raise the question as to why the overactive signaling phenotype of Gap1ΔC6$_{(14aa)}$ is restricted to a specific genetic background. We entertained the notion that the *gap1*Δ strain in which we obtain the overactive phenotype, may contain an additional genomic mutation(s) that proves essential for the overactive Gap1ΔC6$_{(14aa)}$ signaling. To examine the importance of the genetic background on this phenotype, we constructed Gap1ΔC6$_{(14aa)}$ mutants in various genetic backgrounds, including BY, W303-1A and wild-type Σ1278b strains, and measured the trehalose accumulated by these strains after nitrogen starvation. As shown in Figure 2.11B, all the new Gap1ΔC6$_{(14aa)}$ strains constructed, including the new Σ1278b Gap1ΔC6$_{(14aa)}$ mutant, exhibited trehalose levels comparable to that of the wild-type, and are as such indicative of a wild-type PKA phenotype. These results indicate that the overactive signaling phenotype depends on both the truncated allele and a genomic mutation(s) present in the original *gap1*Δ strain.

2.3.3. The background mutation(s) also has profound effects on the phenotype caused by other Gap1 truncated alleles

In light of the importance of the genetic background for the high PKA phenotype caused by Gap1ΔC6$_{(14aa)}$, we decided to re-evaluate the previous data obtained with the other Gap1 truncated alleles as presented in Donaton et al. (2003). All these results were obtained in the presence of the background mutation(s). Hence, when

expressed in wild-type strains, their effect may also disappear, as found for the Gap1ΔC6$_{(14aa)}$ allele. For this purpose, we monitored L-citrulline-induced mobilization of trehalose and glycogen in the new Σ1278b *gap1*Δ strain complemented with various truncated Gap1 alleles (see Figure 2.1). As shown in Figure 2.12, three different classes of truncated alleles can be identified based on their phenotypic properties in the original (mutant) and new *gap1*Δ (wild-type) genetic backgrounds.

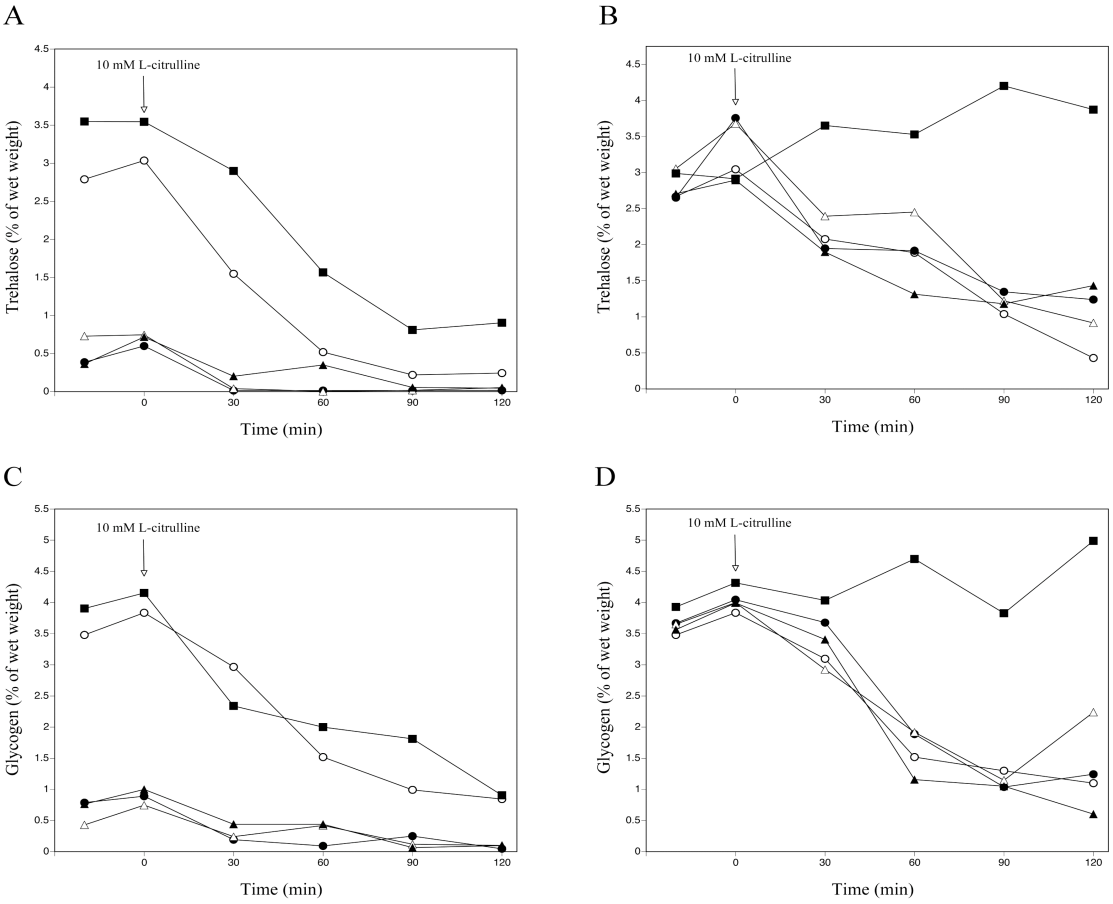

Figure 2.12: The background mutation(s) has profound effects on the phenotype caused by other Gap1 truncations.

Mobilization of trehalose (**A** and **B**) and glycogen (**C** and **D**) after the addition of 10 mM L-citrulline to nitrogen-starved cells. (**A** and **C**). Gap1ΔC6$_{(14aa)}$ (●), Gap1ΔC7$_{(3aa)}$ (○), Gap1ΔC11$_{(15aa)}$ (▲), Gap1ΔC12$_{(20aa)}$ (△), and Gap1ΔC14$_{(42aa)}$ (■). (**B** and **D**). ∑1278b *gap1*Δ + pFL38-*GAP1*Δ*C6*$_{(14aa)}$ (●), ∑1278b *gap1*Δ + pFL38-*GAP1*Δ*C7*$_{(3aa)}$ (○), ∑1278b *gap1*Δ + pFL38-*GAP1*Δ*C11*$_{(15aa)}$ (▲), ∑1278b *gap1*Δ + pFL38-*GAP1*Δ*C12*$_{(20aa)}$ (△), and ∑1278b *gap1*Δ + pFL38-*GAP1*Δ*C14*$_{(42aa)}$ (■).

The first type of alleles, consisting only of Gap1ΔC7$_{(3aa)}$, causes a wild-type PKA phenotype both in the presence and absence of the background mutation(s): trehalose and glycogen levels are similar in the mutant and wild-type strain when starved for nitrogen. A second type of truncated alleles, represented only by Gap1ΔC14$_{(42aa)}$, functions as wild-type allele only in the presence of the background mutation(s); in its absence, this allele displays an interesting phenotype in that it does not show L-citrulline-induced mobilization of trehalose or glycogen. The third type of alleles, comprising Gap1ΔC6$_{(14aa)}$, Gap1ΔC11$_{(15aa)}$ and Gap1ΔC12$_{(20aa)}$, demonstrates an overactive signaling phenotype in the mutant background, but a wild-type phenotype when expressed in a strain lacking the background mutation(s).

We also performed western analysis on extracts of wild-type- and mutant *gap1*Δ cells expressing the *GAP1*Δ*C6*$_{(14aa)}$ and *GAP1*Δ*C14*$_{(42aa)}$ alleles. The results of this analysis are shown in Figure 2.13. The Gap1ΔC6$_{(14aa)}$ allele shows a significant increase in expression, compared to the wild-type, when expressed in the mutant background. Based on this result, it is tempting to hypothesize that the increased expression of *GAP1*Δ*C6*$_{(14aa)}$ also increases the truncated permease's basal signaling capacity, which in turn would result in the constitutive activation of the cAMP-PKA pathway. Furthermore, as evident from Figure 2.13, the Gap1ΔC14$_{(42aa)}$ allele only reaches the plasma membrane when expressed in the mutant background.

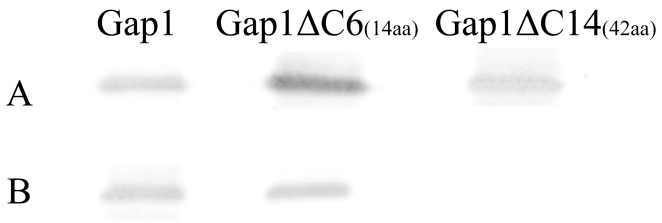

Figure 2.13: A Gap1 allele lacking an ER exit signal reaches the plasma membrane when expressed in the mutant *gap1*Δ background. (In collaboration with Ole Lagatie)

Western analysis of Gap1 expression in cell extracts of mutant (**A**) and wild-type (**B**) cells expressing the wild-type *GAP1*, *GAP1*Δ*C6*$_{(14aa)}$ and *GAP1*Δ*C14*$_{(42aa)}$ alleles, respectively.

Strikingly, in a background lacking the genomic mutation(s), the presence of Gap1ΔC14$_{(42aa)}$ in the plasma membrane is undetectable. This indicates that the background mutation(s) causes certain truncated alleles to be secreted to the plasma membrane, whereas in wild-type cells these truncated alleles are unable to reach the plasma membrane. These results also lend further support to the beforementioned data on storage carbohydrate mobilization.

Consistent with our localization data, Malkus et al. (2002) demonstrated the requirement of a short di-acidic sequence within the C-terminal tail of Gap1 essential for the permease's concentrative sorting to the plasma membrane. Mutations within this region, known as the ER exit signal, severely reduce the permease's packaging into COPII transport vesicles, culminating in Gap1's retention in the ER, and eventual degradation by the organelle's quality control system (see Figure 2.1 and "Chapter I", section 1.4.1.). The background mutation(s), on the other hand, seems to overcome the requirement for an ER exit signal for Gap1 and was therefore named 'suppressor of ER-exit deficient Gap1', or *seg1-1*, accordingly.

We next analyzed whether the overactive signaling phenotype of Gap1ΔC6$_{(14aa)}$ in the *seg1-1* mutant strain is correlated with its overaccumulation at the plasma membrane. We tested this hypothesis by overexpressing *GAP1ΔC6*$_{(14aa)}$ on a multi-copy plasmid. As the expression of *GAP1* is tightly regulated, both at the transcriptional- and post-translational level, we performed the overexpression of *GAP1ΔC6*$_{(14aa)}$ both in a wild-type- and *npi1-1* strain (Figure 2.14). The *npi1-1* mutation inhibits the Rsp5 ubiquitin ligase-dependent downregulation of Gap1, which allows the permease to be present *en masse* at the plasma membrane during nutritional conditions in which it is normally rapidly downregulated (De Craene et al., 2001). Hence, overexpression of *GAP1ΔC6*$_{(14aa)}$ in the *npi1-1* mutant should result in strong expression of the truncated allele in the plasma membrane.

Contrary to expectation, the overexpression of *GAP1ΔC6*$_{(14aa)}$ in the *npi1-1* mutant did not result in a constitutive signaling phenotype. Initial trehalose levels in the overexpression strains are identical to that of the wild-type strain. The rate of L-citrulline-induced mobilization of trehalose, however, is increased in the *npi1-1*

strains overexpressing wild-type *GAP1*, compared to the overexpressing *NPI1* wild-type strains. This increased signaling capacity also correlates with an increase in transport activity in the *npi1-1* strains (personal communication, Ole Lagatie).

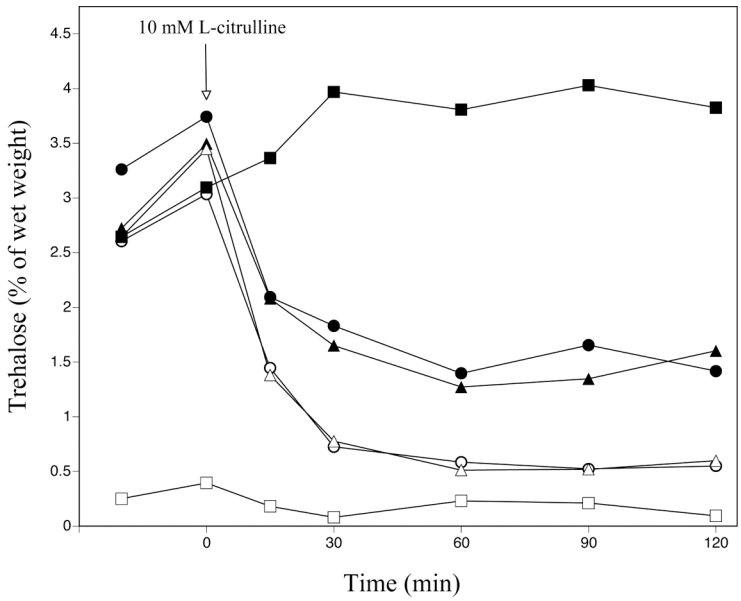

Figure 2.14: Overexpression of *GAP1*Δ*C6*$_{(14aa)}$ does not confer a constitutive signaling phenotype in the absence of *seg1-1*.

Mobilization of trehalose after the addition of 10 mM L-citrulline to nitrogen-starved cells of ∑1278b *gap1*Δ + pFL44L-*GAP1* (●), *npi1-1* + pFL44L-*GAP1* (○), ∑1278b *gap1*Δ + pFL44L-*GAP1*Δ*C6*$_{(14aa)}$ (▲), *npi1-1* + pFL44L-*GAP1*Δ*C6*$_{(14aa)}$ (△), ∑1278b *gap1*Δ + pFL44L (■), and Gap1ΔC6$_{(14aa)}$ + pFL44L (□).

This fits with the previous observations that the *npi1-1* mutation causes a higher expression of *GAP1* at the plasma membrane. Hence, the quicker mobilization of trehalose may be due to the stronger signaling capacity of the overexpressed *GAP1* at the plasma membrane. The mobilization is also more pronounced which may be due to the absence of Gap1 internalization and breakdown at the vacuole.

The fact that the overexpression of *GAP1*Δ*C6*$_{(14aa)}$ failed to mimic the *seg1-1* Gap1ΔC6$_{(14aa)}$ phenotype, suggests that the overaccumulation of Gap1ΔC6$_{(14aa)}$ at the plasma membrane is not (exclusively) responsible for the constitutive signaling. It has to be noted that overexpression studies were performed in strains lacking the

seg1-1 mutation, which in itself is an indication that the background mutation(s) contributes more to the overactive signaling phenotype than merely ensuring the overaccumulation of the truncated Gap1 allele at the plasma membrane.

Chapter III

IDENTIFICATION OF THE BACKGROUND MUTATION REQUIRED FOR CONSTITUTIVE SIGNALING BY TRUNCATED GAP1 ALLELES IN YEAST

3.1. ABSTRACT

We have previously shown that the constitutively high PKA phenotype observed in Gap1ΔC6$_{(14aa)}$ cells depend on both the truncated permease and an unknown background mutation. Here, we show that *seg1-1* mutation is both a single and a recessive mutation. Single-copy suppressor analysis of the mutation identifies a role for the retromer in the constitutively signaling phenotype. We subsequently performed genetic mapping of the mutation and identified a 40 kb region on chromosome VIII most likely linked to the mutation. We focused first on a Golgi-localized v-SNARE, Gos1, which was previously shown to cause clear secretory defects upon disruption. Biochemical analyses of the *gos1*Δ mutant support a role for Gos1 in the overactive signaling phenotype.

3.2. INTRODUCTION

Allelic variation is quite common in different strains and in different individuals in a population. The frequency of genetic variation between common laboratory strains of yeast is believed to be as high as 1% (Nelson et al., 1993). A fundamental challenge in genetics therefore, is to understand how different genetic loci contribute to specific traits. In model organisms such as yeast, genetic interactions are typically identified using reverse genetic approaches, in which different genes are systematically knocked out to create a collection of deletion mutants. Deletion strains are then subjected to various forms of phenotypical characterization, and the outcome of these tests is usually assigned as a (putative) function(s) of the gene product concerned.

Here, we describe the identification of a genomic mutation, dubbed *seg1-1*, present in a specific Σ1278b *gap1*Δ strain, 25.969b (stocked as JT 4505), employed in our studies. The mutation is not present in any other strain tested. The background mutation, in combination with a C-terminally truncated allele of Gap1, Gap1ΔC6$_{(14aa)}$, results in cells that display a constitutively high PKA phenotype, even in the absence of any nitrogen source (Donaton et al., 2003). The high PKA phenotype is independent of the carbon source in the growth medium, and is also observed in the

presence of ammonium as sole nitrogen source. *seg1-1* cells harboring Gap1ΔC6$_{(14aa)}$ typically have a low trehalose and glycogen content and a severely reduced expression of STRE-regulated genes, causing very high stress sensitivity. Amino acid-induced trehalase activation, however, is slightly reduced.

As opposed to Gap1ΔC6$_{(14aa)}$, the Gap1ΔC14$_{(42aa)}$ allele, which has a slightly longer truncation of 42 amino acids, does not cause a high PKA phenotype in the *seg1-1* strain. It is, however, only in the *seg1-1* background that Gap1ΔC14$_{(42aa)}$ reaches the plasma membrane where it functions as a wild-type allele for both transport and signaling; a wild-type *SEG1* strain carrying only Gap1ΔC14$_{(42aa)}$ displays a "*gap1*Δ-phenotype".

In this chapter, we made use of several approaches to identify the gene with the *seg1-1* mutation. First, we utilized Gap1's unique ability to transport toxic D-amino acids as a basis for a suppressor screen in which we tried to identify the *SEG1* gene by complementation of the *seg1-1* mutant. We next employed a novel genetic mapping technology in the screening process, which pointed to a specific v-SNARE protein as a likely candidate for the mutation. We show that the constitutively high PKA phenotype is synergistically dependent on both the Gap1ΔC6$_{(14aa)}$ allele and disruption of the v-SNARE; an attribute reminiscent to that of the *seg1-1* mutation.

3.3. RESULTS AND DISCUSSION

3.3.1. The *seg1-1* mutation is both single and recessive

Having determined that the overactive signaling phenotype of the Gap1ΔC6$_{(14aa)}$-carrying cells depends both on the truncated form of the permease and a background mutation(s), provisionally called *seg1-1*, present in a specific Σ1278b *gap1*Δ strain, we next tested whether the *seg1-1* mutation(s) itself is dominant or recessive. We crossed the *seg1-1* strain with a Σ1278b *gap1*Δ strain lacking the mutation(s) and transformed the resulting heterozygous *seg1-1/SEG1* diploid strain with plasmid-borne copies of either the *GAP1*Δ*C6*$_{(14aa)}$ or *GAP1*Δ*C14*$_{(42aa)}$ allele. As depicted in Figure 3.1A, the phenotypes of the respective diploid strains bear resemblance to that of the haploid strain without the mutation, i.e. *seg1-1* is a recessive mutation.

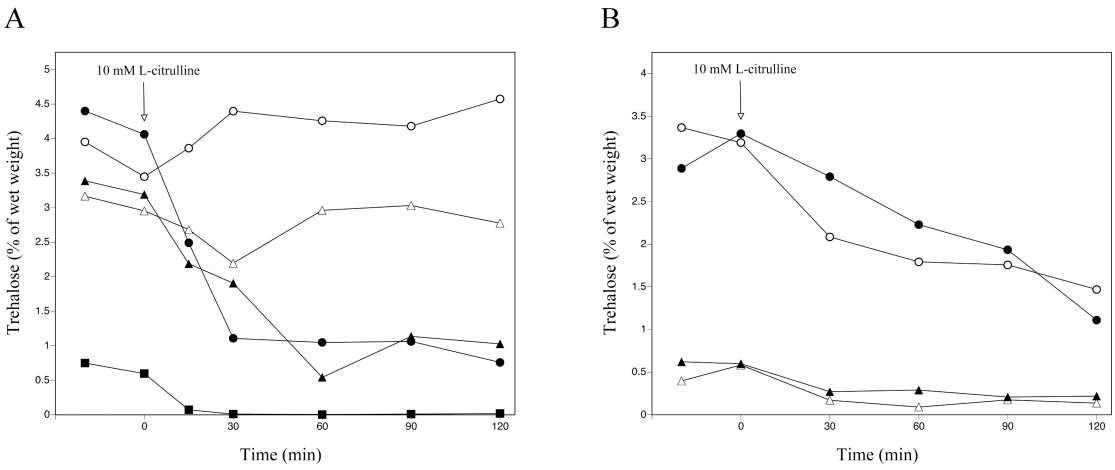

Figure 3.1: The *seg1-1* mutation is a single and recessive mutation.

Mobilization of trehalose after the addition of 10 mM L-citrulline to nitrogen-starved cells. **(A).** Σ1278b wild-type (●), Σ1278b *gap1*Δ (○), *seg1-1*/*SEG1 GAP1*Δ*C6*$_{(14aa)}$ (▲), *seg1-1*/*SEG1 GAP1*Δ*C14*$_{(42aa)}$ (△), and *seg1-1 GAP1*Δ*C6*$_{(14aa)}$ (■). **(B).** *SEG1 GAP1*Δ*C6*$_{(14aa)}$ segregant 1 (●), *SEG1 GAP1*Δ*C6*$_{(14aa)}$ segregant 2 (○), *seg1-1 GAP1*Δ*C6*$_{(14aa)}$ segregant 3 (▲), and *seg1-1 GAP1*Δ*C6*$_{(14aa)}$ segregant 4 (△). A representative experiment is shown.

In addition, the haploid meiotic progeny of the *seg1-1*/*SEG1 GAP1*Δ*C6*$_{(14aa)}$ diploid strain exhibits a segregation ratio of 2:2, with respect to the levels of trehalose accumulated after starvation for nitrogen, suggesting that *seg1-1* is a mutation in a single gene (Figure 3.1B). As the results of this experiment have a considerable bearing on any future strategy for identification of the *SEG1* gene, we confirmed the original results several times with independent meiotic segregants and transformants.

3.3.2. Identification of the cognate gene for *seg1-1*

3.3.2.1. Screening strategy

As *seg1-1* is both a single and recessive mutation, we sought to identify the mutant locus by cloning the cognate gene from a yeast genomic DNA library. Our strategy for the screening process exploited the unique properties of both the Gap1 permease, in general, and the *seg1-1 GAP1*Δ*C14*$_{(42aa)}$ strain specifically. The latter strain contains a transport-competent Gap1 allele and is, as a consequence, inviable on a medium supplemented with toxic D-histidine, an amino acid of which the uptake is solely mediated by Gap1 (Regenberg and Hansen, 2000). Complementing the *seg1-1* mutation with the corresponding wild-type *SEG1* gene would therefore result in a strain lacking a functional Gap1 allele, i.e. a *gap1*Δ mutant, which in turn would allow the latter strain to grow in the presence of D-histidine.

3.3.2.2. Screening results

We transformed the *seg1-1 GAP1*Δ*C14*$_{(42aa)}$ strain with a single-copy yeast genomic library in YCp50, and recovered an estimated 30,000 transformants. The transformants were plated out on minimal L-proline plus D-histidine (MPDHis) medium. The plasmids from viable clones were isolated and the genomic DNA inserts were identified by sequence analysis. We verified that the D-histidine-insensitivity of the viable clones is due to the single-copy plasmids, by counter-selecting for the loss of the *URA3*-based YCp50 plasmid on 5-fluoro-orotic acid (5-FOA) plates (Boeke et al., 1987). The 5-FOA growers, i.e. *ura3* cells lacking the YCp50 library, were

evaluated for growth on MPDHis medium, and were found to be non-viable (results not shown). We also re-introduced the plasmids isolated from the viable clones into the original *seg1-1* *GAP1*Δ*C14*$_{(42aa)}$ strain, which bestowed the same D-histidine-insensitivity on the transformants as witnessed in our screen (results not shown). The genes identified in this screen are listed in Table 3.1.

Table 3.1: Genes identified as single-copy suppressors of the *seg1-1* mutation.

Gene	General function	Description
Erp2	Secretory pathway	Member of the highly-conserved p24 family of proteins that are involved in ER to Golgi transport; localized to COPII vesicles (Marzioch et al., 1999)
Erp4	Secretory pathway	Functionally redundant member of the p24 family of proteins; closely related to Erp2 (Springer et al., 2000)
Vps26	Secretory pathway	Vacuolar protein sorting protein that, together with Vps29, Vps35, Vps5 and Vps17 form a multimeric complex, mainly on vesicular and tubulovesicular membranes. The complex, called the retromer complex, assembles onto the membrane from two distinct subcomplexes, comprising (a) Vps35, Vps29, and Vps26; and (b) Vps5 and Vps17. Essential for endosome-to-Golgi retrograde transport (Seaman et al., 1998)
Vps29	Secretory pathway	Endosomal protein that is a subunit of the retromer complex; essential for endosome-to-Golgi retrograde transport (Reddy and Seaman, 2001)
Vps35	Secretory pathway	Vps35 acts as a "receptor" protein for recognition of the retrieval signals of cargo proteins during their recruitment into retrograde vesicles (Nothwehr et al., 2000)
Stp2	Transcription factor	Stp2 is a transcription factor that binds to specific sequences within the promoters of SPS-regulated amino acid permease genes (Andréasson and Ljungdahl, 2002)
Dia4	Translation initiation	Probable mitochondrial seryl-tRNA synthetase; deletion mutant displays increased invasive and pseudohyphal growth (Arnez and Moras, 1997)
Caj1	Protein folding and chaperone activity	A type II heat shock protein of the bacterial dnaJ family, which facilitates the molecular chaperone Hsp70's interaction with polypeptide substrates (Walsh et al., 2004)

The most abundant class of proteins we isolated as potential wild-type counterparts of the *seg1-1* mutation, all function within the early secretory pathway, i.e. transport between the ER and the Golgi apparatus, or *vice versa*. The Vps26, Vps29 and Vps35 proteins, for example, constitute the cargo-selection subcomplex of the retromer complex; the latter being a conserved cytoplasmic coat that functions in endosome-to-Golgi retrieval. Loss of the retromer function results in a protein

missorting defect to the vacuole, and subsequent mislocalization of the vacuolar hydrolase carboxypepetidase Y to the plasma membrane (Seaman, 2004; Gokool et al., 2007).

The Erp2 and Erp4 (for Emp24- and Erv25-related proteins) proteins are the founding members of the evolutionary-conserved p24 family of proteins. This family of transmembrane proteins has been suggested to limit the entry of specifically unfolded proteins into COPII vesicles. Given their ability to strongly interact with the COPII coat proteins, p24 complexes may act as 'placeholders' to prevent other proteins with a lower affinity to COPII proteins from entering COPII vesicles. Cargo proteins that efficiently interact with COPII components could then displace p24 complexes from COPII budding sites, and as such secure a space for themselves in a COPII vesicle (see "Chapter I", section 1.4.2.). A similar mechanism is proposed to act in the COPI-dependent, endosome-to-Golgi retrieval pathway (Springer et al., 2000; Caldwell et al., 2001).

In addition to the single-copy suppressor screen, we also performed a multi-copy suppressor analysis that functioned on the same principle as the single-copy screen (see section 3.3.2.1.). We isolated 26 suppressors, which represented 11 different genes (Table 3.2).

Table 3.2: Genes identified as multi-copy suppressors of the *seg1-1* mutation.

Gene	General function	Description
Isolated 13 times		
Put4	Amino acid transport	Proline permease required for high-affinity transport of proline; also transports the toxic proline analog azetidine-2-carboxylate (AzC); *PUT4* transcription is repressed in ammonia-grown cells (Andréasson et al., 2004)
Isolated 4 times		
Stp2	Transcription factor	Stp2 is a transcription factor that binds to specific sequences within the promoters of SPS-regulated amino acid permease genes (Andréasson and Ljungdahl, 2002)

Isolated once		
Gcd14	Translation/transcription	One of the subunits of tRNA methyltransferase, and is required for the modification of the adenine at position 58 in tRNAs, especially tRNAi-Met; was first identified as a negative regulator of *GCN4* expression (Cuesta et al., 1998)
Agp1	Amino acid transport	Low-affinity amino acid permease with broad substrate range; involved in uptake of most uncharged amino acids, including asparagine, glutamine and leucine; expression is under control of the SPS amino acid sensor system (Abdel-Sater et al., 2004)
Bdf1	Transcription factor	*BDF1* encodes a bromodomain-containing transcription factor involved in transcription initiation at TATA-containing promoters; corresponds to the C-terminal region of mammalian TAF1 (Liu et al., 2009)
Kar4	Transcription factor	Putative transcription factor required for the induction of *CIK1* and *KAR3* during mating and meiosis, and for the efficient transit from the G_1 phase during mitosis (Lahav et al., 2006)
Hsp82	Protein folding and chaperone activity	Hsp90 molecular chaperone required for pheromone signaling and negative regulation of Hsf1; chaperone activity of Hsp82 is unique in that it acts on partially folded proteins that are recruited by the sequential activity of Hsp40 and Hsp70 (Tapia and Morano, 2010)
Exo84	Exocyst	Essential protein which mediates polarized targeting of secretory vesicles to active sites of exocytosis; specifically localizes to the bud tip or the mother/daughter connection (Guo et al., 1999)
Ssb2	Translation	Ribosome-associated chaperone that may be involved in the folding of newly-synthesized polypeptide chains; member of Hsp70 family associated with ribosomes (Pfund et al., 1998)
Sec16 (N-term.)	Secretion	COPII vesicle coat protein required for ER transport vesicle formation and physically interacts with all of the COPII components, except Sec13; deletion of *SEC16* blocks ER to Golgi transport (Connerly et al., 2005)
Mth1 (N-term.)	Other	Negative regulator of the glucose-sensing signal transduction pathway, required for repression of transcription by Rgt1; interacts with both the Snf3 and Rgt2 glucose sensors; phosphorylated by Yck1 (Lakshmanan et al., 2003)

Remarkably, this set of suppressor clones was comprised of mainly two distinct clusters of genes: one group of genes that codes for amino acid permeases (e.g. the proline permease-encoding *PUT4* and the low-affinity amino acid permease-encoding *AGP1*), and another that includes transcription factors specific for the expression of

amino acid permease genes, like Stp2 and the Gcn4-specific regulator Gcd14. It is important to note that only amino acid permeases, and no other nutrient carriers, were isolated as multi-copy suppressors of the *seg1-1* mutation. Based on this observation, it is tempting to hypothesize that *seg1-1* specifically modulates the ER-to-Golgi transit of amino acid transporters. Moreover, overexpression of the amino acid transporters apparently strengthens the ER quality control system (and/or saturates the recruitment of the secreted proteins into the COPII transport vesicles) in such a manner that the Gap1ΔC14$_{(42aa)}$ allele apparently no longer is able to reach the plasma membrane.

3.3.2.3. Is one of the single-copy suppressors *SEG1*?

To determine whether one of the single-copy suppressors is the *SEG1* gene, we mated a Σ1278b *gap1*Δ strain with the corresponding deletion mutants in the genes we picked up as suppressors. After sporulation and tetrad analysis, the appropriate haploid double deletion strains were transformed with the plasmid-borne Gap1ΔC6$_{(14aa)}$ allele, and the resulting mutants were monitored for L-citrulline-induced mobilization of trehalose.

However, contrary to expectation, none of the deletions had any impact on the PKA phenotype of the respective mutant strains, as evident from the high levels of trehalose accumulated by the various strains during nitrogen starvation (Figure 3.2). It therefore appears that none of the single-copy suppressor genes, as listed in Table 3.1, is actually identical to the *SEG1* gene. The remaining explanation that the point mutant would give a different phenotype compared to the deletion mutant appears unlikely, because of the recessive character of the *seg1-1* mutation. Hence, *seg1-1* is probably a (partial) inactivation mutation.

Although not relevant to our study, it is interesting to note that the *vps29*Δ mutant displays a "*gap1*Δ-phenotype", despite carrying a copy of the truncated permease. This may be in part due to a defect in retromer-dependent trafficking (Seaman, 2008).

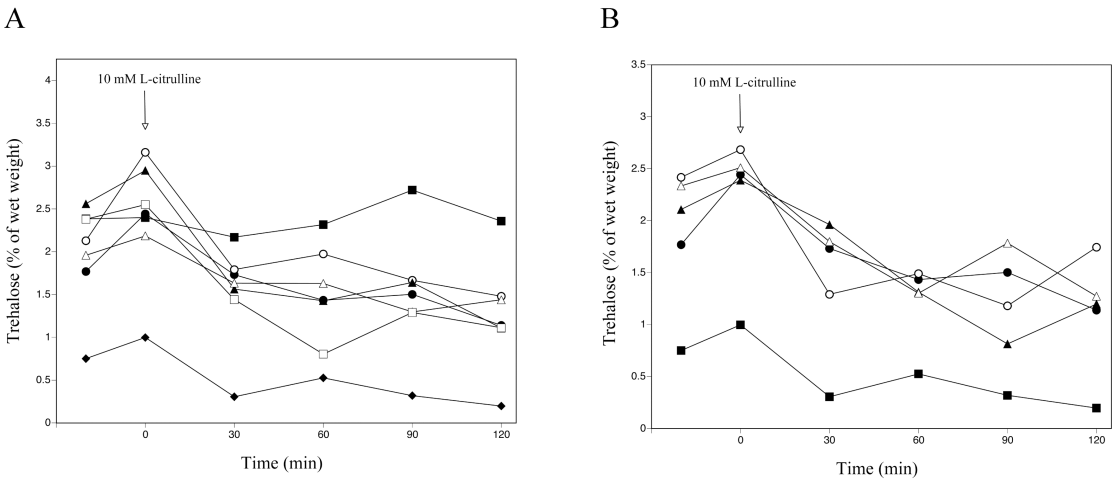

Figure 3.2: None of the deletion strains in the single-copy suppressors could support the high PKA phenotype caused by Gap1ΔC6$_{(14aa)}$ in the *seg1-1* mutant.
Mobilization of trehalose after the addition of 10 mM L-citrulline to nitrogen-starved cells. **(A).** Σ1278b *gap1*Δ + pFL38-*GAP1*Δ*C6*$_{(14aa)}$ (●), *erp2*Δ + pFL38-*GAP1*Δ*C6*$_{(14aa)}$ (○), *erp4*Δ + pFL38-*GAP1*Δ*C6*$_{(14aa)}$ (▲), *vps26*Δ + pFL38-*GAP1*Δ*C6*$_{(14aa)}$ (△), *vps29*Δ + pFL38-*GAP1*Δ*C6*$_{(14aa)}$ (■), *vps35*Δ + pFL38-*GAP1*Δ*C6*$_{(14aa)}$ (□), and *seg1-1* + pFL38-*GAP1*Δ*C6*$_{(14aa)}$ (◆). **(B).** Σ1278b *gap1*Δ + pFL38-*GAP1*Δ*C6*$_{(14aa)}$ (●), *stp2*Δ + pFL38-*GAP1*Δ*C6*$_{(14aa)}$ (○), *dia4*Δ + pFL38-*GAP1*Δ*C6*$_{(14aa)}$ (▲), *caj1*Δ + pFL38-*GAP1*Δ*C6*$_{(14aa)}$ (△), and *seg1-1* + pFL38-*GAP1*Δ*C6*$_{(14aa)}$ (■).

Albeit a major advantage as a genetic system, identifying a mutant locus in yeast by cloning the cognate gene from a plasmid library may sometimes prove difficult. A gene may, for example, be underrepresented in a library or toxic in *E. coli*, gene dosage effects may result in unexpected phenotypes, or false positives may be more easily recovered than the gene of interest (Agnan et al., 1997; Wiatrowski and Carlson, 2001). However, the advent of new technologies, like genome-wide mapping and single nucleotide polymorphism (SNP) genotyping, and its application in the identification of mutant loci by linkage analysis, has circumvented many of the above-mentioned problems associated with the conventional cloning system.

Here we describe a novel, alternative approach, named 'Artificial Marker Track Exclusion Mapping' (AMTEM), with which we proceeded for the identification of the mutation.

3.3.3. Identifying the genomic locus of *seg1-1* using AMTEM

3.3.3.1. Screening strategy

The AMTEM technology was developed in our laboratory, and makes use of a standard artificially-marked yeast strain (AMS; S288c genetic background) that contains approximately 600 different markers in its genome. The artificial markers are specific 20 bp oligonucleotides introduced at predefined, neutral (intergenic) positions in the genome, at a distance of roughly 20 kb from one another. They cover the whole yeast genome genetically. Mapping is performed by crossing the AMS with any other strain displaying a trait of interest; in our case the high PKA phenotype caused by the *seg1-1* mutation in a strain expressing *GAP1*Δ*C6*$_{(14aa)}$ or the D-histidine sensitivity caused by *seg1-1* in a strain expressing *GAP1*Δ*C14*$_{(42aa)}$. The segregants of this cross are phenotyped and those with the desired trait are selected. About 20 of these segregants are pooled, their genomic DNA extracted and the artificial markers are scored using a custom-made micro-array carrying oligonucleotides that match the artificial markers (Figure 3.3).

Because all loci that are required for the trait of interest in the segregants, have to originate from the unmarked parent strain carrying the desired trait, the positions of these loci are indicated by the different gaps in the track of markers. Moreover, due to crossing-over events in the mapped locus (at a rate of about 1 in every 12 segregants), the markers are not necessarily completely absent but may have a strongly reduced signal intensity. This is true for genetic elements that are essential for the trait of interest. When they are only important, and not truly essential, the markers will be reduced in intensity to some extent depending on the importance of the genetic element. When the markers are scored in the individual segregants, loci that are not linked with the trait of interest will show about 50% marker presence, whereas in the loci linked to the desired trait the presence of the marker drops well below 50% - the lower the percentage, the stronger the linkage with the trait of interest.

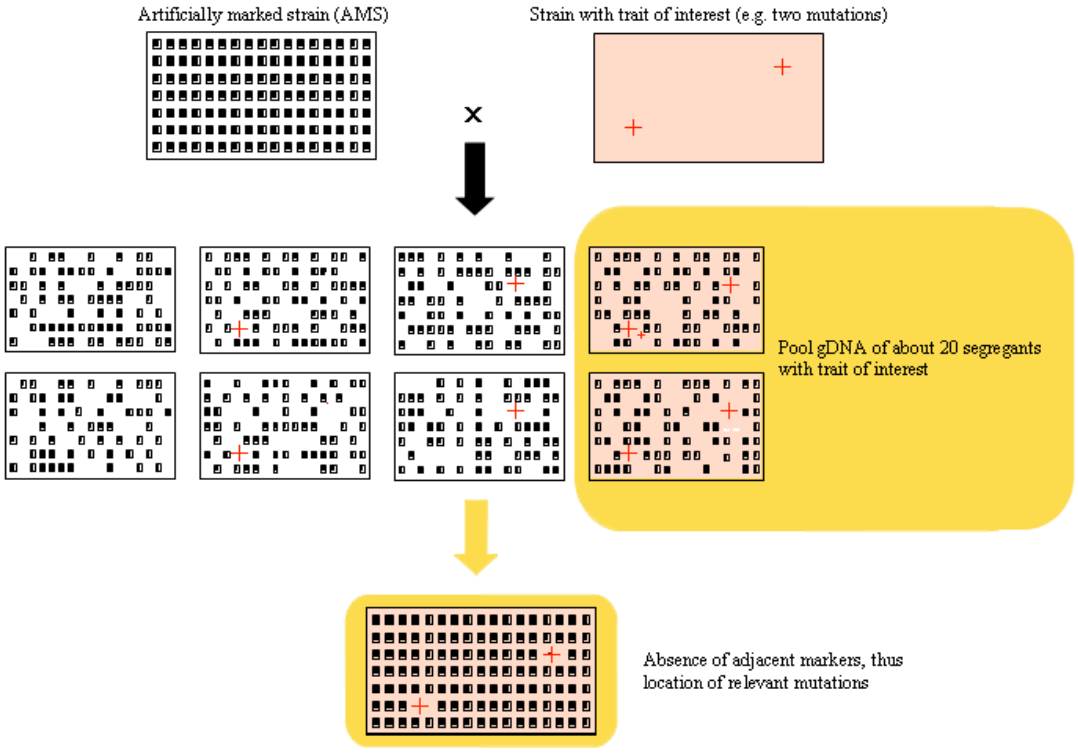

Figure 3.3: Schematic depiction of the principle of the AMTEM technology.

Black squares represent the markers detected by micro-array; red crosses denote the mutations responsible for the trait of interest; pink-filled squares constitute the trait of interest. Meiotic segregants of a cross between the AMS and a strain of interest each contain approximately 50% of the markers. About 20 segregants with the desired phenotype are selected and their genomic DNA pooled. In a pool of 20 segregants, all unlinked markers are detected, while the markers adjacent to the genetic element(s) required for the trait of interest are either absent or have very low signal intensity. Hence, the gap(s) in the marker track will indicate the genomic location of the responsible mutation(s). The very low signal intensity can be due to the presence of interval recombinants (strains with a crossing-over in the mapped locus between the mutation and the adjacent marker). As there are approximately 50 crossing-overs in one meiotic event and there are 600 markers in the genome, the mean frequency of interval recombinants between two markers is roughly 1 in 12.

During the course of this study, the completely marked strain was not available yet, which meant that we had to cross with several AMS strains covering most of the genome genetically. The first strain we used had 61 markers.

3.3.3.2. Screening results

We crossed the *seg1-1* mutant strain with an AMS containing 61 markers, and subjected the diploid to tetrad analysis. We transformed the meiotic progeny with a plasmid-borne copy of the *GAP1*Δ*C6*$_{(14aa)}$ allele, and measured the amount of trehalose accumulated by each transformed segregant after nitrogen starvation. We isolated 11 segregants that displayed the high-PKA phenotype, i.e. low levels of trehalose. The genomic DNA from these strains was isolated, pooled and used in our marker-detection micro-array (see "Materials and Methods", section 6.2.7.). Segregants that displayed the wild-type PKA phenotype, i.e. high levels of trehalose, were included as control.

Application of the marker-detection methodology resulted in negative signals for three adjacent markers (no. 249 – 251). They were absent in the genomic DNA of all 11 low-trehalose segregants. In contrast, all of the markers were present in the genomic DNA of the high-trehalose segregants selected. We confirmed the micro-array data by scoring the presence, or absence, of each marker in each individual low-trehalose segregant. We employed a standard PCR protocol in the process, in which we used the specific marker as one primer, and an appropriate downstream sequence of the same length as the second primer. The PCR confirmation results are shown in Table 3.3.

Table 3.3: Confirmation of the micro-array data by marker-specific PCR detection.
The "+" sign denotes the presence of a marker, whereas a "-" sign indicates its absence.

Chromosome VIII	Marker 249	Marker 250	Marker 251
Low-trehalose segregant 1	-	-	+
2	-	-	-
3	+	-	-
4	-	-	-
5	-	-	-
6	-	-	-
7	-	-	-

8	-	-	-
9	+	-	+
10	-	-	-
11	+	-	-
PCR controls			
Marker strain	+	+	+
S288c wild-type (unmarked)	-	-	-

The area covered by markers 249 to 251 comprises of a 40 kb region between bp 18,226 and 58,935 near the beginning of chromosome VIII. The probability (*P* value) of this region being relevant to the *seg1-1* phenotype was calculated at 4.338×10^{-4} (see "Materials and Methods", section 6.2.8.). Given that the mathematical cut-off for the significance of a specific gene or chromosomal region contributing to a phenotype, has been specified at 0.005, our data suggest a high true-positive-to-false discovery ratio, i.e. there is a very good mathematical probability that the *seg1-1* mutation is contained within the 40 kb region (Steinmetz et al., 2002; Segrè et al., 2006). Table 3.4 lists all the genes of chromosome VIII within this specific region.

Table 3.4: Genes within the 18,226 to 58,935 bp region of chromosome VIII.

Gene	General function	Description
Arn1	Transport	Member of the ARN family of transporters that specifically recognize siderophore-iron chelates (Heymann et al., 2000)
Yhl039w	Unknown	Putative protein of unknown function; localizes to the cytoplasm
Cbp2	Transcription	Mitochondrial protein required for splicing of the group I intron aI5 of the COB pre-mRNA by binding to the RNA to promote its splicing (Tirupati et al., 1999)
Yhl037c	Unknown	Dubious open reading frame unlikely to encode a functional protein
Mup3	Transport	Low-affinity methionine permease, similar to Mup1 (Menant et al., 2006)
Vmr1	Transport	Member of the ATP-binding cassette (ABC) superfamily of multi-drug transporters (Paumi et al., 2009)
Yhl034w-a	Unknown	Dubious open reading frame unlikely to encode a functional protein

Sbp1	Translation	Putative RNA binding protein involved in translational repression (Segal et al., 2006)
Rpl8a	Translation	Ribosomal protein L4 of the large (60S) ribosomal subunit; mutation results in decreased amounts of free 60S subunits (Zhao et al., 2006)
Gut1	Glycerol utilization	Glycerol kinase that converts glycerol to glycerol-3-phosphate; glucose repression of expression is mediated by Adr1 and Ino2-Ino4 (Grauslund et al., 1999)
Yhl030w-a	Unknown	Dubious open reading frame unlikely to encode a functional protein
Gos1	Secretion pathway (ER-Golgi and intra-Golgi)	v-SNARE protein localized to the Golgi compartment and likely homolog of the mammalian protein GOS-28/GS28; may play a role in multiple transport steps (McNew et al., 1998)
Ecm29	Proteasome function	Major component of the proteasome; tethers the proteasome core particle to the regulatory particle, and enhances the stability of the proteasome (Leggett et al., 2002)
Oca5	Unknown	Cytoplasmic protein required for replication of the Brome mosaic virus in S. cerevisiae (Kushner et al., 2003)
Wsc4	Cell wall integrity / protein targeting to ER	ER-localized protein involved in the translocation of soluble secretory proteins and insertion of membrane proteins into the ER membrane; may also have a role in the stress response (Zu et al., 2001)
Rim101	Cell wall biogenesis	Transcriptional repressor involved in response to pH and in cell wall construction; required for alkaline pH-stimulated haploid invasive growth and sporulation, and is activated by proteolytic processing (Castrejon et al., 2006)
Yhl026c	Unknown	Putative protein of unknown function
Snf6	Chromatin remodeling	Subunit of the SWI/SNF chromatin remodeling complex involved in transcriptional regulation (Smith et al., 2003)
Rim4	Meiosis	Putative RNA-binding protein required for the expression of early and middle sporulation genes (Deng and Saunders, 2001)

Based on our previous data (see "Chapter II"), we focused our study first on the two candidate genes functioning within the yeast's secretion pathway, namely the v-SNARE *GOS1* and the ER membrane protein *WSC4*. Gos1 has been localized primarily to the Golgi complex and likely participates in ER-Golgi and / or intra-Golgi transport. It is thus not surprising then that the deletion of *GOS1* causes clear secretory defects. The ER chaperone, Kar2 (see "Chapter I", section 1.4.1.), is secreted five-fold more in *gos1*Δ mutants than in wild-type cells, indicative of the ER-retention defective (*erd*) phenotype that *gos1*Δ cells suffer from. It was also reported that the proteolytic processing of carboxypeptidase Y (CPY) significantly

decreased in *gos1*Δ mutants, such that both the p1CPY and p2CPY precursors accumulated in these cells (McNew et al., 1998). Moreover, during the course of this study, Gos1 was identified in a split-ubiquitin screen as an interacting partner of wild-type Gap1 (Griet Van Zeebroeck, personal communication).

Wsc4, on the other hand, is an essential component of the signal recognition particle (srp) - dependent translocation of secretory proteins through, or into, the ER. Deletion of *WSC4* causes significant defects in the translocation of both soluble and membrane secretory proteins, resulting in the accumulation of pre-CPY, prepro-α-factor, preinvertase as well as the integral membrane protein dipeptidyl-aminopeptidase B (Mamoun et al., 1999). The role of Wsc4 in the yeast cell's response to environmental stress, however, is far less clear, with earlier data suggesting that the function of Wsc4 may partially overlap with that of the other *WSC* family members (Zu et al., 2001).

3.3.4. Is *GOS1* or *WSC4* identical to *SEG1*?

We next sought to test whether the *GOS1* or the *WSC4* genes could be identical to *SEG1*. We deleted *GOS1*, or *WSC4*, in a Σ1278b *gap1*Δ strain, transformed the double deletion mutant with plasmid-borne Gap1ΔC6$_{(14aa)}$, and determined the trehalose levels in the respective strains when starved for nitrogen (Figures 3.4A and B, respectively). In contrast to the *GOS1* wild-type strain, trehalose levels in the *gos1*Δ mutant were significantly reduced. Initial trehalose levels in the deletion strain were in fact very similar to that of the *seg1-1* Gap1ΔC6$_{(14aa)}$ mutant, suggesting that *GOS1* may be identical to *SEG1*. Additional trehalose experiments with independent transformants confirmed the original result, which justified taking a closer look at *GOS1* as the potential wild-type counterpart of *seg1-1*.

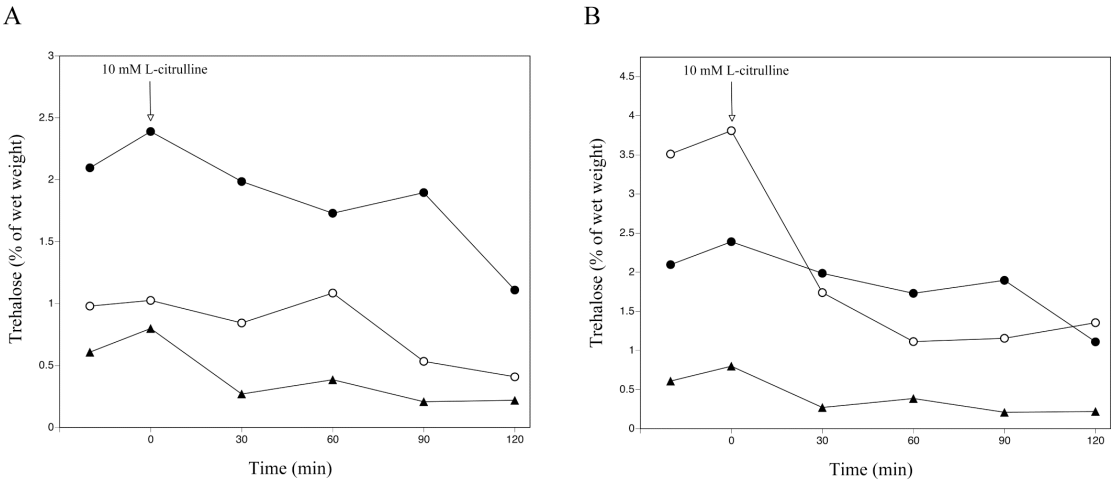

Figure 3.4: Deletion of *GOS1* in a strain expressing *GAP1ΔC6*$_{(14aa)}$ results in a low trehalose level.

Mobilization of trehalose after the addition of 10 mM L-citrulline to nitrogen-starved cells. **(A).** Σ1278b *gap1*Δ + pFL38-*GAP1ΔC6*$_{(14aa)}$ (●), Σ1278b *gap1*Δ *gos1*Δ + pFL38-*GAP1ΔC6*$_{(14aa)}$ (○), and *seg1-1* + pFL38-*GAP1ΔC6*$_{(14aa)}$ (▲). **(B).** Σ1278b *gap1*Δ + pFL38-*GAP1ΔC6*$_{(14aa)}$ (●), Σ1278b *gap1*Δ *wsc4*Δ + pFL38-*GAP1ΔC6*$_{(14aa)}$ (○), and *seg1-1* + pFL38-*GAP1ΔC6*$_{(14aa)}$ (▲).

Contrary to the *gos1*Δ results, the disruption of *WSC4* did not result in a high PKA phenotype. The trehalose levels in the *wsc4*Δ strain expressing *GAP1*Δ*C6*$_{(14aa)}$ was even higher than in the *WSC4* wild-type strain carrying Gap1ΔC6$_{(14aa)}$ (Figure 3.4B). This actually suggests a further decrease in PKA activity in *wsc4*Δ cells, and is as such not relevant to our study. The remainder of this particular study therefore focuses on understanding the role of Gos1 in the overactive signaling phenotype of the *seg1-1* mutant.

3.3.4.1. Deletion of *GOS1* in combination with Gap1ΔC6$_{(14aa)}$ mimics the overactive phenotype

We also mated the *gos1*Δ Gap1ΔC6$_{(14aa)}$ strain with the *seg1-1* Gap1ΔC6$_{(14aa)}$ mutant and measured trehalose mobilization in the diploid after starvation for nitrogen (Figure 3.5).

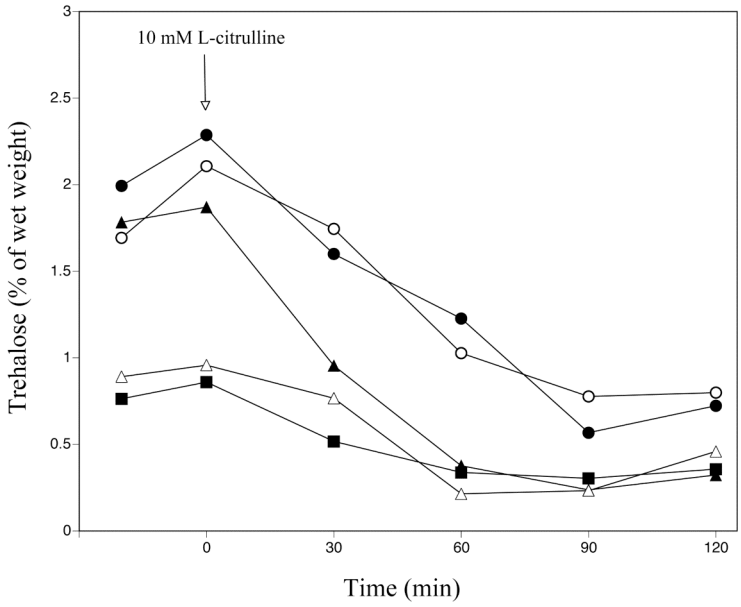

Figure 3.5: The *seg1-1*/*gos1*Δ diploid displays phenotypes identical to the *seg1-1*/*seg1-1* diploid strain.

Mobilization of trehalose after the addition of 10 mM L-citrulline to nitrogen-starved cells of the *seg1-1*/*seg1-1* diploid + pFL38-*GAP1* (●), Σ1278b *gap1*Δ + pFL38-*GAP1*Δ*C6*$_{(14aa)}$ (○), *seg1-1*/*gos1*Δ diploid + pFL38-*GAP1* (▲), *seg1-1*/*gos1*Δ diploid + pFL38-*GAP1*Δ*C6*$_{(14aa)}$ (△), and *seg1-1*/*seg1-1* diploid + pFL38-*GAP1*Δ*C6*$_{(14aa)}$ (■).

We included a *seg1-1*/*gos1*Δ diploid strain carrying a plasmid-borne wild-type copy of Gap1 as control. Similar to the individual haploid stains, the *seg1-1*/*gos1*Δ Gap1ΔC6$_{(14aa)}$ diploid displayed the characteristically low levels of trehalose that has become the hallmark of the overactive PKA phenotype. More importantly, the *seg1-1*/*gos1*Δ diploid harboring the plasmid-borne Gap1 exhibited trehalose levels identical to that of the *seg1-1* homozygous diploid carrying wild-type Gap1. This suggests that, analogous to the *seg1-1* mutant strain, the high PKA phenotype of a *gos1*Δ strain is only observed in combination with the Gap1ΔC6$_{(14aa)}$ allele.

This is an important finding since it corroborates the synergistic nature of the overactive phenotype – both the background mutation and Gap1 truncated allele is required for the constitutive signaling phenotype (see "Chapter II", section 2.3.3.).

These results also show that the *gos1*Δ and *seg1-1* mutations do not complement each other, which strongly suggests that *GOS1* and *SEG1* is the same gene.

We confirmed the mobilization data by sporulating the respective diploid strains and measuring the accumulation of trehalose in all four of the meiotic progeny (Figure 3.6).

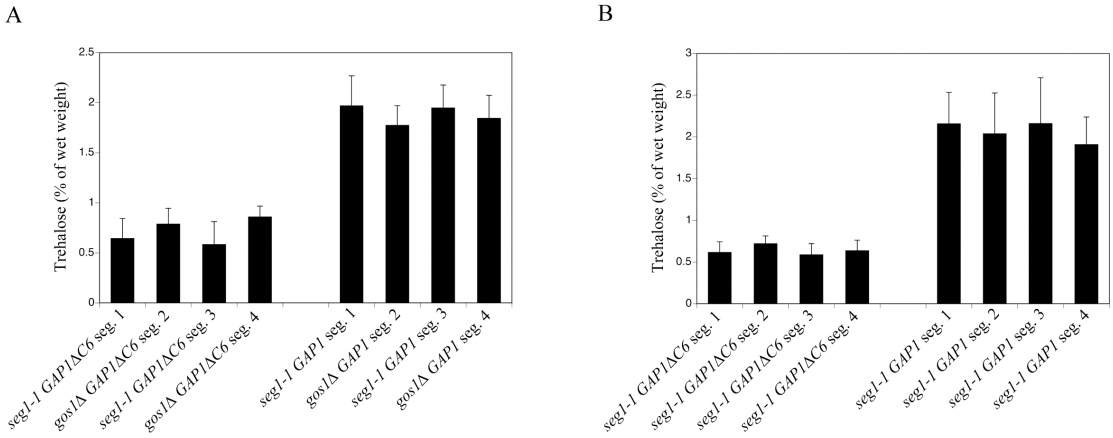

Figure 3.6: Trehalose levels of the individual segregants confirm the original mobilization data.

Trehalose levels as accumulated by the haploid meiotic progeny of the respective strains when starved overnight for nitrogen on a glucose-containing medium.

Consistent with the data on trehalose mobilization, the *gos1*Δ Gap1ΔC6$_{(14aa)}$ segregants (as confirmed by PCR analysis) accumulated very little trehalose during the starvation period. The *gos1*Δ Gap1 segregants, on the other hand, accumulated wild-type levels of the storage carbohydrate, which essentially underscores our earlier findings. Taken together, these data provide a strong argument for *GOS1* being the wild-type equivalent of the *seg1-1* mutation.

3.3.4.2. Sequence analysis of the *GOS1* ORF, promoter and terminator regions in the *seg1-1* background does not reveal any mutation

Because the previous results strongly suggested that *GOS1* was identical to *SEG1*, we searched for the presence of mutations in the *GOS1* ORF, promoter and terminator in the *seg1-1* background. We sequenced the 672 bp *GOS1* ORF, and about 1,000 bp

upstream and downstream thereof, in both the *seg1-1* and Σ1278b wild-type parental strain. We employed the conventional dideoxynucleotide PCR-based method, and compared the sequence data to that of the S288c reference strain (*Saccharomyces* Genome Database; http://www.yeastgenome.org). However, to our surprise, no loss-of-function (missense, frameshift, or nonsense) mutations were detected in the *GOS1* coding sequence, promoter or terminator regions originating from the *seg1-1* mutant; the sequence data of all three strains were in complete agreement. This is practically in contrast to our previous data suggesting that *GOS1* is identical to *SEG1*.

We argued that the expression of *GOS1* in the *seg1-1* background may be severely compromised, to the extent that the *seg1-1* strain symbolizes a "*gos1*Δ" strain, i.e. a strain lacking functional Gos1 protein. This seems reasonable, as several recent studies have shown that sequence variation, i.e. polymorphism, in DNA sequences upstream and downstream of coding sequences have profound effects on gene expression and, as a result, on phenotype (Yvert et al., 2003; Wang et al., 2007). Ronald and colleagues (2005) for example found that up to a quarter of all yeast genes are affected by polymorphisms in both their promoter regions and upstream transcription factor binding sites. Similar findings in mouse suggest that polymorphic variation is probably an evolutionary conserved phenomenon (Doss et al., 2005).

To test our hypothesis, we determined by real-time quantitative PCR (qPCR) the expression levels of *GOS1* mRNA in nitrogen-starved, *seg1-1* Gap1ΔC6$_{(14aa)}$ cells, including relevant control strains for this experiment (Figure 3.7).

However, contrary to expectation, the expression of *GOS1* mRNA in the *seg1-1* Gap1ΔC6$_{(14aa)}$ strain increased significantly, compared to the mutant carrying wild-type Gap1. This discrepancy in expression can only be attributed to the Gap1ΔC6$_{(14aa)}$ allele, although the exact mechanism by which the truncated permease could influence the expression of the v-SNARE is not clear. Important to note is that the mRNA levels do not necessarily equate to the amount of Gos1 protein found in the *seg1-1* Gap1ΔC6$_{(14aa)}$ strain. Translational efficiency, i.e. *GOS1* mRNA to Gos1 protein, should therefore be determined by western analysis.

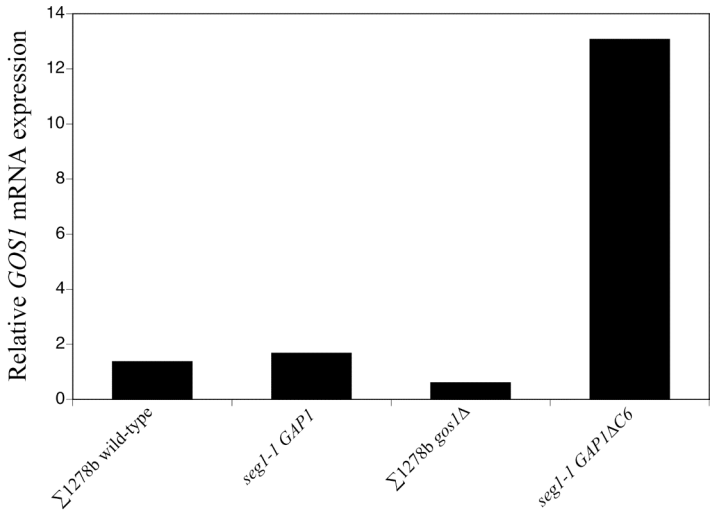

Figure 3.7: The Gap1ΔC6$_{(14aa)}$ allele causes a dramatic increase in *GOS1* mRNA levels.
Relative expression of *GOS1* mRNA in the individual strains after overnight starvation for nitrogen. Expression of *18S* mRNA was used for normalization. Cells were grown to mid-exponential phase before their transfer to nitrogen-starvation medium supplemented with 4% glucose.

If the level of Gos1 protein is also strongly elevated, we have to conclude that both the disruption and overexpression of *GOS1* support the overactive Gap1 allele, or at least that both are correlated with the overactive effect. This may be possible as the overexpression of *GOS1* may also disrupt its normal interaction with the t-SNARE proteins (see "Chapter I", section 1.4.3.).

3.3.4.3. Sequence analysis of the regions around *GOS1* identifies a polymorphism in the *ECM29* gene of the *seg1-1* strain

We proceeded by sequencing 20 kb upstream and downstream of the *GOS1* ORF, thereby covering the whole locus previously identified by genetic mapping. We employed the recently developed Illumina GAII^{TM} Next-Generation sequencing technology (Cofactor Genomics, St. Louis, MO) in the process, and recovered 227 potential SNPs in total for the 40 kb sequenced region. However, analysis of the raw data indicated that most (approximately 200) were actually sequencing errors, and that of the remaining SNPs, only one exhibited a very high 'confidence rate'. Table 3.5 summarizes this result.

Table 3.5: A high confidence filtered list of the total SNPs.

The most important values for defining a high 'confidence rate' of SNP candidates are those of the Total Count, Count Ratio and the Quality Base. In a 20× coverage sequencing project, like ours, one would expect a minimum coverage of 3×, a Count Ratio of 0.4, and a Quality Base value of at least 30.

Reference Sequence ID	Pos.[a]	Base[b]	Base Count[c]	Total Count[d]	Count Ratio[e]	Qual. Base[f]	Qual. Total[g]	Qual. Ratio[h]
NODE 71 length 115 bp coverage 3.7	19	G	3	3	1	180	180	1

[a]position of the SNP / insertion/deletion (indel) in the reference sequence; [b]base or indel observed at this position; [c]number of times this polymorphism is observed; [d]coverage at this base, counting all matches and mismatches; [e](polymorphism count) / (total count); [f]sum of qualities for this polymorphism; [g]sum of qualities for ALL bases at this position; [h](polymorphism quality value sum) / (total quality value sum at this position)

The SNP is located within the *ECM29* ORF, with *ECM29* being the next gene on the chromosome but on the opposite strand, i.e. the Watson strand, to *GOS1* (Figure 3.8). The nucleotide at bp 5524, an adenine in both the S288c and the Σ1278b wild-type strains, is changed to a guanine in the *seg1-1* mutant. This leads to an amino acid change where the amino acid residue at position 1842, an asparagine (N), is substituted for aspartic acid (D).

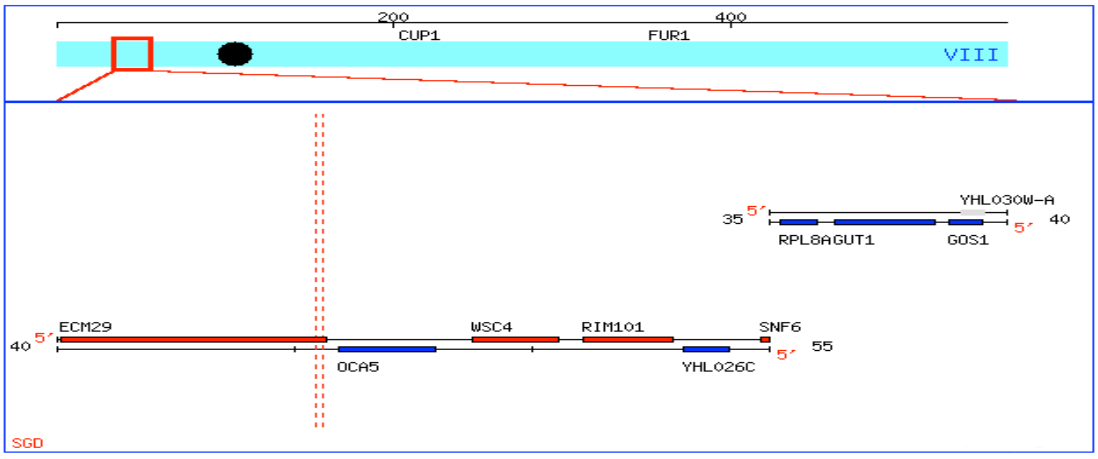

Figure 3.8: The SNP is located within the *ECM29* ORF of the *seg1-1* strain.

Chromosome VIII features that span coordinates bp 35,000 to 55,000. The specified map is indicated by the region between the two vertical red dashed lines (coordinates bp 45,479 to bp 45,593).

The role that Ecm29 may play in the overactive signaling phenotype is not clear yet, and requires further investigation. First, the point mutation identified has to be introduced into a wild-type strain expressing *GAP1*Δ*C6*$_{(14aa)}$, to evaluate whether it truly is the same as the *seg1-1* mutation that supports the high PKA phenotype. In addition, it should be investigated whether *ecm29*Δ also supports the high PKA phenotype and whether *gos1*Δ affects the expression of *ECM29*.

Ecm29 enhances the stability of the proteasome by tethering the organelle's core catalytic particle to its regulatory particle, which in turn stimulates the *in vivo* activity of the proteasome's de-ubiquitinating enzyme, Ubp6. Curiously, the inactivation of *UBP6* causes a two-fold reduction in the internalization of Gap1 present at the plasma membrane (Nikko and André, 2007a). The internalization of Gap1 in *ubp6*Δ mutants relies on the regular Gap1 ubiquitination, thus ubiquitination of lysine^{9} and lysine^{16}. The function of Ecm29 may also explain the secretion of the truncated Gap1ΔC14$_{(42aa)}$ protein and the oversecretion of Gap1ΔC6$_{(14aa)}$ to the plasma membrane in the *seg1-1* mutant, since the proteasome is involved in the degradation of incorrect ER-produced proteins that do not pass the organelle's quality control system (see "Chapter II", section 2.3.3.)

We are also considering the possibility that a polymorphism in one gene, e.g. *ECM29*, can affect the expression of the *GOS1* gene. Such *trans*-regulatory variation is known to affect the timing, level, or activity of the transcription factors or other regulators that control the expression of specific genes. The question that begs an answer, though, is what role the Gap1ΔC6$_{(14aa)}$ allele plays in the regulation of *GOS1* expression in the *ecm29*Δ mutant, since the increased expression of *GOS1* is only observed in a *seg1-1* strain carrying Gap1ΔC6$_{(14aa)}$. It would be interesting to also check whether the Gap1ΔC14$_{(42aa)}$ allele, which does not cause a high PKA phenotype, also causes elevated expression of *GOS1*.

Finally, it remains unclear why the *gos1*Δ mutation fails to complement the *seg1-1* mutation if *seg1-1* is the same as the *ecm29*^{N1842D} mutation. A *gos1*Δ strain should have a wild-type *ECM29* gene that should complement the *ecm29*^{N1842D} mutation if it is *seg1-1*, since we showed that *seg1-1* is a recessive mutation. In addition, the *seg1-1*

mutant should have a wild-type *GOS1* gene that in principle should be able to complement the *gos1*Δ mutation.

Chapter IV

GLUCOSE-INDUCED ACTIVATION OF PROTEIN PHOSPHATASES PP2A AND PP1 IN YEAST

4.1. ABSTRACT

Reversible protein phosphorylation regulates practically every signaling pathway in the eukaryotic cell. Here, we reveal that both protein phosphatases PP2A and PP1 are under direct control of glucose sensing. We show that glucose addition to glucose-deprived yeast cells triggers rapid activation of both PP2A and PP1 phosphatase activity. The glucose-induced activation of PP2A requires the catalytic subunits Pph21 and Pph22. Of the regulatory subunits, only Rts1 is involved; the Tpd3 structural subunit is dispensable for this activity. Cells deficient in Ppm1-directed carboxymethylation of the catalytic subunits exhibit a slight decrease in PP2A activation upon glucose addition. Moreover, methylation of PP2A's catalytic subunits increased in response to glucose re-addition. We also identify four different regulatory subunits required for glucose-dependent activation of PP1.

4.2. INTRODUCTION

The serine/threonine-specific protein phosphatases PP2A and PP1 are major regulators of numerous cellular processes in yeast and other eukaryotes. Distinct functions of PP2A and PP1 are generated through the association of their catalytic subunit(s) with a broad range of regulatory subunits. In yeast, two related genes, *PPH21* and *PPH22*, encode the catalytic (C) subunits of PP2A. The *TPD3* gene codes for the only structural (A) subunit in *S. cerevisiae*, which serves as a scaffolding protein to accommodate one catalytic subunit and one of the two mutually exclusive regulatory (B) subunits, encoded by *RTS1* and *CDC55* respectively (Jiang, 2006). Interestingly, the lack of a structural subunit in a PP2A complex has been reported for yeast (Koren et al., 2004). Formation of the PP2A holoenzyme is regulated by the reversible methylation of the carboxyl terminus of the catalytic subunits. Inhibition of methylation, e.g. through the inactivation of the *PPM1*-encoded methyltransferase, reduces the interaction of the catalytic subunits with the regulatory subunits.

The catalytic subunit of PP1 in yeast is encoded by a single gene, *GLC7*. Yeast Glc7 is essential for viability and critically regulates processes as diverse as glucose and glycogen metabolism, sporulation, chromosome segregation, meiosis and protein synthesis. As for PP2A, the activity of PP1 is controlled by specific association with a wide variety of subunits. These include proteins such as Pig1 (and possibly Pig2), Reg1 and Reg2, Red1, Gip1 and Gip2, Gac1, Shp1, Bni4, Bud14 and Glc8; each of which has a well-characterized role as a modulator of Glc7 function (Walsh et al., 2002; Logan et al., 2008). The subunits target Glc7 to the appropriate subcellular location, determine the substrate specificity, and modulate the enzymatic activity accordingly. Thus, rather than being a promiscuous phosphatase, the yeast PP1 represents a large family of diverse enzymes that have individual specificity but share a common catalytic subunit.

In line with a proposed role in nutrient-induced signaling, moderate overexpression of *PPH22* was shown to trigger activation of the cAMP-PKA pathway, even in the absence of nutrients. Overexpression of *PPH22* affected all the PKA targets investigated, with the *PPH22*-overexpressing mutants demonstrating an increased trehalase activity, low trehalose levels, heat sensitivity and a constitutive repression of STRE-controlled genes; a phenotype commonly referred to as a 'high PKA phenotype'. Deletion of *SCH9* in the *PPH22*-overexpressing cells restores the glucose-induced activation of trehalase, suggesting that Sch9 is required to mediate the nutrient-induced signaling effects of Pph22 and may as such represent a novel Pph22 target (Sugajska et al., 2001). The kinase-phosphatase relationship in yeast therefore appears to be more intimate than previously thought. Similar signal transduction 'cassettes' have been described for higher eukaryotes in which a protein kinase and phosphatase interact directly or via a common scaffolding protein (Millward et al., 1999; Takahashi et al., 1999).

Previous work by Somers (2006) revealed, for the first time, the rapid activation of the protein phosphatases upon addition of glucose to glycerol-grown cells, i.e. glucose-starved cells. This activation is not inhibited by cycloheximide, which together with the rapidity of the response (within one minute) suggests a post-translational mechanism. In addition, it was demonstrated that glucose activation of PP2A requires only one of the known glucose-sensing mechanisms for activation

of the cAMP-PKA pathway: either the glucose- and sucrose-sensing GPCR, Gpr1, or the glucose phosphorylation-dependent system. Such a rapid change in phosphatase activity in response to an environmental stimulus has not been reported in yeast.

In this chapter, we focus on the mechanism by which glucose stimulates the activation of protein phosphatases in glucose-deprived cells. We demonstrate the requirement of specific regulatory and catalytic subunits for the activation of both PP2A and PP1. In addition, we provide evidence of the increase in methylation of PP2A brought about by glucose re-addition. This suggests a role for the nutrient in PP2A enzyme assembly.

4.3. RESULTS AND DISCUSSION

4.3.1. Glucose triggers rapid activation of PP2A and PP1 in derepressed cells

The addition of glucose to glucose-starved cells of *S. cerevisiae* triggers rapid stimulation of phosphatase activity (Figure 4.1). We have determined this increase in phosphoserine/phosphothreonine-specific catalytic activity by employing a routinely-used phosphatase activity assay (see "Materials and Methods", section 6.2.14.3.). Briefly, crude cell extracts are incubated with the ^{32}P-labeled glycogen phosphorylase a substrate. The reaction is terminated by addition of trichloroacetic acid, at which point the $^{32}P_i$ liberated by the phosphatase activity in the cell extract, is counted in a scintillation counter. The cpm values serve as indication of the protein phosphatase activity present in the cell extract. In all experiments, equal amounts of cells were extracted. The assay values were normalized to the amount of protein, as determined by Bradford analysis (Bradford, 1976).

The basal level of phosphatase activity in the cell extracts, as well as the profile of the glucose-induced increase in activity, varied to some extent between experiments. The exact reason for this is unclear, but it may reflect the complexity of the process, or possibly the sensitivity of the activity assay to the prevailing experimental conditions. However, despite some experimental variability, the rapid increase in activity after addition of glucose remained clearly recognizable throughout the course of this study.

The use of different glucose concentrations revealed that 20 mM led to maximum activation of phosphatase activity; both lower and higher concentrations of the carbon source reduced the magnitude of activation (Figure 4.1). This may be due to stronger feedback inhibition of the mechanism at higher glucose concentrations. Addition of other easily-fermentable sugars, like fructose and sucrose, at concentrations of 20 mM activated the phosphatases to the same extent as glucose; the non-metabolizable carbon sources sorbitol and 6-deoxyglucose had no effect on phosphatase activity (Somers, 2006).

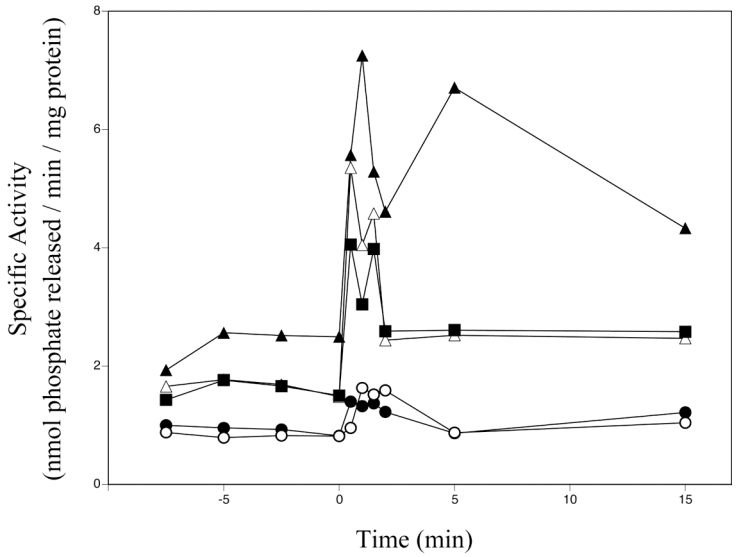

Figure 4.1: Glucose elicits the rapid activation of protein phosphatases in glucose-deprived cells. (In collaboration with Ils Somers)
Different glucose concentrations were added to glucose-starved wild-type cells at time zero. 1 mM (●), 5 mM (○), 20 mM (▲), 60 mM (△), and 100 mM (■).

To distinguish between PP2A activity and PP1 activity *in vitro*, we employed two highly selective phosphatase inhibitors: the naturally occurring inhibitor-2 and the tumor-inducing toxin okadaic acid (Foulkes and Cohen, 1980; MacKintosh et al., 1990). Inhibitor-2 inhibits PP1 specifically, whereas okadaic acid inhibits PP2A in the concentration range of 1-5 nM and also PP1 at higher concentrations. We therefore used inhibitor-2 and okadaic acid at concentrations of 0.2 μM and 2 nM, respectively, unless stated otherwise. As shown in Figure 4.2, both PP2A and PP1 are rapidly activated by addition of glucose to cells starved for the carbon source. The contribution of PP1 to the overall glucose-induced phosphatase activity, however, is slightly lower than that of PP2A. Moreover, the combined addition of both inhibitors completely suppressed activation of the phosphatases, which in itself underlines the specificity of the inhibitors at the concentrations used. In an additional control experiment, we showed that the glucose-induced activation of PP1 was not influenced by deletion of the PP2A or PP2A-like (e.g. *PPG1*, *SIT4*, and *PPH3*) phosphatase-encoding genes (Somers, 2006).

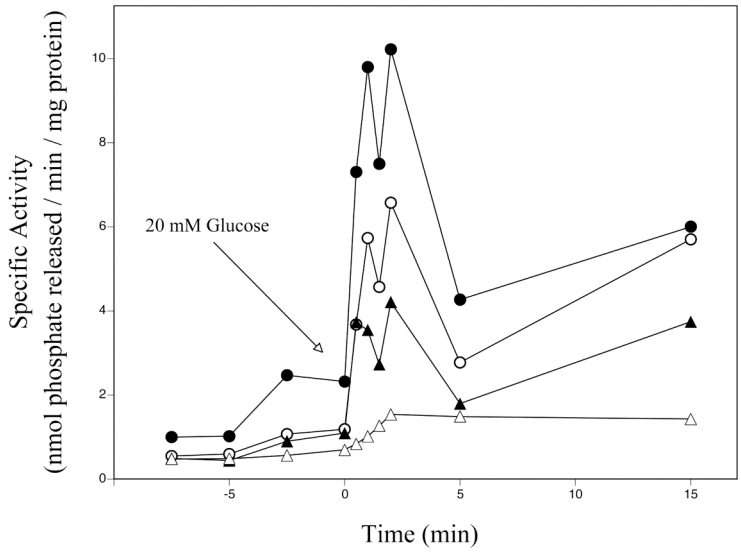

Figure 4.2: Glucose causes the rapid activation of both PP2A and PP1 in derepressed cells.

At time zero, 20 mM glucose was added to glucose-starved wild-type cells. Protein phosphatase activity was measured in cell extracts in the absence of an inhibitor (●), in the presence of 0.2 μM inhibitor-2 (○), 2 nM okadaic acid (▲), or 0.2 μM inhibitor-2 and 2 nM okadaic acid (△).

4.3.1.1. Glucose activation of PP2A requires Pph21 and Pph22

In yeast, as in higher eukaryotes, PP2A often exists as a multiprotein complex, composed of a catalytic subunit, a scaffolding subunit, and a variable regulatory subunit. To analyze the subunit makeup of the PP2A heterotrimer activated by glucose, we measured glucose-induced activation of PP2A in strains lacking either Pph21 or Pph22, or both. Disruption of *PPH21* reduced the extent of activation, and this was the case for deletion of *PPH22* as well, although to a lesser degree. Deletion of both catalytic subunits completely abolished the glucose stimulation of PP2A activity (Figure 4.3). The increased reduction observed for the *pph21*Δ cells is in agreement with previous data indicating that the individual loss of *PPH21* and *PPH22* reduced measurable PP2A activity by 51% and 33%, respectively (Wei et al., 2001). Deletion of the other PP2A-related catalytic subunits, *PPG1*, *SIT4*, and *PPH3*, had no impact on the glucose-induced stimulation of PP2A activity (results not shown).

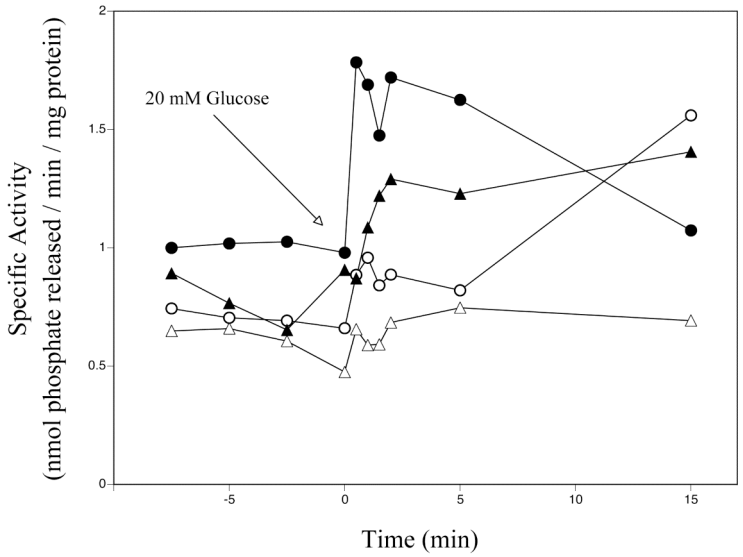

Figure 4.3: PP2A catalytic subunits Pph21 and Pph22 are required for glucose-induced activation of PP2A. (In collaboration with Ils Somers)

At time zero, 20 mM glucose was added to glucose-starved cells. Protein phosphatase activity was measured in cell extracts of the wild-type (●), *pph21*Δ (○), *pph22*Δ (▲), and *pph21*Δ *pph22*Δ (△) strains in the presence of 0.2 μM inhibitor-2.

Additional evidence that the catalytic subunits of PP2A are responsible for glucose-induced activation of the enzyme came from subsequent experiments with immunoprecipitated Pph21. We expressed hemagglutinin (HA)-tagged Pph21 in cells lacking both PP2A catalytic subunits, and tested the anti-HA-tag immunoprecipitates (one for each time point of the assay) for catalytic activity towards phosphorylase a. Pph21 activity was also measured in cell extracts (Figure 4.4B).

As shown in Figure 4.4A, a clear increase in phosphatase activity was observed for the immunoprecipitated Pph21, whereas for the *pph21*Δ *pph22*Δ mutant carrying the empty vector, no glucose-induced activation could be measured. This correlates well with the fact that no detectable Pph21 protein was immunoprecipitated in the latter strain. Similarly, we found that Pph21 restored phosphatase activity to the double deletion strain (in the cell extracts); reinforcing the idea that activation of PP2A by glucose is apparently due to the enzyme's catalytic subunits (Figure. 4.4B).

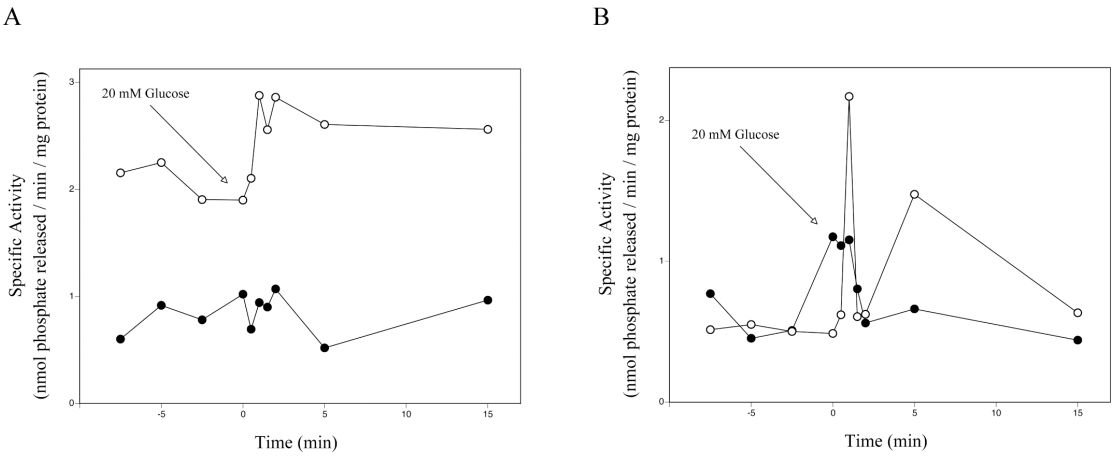

Figure 4.4: Pph21 restores glucose-inducible phosphatase activity to a strain lacking all PP2A catalytic subunits.

At time zero, 20 mM glucose was added to glucose-starved cells. Protein phosphatase activity was measured in immunoprecipitates **(A)** and cell extracts **(B)** in the presence of 0.2 μM inhibitor-2**. (A).** Anti-HA immunoprecipitates from lysates of *pph21*Δ *pph22*Δ cells expressing pYX142 (●), or pYX142-HA-*PPH21* (○).

(B). Cell extracts of the *pph21*Δ *pph22*Δ cells expressing pYX142 (●), or pYX142-HA-*PPH21* (○).

An unexpected result of the immunoprecipitation experiment is the subtle but reproducible increase in the basal level activity of the *PPH21*-expressing strain (Figure 4.4A). We ruled out the involvement of another (co-immunoprecipitated) phosphatase by performing the assay on immunoprecipitated Pph21 in the presence of either inhibitor-2 or okadaic acid. Addition of inhibitor-2 neither affected the high basal level nor the increase in PP2A activity, thus excluding PP1's participation in the non-induced phosphatase activity (see Figure 4.4A). Moreover, addition of okadaic acid completely blocked all immunoprecipitated Pph21 activity, suggesting that both the high basal level and the increase in activity are solely due to PP2A (results not shown).

Whereas PP2A usually exists as a heterotrimeric protein *in vivo*, cell extracts mostly contain catalytically-active AC dimers and free catalytic subunits (Cohen, 1989; Wu et al., 2000). It is thus tempting to speculate that the high basal level seen in the

immunoprecipitation experiments may simply derive from unspecific phosphatase activity by the ABC heterotrimeric complex as a whole, or perhaps from the binding of an unknown activator to immunoprecipitated Pph21.

To test this possibility, we measured glucose-inducible catalytic activity of immunoprecipitated Pph21 that was stripped of all associated proteins. Disruption of Pph21 complexes, and the concomitant isolation of monomeric Pph21 by immunoprecipitation, is achieved by treating cell lysates with an alkaline pH shift to disturb protein complexes, followed by neutralization (see "Materials and Methods", section 6.2.15.).

Surprisingly, activity from the monomeric Pph21 was largely abolished, as shown in Figure 4.5. This result suggests that there is an additional component(s) critical to the glucose-inducible PP2A phenomenon, most likely the regulatory and/or structural subunits of the enzyme.

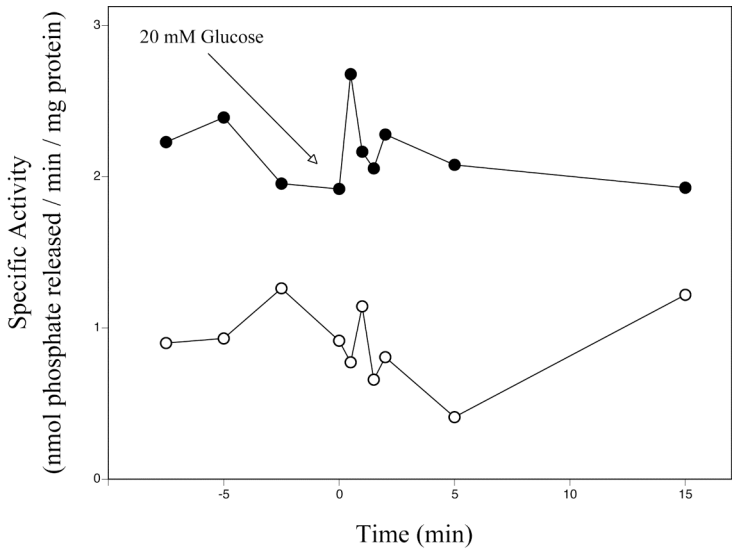

Figure 4.5: Monomeric Pph21 exhibits a severe defect in glucose-induced stimulation of PP2A activity.

At time zero, 20 mM glucose was added to glucose-starved wild-type cells expressing pYX142-HA-*PPH21*. Protein phosphatase activity was measured in anti-HA immunoprecipitates from untreated lysates **(●),** and from pH-treated lysates **(○)** in the presence of 0.2 μM inhibitor-2**.**

The overall basal activity of the treated lysates also dropped by about three-fold to levels seen with cell extracts, thus corroborating our earlier hypothesis that the high basal level is in part due to unspecific, i.e. non-induced, activity of the PP2A heterotrimeric enzyme.

4.3.1.2. Glucose activation of PP2A is dependent on Rts1 but not on Cdc55 and Tpd3

Work from several laboratories has demonstrated the importance of the PP2A regulatory and scaffolding subunits in many cellular processes. Deletion of *CDC55* or *TPD3*, for example, renders growth cold sensitive and causes clear morphological and cytokinetic defects (Healy et al., 1991; Yang et al., 2000a; Janssens and Goris, 2001). Disruption of *RTS1*, on the other hand, results in temperature-sensitive growth and, more importantly, diminishes the mRNA levels of the Hsp60 chaperone, thus impairing the deletion mutant's overall stress response (Shu et al., 1997; Wu et al., 2000).

Based on our earlier findings, we asked whether the A and/or B subunits may have an additional, previously unknown, role in glucose-induced activation of PP2A. To this end, we constructed mutants deleted for the regulatory subunits *RTS1* and *CDC55*, and the scaffolding subunit *TPD3*.

As shown in Figure 4.6A, inactivation of *RTS1* completely abrogated glucose-induced activation of PP2A. In contrast, cells lacking either *CDC55* (Figure 4.6A) or *TPD3* (Figure 4.6B) exhibited no such defects and, as in the case of *tpd3*Δ cells, caused a somewhat stronger glucose-induced stimulation of PP2A activity. The *rts1*Δ *cdc55*Δ double deletion mutant, however, lost all PP2A-specific activity (Figure 4.6A).

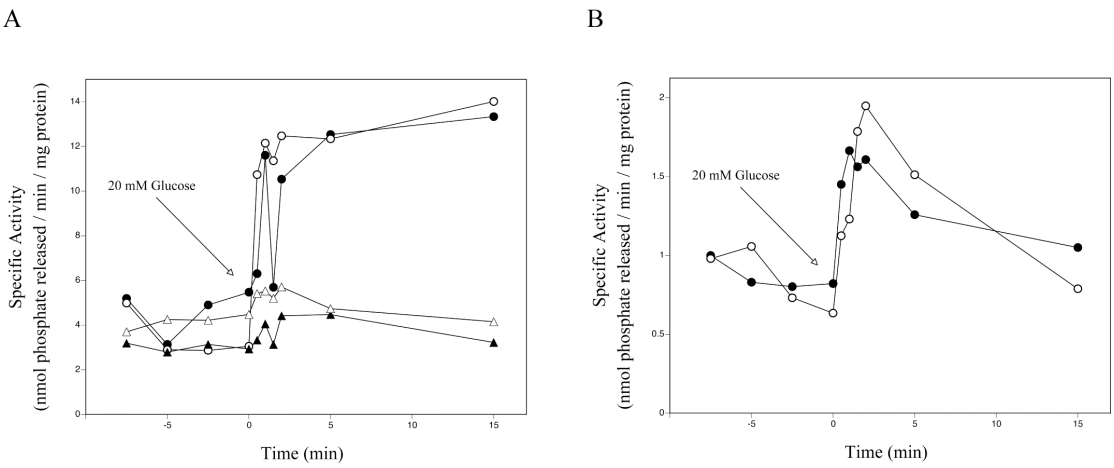

Figure 4.6: The regulatory subunit Rts1 is required for glucose activation of PP2A, as opposed to Cdc55 and Tpd3 which are both dispensable for this activity.

At time zero, 20 mM glucose was added to glucose-starved cells. Protein phosphatase activity was measured in cell extracts in the presence of 0.2 μM inhibitor-2**. (A).** wild-type (●), *cdc55*Δ (○), *rts1*Δ (▲), and *rts1*Δ *cdc55*Δ (△). **(B).** wild-type (●), and *tpd3*Δ (○).

Also, it has recently been reported that Rts1 is a key component of the pathways that integrate nutrient availability, cell size, and eventual entry into the cell cycle (Artiles et al., 2009). Cells deficient in Rts1 fail to undergo nutrient-based modulation of cell size.

In addition to the association with the A and B subunits, PP2A catalytic subunits also exist in complex with the essential protein Tap42, a downstream target of TORC1 (see "Chapter I", section 1.5.1.2.). Deletion of *CDC55* or *TPD3* enhances this association, which also correlates with the increased rapamycin resistance observed in *cdc55*Δ or *tpd3*Δ cells. Inhibition of TORC1 activity by rapamycin treatment or nutrient deprivation causes dissociation of Tap42 from the PP2A C subunit and subsequently inactivates the complex (Jiang and Broach, 1999; Wang et al., 2003).

To assess whether glucose-induced activation of phosphatases functions via TORC1, we pre-incubated glucose-starved wild-type cells with 300 ng/ml rapamycin for 3 hours. Evaluation of growth confirmed that TORC1 activity was completely blocked under these conditions. Addition of rapamycin, however, had no effect on the

stimulation of PP2A activity by glucose, suggesting that both TORC1 and Tap42 are apparently not involved in this process (Somers, 2006).

4.3.1.3. Addition of glucose to carbon-starved cells leads to carboxymethylation of Pph21

During the course of our study, the Ogris group published a series of reports on the biogenesis of catalytically-active PP2A heterotrimers. The authors proposed a model whereby the generation of catalytic subunits and assembly of the enzyme require a series of highly-regulated steps that occur under scrutiny of both Ppe1 and Ppm1 (Fellner et al., 2003a; Fellner et al., 2003b; Hombauer et al., 2007).

Although carboxymethylation of the catalytic subunits is not an absolute requirement for phosphatase activity, it plays a major, if not indispensable, role in the assembly of the PP2A heterotrimeric enzyme. Accordingly, we investigated the methylation status of immunoprecipitated Pph21 with the methylation-specific monoclonal antibody 2A10 (Fellner et al., 2003a).

As shown in Figure 4.7, the addition of glucose to glycerol-grown cells causes a clear increase in carboxymethylation of the Pph21 protein, a phenomenon that was cumulative over the first 90 min.

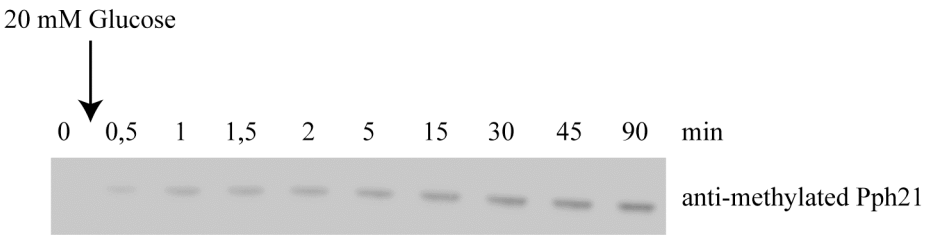

Figure 4.7: Glucose re-addition stimulates PP2A catalytic subunit methylation.

At time zero, 20 mM glucose was added to glucose-starved wild-type cells expressing pYX142-HA-*PPH21*. Anti-HA immunoprecipitates were subjected to western analysis with the indicated antibody.

To confirm the beforementioned data, we also employed a methylation-sensitive mouse monoclonal antibody (1d6) to evaluate PP2A's methylation status during carbon source re-addition (Figure 4.8). 1d6 specifically detects only unmethylated Pph21 and Pph22, since its binding to the catalytic subunits is strongly inhibited by methylation of the C-terminal leucine (Ogris et al., 1999; Wei et al., 2001).

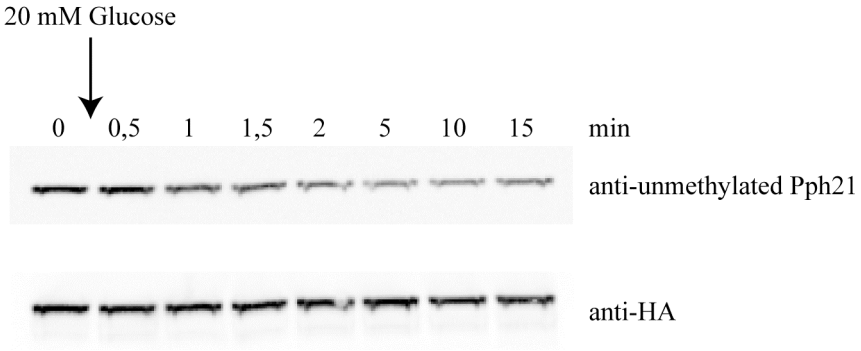

Figure 4.8: Unmethylated catalytic subunit levels decrease upon glucose re-addition.
At time zero, 20 mM glucose was added to glucose-starved wild-type cells expressing pYX142-HA-*PPH21*. Anti-HA immunoprecipitates were subjected to western analysis with the indicated antibody.

Figure 4.8 shows a clear decrease over time in 1d6 signal intensity upon glucose addition, which indicates the generation of a predominantly methylated form of Pph21 after glucose re-supplementation, and essentially, underscores our earlier finding. Taken together, our data suggest that glucose stimulates methylation of the catalytic subunits, and as such contributes to the biogenesis of active catalytic subunits and, moreover, to the generation of stable PP2A heterotrimeric enzymes.

We next analyzed the glucose-induced activation of PP2A in strains deficient for Ppm1. In yeast, *PPM1* encodes the carboxymethyltransferase solely responsible for PP2A methylation (Leulliot et al., 2004). Deletion of *PPM1* reduced PP2A activation with about 40% compared to the wild-type, as evident from Figure 4.9. This result is consistent with previous data highlighting Ppm1's minimal effect on PP2A phosphatase activity. Blocking methylation in yeast results in phenotypes typically associated with impaired PP2A enzyme formation (Ikehara et al., 2007).

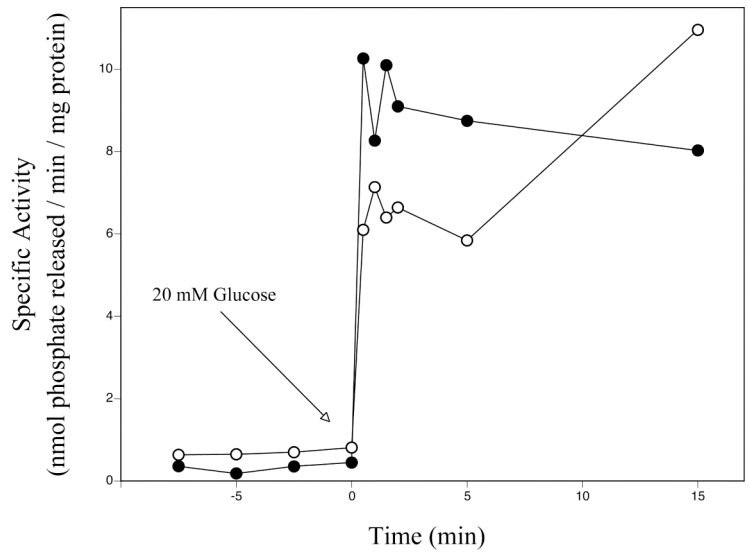

Figure 4.9: Loss of *PPM1*-encoded carboxymethyltransferase activity has only a limited effect on glucose-induced activation of PP2A.

At time zero, 20 mM glucose was added to glucose-starved cells. Protein phosphatase activity was measured in cell extracts of the wild-type (●), and *ppm1*Δ (○) strains in the presence of 0.2 μM inhibitor-2**.**

As expected, methylation of Pph21 in *ppm1*Δ cells, as measured with the methylation-specific antibody, was completely abolished (results not shown).

The methylated state of PP2A is in a dynamic equilibrium between the opposing actions of Ppm1 and the methylesterase Ppe1 that catalyzes the removal of the methyl group from the enzyme. Recent experimental evidence identified an additional role for the methylesterase. It was shown that Ppe1 regulates PP2A assembly by preventing the premature methylation of the catalytic subunit(s) that has not been activated by binding to the structural subunit, thus preventing the potential risk of unspecific dephosphorylation events *in vivo* (Hombauer et al., 2007).

We next determined whether the loss of Ppe1 affects glucose-induced stimulation of PP2A activity. As shown in Figure 4.10, loss of Ppe1 function resulted in a strong increase in glucose-stimulated PP2A activity, albeit at a slower rate than the wild-type. We attribute this increase in phosphatase activity to the fact that the catalytic subunits in *ppe1*Δ cells are all in a hypermethylated state (due to the

unregulated activity of Ppm1), which may contribute to an increase in uncontrolled C-subunit catalytic activity, especially when stimulated by glucose re-supplementation (also see Figure 4.11).

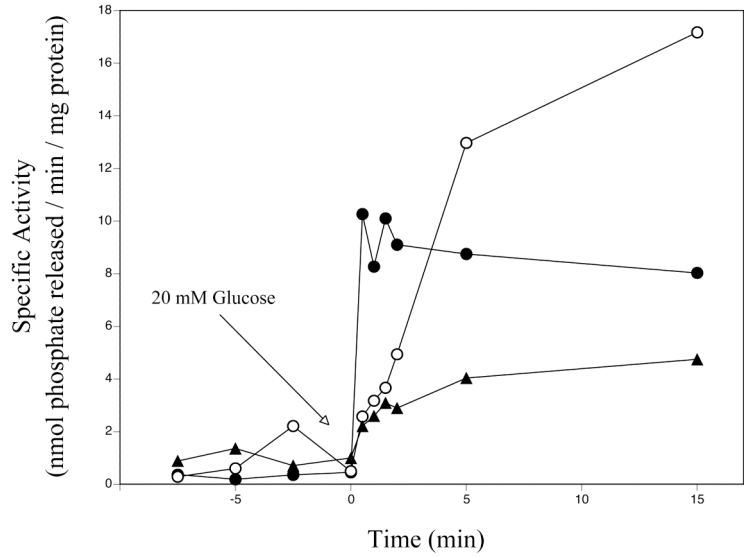

Figure 4.10: Disruption of *PPE1* causes a significant increase in glucose-dependent PP2A activity.

At time zero, 20 mM glucose was added to glucose-starved cells. Protein phosphatase activity was measured in cell extracts of the wild-type (●), *ppe1*Δ (○), and *ppm1*Δ *ppe1*Δ (▲) strains in the presence of 0.2 μM inhibitor-2**.**

We also evaluated *ppe1*Δ *ppm1*Δ cells for their glucose-induced activation of PP2A and found that the extent of activation was severely reduced in the double deletion mutant when compared to either the wild-type or *ppe1*Δ cells, which in effect highlights the requirement of both Ppm1 and Ppe1 in the generation of a catalytically-active and stable PP2A enzyme (Figure 4.10).

Immunoblot analysis of Pph21 protein from *ppe1*Δ cells revealed a large drop in the unmethylation level, and therefore a strong increase in methylation of the catalytic subunit, as judged from the strong signal intensity with the methylation-sensitive antibody 1d6 present in all the samples (Figure 4.11).

We confirmed this result via a different approach (see "Materials and Methods", section 6.2.16.). Because alkali treatment was shown to demethylate the catalytic subunit, a cell lysate containing predominantly methylated C subunits will exhibit a clear increase in 1d6 signal intensity upon alkali treatment, whereas a lysate with only unmethylated C subunits will have no such increase (Favre et al., 1994; Wei et al., 2001).

As shown in Figure 4.11, NaOH-treatment of one of the samples, sample "0", reveals a large increase in immunoreactivity compared to the untreated samples; suggestive of Pph21's strongly methylated state in *ppe1*Δ cells prior to alkali treatment.

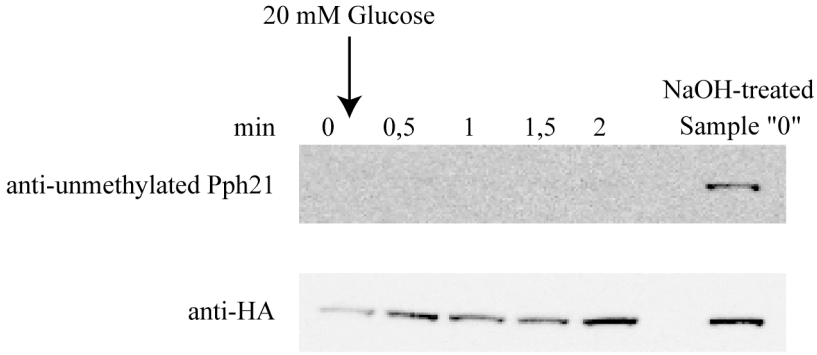

Figure 4.11: Strains lacking *PPE1*-encoded methylesterase activity display increased catalytic subunit methylation; a phenomenon independent of the carbon source in the growth medium.

At time zero, 20 mM glucose was added to glucose-starved *ppe1*Δ cells expressing pYX142-HA-*PPH21*. Anti-HA immunoprecipitates were subjected to western analysis with the indicated antibody. NaOH stripping of the C subunit methyl groups confirmed the reactivity of the antibody.

4.3.1.4. The Rrd proteins are required for glucose-induced stimulation of PP2A activity

As in mammalian cells, yeast PP2A is regulated by a set of evolutionary-conserved proteins known as Rrd1 and Rrd2 (Rrd1/2), the yeast homologs of the mammalian phosphotyrosyl phosphatase activator (PTPA) (Van Hoof et al., 2005). The loss of Rrd1/2 results in the generation of C subunits with severely impaired

phosphoserine/phosphothreonine-specific catalytic activity, indicating an essential function for Rrd1/2 in the formation of native PP2A (Fellner et al., 2003a). To investigate whether the Rrd proteins may also play a role in the glucose-induced activation, we determined activity of PP2A in cells deleted for *RRD1* and/or *RRD2* after addition of glucose. Deletion of both *RRD* genes is synthetically lethal, but can be rescued by expression of the *SSD1* gene (see "Chapter I", section 1.5.1.1.). Cells deficient for Rrd1 showed a distinct drop in glucose activation compared to the wild-type, with the loss of Rrd2 imposing an even bigger reduction on the stimulation of PP2A activity by glucose (Figure 4.12).

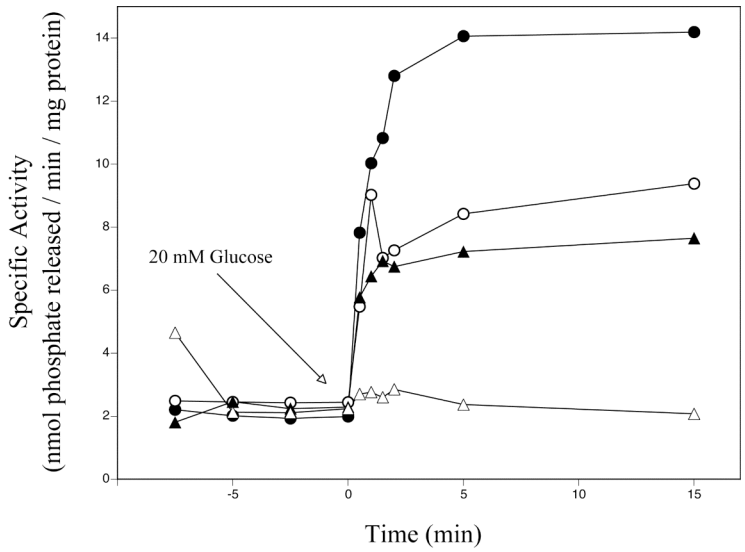

Figure 4.12: Loss of Rrd function abolishes the activation of PP2A by glucose.
At time zero, 20 mM glucose was added to glucose-starved cells. Protein phosphatase activity was measured in cell extracts of the wild-type (●), *rrd1*Δ (○), *rrd2*Δ (▲), and *rrd1*Δ *rrd2*Δ (△) strains in the presence of 0.2 μM inhibitor-2**.**

Moreover, the double deletion mutant showed no glucose-stimulated PP2A activity. We ascribe the reduction in catalytic activity, or lack thereof, observed in these mutants to an unstable PP2A enzyme comprised of a biochemically altered C-subunit (Hombauer et al., 2007).

The PP2A C subunits of strains deleted for the *RRD* genes typically exhibit an increase in phosphotyrosine catalytic activity, as opposed to the loss in phosphoserine/phosphothreonine activity. It would therefore be interesting to also evaluate *rrd*Δ cells for their glucose-induced PP2A activity towards a phosphotyrosine substrate, like para-nitrophenyl phosphate (pNPP). Fellner and colleagues (2003a), for example, reported a dramatic increase (about six-fold) in phosphotyrosine-specific catalytic activity in *rrd1*Δ *rrd2*Δ mutants compared to the wild-type.

4.3.2. Structure of PP1 activated by glucose

Unlike all eukaryotes, yeast only contains one gene encoding a PP1 catalytic subunit, termed *GLC7*. As in higher eukaryotes, Glc7 regulates numerous processes in yeast, including glucose and glycogen metabolism, sporulation and transcriptional responses. One hallmark of PP1 enzymes is the association of the catalytic subunit with a variety of regulatory subunits – at least 100 putative PP1 regulatory subunits have been identified in mammalian cells (Moorhead et al., 2007; Shi, 2009).

In yeast, PP1 regulatory subunits are encoded by *REG1* and *REG2*, *GIP1* and *GIP2*, *PIG1* and *PIG2*, *GAC1*, *SHP1*, *RED1, BNI4, BUD14* and *GLC8*, amongst others (for a detailed overview on the functions of the respective subunits, see "Chapter I", section 1.5.2.). To investigate the possible involvement of these regulatory subunits in the glucose-induced stimulation of PP1 activity, we measured phosphatase activity in a strain deleted for a particular subunit. We ensured specificity of the assay by performing the phosphatase activity measurements in the presence of the PP2A inhibitor okadaic acid, thus focusing only on the contribution of PP1 to the phosphatase activity observed. With the exception of Shp1, Glc8, Gac1, and Red1, none of the remaining regulatory subunits are required for stimulation of PP1 activity by glucose (results not shown).

However, deletion of *SHP1*, or the yeast homolog of mammalian inhibitor-2, *GLC8*, completely abolished PP1 activation, as shown in Figure 4.13A and Figure 4.13B,

respectively. Strains deficient for Gac1 or Red1 show only a partial decrease in glucose-induced activation of PP1 compared to the wild-type (Figure 4.13C and Figure 4.13D, respectively). The partial reduction in PP1 activity observed for the *gac1*Δ mutant may be a consequence of the weak association between Glc7 and Gac1 that exists in the presence of glucose (Stark, 1996). This is consistent with the fact that glycogen synthesis, regulated by Gac1, only commences once glucose becomes limiting. Hence, the loss of Gac1 in cells supplemented with glucose may have only a limited effect on Glc7 catalytic activity.

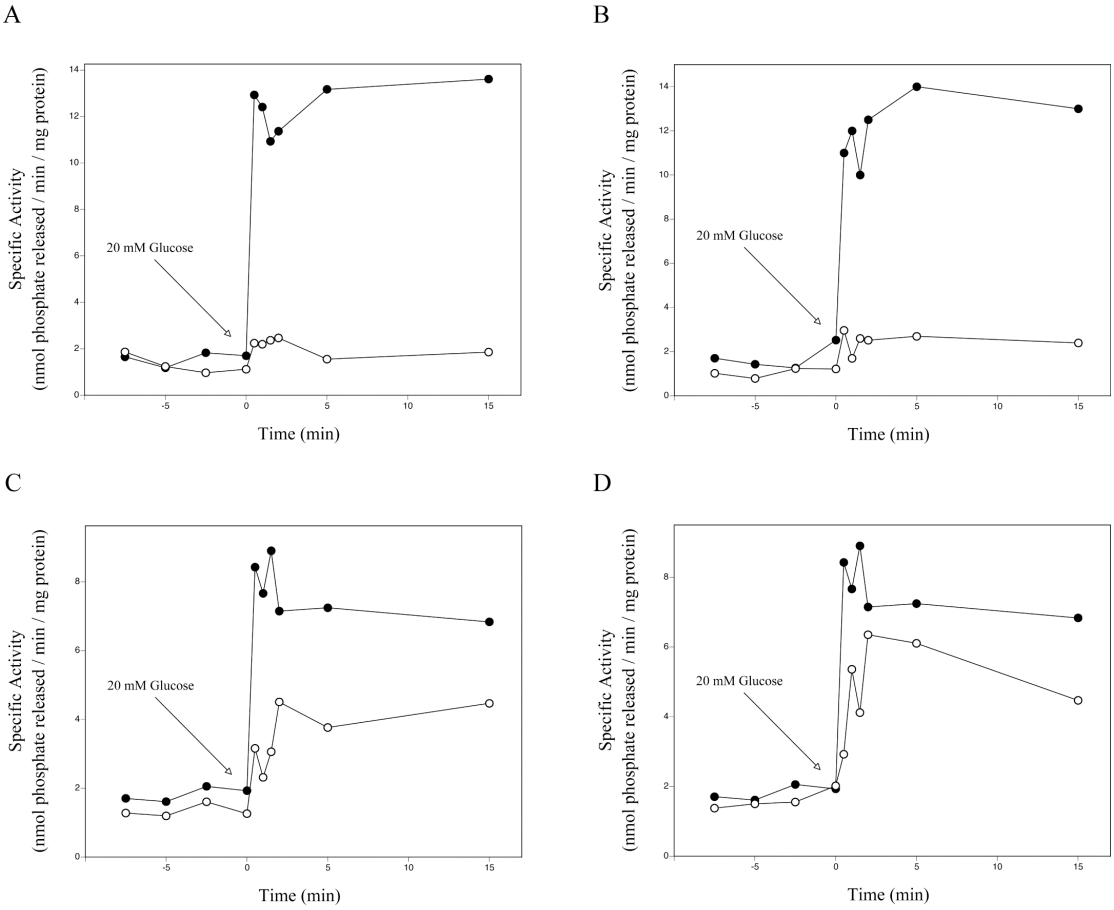

Figure 4.13: The PP1 regulatory subunits Shp1, Glc8, Gac1, and Red1 are all required for maximum activation of PP1 upon glucose re-supplementation.

At time zero, 20 mM glucose was added to glucose-starved cells. Protein phosphatase activity was measured in cell extracts in the presence of 2 nM okadaic acid**. (A).** wild-type (●), and *shp1*Δ (○); **(B).** wild-type (●), and *glc8*Δ (○); **(C).** wild-type (●), and *gac1*Δ (○); and **(D).** wild-type (●), and *red1*Δ (○).

Both Red1 and Gip1 are required for early meiosis, and it is this (partial) overlap in function between the two proteins that perhaps masks the effect losing only one of them may have on glucose-induced stimulation of PP1 activity (Tu et al., 1996). It may therefore prove useful to test the *red1*Δ *gip1*Δ double mutant for its PP1 activity.

Chapter V

GENERAL DISCUSSION

To grow and proliferate, all microorganisms must sense and respond to the availability of nutrients in their immediate surroundings. The unicellular eukaryote *S. cerevisiae* has therefore evolved numerous developmental options that ensure its quick adaptation to the prevailing growth conditions. Thus, when sufficient levels of carbon, nitrogen, phosphor and sulfur are detected, yeast cells embark on a period of rapid growth, characterized by, amongst others, the preferential use of glucose and the repression of genes required for utilization of other sugars. Starving yeast cells for any of these essential nutrients results in a dramatic restructuring of the cell's transcriptional profile. For instance, transcription of ribosomal protein genes is largely repressed, whereas expression of STRE-regulated genes, like *TPS1* and *NTH1*, is induced; the latter culminating in the starved cells acquiring a so-called 'stress resistance' phenotype (Rubio-Texeira et al., 2010).

The response of *S. cerevisiae* to the quality and quantity of nutrients in its environment is mediated by numerous signaling pathways, among which two are prominent: the well-studied cAMP-PKA pathway and the FGM pathway. Whereas the cAMP-PKA pathway is activated by addition of glucose to non-fermenting or stationary phase cells, activation of the FGM pathway requires a complete growth medium in which all essential nutrients are present.

Several nutrient-related sensors mediating nutrient-induced activation of the cAMP-PKA and FGM pathways have been identified. Detection of extracellular glucose and sucrose, for example, occurs through a GPCR system that is comprised of the receptor Gpr1 and its G protein Gpa2 (Lemaire et al., 2004). External amino acids are sensed and transported by Gap1, inorganic phosphate is sensed by Pho84 and Pho87, and Mep1 and Mep2 sense ammonium (Thevelein and Voordeckers, 2009; Popova et al., 2010). Interestingly, activation of the FGM pathway by the transported nutrient does not require its metabolization.

The intracellular part of the pathway that connects the signal generated by the nutrient transporter/receptor, or transceptor, to its downstream effector, PKA, remains poorly understood. Strong experimental evidence, however, suggests that the protein kinase Sch9 acts downstream of the nitrogen (but not phosphate) sensors (Crauwels et al., 1997; Giots et al., 2003).

In an attempt to identify domains of Gap1 specifically involved in signaling, short truncations of the extreme N- and C-termini of the permease were constructed. Partial removal of the Gap1 C terminal domain (14 amino acids; Gap1ΔC6$_{(14aa)}$), however, transformed the permease into a constitutive signaling form that caused permanent activation of the PKA pathway under all nutrient conditions tested (Donaton et al., 2003). To our knowledge, these mutant proteins represent the first example of an active nutrient transporter that causes permanent activation of a signaling pathway in eukaryotic cells. Further investigation revealed that this phenotype is dependent on a background mutation in the specific *gap1*Δ strain employed in our studies. The first part of the study therefore focused on additional characterization of the constitutive signaling phenotype, as well as identification of the background mutation.

Characterization of the constitutive signaling Gap1 transceptor

The constitutive signaling Gap1ΔC6$_{(14aa)}$ phenotype is characterized by low levels of the storage carbohydrates trehalose and glycogen, no repression of ribosomal protein genes, reduced expression of STRE-regulated genes, and an overall weak resistance to environmental stresses. In fact, of all the known PKA targets tested, only the activity of the trehalase enzyme remained unaffected by expression of the Gap1ΔC6$_{(14aa)}$ allele. The reason for this remains unclear, but may be due to additional inhibition of trehalase activity during nitrogen starvation in Gap1ΔC6$_{(14aa)}$-carrying cells. Consequently, we employed mostly L-citrulline-induced mobilization of trehalose and glycogen as a more reliable read-out of overactive PKA activity in this study.

We studied the contribution of known nutrient signaling pathways to the overactive signaling phenotype by, for example, blocking these pathways through the use of specific inhibitors. Inhibition of TORC1 activity by addition of the immunosuppressive drug, rapamycin, to yeast cells elicits profound physiological changes that include trehalose accumulation and the downregulation of amino acid transporters. However, exposing Gap1ΔC6$_{(14aa)}$-expressing cells to rapamycin had no effect on the amount of trehalose accumulated by these mutants; levels of the storage carbohydrate remained consistently low throughout the treatment. Growth in the presence of rapamycin of an adenylate cyclase mutant carrying Gap1ΔC6$_{(14aa)}$ was

also unaffected, suggesting that Tor Complex 1 is dispensable for the overactive signaling phenotype. Similar observations were also made for the phosphoinositide 4-kinase, Stt4. Blocking Stt4 activity with the antifungal antibiotic, wortmannin, left the Gap1ΔC6$_{(14aa)}$ cells unaffected, whereas similar treatment of the wild-type Gap1 cells elicited the rapid accumulation of trehalose. Thus, as for TORC1, Stt4 activity seems to be obsolete for the constitutive signaling phenotype.

Another serine/threonine protein kinase with a well-documented role in nutrient-sensing is the yeast PKB/S6K ortholog Sch9. Not only does the overexpression of *SCH9* mitigate the growth-inhibitory properties of wortmannin, deletion of the kinase also renders the cells incapable of properly entering the G_0 phase when starved for nitrogen. Overexpression of *SCH9* in Gap1ΔC6$_{(14aa)}$ cells, however, did not suppress the high PKA phenotype, as judged from the low levels of trehalose accumulated by the Gap1ΔC6$_{(14aa)}$ strain after starvation. This would suggest that Gap1ΔC6$_{(14aa)}$ does not signal through Sch9.

As all PKA targets, with the exception of trehalase, are affected by expression of *GAP1*Δ*C6*$_{(14aa)}$, we next investigated the role of PKA itself in this phenomenon. We considered the possibility that Gap1ΔC6$_{(14aa)}$ enhances adenylate cyclase activity, which in turn could lead to the hyperactivation of PKA and, as a result, to the "high PKA" phenotype observed in the mutant cells. This seems reasonable, as earlier work by Amitrano et al. (1997) demonstrated a clear link between cAMP levels and Gap1 activity: L-citrulline uptake in *cyr1-1* mutant increased as the exogenously-added cAMP levels were increased from 0.25 to 1.0 mM. Deletion of *CYR1* is lethal, but can be rescued through the additional deletion of *PDE2* and culturing of the double deletion strain on cAMP-supplemented media. Remarkably, expression of *GAP1*Δ*C6*$_{(14aa)}$ in the *cyr1*Δ *pde2*Δ strain completely abolishes the requirement for exogenously-added cAMP, suggesting that the truncated permease functions downstream of the signaling pathways known to affect cAMP synthesis. This result also excludes the possibility that the constitutive signaling phenotype is mediated through either an increased affinity of the *BCY1*-encoded regulatory subunit (of PKA) for cAMP, or through a decreased affinity of Bcy1 for the PKA catalytic subunits. For the latter, one would still expect the requirement of cAMP for growth, although at a

reduced concentration compared to, for example, the *cyr1*Δ *pde2*Δ Gap1 strain. However, as no cAMP is required for growth, the most plausible explanation is that Gap1ΔC6$_{(14aa)}$ functions either directly through PKA, or by overactivation of a downstream effector of PKA involved in growth control, and/or by constitutively blocking a downstream inhibitor with a similar function. Interesting to note, is the recent discovery of an adenylate cyclase-independent regulatory mechanism controlling activity of PKA in the human pathogenic fungus *Cryptococcus neoformans* (Palmer et al., 2006).

Subsequently, by inactivating all the PKA catalytic subunits, we could demonstrate the requirement of PKA for the overactive Gap1ΔC6$_{(14aa)}$ signaling phenotype. Hence, Gap1ΔC6$_{(14aa)}$ apparently acts at the level of PKA itself. These results probably also rule out the involvement of any additional component downstream of PKA as target of Gap1ΔC6$_{(14aa)}$.

Of particular relevance is the connection made between PKA and TORC1 in this work. Previous work by Schmelzle et al. (2004) showed that constitutive activation of the cAMP-PKA pathway prevented several of the typical rapamycin-induced responses, i.e. the accumulation of glycogen or the down-regulation of ribosomal protein gene expression. These data are in line with our own observations, and was further supported by the finding that we could restore rapamycin-sensitivity to the Σ1278b genetic background, known for its hyperactive PKA pathway, by lowering its PKA activity. We could therefore employ the Gap1ΔC6$_{(14aa)}$ strain in a suppressor screen, in which suppressors of the overactive signaling phenotype may well provide new information on the link between these two nutrient-sensing pathways.

Apart from the well-established adenylate cyclase-controlled stimulation of PKA activity, an alternative cAMP-independent bypass pathway for the activation of PKA was identified. Surprisingly, deletion of the *KRH* genes in the Gap1ΔC6$_{(14aa)}$ strain caused a clear reversal of the high PKA phenotype, with the single *krh1*Δ strain demonstrating the most pronounced turnaround in PKA activity, as deduced from the massive increase in trehalose levels in this strain. Moreover, the typical phenotypic differences between the wild-type Gap1 and Gap1ΔC6$_{(14aa)}$ strains, i.e. high trehalose

vs. low trehalose levels after nitrogen deprivation, are completely absent upon deletion of the *KRH* genes. In contrast, the Σ1278b *krh1*Δ *KRH2* strain carrying a plasmid-borne copy of *GAP1* continued to exhibit the high PKA phenotype that is typical of *krh*Δ strains.

These results ofcourse raise the question as to why two seemingly similar *krh1*Δ strains in the same genetic background carrying the same copy of wild-type Gap1 can display such opposite PKA phenotypes. We entertained the notion that the original Σ1278b *gap1*Δ strain in which we obtain the overactive phenotype, may contain a genomic mutation that proves crucial for Gap1ΔC6$_{(14aa)}$ signaling. Furthermore, the fact that deletion of the *KRH* genes in this (mutant) background abolishes the high PKA phenotype, suggests that both Gap1ΔC6$_{(14aa)}$ and the Krh proteins converge on the same component additionally required for the constitutive signaling. Since deletion of the *KRH* genes enhance PKA activity, the Krh proteins are normally considered as inhibitors of PKA. If the Krh proteins are a target of Gap1ΔC6$_{(14aa)}$, one possibility could be that Gap1ΔC6$_{(14aa)}$ switches the Krh proteins from inhibitors to activators. This would explain why deletion of the *KRH* genes in the Gap1ΔC6$_{(14aa)}$ strain reduces or abolishes the high PKA phenotype. Together, these results indicate a potential role for the Krh proteins in the Gap1ΔC6$_{(14aa)}$ phenotype, but clearly require more investigation.

Through various biochemical assays we confirmed the presence of a single and recessive genomic mutation, named *seg1-1*, present only in the original Σ1278b *gap1*Δ strain we employed in our Gap1ΔC6$_{(14aa)}$ characterization experiments. Our data also demonstrates the synergistic nature of the overactive signaling phenotype – both the truncated permease and *seg1-1* is required for the high PKA phenotype; the absence of either results in wild-type PKA activity. When expressed in the *seg1-1* strain, Gap1 alleles lacking a functional ER-exit domain, e.g. Gap1ΔC14$_{(42aa)}$, are not retained in the ER but instead show normal plasma membrane localization. Also, expression of *GAP1ΔC6*$_{(14aa)}$ in the *seg1-1* strain results in its strong overaccumulation at the plasma membrane. Notably, the latter truncation of Gap1 lacks the last 11 amino acids essential for its NH_4^+-induced inactivation and

internalization, thus resulting in a far less efficient ubiquitination and downregulation of the permease (Hein and André, 1997; Springael and André, 1998).

Based on these observations, we hypothesized that the overactive signaling phenotype of Gap1ΔC6$_{(14aa)}$ in the *seg1-1* strain is correlated with both its poor ubiquitination and concomitant overaccumulation at the plasma membrane. However, when tested in an *npi1-1 SEG1* strain deficient for Rsp5-mediated ubiquitination, overexpression of *GAP1ΔC6*$_{(14aa)}$ on a multi-copy plasmid did not result in an overactive signaling phenotype. This would suggest that *seg1-1* contributes more to the overactive signaling phenotype than only ensuring the overaccumulation of Gap1ΔC6$_{(14aa)}$ at the plasma membrane.

It may prove worthwhile to evaluate other amino acid transporters lacking an ER export signal for their subcellular localization in *seg1-1* cells. The di-acidic sequence (-DxD-; residues 564-566) of Gap1 essential for its sorting to the plasma membrane, is highly conserved among yeast amino acid permeases. In addition, Malkus and colleagues (2002) demonstrated the apparent universality of the permease export signal by creating an arginine permease molecule that contained the Gap1 ER exit signal. Appending Gap1's ER exit signal to Can1 resulted in a chimeric molecule that was packaged into COPII transport vesicles even more efficiently than full-length Can1.

Identification of the cognate gene for *seg1-1*

We employed several approaches to identify the gene containing the *seg1-1* mutation. In our single- and multi-copy suppressor screens, we made use of the unique properties of both the Gap1 transporter, in general, and the *seg1-1 GAP1ΔC14*$_{(42aa)}$ strain specifically. Keeping in mind that the Gap1ΔC14$_{(42aa)}$ allele is only properly localized to the plasma membrane in the *seg1-1* strain, we set out to complement the mutation by virtue of growth on a medium supplemented with D-histidine; a toxic amino acid transported only by Gap1. We isolated eight different single-copy suppressors, most of which functions within the yeast's early secretory pathway. In the multi-copy suppressor analysis, we isolated only amino acid carriers and no other

nutrient transporters, suggesting that *seg1-1* specifically modulates the ER exit of amino acid permeases. Subsequent genetic analysis showed that also none of the single-copy suppressors were identical to the *SEG1* gene.

We ascribe the failure to isolate *SEG1* by the conventional 'cloning-by-complementation' procedure, to the typical shortcomings associated with this method. For instance, a gene may be underrepresented in a library or toxic in *E. coli*, or false positives may be more readily isolated than the gene of interest. Also, *SEG1* may well be a large gene, which could make isolating the full-length *SEG1* from a 5-10 kb gDNA library, such as the one we used, more difficult.

We therefore switched to a genetic mapping strategy, AMTEM, for the purpose of identifying *SEG1*. As a first step in the AMTEM methodology, we crossed the *seg1-1* mutant strain with several artificially-marked strains carrying 20 bp oligonucleotide markers inserted all over the genome. We isolated 11 segregants that displayed the overactive signaling phenotype, i.e. low levels of trehalose. Although recommended to take about 20 segregants carrying the desired trait, we took extreme care to only select those segregants which showed a clearly reduced level of the reserve carbohydrate (0.6-0.8% of trehalose per wet weight) after overnight nitrogen deprivation. Segregants with trehalose levels of 1% or more were excluded from the experiment. Similarly, for the segregants we selected as a negative control, i.e. those with wild-type PKA activity, we only focused on the segregants with a clearly increased level of trehalose after nitrogen starvation (2% or more).

Application of the marker-detection micro-array resulted in negative signals for three adjacent markers located in a 40 kb region near the beginning of chromosome VIII. Further investigation revealed that, in addition to a variety of other genes, this region also contained a v-SNARE protein, Gos1, known to participate in multiple transport steps, most notably in the ER-Golgi transit. Deletion of *GOS1* is characterized by the uncontrolled secretion of the ER-resident chaperone Kar2, indicative of an ER-retention defective (*erd*) phenotype.

The critical role of Gos1 in the secretory pathway was further highlighted by the discovery that some SNARE proteins, like Gos1, not only ensure the efficient fusion

of a transport vesicle with an acceptor compartment, but also contribute to the specificity of intracellular transport. This was based on the finding that certain combinations of v- and t-SNAREs that actually inhibits vesicle fusion, e.g. Sed5-Sec22-Gos1-Bet1, are still found to assemble into non-fusogenic complexes *in vivo*. Originally, this was interpreted as evidence of SNARE proteins' promiscuous nature. However, a study by Varlamov et al. (2004) demonstrated that these non-fusogenic complexes indeed have a biological function: that of inhibitory-SNARE (i-SNARE) complexes. i-SNARE proteins are thought to fine-tune the movement of transport vesicles through the secretory pathway by 'removing' fusogenic-competent SNARE complexes from the transport process and replacing them with non-fusogenic complexes, which in effect blocks vesicular traffic.

Strikingly, when complemented with the Gap1ΔC6$_{(14aa)}$ allele, *gos1*Δ cells exhibited the same constitutive signaling phenotype as the *seg1-1* Gap1ΔC6$_{(14aa)}$ mutant strain. Moreover, *gos1*Δ cells carrying wild-type Gap1 exhibited trehalose levels similar to that of the *seg1-1* Gap1 strain, indicative of the wild-type PKA phenotype of the *gos1*Δ Gap1 strain. More importantly, though, is the fact that the high PKA phenotype of a *gos1*Δ strain is only observed in combination with the Gap1ΔC6$_{(14aa)}$ allele, which essentially corroborates our earlier findings on the synergistic character of the constitutive signaling phenotype.

Sequence analysis of the *GOS1* ORF, promoter and terminator regions in the *seg1-1* background, however, revealed no missense or any other potentially relevant mutations. This contrasts with the earlier data suggesting that *GOS1* is identical to *SEG1*. The exact reason for this seemingly contradictory observation is not yet clear. We hypothesized that the expression of *GOS1* may be affected by sequence variation in DNA sequences upstream and downstream of the *GOS1* coding sequences. Surprisingly, qPCR analysis of the expression of *GOS1* mRNA in the *seg1-1* Gap1ΔC6$_{(14aa)}$ strain revealed a dramatic increase in *GOS1* mRNA levels, whereas the levels of *GOS1* mRNA in the *seg1-1* Gap1 strain were unaffected. Hence, the differences in expression can only be attributed to the Gap1ΔC6$_{(14aa)}$ allele. The exact mechanism by which Gap1ΔC6$_{(14aa)}$ can influence the expression of Gos1 is not clear. We should, however, confirm the overexpression data at the protein level, i.e.

determine translational efficiency of the *GOS1* mRNA to protein. If the level of Gos1 protein is also strongly elevated, we have to conclude that both the disruption and overexpression of *GOS1* support the overactive Gap1 allele.

We sequenced the rest of the 40 kb region identified in the AMTEM screen and identified a point mutation within the *ECM29* ORF. The nucleotide at bp 5524, an adenine in the Σ1278b wild-type parental strain, is substituted for a guanine in the *seg1-1* mutant. This leads to an amino acid change where the amino acid residue at position 1842, an asparagine, is replaced by aspartic acid. This asparagine at position 1842 is not evolutionary-conserved.

The role that Ecm29 may play in the overactive signaling phenotype is not clear yet, and requires more investigation. Ecm29 was shown to enhance the stability of the proteasome by binding the organelle's core catalytic particle to its regulatory particle, which in turn activates the proteasome's de-ubiquitinating enzyme, Ubp6. Curiously, the disruption of *UBP6* causes a two-fold decrease in the internalization of plasma membrane-localized Gap1 (Nikko and André, 2007a).

Taken together, our results demonstrate a multi-faceted role for *seg1-1*. Expressing a secretion-incompetent Gap1 allele in the mutant background results in its localization to the plasma membrane where it exhibits wild-type function and stability. Moreover, expression in *seg1-1* of a Gap1 allele lacking part of the C-terminus required for NH_4^+-induced downregulation, causes its overaccumulation at the plasma membrane (although this may be an indirect consequence of decreased ubiquitination and internalization). Hence, these results points to a mutation in a gene functioning within the secretory pathway, most probably in one of the principal genes regulating ER exit. However, when combined with the Gap1Δ6 allele$_{(14aa)}$, *seg1-1* also results in constitutively-high PKA activity, a phenotype that was shown to be dependent on PKA itself. The high PKA phenotype is specific for the Gap1Δ6$_{(14aa)}$ allele, and is not observed when (much) longer or shorter truncations are employed, thus highlighting the importance of the specific truncation to the overall phenotype.

Glucose-induced activation of PP2A and PP1

The second part of this study focuses on the glucose-induced activation of the ubiquitously-expressed protein phosphatases PP2A and PP1. Previous work in our laboratory has defined a role for the PP2A C subunits in nutrient-induced signaling: overexpression of *PPH22* in wild-type cells was shown to trigger activation of the trehalase enzyme. On closer examination of the phenotype, it was revealed that *PPH22*-overexpression leads to the activation of all PKA targets investigated, i.e. a high PKA phenotype (Sugajska et al., 2001).

In an earlier study by Somers (2006), it was shown that addition of glucose to glucose-derepressed cells triggers rapid activation of both PP2A and PP1. The activation is not blocked by addition of the protein synthesis inhibitor cycloheximide, which together with the rapidity of the response, indicates a post-translational mechanism. Maximum phosphatase activation is achieved with 20 mM glucose; employing higher or lower concentrations reduces the extent of activation.

By using specific inhibitors, we were able to distinguish between PP2A and PP1 activity *in vitro*. The contribution of PP2A to the total glucose-induced phosphatase activity was shown to be higher than that of PP1, with Pph21 supplying the bulk of the PP2A activity. We confirmed the role of the C-subunits in the carbon-induced activation of PP2A by reconstituting glucose-induced phosphatase activity in a *pph21*Δ *pph22*Δ strain with immunoprecipitated Pph21. Moreover, disruption of the PP2A-like catalytic subunits, *PPG1*, *SIT4*, and *PPH3*, had no influence on the glucose-induced stimulation of PP2A activity. Deletion of the regulatory subunit *RTS1*, however, completely abolished glucose-induced activation of PP2A. On the other hand, cells lacking Cdc55 or the structural subunit Tpd3 displayed no such defects. Although the exception rather than the rule, it was shown that functionally-stable PP2A complex do exist in the absence of Tpd3 (Koren et al., 2004). Interesting to note, is that Rts1 is 12 times as abundant as Cdc55, implying that there will always be a free pool of Rts1 in the cell (Janssens et al., 2008).

In a screen aimed at identifying components required for downregulation of the SPS amino acid-sensing pathway, Rts1 was isolated as a negative regulator of this pathway. Deletion of *RTS1* caused the constitutive expression of SPS-responsive genes, such as *AGP1* and *BAP2* coding for amino acid transporters. These results propose a role for PP2A involvement in the SPS pathway, suggesting a dephosphorylation event may be required to downregulate signaling in the absence of extracellular amino acids (Eckert-Boulet et al., 2006). Recently, Rts1 was also identified as a novel upstream regulator of nutrient-dependent G_1 cyclin transcription, the latter being required for entry into the cell cycle (Artiles et al., 2009). Together with our discovery of a role for Rts1 in glucose-induced activation of PP2A, the role of Rts1 as an integrator of nutrient signals is thus firmly entrenched.

The addition of glucose to glycerol-grown cells was shown to also cause methylation of the PP2A catalytic subunit. This is an important finding, as it identifies a role for a nutrient (glucose) in the generation of functional PP2A complexes. Carboxymethylation of the catalytic subunits plays an important role in the binding of Pph21 and Pph22 to Cdc55; binding of Rts1 and Tpd3 to catalytic subunits is, however, somewhat less affected by the absence of methylation (Janssens et al., 2008). Hence, changes in PP2A methylation might regulate the specificity of the enzyme in cells. In contrast to its role in assembly, methylation of the PP2A C subunits is not an absolute requirement for phosphatase activity. This observation is in line with our own data on PP2A activity in *ppm1*Δ cells; deletion of the major methyltransferase in yeast, *PPM1*, reduced glucose-induced PP2A activity with about 40%. This result also lends further support to our earlier findings on the requirement of Rts1 for PP2A activation by glucose. As the association between unmethylated C subunits and Rts1 (and Tpd3) are only reduced and not fully abrogated, PP2A activity in *ppm1*Δ cells is only minimally affected.

Loss of methylesterase activity in *ppe1*Δ cells resulted in a significant increase in glucose-stimulated PP2A activity when compared to the wild-type. This is somewhat surprising, as no obvious phenotype has been described for yeast cells lacking Ppe1 (Wu et al., 2000). Our results, however, may be explained in context of the new model for PP2A holoenzyme assembly recently offered by Hombauer et al. (2007).

The authors proposed a model whereby Ppe1 represents a surveillance mechanism that prevents untimely methylation of the catalytic subunits in the absence of the structural subunit. In doing so, Ppe1 limits the risk of unspecific dephosphorylation events originating from inappropriate C subunit activation. The latter is associated with debilitating conditions in mammals such as cancer and Alzheimer's disease (Leulliot et al., 2004). Thus, the increase in phosphatase activity exhibited by *ppe1*Δ cells may well be due to the fact that the C subunits in such cells are all in a hypermethylated state (due to uncontrolled methylation), resulting in an increase in unregulated C-subunit catalytic activity. Western analysis of the C subunits in *ppe1*Δ cells confirmed their hypermethylated state.

The Hombauer model is particularly attractive as it also incorporates the activities of the yeast homologs of mammalian phosphotyrosyl phosphatase activator (PTPA), Rrd1 and Rrd2, in the generation of catalytically-active PP2A holoenzymes. It was shown that Rrd2 physically associates with Tpd3 and that this Tpd3-Rrd2 interaction is an essential prerequisite for binding the (unmethylated) Pph21/Pph22-Ppe1 complex. Once bound to the unmethylated C subunits, Ppe1 is replaced and Ppm1-directed methylation of the C subunits can occur (Hombauer et al., 2007). We showed that loss of Rrd function completely abolishes the glucose-induced stimulation of PP2A activity. The lack of phosphatase activity in the *rrd*Δ mutants may be attributed to the formation of PP2A enzymes comprised of biochemically- and conformationally-altered C-subunits. Typically, such enzymes exhibit an increase in phosphotyrosine activity combined with a loss of phosphoserine/phosphothreonine-specific catalytic activity.

We also investigated the role of the main regulatory subunits of PP1 in the glucose-induced stimulation of its activity. We found that deletion of *SHP1* and *GLC8* completely abolished PP1 activity; cells deficient for Gac1 or Red1 show only a partial reduction in glucose activation of the enzyme. Our data on Glc8 fits with an earlier report by Tung et al. (1995) who showed that Glc8, the yeast ortholog of mammalian inhibitor-2, functions both as activator and inhibitor of Glc7. When overproduced under certain physiological conditions, Glc8 binds to Glc7 at a low-affinity site, causing immediate and permanent inhibition of PP1 catalytic

activity. However, when Glc8 is present in low concentrations, it binds Glc7 at a different, high-affinity site in a 1:1 ratio, resulting in the formation of a temporarily-inactive Glc8-Glc7 complex that can be activated through the phosphorylation of Glc8. This suggests a function of Glc8 as a Glc7 chaperone, and explains our lack of PP1 activity in *glc8*Δ cells.

Both Gac1 and Shp1 are involved in Glc7-regulated glycogen synthesis (Zhang et al., 1995; Wu et al., 2001). The partial decrease in Glc7 activity observed for the *gac1*Δ strain may be an indirect consequence of the weak association that characterizes Glc7-Gac1 complexes in the presence of glucose. As glycogen accumulation only starts once glucose becomes limiting, the loss of Gac1 in cells supplemented with glucose may have a very limited effect on PP1 catalytic activity.

Similarly, it was demonstrated that both Red1 and Gip1 are required for entry into early meiosis (Stark, 1996; Tu et al., 1996). We believe that it is this overlap in function between the two proteins that perhaps masks the effect that losing only one of them may have on glucose-induced activation of PP1. It may therefore prove worthwhile to test the *red1*Δ *gip1*Δ mutant for glucose activation of Glc7 catalytic activity. In addition, we could also evaluate the deletions of the other PP1 regulatory subunits lacking a glucose-activation phenotype for their effect on PP1 activity when combined with the deletion of another glucose-unresponsive PP1 subunit.

The physiological relevance of glucose-induced activation of PP2A and PP1 may stem from the crucial role this carbon source plays on yeast physiology and development. Both PP2A and PP1 have been implicated in cellular processes as diverse as cell cycle progression, meiosis, sporulation, DNA transcription and glucose repression. In fact, the only common denominator in these processes is that they are all regulated by the availability of nutrients, especially glucose. As glucose activation of PP2A and PP1 occurs under the same conditions as glucose activation of the cAMP-PKA pathway, it is tempting to envision a process whereby the glucose-induced activation of the protein kinase-mediated signaling pathways is kept in check by the glucose-induced downregulation of the pathways, i.e. glucose could

bring balance in the activity of signaling pathways by stimulating also the activity of the opposing enzymes.

Chapter VI

MATERIALS AND METHODS

6.1. STRAINS AND PLASMIDS

6.1.1. Yeast strains

Saccharomyces cerevisiae strains used in this study are listed in Table 6.1. All experiments were performed with isogenic wild-type and mutant strains.

Table 6.1: *Saccharomyces cerevisiae* strains used in this study.

Strain	Relevant genotype	Source/Reference
Chapter II		
∑1278b (JT 4500)	*MATα ura3*	Grenson et al., 1970
BY4742	*MATα his3 leu2 lys2 ura3*	Brachmann et al., 1998
W303-1A	*MAT*a *leu2-3,112 trp1-1 can1-100 ura3-1 ade2-1 his3-11,15 GAL mal SUC2*	R. Rothstein
IH 73	∑1278b *gap1*Δ*::KanMX ura3*	I. Holsbeeks
25.969b (JT 4505)	∑1278b *seg1-1 gap1*Δ*::KanMX ura3*	B. André
JK 8	∑1278b *seg1-1 GAP1 ura3*	This study
IH 24	∑1278b *seg1-1 GAP1*Δ*C6*$_{(14aa)}$ *ura3*	I. Holsbeeks
IH 26	∑1278b *seg1-1 GAP1*Δ*C14*$_{(42aa)}$ *ura3*	I. Holsbeeks
JK 32	∑1278b + pFL38	This study
JK 33	∑1278b + pFL38-*GAP1*	This study
JK 34	∑1278b + pFL38-*GAP1*Δ*C6*$_{(14aa)}$	This study
JT 20425	∑1278b + pYX212	I. Holsbeeks
OL 9	∑1278b + pYX212-*SCH9*	O. Lagatie
JK 24	∑1278b *gap1*Δ*::KanMX* + pYX212	This study
OL 8	∑1278b *gap1*Δ*::KanMX* + pYX212-*SCH9*	O. Lagatie
JK 25	∑1278b *seg1-1 GAP1*Δ*C6*$_{(14aa)}$ + pYX212	This study
OL 11	∑1278b *seg1-1 GAP1*Δ*C6*$_{(14aa)}$ + pYX212-*SCH9*	O. Lagatie
JK 35	∑1278b *seg1-1 gap1*Δ*::KanMX sch9*Δ*::KanMX* + pFL38-*GAP1*	This study
JK 36	∑1278b *seg1-1 gap1*Δ*::KanMX sch9*Δ*::KanMX* + pFL38-*GAP1*Δ*C6*$_{(14aa)}$	This study
JK 39	∑1278b *seg1-1 GAP1*Δ*C6*$_{(14aa)}$ + pFL38	This study

JK 41	∑1278b *seg1-1 tpk1Δ::KanMX tpk2^{ts} tpk3Δ::URA3 GAP1*	This study
JK 42	∑1278b *seg1-1 tpk1Δ::KanMX TPK2 tpk3Δ::URA3 GAP1*	This study
JK 43	∑1278b *seg1-1 tpk1Δ::KanMX tpk2^{ts} tpk3Δ::URA3 GAP1ΔC6$_{(14aa)}$*	This study
JK 44	∑1278b *seg1-1 tpk1Δ::KanMX TPK2 tpk3Δ::URA3 GAP1ΔC6$_{(14aa)}$*	This study
JK 2	∑1278b *seg1-1 cyr1Δ::KanMX pde2Δ:: URA3 GAP1ΔC6$_{(14aa)}$*	This study
JK 1	∑1278b *seg1-1 cyr1Δ::KanMX pde2Δ:: URA3 GAP1*	This study
JK 50	∑1278b *seg1-1 gap1Δ::KanMX krh1Δ::hisG KRH2* + pFL38-*GAP1*	This study
JK 51	∑1278b *seg1-1 gap1Δ::KanMX krh1Δ::hisG KRH2* + pFL38-*GAP1ΔC6$_{(14aa)}$*	This study
JK 52	∑1278b *seg1-1 gap1Δ::KanMX krh1Δ::hisG krh2Δ::hisG* + pFL38-*GAP1*	This study
JK 53	∑1278b *seg1-1 gap1Δ::KanMX krh1Δ::hisG krh2Δ::hisG* + pFL38-*GAP1ΔC6$_{(14aa)}$*	This study
JT 20445	∑1278b *seg1-1 gap1Δ::KanMX* + pFL38-*GAP1ΔC6$_{(14aa)}$*	Donaton et al., 2003
JK 55	∑1278b *seg1-1 gap1Δ::KanMX KRH1 krh2Δ::hisG* + pFL38-*GAP1*	This study
JK 56	∑1278b *seg1-1 gap1Δ::KanMX KRH1 krh2Δ::hisG* + pFL38-*GAP1ΔC6$_{(14aa)}$*	This study
JK 57	∑1278b *SEG1 gap1Δ::KanMX krh1Δ::hisG KRH2* + pFL38-*GAP1*	This study
JK 59	∑1278b *SEG1 gap1Δ::KanMX krh1Δ::hisG krh2Δ::hisG* + pFL38-*GAP1*	This study
OL 85	∑1278b *seg1-1 GAP1ΔC6$_{(14aa)}$* + pFL38-*GAP1*	O. Lagatie
JK 46	BY *gap1Δ::KanMX* + pFL38-*GAP1ΔC6$_{(14aa)}$*	This study
JT 20545	W303-1A *gap1Δ::KanMX* + pFL38-*GAP1ΔC6$_{(14aa)}$*	I. Holsbeeks
JK 47	∑1278b *gap1Δ::KanMX* + pFL38-*GAP1ΔC6$_{(14aa)}$*	This study
IH 88	∑1278b *seg1-1 gap1Δ::KanMX* + pFL38-*GAP1ΔC7$_{(3aa)}$*	I. Holsbeeks
IH 91	∑1278b *seg1-1 gap1Δ::KanMX* + pFL38-*GAP1ΔC11$_{(15aa)}$*	I. Holsbeeks
IH 92	∑1278b *seg1-1 gap1Δ::KanMX* + pFL38-*GAP1ΔC12$_{(20aa)}$*	I. Holsbeeks
JT 20417	∑1278b *seg1-1 gap1Δ::KanMX* + pFL38-*GAP1ΔC14$_{(42aa)}$*	I. Holsbeeks
JK 73	∑1278b *gap1Δ::KanMX* + pFL38-*GAP1ΔC6$_{(14aa)}$*	This study
JK 74	∑1278b *gap1Δ::KanMX* + pFL38-*GAP1ΔC7$_{(3aa)}$*	This study
JK 75	∑1278b *gap1Δ::KanMX* + pFL38-*GAP1ΔC11$_{(15aa)}$*	This study

JK 76	∑1278b *gap1*Δ*::KanMX* + pFL38-*GAP1*Δ*C12*$_{(20aa)}$	This study
JK 77	∑1278b *gap1*Δ*::KanMX* + pFL38-*GAP1*Δ*C14*$_{(42aa)}$	This study
OL 65	∑1278b *gap1*Δ*::KanMX* + pFL44L-*GAP1*	O. Lagatie
OL 66	∑1278b *npi1-1* + pFL44L-*GAP1*	O. Lagatie
JK 80	∑1278b *gap1*Δ*::KanMX* + pFL44L-*GAP1*Δ*C6*$_{(14aa)}$	This study
JK 81	∑1278b *npi1-1* + pFL44L-*GAP1*Δ*C6*$_{(14aa)}$	This study
JK 82	∑1278b *gap1*Δ*::KanMX* + pFL44L	This study
JK 83	∑1278b *seg1-1 GAP1*Δ*C6*$_{(14aa)}$ + pFL44L	This study
Chapter III		
OL 43	∑1278b *gap1*Δ*::KanMX / gap1*Δ*::KanMX seg1-1 / SEG1* + pFL38-*GAP1*Δ*C6*$_{(14aa)}$	O. Lagatie
OL 44	∑1278b *gap1*Δ*::KanMX / gap1*Δ*::KanMX seg1-1 / SEG1* + pFL38-*GAP1*Δ*C14*$_{(42aa)}$	O. Lagatie
JK 63	*gap1*Δ*::KanMX erp2*Δ*::KanMX* + pFL38-*GAP1*Δ*C6*$_{(14aa)}$	This study
JK 64	*gap1*Δ*::KanMX erp4*Δ*::KanMX* + pFL38-*GAP1*Δ*C6*$_{(14aa)}$	This study
JK 65	*gap1*Δ*::KanMX vps26*Δ*::KanMX* + pFL38-*GAP1*Δ*C6*$_{(14aa)}$	This study
JK 66	*gap1*Δ*::KanMX vps29*Δ*::KanMX* + pFL38-*GAP1*Δ*C6*$_{(14aa)}$	This study
JK 67	*gap1*Δ*::KanMX vps35*Δ*::KanMX* + pFL38-*GAP1*Δ*C6*$_{(14aa)}$	This study
JK 68	*gap1*Δ*::KanMX stp2*Δ*::KanMX* + pFL38-*GAP1*Δ*C6*$_{(14aa)}$	This study
JK 69	*gap1*Δ*::KanMX dia4*Δ*::KanMX* + pFL38-*GAP1*Δ*C6*$_{(14aa)}$	This study
JK 70	*gap1*Δ*::KanMX caj1*Δ*::KanMX* + pFL38-*GAP1*Δ*C6*$_{(14aa)}$	This study
JK 92	∑1278b *gap1*Δ*::KanMX gos1*Δ*::KanMX* + pFL38-*GAP1*Δ*C6*$_{(14aa)}$	This study
JK 93	∑1278b *gap1*Δ*::KanMX wsc4*Δ*::KanMX* + pFL38-*GAP1*Δ*C6*$_{(14aa)}$	This study
JK 96	∑1278b *gap1*Δ*::KanMX / gap1*Δ*::KanMX seg1-1 / seg1-1* + pFL38-*GAP1*	This study
JK 97	∑1278b *gap1*Δ*::KanMX / gap1*Δ*::KanMX seg1-1 / gos1*Δ*::KanMX* + pFL38-*GAP1*	This study
JK 99	∑1278b *gap1*Δ*::KanMX / gap1*Δ*::KanMX seg1-1 / gos1*Δ*::KanMX* + pFL38-*GAP1*Δ*C6*$_{(14aa)}$	This study
JK 98	∑1278b *gap1*Δ*::KanMX / gap1*Δ*::KanMX seg1-1 / seg1-1* + pFL38-*GAP1*Δ*C6*$_{(14aa)}$	This study
Chapter IV		
BY4742	*MATα his3 leu2 lys2 ura3*	Brachmann et al., 1998

Record nr. 13832	BY4742 *pph21*Δ*::KanMX*	Giaever et al., 2002
Record nr. 13886	BY4742 *pph22*Δ*::KanMX*	Giaever et al., 2002
JT 21039	BY4742 *pph21*Δ*::KanMX pph22*Δ*::KanMX*	I. Somers
JK 109	BY4742 *pph21*Δ*::KanMX pph22*Δ*::KanMX* + pYX142	This study
JK 114	BY4742 *pph21*Δ*::KanMX pph22*Δ*::KanMX* + pYX142-HA-*PPH21*	This study
JK 113	BY4742 + pYX142-HA-*PPH21*	This study
JK 117	BY4742 *cdc55*Δ*::LEU2*	This study
Record nr. 11790	BY4742 *rts1*Δ*::KanMX*	Giaever et al., 2002
JK 118	BY4742 *rts1*Δ*::KanMX cdc55*Δ*::LEU2*	This study
Record nr. 16866	BY4742 *tpd3*Δ*::KanMX*	Giaever et al., 2002
JK 123	BY4742 *ppm1*Δ*::KanMX*	This study
JK 124	BY4742 *ppe1*Δ*::KanMX*	This study
JK 126	BY4742 *ppm1*Δ*::KanMX ppe1*Δ*::KanMX*	This study
JK 125	BY4742 *ppe1*Δ*::KanMX* + pYX142-HA-*PPH21*	This study
Record nr. 12312	BY4742 *rrd1*Δ*::KanMX*	Giaever et al., 2002
Record nr. 12100	BY4742 *rrd2*Δ*::KanMX*	Giaever et al., 2002
JK 116	BY4742 *rrd1*Δ*::KanMX rrd2*Δ*::KanMX*	This study
Record nr. 13084	BY4742 *shp1*Δ*::KanMX*	Giaever et al., 2002
Record nr. 16451	BY4742 *glc8*Δ*::KanMX*	Giaever et al., 2002
Record nr. 12434	BY4742 *gac1*Δ*::KanMX*	Giaever et al., 2002
Record nr. 15172	BY4742 *red1*Δ*::KanMX*	Giaever et al., 2002

6.1.2. Bacterial strain

The *Escherichia coli* strain used in this study is listed in Table 6.2. The *E. coli* TOP10 strain was used for molecular cloning and plasmid propagation.

Table 6.2: *Escherichia coli* strain used in this study.

Strain	Relevant genotype	Source/Reference
TOP10	F- mcrA Δ(mrr-hsdRMS-mcrBC) φ80lacZΔM15 ΔlacX74 nupG recA1 araD139 Δ(ara-leu)7697 galE15 galK16 rpsL(Str^R) endA1 λ^-	Invitrogen

6.1.3. Plasmids

All plasmids used in this study are summarized in Table 6.3.

Table 6.3: Plasmids used in this study

Plasmid	Insert	Source/Reference
Chapter II and Chapter III		
pFL38		Bonneaud et al., 1991
pYX212		Ingenius, Madison, WI
pFL44L		Bonneaud et al., 1991
pFL38-*GAP1*	*GAP1*	Hein and André, 1997
pFL38-*GAP1*Δ*C6*$_{(14aa)}$	*GAP1*Δ*C6*$_{(14aa)}$	I. Holsbeeks
pFL38-*GAP1*Δ*C7*$_{(3aa)}$	*GAP1*Δ*C7*$_{(3aa)}$	I. Holsbeeks
pFL38-*GAP1*Δ*C11*$_{(15aa)}$	*GAP1*Δ*C11*$_{(15aa)}$	I. Holsbeeks
pFL38-*GAP1*Δ*C12*$_{(20aa)}$	*GAP1*Δ*C12*$_{(20aa)}$	I. Holsbeeks
pFL38-*GAP1*Δ*C14*$_{(42aa)}$	*GAP1*Δ*C14*$_{(42aa)}$	I. Holsbeeks
pYX212-*SCH9*	*SCH9*	I. Geyskens
pFL44L-*GAP1*	*GAP1*	O. Lagatie
pFL44L-*GAP1*Δ*C6*$_{(14aa)}$	*GAP1*Δ*C6*$_{(14aa)}$	This study
pFL44L-multi-copy yeast genomic library	*S. cerevisiae* genomic DNA; 3 to 4 kb insert	Bonneaud et al., 1991
YCp50-single-copy yeast genomic library	*S. cerevisiae* genomic DNA; 5 to 10 kb insert	Rose et al., 1987
Chapter IV		
pYX142-HA-*PPH21*	HA-*PPH21*	Fellner et al., 2003

6.2. METHODS

6.2.1. Bacterial culture conditions

Escherichia coli cells were grown at 37°C in Luria-Bertani medium (1% w/v NaCl, 1% w/v Bactotryptone and 0.5% w/v yeast extract; pH 7.5). For Amp^r selection, ampicillin was added to a final concentration of 100 µg/ml. Solid medium contained 1.5% w/v agar in addition.

6.2.2. Yeast culture conditions

Yeast cells were cultured under continuous shaking at 30°C, unless stated otherwise. When selection for a specific nutritional marker was required, cells were grown in defined minimal media containing 0.17% w/v Yeast Nitrogen Base without amino acids and ammonium sulfate, 2% w/v glucose or 3% w/v glycerol, 0.5% w/v ammonium sulfate and supplemented with the appropriate synthetic amino acid/nucleotide mixture. The pH was adjusted to 5.5 with 4 M KOH. For solid medium, 1.5% w/v agar was added and the pH was adjusted to 6.5 with 4M KOH. When no minimal media was required for the selection of plasmids, cells were grown on nutrient-rich YP medium, containing 1% w/v yeast extract, 2% w/v Bactopeptone and 2% w/v glucose (for YPD) or 3% glycerol (for YPGly). In all experiments care was taken to use strains with identical autotrophies in order to avoid any potential marker effects on growth; when necessary, empty plasmids were introduced. For selection of geneticin-resistant mutants, geneticin was added to a final concentration of 100 µg/ml.

For experiments with nitrogen-starved cultures, cells were first grown to mid-exponential phase (OD_{600} = 1.5 – 2.0), harvested under sterile conditions and resuspended in nitrogen starvation medium (0.17% w/v Yeast Nitrogen Base without amino acids and ammonium sulfate, supplemented with 4% w/v glucose). Cultures were then incubated under continuous shaking for 24 h, while care was taken that glucose levels remained high throughout the entire period of starvation.

6.2.3. General molecular biology methods

Polymerase chain reaction (PCR) was performed with *Pfu*Turbo (Stratagene) or ExTaq (Takara) for cloning and diagnostic PCR respectively, according to the manufacturer's recommendations. Cloning was performed using standard restriction and ligation procedures, as described by Sambrook et al. (1989). Restriction digests were performed by incubation of DNA with the specific restriction enzymes and supplied reaction buffers for 2 h at the required temperature. Ligations were performed with the rapid ligation kit (Roche). *E. coli* transformations were performed according to the $CaCl_2$-procedure as described by Sambrook et al. (1989). Plasmid DNA was prepared from *E. coli* cells as described by Del Sal et al. (1988). DNA sequencing was performed by the dideoxy chain-termination method, unless stated otherwise. Detection was performed with an Applied Biosystems model 3100 Avant Genetic Analyzer according to the manufacturer's instructions, unless stated otherwise. Genomic and plasmid DNA was extracted from yeast with PCI (phenol/chloroform/isoamyl alcohol; 25:24:1), according to Hoffman and Winston (1987). Yeast was transformed according to Gietz et al. (1995), with the exception that the heat-shock treatment of temperature-sensitive strains occurred at 37°C.

6.2.4. Tetrad analysis

Crossing and sporulation was done following standard procedures as described by Sherman and Hicks (1991). Diploid strains were sporulated for 5 to 7 days at 23°C on solid sporulation medium A (1% w/v potassium acetate and 1.5% w/v agar). The ascus walls of the tetrads were digested with lyticase (500 U/ml) for 10 min at room temperature. Individual tetrads were separated and dissected using a micromanipulator (MSM System Series 3000, Singer Instruments). Growth of all yeast strains derived from crossing and subsequent sporulation was tested on the appropriate selective media to determine the presence of the auxotrophic markers used to delete the genes. Genotype characterization of all segregants was additionally checked by PCR analysis.

6.2.5. Single-copy suppressor analysis of *seg1-1*

Strain IH26 was transformed with 50 µg plasmid DNA from the single-copy yeast genomic library in YCp50 (Rose et al., 1987). Transformants were plated on MPDHis media (0.16% w/v D-histidine, 0.1% w/v L-proline, 1% w/v succinic acid, 0.6% w/v NaOH, 0.16% w/v Yeast Nitrogen Base without amino acids and ammonium sulfate, 2% w/v glucose, and 1.5% w/v agar). The total number of transformants was estimated at 30,000. Plasmids were isolated from viable transformants and the genomic DNA inserts were identified by sequence analysis.

6.2.6. Multi-copy suppressor analysis of *seg1-1*

Similar to the single-copy suppressor analysis, strain IH26 was transformed with 50 µg plasmid DNA from the multi-copy yeast genomic library in pFL44L (Bonneaud et al., 1991). Transformants were plated on MPDHis media. The total number of transformants was estimated at over 50,000. Plasmids were isolated from viable transformants and the genomic DNA inserts were identified by sequence analysis

6.2.7. Marker-detection micro-array

Micro-arrays were custom-made by Agilent. In total, 25 60 bp-probes were spotted per marker. These probes form a sliding window starting with a probe with 32 bases of the upstream sequence up to the end of the marker and sliding one base at a time to a probe with the marker followed by 32 bases of its downstream sequence. Of the 33 possible probes obtained per marker in this way, 8 were omitted for purposes of slide design.

Genomic DNA of a test strain and genomic DNA of the control strain (S288c without any artificial marker) was first digested with two mixtures of three enzymes (*Hin*dIII, *Bgl*II, *Xba*I and *Sac*II, *Mje*I, *Dra*I) and then mixed again. Labeling and subsequent purification was done with the BioPrime® Total Genomic Labeling System (Invitrogen), according to the manufacturer's recommendations. A competitive hybridization was then performed according to the Agilent Oligo acGH/ChIP-on-Chip protocol.

Statistical data analysis was performed on the processed Cy3 and Cy5 intensities, as provided by the Agilent Feature Extraction software version 9.1. The control spots (i.e. spots with Control Type equal to -1 or 1) were removed from the data set. Further analysis was performed in the R programming environment, in conjunction with the packages developed within the Bioconductor project (http://www.bioconductor.org; Gentleman et al., 2004). For each hybridization, we computed for each marker the regression coefficients of the regression line of the Cy5 intensities on the x-axis (control strain) *vs*. the Cy3 intensities on the y-axis (test strain). Plotting the intercepts *vs*. the slopes of the regressions showed a clear separation in the data. We clustered the data with K-means for K=2. The group of markers with slope values close to zero and high intercept values, consists out of present markers. The group with slope values close to one and intercept values close to zero corresponds to the absent markers

6.2.8. Statistical analysis

The probability of observing a given marker segregation by chance was calculated as a product of a binomial probability:

$$b(x; n, P) = {}_nC_x \times P^x \times (1 - P)^{n - x}$$

where “x” is the number of successes that result from the binomial experiment (all 11 segregants lack marker 250), “n” is the number of trials in the binomial experiment (total of 11 segregants checked), “P” is the probability of success on an individual trial (50% chance that an individual segregant contains a marker), b(x; n, P) is the binomial probability, i.e. the probability that an “n”-trial binomial experiment results in exactly “x” successes, when the probability of success on an individual trial is “P”, and ${}_nC_r$ is the number of combinations of “n” things, taken “r” at a time.

6.2.9. Determination of trehalose and glycogen content

Nitrogen-starved, glucose-repressed cells were cooled on ice for 30 min, harvested by centrifugation, washed with ice-cold 25 mM MES buffer pH 6.0, and resuspended at a cell density of 25 mg/ml cells (wet weight) in fresh nitrogen starvation medium

supplemented with 4% glucose. Cells were pre-incubated at 30°C for 20 min before sampling started at the indicated time points. Samples of 25 to 35 mg cells were collected by filtration, washed twice with ice-cold water, weighed and flash-frozen in liquid nitrogen. Frozen cells were thawed on ice, resuspended in 500 µl 0.25 M Na_2CO_3 and incubated for 1 h at 95°C. Trehalose and glycogen levels were determined as described previously by Colombo et al. (1998). The samples for trehalose determination were spun down and 10 µl of the clear supernatant was used. The samples for glycogen determination were instead mixed well and used directly (10 µl). All samples were neutralized by addition of 5 µl of 1 N acetic acid. For trehalose determination, 25 µl trehalase (extracted from *Humicola*) in buffer (60 mM NaAc, 6 mM $CaCl_2$; pH 5.5) was added, and samples were incubated for 1 h at 40°C. For glycogen determination, 25 µl amyloglucosidase (extracted from *Aspergillus niger*) in buffer (400 mM NaAc; pH 4.7) was added and incubated for 1 h at 40°C. After centrifugation, 20 µl of the supernatant from both the trehalose and glycogen samples were transferred to a microtiter plate. To determine the amount of glucose liberated from trehalose and glycogen, 200 µl GOD-PAP reagent (Dialab) were added and absorbance measured at 505 nm. Trehalose and glycogen levels are expressed as % of trehalose or glycogen, i.e. mg trehalose or glycogen per 100 mg cells, wet weight.

6.2.10. Real-time quantitative PCR (qPCR)

Culture samples for total RNA extraction were harvested by centrifugation; the pellet was flash-frozen in liquid nitrogen, and stored at -80°C. Total RNA was extracted from yeast cells using PCI. From 1 µg of total RNA, first-strand cDNA was prepared with the Promega AMV Reverse Transcription system according to the manufacturer's instructions. The relative quantification of genes was determined by qPCR using the KAPA fast SYBR mix (KAPA Biosystems). The PCR reaction was made up to 20 µl, consisting of 10 µl KAPA fast SYBR mix, 0.4 µl of each primer (10 µM), 5 µl of cDNA (10 ng/µl) and 4.2 µl RNase-free H_2O. Primers were designed according to the manufacturer's instructions and were probed for dimer formation. The qPCR was monitored with the ABI Prism 7000 Sequence Detection System (Applied Biosystems). The expression of *RDN18-1* (18S) was used as a reference.

6.2.11. Immunopurification of yeast proteins

To prepare crude extracts of yeast cells expressing tagged proteins, cells were resuspended in 500 µl ice-cold lysis buffer (PBS buffer, 0.1% Triton X-100, 10% glycerol, 2.5 mM $MgCl_2$, 1 mM EDTA pH 8.0, 1 mM DTT, 10 mM NaF, 0.4 mM Na_3VO_4, 0.1 mM β-glycerophosphate, containing protease inhibitor cocktail (complete, EDTA-free; Roche)). The same volume glass beads were added and cells were lysed by vigorous vortexing (4 × 1 min, with cooling on ice in between vortexing steps). Lysates were cleared by centrifugation (10 min, 14,000g, 4°C). The supernatant was transferred to a new Eppendorf tube, and centrifuged for a second time at the specifications described before. Cleared cell extracts were incubated with 100 µl of a 50:50 slurry of protein G agarose beads (washed with lysis buffer; Roche) and 5 µl of the appropriate antibody for 1 h on a rollerdrum (4°C). Bead-bound immunocomplexes were collected by centrifugation and beads were extensively washed with lysis buffer. Finally, beads were resuspended in SDS-supplemented sample buffer (added to a final concentration of 50 mM Tris pH 8.0, 10 mM β-mercapto-ethanol, 0.1% w/v bromophenol blue, 10% v/v glycerol, and 2% w/v SDS), boiled for 5 min at 95°C, and proteins were analyzed via SDS-PAGE and western blotting.

6.2.12. Western blotting

Total protein concentrations of crude cell extracts were determined using the Bradford method (Bradford, 1976). After the addition of sample buffer, samples were boiled for 5 min at 95°C. Solubilized proteins were separated via SDS-PAGE (NuPAGE® 4-12% Bis-Tris gel; Invitrogen) in NuPAGE® MOPS SDS running buffer (Invitrogen) at a constant voltage of 120 V. After electrophoresis, proteins were transferred onto nitrocellulose membranes (HybondC extra; GE Healthcare) by blotting for 90 min at 300 mA in blotting buffer (NuPAGE® MOPS SDS running buffer supplemented with 20% v/v methanol). Aspecific antibody binding was prevented by incubating the membrane in blocking buffer (5% w/v skim milk powder in TBS-Tween (TBST) buffer (25 mM Tris-HCl pH 8.0, 150 mM NaCl, and 0.05 % v/v Tween-20)) for 1 h at room temperature. Subsequently, blots were incubated overnight at 4°C with the

appropriate primary antibody dissolved in blocking buffer. Following overnight incubation, blots were washed three times with TBST buffer and incubated with the appropriate secondary antibody dissolved in blocking buffer. After washing three times with TBST, membranes were incubated with Supersignal chemiluminescence substrate (Pierce). Proteins were visualized either by exposure of the membrane to light-sensitive film (TebuBio) or by the LAS4000 mini digital system (Fujifilm). Signals were quantified with Aida software.

6.2.13. Antibodies used

Anti-HA (12CA5; Roche) for immunoprecipitation of HA-tagged proteins

Primary antibodies

- Anti-HA (high affinity, mouse; Roche), 1:1000 in TBST + 2.5% milk, coupled to HRP, used for detection of HA-tagged proteins in Western blot
- Anti-Gap1 (rabbit; gift from Bruno André, Université Libre de Bruxelles), 1:5000 in TBST + 2.5% milk
- Anti-methylated PP2A C subunit (clone 2A10, mouse; Millipore), 1:1000 in TBST + 2.5% milk
- Anti-unmethylated PP2A C subunit (clone 1d6, mouse; Millipore), 1:200 in TBST + 2.5% milk

Secondary antibodies

- Anti-mouse, HRP-conjugated (GE Healthcare), 1:5000 in TBST + 2.5% milk
- Anti-rabbit, HRP-conjugated (GE Healthcare), 1:5000 in TBST + 5% BSA

6.2.14. Phosphatase activity assay

6.2.14.1. Preparation of ^{32}P-phosphorylase a

To obtain ^{32}P-labeled phosphorylase a, 30 mg of glycogen phosphorylase b (Sigma) was dissolved in 1 ml of buffer (pH 7.5) containing 50 mM β-glycerophosphate, 10 % v/v glycerol, 0.1% v/v β -mercapto-ethanol, and 0.1 mM EDTA. To this solution, 155 µl 2 mM ATP, 125 µl 50 mM $Mg{\cdot}(CH_3COO)_2$, 5 µl 100 mM $CaCl_2$, 80 µl 0.5 M

Tris-HCl pH 8.0, 100 U glycogen phosphorylase kinase (Sigma), 520 µl H_2O, and 15 µl of [γ^{32}P]ATP (10 µCi/µ l) was added to initiate the phosphorylation of phosphorylase b. After 90 min at 30°C, proteins were precipitated by addition of 2 ml ice-cold saturated ammonium sulfate (pH 7.0). EDTA (3 mM) and NaF (15 mM) were added to inhibit the glycogen phosphorylase kinase. After 2 h on ice and subsequent centrifugation (10 min, 14,000g, 4°C), the pellet is dissolved in dialysis buffer (50 mM Tris-HCl pH 7.0, 0.1% v/v β-mercapto-ethanol) and dialyzed (4 × 1 L, 4°C). The ^{32}P-labeled phosphorylase a substrate was stored for no longer than one week at 4°C.

6.2.14.2. Sampling

Cultures (1 L) of glucose-deprived cells were harvested by centrifugation (3000g, 5 min, 4°C), washed with ice-cold MES buffer (25 mM, pH 6.0), and resuspended in 40 ml growth medium lacking glucose. Cells were pre-incubated at 30°C for 20 min before sampling started at the indicated time points. Four samples of 3 ml containing approximately 100 mg cells were removed prior to induction with 20 mM glucose. Following induction at time "0", additional samples were taken at time 0.5, 1, 1.5, 2.5, and 15 min. All samples were immediately spun down, flash-frozen in liquid nitrogen, and stored at -80°C.

6.2.14.3. Phosphatase activity assay

Cell pellets were thawed on ice and dissolved in 100 µ l of ice-cold lysis buffer (50 mM Tris-HCl pH 7.4, 0.1 mM EDTA, 0.1% v/v β-mercapto-ethanol) to which protease inhibitors (complete, EDTA-free; Roche) were added. The same volume glass beads were added and cells were lysed by vigorous vortexing (4 × 1 min, with cooling on ice in between vortexing steps). After clearing the lysates by centrifugation (10 min, 14,000g, 4°C), 10 µl of the supernatant was added to 10 µl of Buffer I (lysis buffer supplemented with 1 mg/ml BSA). In the experimental conditions where specifically PP2A activity was measured, inhibitor-2 (rabbit skeletal muscle; New England Biolabs) was included at a final concentration of 0.2 µM. The phosphatase reaction was initiated by addition of 10 µ l of a glycogen phosphorylase a solution

(30% v/v ^{32}P-labeled phosphorylase a, 50% v/v lysis buffer, and 20% v/v caffeine (75 mM)). After incubating the reaction for 30 min at 30°C, it was stopped by addition of 30 µl ice-cold TCA (30% v/v). Following centrifugation (10 min, 14,000g, 4°C), the supernatant was transferred to scintillation liquid and counted in a scintillation counter (Beckman Coulter LS6500). Protein concentrations of the samples were determined using the Bradford method (Bradford, 1976). Specific phosphatase activity is expressed as nmol phosphatase released per min per mg protein. Phosphatase release from glycogen phosphorylase a by phosphatases present in cell extracts was linear over at least 30 min.

6.2.15. Disruption of PP2A complexes and isolation of the monomeric catalytic subunit

Monomeric HA-Pph21 was isolated by immunoprecipitation of cell lysates, which had been treated with a basic pH shift to disrupt PP2A complexes, followed by neutralization. The lysates were generated as described before, except that the lysis buffer contained 10 mM instead of 50 mM Tris-HCl (section 6.2.14.3.). The basic pH shift (pH 11.5) was obtained by adding 6.25 µl of triethylamine (Sigma) to 500 µl of cell lysates. After 5 min incubation at room temperature, the reaction was neutralized by adding 330 µl of 0.1 N HCl and was used for immunoprecipitation experiments.

6.2.16. Demethylation of the PP2A catalytic subunit

Lysates were generated as described before, except that cell extracts were prepared in the presence of 2 nM okadaic acid to prevent further methylation and demethylation of C subunits. 20 µl of each lysate was placed on ice and demethylated by addition of 10 µ l of 0.5 M NaOH. After 5 min incubation, the samples were neutralized by addition of 10 µ l of 0.5 M HCl and 5 µ l of 2 M Tris (pH 6.8), and used for immunoprecipitation experiments.

Reproducibility of results

All experiments in this study were repeated at least twice. The results always showed consistent trends, i.e. differences between strains and mutants were highly reproducible. In all cases, results from representative experiments are shown.

The results of single time point measurements (e.g. accumulation of trehalose) are based on three independent measurements and standard deviations are indicated by means of the error bars in the graphs. Time course experiments (e.g. mobilization of trehalose after addition of L-citrulline) are repeated at least twice. The output of the time course experiments depicted in this study are the results of one of those experiments. The relative order of activation of the used strain was compared to the proper controls included in each experiment. The relative order of activation was highly reproducible.

SUMMARY

For microorganisms, nutrients represent one of the key environmental determinants controlling many aspects of cell function, including growth and proliferation. For example, addition of amino acids to nitrogen-deprived, glucose-grown cells of the yeast *Saccharomyces cerevisiae* triggers a rapid reversal of the stationary phase phenotype that characterizes such cells, i.e. trehalose and glycogen are mobilized, and cells lose their overall stress resistance and resume growth. Two major nutrient-sensing pathways in yeast, the cAMP-Protein Kinase A (PKA) pathway and the Fermentable Growth Medium-induced (FGM) pathway, couple nutrient cues to the cell's physiological and developmental program. Whereas the cAMP-PKA pathway is activated in response to fermentable carbon sources, activation of the FGM pathway requires a complete growth medium in which nitrogen, sulphur, phosphate and a fermentable carbon source are present in adequate amounts.

In addition to its well-documented function as an amino acid transporter, it has recently been shown that the general amino acid permease Gap1 also acts as a receptor. The dual function of Gap1 as amino acid transporter/receptor (transceptor) was supported by the isolation of constitutively activating alleles. These Gap1 mutant alleles contain short truncations, e.g. 14 amino acids for Gap1ΔC6$_{(14aa)}$, of the extreme carboxyl tail of the permease, with their expression resulting in a constitutively high PKA phenotype. This was observed under all growth conditions tested, even in medium with ammonium as sole nitrogen source.

In the first part of this study, we focused on characterizing the high PKA phenotype observed in cells carrying these truncated Gap1 mutant proteins. By blocking known nutrient signaling pathways, either through the disruption of an activating protein or the use of specific inhibitors, we show that the phenomenon is not caused by overactivation of either the rapamycin-sensitive TORC1 kinase, the phosphoinositide 4-kinase Stt4 or the protein kinase Sch9. We also provide experimental evidence that the mutant proteins mediate the overactive PKA phenotype in a cyclic AMP (cAMP)-independent, but PKA-dependent manner. Subsequent work showed that the

overactive signaling phenotype is synergistically dependent on both the truncated permease and a background mutation in the specific Σ1278b *gap1*Δ strain used, called *seg1-1*. The *seg1-1* mutation, for "Suppressor of ER exit-deficient Gap1", causes the secretion to the plasma membrane of truncated Gap1 alleles that lack a C-terminally-based ER exit signal which, in wild-type cells, are retained in the ER by the organelle's quality control system.

Genetic evidence indicated that the *seg1-1* mutation is both single and recessive. We employed a novel genetic mapping technology developed in our laboratory, AMTEM, for identification of the wild-type counterpart of *seg1-1*. AMTEM makes use of artificially-marked yeast strains which contain 600 different markers, inserted at neutral positions throughout the whole genome. In the screening process, we identified a 40 kb region between bp 18,226 and 58,935 near the beginning of chromosome VIII that is linked to the high PKA phenotype. Based on our earlier data, we first focused on a candidate gene (within the determined region) which functions within the yeast's secretion pathway, namely the Golgi-localized v-SNARE *GOS1*. Through detailed biochemical analyses, we showed that the expression of Gap1ΔC6$_{(14aa)}$ in *gos1*Δ cells causes PKA phenotypes identical to those observed in *seg1-1* Gap1ΔC6$_{(14aa)}$ cells, i.e. trehalose levels remain very low, even when these mutants are starved for nitrogen. Sequence analysis of the *GOS1* ORF, promoter and terminator regions in the *seg1-1* background, however, did not reveal any missense or other potentially relevant mutations.

We sequenced the rest of the 40 kb region, and identified a point mutation within the *ECM29* ORF, located at bp 5524. *ECM29* is the next gene on chromosome VIII, but located on the opposite strand to *GOS1*. The nucleotide at bp 5524, an adenine in both the S288c and the Σ1278b wild-type strains, is changed to a guanine in the *seg1-1* mutant. This leads to an amino acid change in which the amino acid residue at position 1842, an asparagine (N), is substituted for aspartic acid (D). The role that Ecm29 may play in the overactive signaling phenotype is not clear yet, and requires further investigation.

The next part of this study deals with the mechanism by which glucose addition to glucose-deprived yeast cells causes rapid activation of the serine/threonine protein phosphatases PP2A and PP1. Previous work has shown that both PP2A and PP1 are under direct control of glucose sensing. Here, we convincingly demonstrate that glucose-induced activation of PP2A requires the catalytic subunits Pph21 and Pph22. Of the PP2A regulatory subunits, only Rts1 is involved; Cdc55 appears to be dispensable for this activity. Furthermore, we show that cells deficient in catalytic subunit methylation exhibit a slight decrease in PP2A activation upon glucose addition. Moreover, methylation of PP2A's catalytic subunits increases in response to glucose re-addition.

We also identified four different regulatory subunits required for glucose-induced activation of PP1, namely Shp1, Glc8, Gac1 and Red1. Strains lacking Gac1 or Red1 show only a partial decrease in glucose-induced activation of PP1, compared to the *shp1*Δ and *glc8*Δ mutants that exhibit a complete loss of PP1-specific activation. We attribute the partial decrease in PP1 activation observed in *gac1*Δ and *red1*Δ cells to an overlap in function.

SAMENVATTING

Nutriënten zijn voor microorganismen één van de voornaamste factoren die vele aspecten van celfuncties, waaronder groei en proliferatie, controleren. Zo resulteert toevoeging van aminozuren aan *Saccharomyces cerevisiae* cellen gegroeid in aanwezigheid van glucosemaar zonder stikstofbron in een snelle omkering van het stationaire fase fenotype dat deze cellen kenmerkt. Trehalose en glycogeen worden gemobiliseerd, cellen verliezen hun verworven stress-resistentie en herstellen hun groei. De twee belangrijkste nutrient-geïnduceerde signaalwegen die hierbij tussenkomen zijn de cAMP proteïne kinase A (PKA) signaalweg en de 'Fermentable Growth Medium' geïnduceerde (FGM) signaalweg. De cAMP-PKA signaalweg wordt geacitveerd door een fermenteerbare koolstofbron, activatie van de FGM signaalweg daarentegen vereist een volledig groeimedium waarin naast een fermenteerbare koolstofbron ook stikstof, fosfaat en sulfaat aanwezig zijn.

Naast zijn reeds lang gekende functie als aminozuurtransporter, werd recent aangetoond dat de algemene aminozuurtransporter Gap1 ook een functie heeft als receptor. Deze dubbele functie van Gap1 als aminozuurtransporter/receptor (transceptor) werd ondersteund door de isolatie van constitutief activerende allelen van Gap1. Deze Gap1 mutanten bevatten korte truncaties van bv. 14 aminozuren (Gap1ΔC6$_{(14aa)}$) in het carboxyl uiteinde van de transporter die resulteren in een constitutief hoog PKA fenotype. Dit fenotype werd waargenomen in verschillende groei condities, zelfs in medium met ammonium als enige stikstofbron.

In het eerste deel van dit werk hebben we het hoge PKA fenotype van cellen met de getrunceerde Gap1 mutanten gekarakteriseerd. Door gekende nutriënt signaalwegen te blokkeren, door uitschakeling van een activerend proteïne of door gebruik van specifieke inhibitoren, konden we aantonen dat dit fenotype niet het gevolg is van een overactivatie van het rapamycine gevoelige TORC1 kinase, het fosfoinositide 4-kinase Stt4, of het proteïne kinase Sch9. Er werd ook aangetoond dat dit overactief PKA fenotype cAMP-onafhankelijk, maar PKA-afhankelijk is. Vervolgens werd aangetoond dat het overactieve signaleringsfenotype een gevolg is van zowel truncatie

van de transporter als een achtergrondmutatie in de specifieke Σ1278b *gap1*Δ stam, verder *seg1-1* genoemd. De *seg1-1* mutatie, voor 'Suppressor of ER exit-deficient Gap1' induceert secretie naar de plasmamembraan van het getrunceerde Gap1 dat het C-terminale ER-exit signaal mist. In wild type cellen worden deze getrunceerde Gap1 proteïnen weerhouden in het ER door het kwaliteitscontrole systeem.

Genetisch onderzoek heeft aangetoond dat de *seg1-1* mutatie zowel enkelvoudig als recessief is. Met behulp van een nieuwe genetische mapping tehnologie, ontwikkeld in ons labo, genaamd AMTEM, hebben we getracht het wild type gen van het mutante *seg1-1* gen te identificeren. AMTEM is gebaseerd op het gebruik van kunstmatig gemerkte giststammen die 600 verschillende merkers bevatten, geïnserered op neutrale posities over het hele genoom. Tijdens deze screen werd een regio van 40 kbp tussen 18,226 en 58,935 bp aan het begin van chromosoom VIII geïdentificeerd. Deze regio is gekoppeld aan het hoge PKA fenotype. Gebaseerd op vroegere gegevens hebben we ons initiëel gefocusseerd op een kandidaatgen (gelegen binen deze regio), *GOS1*, dat een functie heeft in de secretie weg, het codeert namelijk voor een Golgi gelokaliseerde v-SNARE. Na biochemische analyse konden we aantonen dat expressie van Gap1ΔC6$_{(14aa)}$ in *gos1*Δ hetzelfde PKA fenotype vertoont als dat in de *seg1-1* Gap1ΔC6$_{(14aa)}$ stam, namelijk een laag trehalose gehalte zelfs na deprivatie voor stikstof. Desondanks konden geen mutaties gevonden worden met behulp van sequentie analyse in de *GOS1* ORF, promoter en terminator gebieden.

Na sequenering van het volledige 40 kbp grote gebied, werd echter een mutatie gevonden in het *ECM29* ORF, gelegen op 5524 bp. *ECM29* is het volgende gen op chromosoom VIII, op de tegenovergestelde streng van *GOS1*. Het nucleotide op positie 5524, heeft een adenine in zowel S288c als Σ1278b wilde type achtergrond, die veranderd is naar een guanine in de *seg1-1* mutant. Hierdoor is er een verandering in aminozuur op positie 1842, asparagine (N) is vervangen door een aspartaat (D). Welke rol Ecm29 zou spelen in het overactieve signaleringsfenotype is nog niet opgehelderd en vereist verder onderzoek.

Het volgende deel van deze studie handelt over de mechanismen die tussenkomen in de activatie van de serine/threonine fosfatasen PP2A en PP1 door toevoeging van glucose aan glucose-gederepresseerde cellen. Eerder werd aangetoond dat zowel

PP2A als PP1 direct gereguleerd worden door glucose. In deze studie konden we aantonen dat de katalytische subeenheden Pph21 en Pph22 nodig zijn voor de glucose-geïnduceerde activatie van PP2A. Enkel de PP2A regulatorische subeenheid Rts1, en niet Cdc55, is betrokken bij deze signalering. Er werd ook aangetoond dat deficiëntie in methylatie van de katalytische subeenheden resulteert in een reductie van PP2A activatie na toevoegen van glucose. Bovendien neemt methylatie van de katalytische subeenheden van PP2A toe als respons op glucose.

Er werden vier verschillende regulatorische subeenheden, Shp1, Glc8, Gac1 en Red1, gekarakteriseerd als zijnde essentiëel voor de glucose-geïnduceerde activatie van PP1. Deletie van *GAC1* en *RED1* resulteert in gedeeltelijke daling van de activatie van PP1, bij deletie van *SHP1* en *GLC8* daarentegen is de PP1 activatie volledig teniet gedaan. De gedeeltelijke reductie in PP1 activatie is vermoedelijk een gevolg van een overlap in functies.

REFERENCES

Abdel-Sater, F., Iraqui, I., Urrestarazu, A., and Andre, B. (2004). The external amino acid signaling pathway promotes activation of Stp1 and Uga35/Dal81 transcription factors for induction of the AGP1 gene in Saccharomyces cerevisiae. Genetics 166, 1727-1739.

Adami, A., Garcia-Alvarez, B., Arias-Palomo, E., Barford, D., and Llorca, O. (2007). Structure of TOR and its complex with KOG1. Mol Cell 27, 509-516.

Agnan, J., Korch, C., and Selitrennikoff, C. (1997). Cloning heterologous genes: problems and approaches. Fungal Genet Biol 21, 292-301.

Amitrano, A.A., Saenz, D.A., and Ramos, E.H. (1997). GAP1 activity is dependent on cAMP in Saccharomyces cerevisiae. FEMS Microbiol Lett 151, 131-133.

Andreasson, C., and Ljungdahl, P.O. (2002). Receptor-mediated endoproteolytic activation of two transcription factors in yeast. Genes Dev 16, 3158-3172.

Andreasson, C., and Ljungdahl, P.O. (2004). The N-terminal regulatory domain of Stp1p is modular and, fused to an artificial transcription factor, confers full Ssy1p-Ptr3p-Ssy5p sensor control. Mol Cell Biol 24, 7503-7513.

Andreasson, C., Neve, E.P., and Ljungdahl, P.O. (2004). Four permeases import proline and the toxic proline analogue azetidine-2-carboxylate into yeast. Yeast 21, 193-199.

Araki, T., Uesono, Y., Oguchi, T., and Toh, E.A. (2005). LAS24/KOG1, a component of the TOR complex 1 (TORC1), is needed for resistance to local anesthetic tetracaine and normal distribution of actin cytoskeleton in yeast. Genes Genet Syst 80, 325-343.

Arnez, J.G., and Moras, D. (1997). Structural and functional considerations of the aminoacylation reaction. Trends Biochem Sci 22, 211-216.

Artiles, K., Anastasia, S., McCusker, D., and Kellogg, D.R. (2009). The Rts1 regulatory subunit of protein phosphatase 2A is required for control of G1 cyclin transcription and nutrient modulation of cell size. PLoS Genet 5, e1000727.

Audhya, A., and Emr, S.D. (2002). Stt4 PI 4-kinase localizes to the plasma membrane and functions in the Pkc1-mediated MAP kinase cascade. Dev Cell 2, 593-605.

Aviram, S., Simon, E., Gildor, T., Glaser, F., and Kornitzer, D. (2008). Autophosphorylation-induced degradation of the Pho85 cyclin Pcl5 is essential for response to amino acid limitation. Mol Cell Biol 28, 6858-6869.

Babst, M. (2004). GGAing ubiquitin to the endosome. Nat Cell Biol 6, 175-177.

Batlle, M., Lu, A., Green, D.A., Xue, Y., and Hirsch, J.P. (2003). Krh1p and Krh2p act downstream of the Gpa2p G(alpha) subunit to negatively regulate haploid invasive growth. J Cell Sci 116, 701-710.

Beck, T., and Hall, M.N. (1999). The TOR signalling pathway controls nuclear localization of nutrient-regulated transcription factors. Nature 402, 689-692.

Bergsma, J.C., Kasri, N.N., Donaton, M.C., De Wever, V., Tisi, R., de Winde, J.H., Martegani, E., Thevelein, J.M., and Wera, S. (2001). PtdIns(4,5)P(2) and phospholipase C-independent Ins(1,4,5)P(3) signals induced by a nitrogen source in nitrogen-starved yeast cells. Biochem J 359, 517-523.

Bertram, P.G., Choi, J.H., Carvalho, J., Ai, W., Zeng, C., Chan, T.F., and Zheng, X.F. (2000). Tripartite regulation of Gln3p by TOR, Ure2p, and phosphatases. J Biol Chem 275, 35727-35733.

Bharucha, J.P., Larson, J.R., Gao, L., Daves, L.K., and Tatchell, K. (2008). Ypi1, a positive regulator of nuclear protein phosphatase type 1 activity in Saccharomyces cerevisiae. Mol Biol Cell 19, 1032-1045.

Bi, X., Corpina, R.A., and Goldberg, J. (2002). Structure of the Sec23/24-Sar1 pre-budding complex of the COPII vesicle coat. Nature 419, 271-277.

Boban, M., and Ljungdahl, P.O. (2007). Dal81 enhances Stp1- and Stp2-dependent transcription necessitating negative modulation by inner nuclear membrane protein Asi1 in Saccharomyces cerevisiae. Genetics 176, 2087-2097.

Boban, M., Zargari, A., Andreasson, C., Heessen, S., Thyberg, J., and Ljungdahl, P.O. (2006). Asi1 is an inner nuclear membrane protein that restricts promoter access of two latent transcription factors. J Cell Biol 173, 695-707.

Boeke, J.D., Trueheart, J., Natsoulis, G., and Fink, G.R. (1987). 5-Fluoroorotic acid as a selective agent in yeast molecular genetics. Methods Enzymol 154, 164-175.

Bonneaud, N., Ozier-Kalogeropoulos, O., Li, G.Y., Labouesse, M., Minvielle-Sebastia, L., and Lacroute, F. (1991). A family of low and high copy replicative, integrative and single-stranded S. cerevisiae/E. coli shuttle vectors. Yeast 7, 609-615.

Bowers, K., and Stevens, T.H. (2005). Protein transport from the late Golgi to the vacuole in the yeast Saccharomyces cerevisiae. Biochim Biophys Acta 1744, 438-454.

Brachmann, C.B., Davies, A., Cost, G.J., Caputo, E., Li, J., Hieter, P., and Boeke, J.D. (1998). Designer deletion strains derived from Saccharomyces cerevisiae S288c: a useful set of strains and plasmids for PCR-mediated gene disruption and other applications. Yeast 14, 115-132.

Bradford, M.M. (1976). A rapid and sensitive method for the quantitation of microgram quantities of protein utilizing the principle of protein-dye binding. Anal Biochem 72, 248-254.

Broach, J.R. (1991). Ras-regulated signaling processes in Saccharomyces cerevisiae. Curr Opin Genet Dev 1, 370-377.

Broach, J.R., Pringle, J.R., and Jones, E.W. (1991). The molecular and cellular biology of the yeast Saccharomyces . Cold Spring Harbor Laboratory press, Cold Spring Harbor, New York.

Cai, H., Yu, S., Menon, S., Cai, Y., Lazarova, D., Fu, C., Reinisch, K., Hay, J.C., and Ferro-Novick, S. (2007). TRAPPI tethers COPII vesicles by binding the coat subunit Sec23. Nature 445, 941-944.

Caldwell, S.R., Hill, K.J., and Cooper, A.A. (2001). Degradation of endoplasmic reticulum (ER) quality control substrates requires transport between the ER and Golgi. J Biol Chem 276, 23296-23303.

Camus, C., Boy-Marcotte, E., and Jacquet, M. (1994). Two subclasses of guanine exchange factor (GEF) domains revealed by comparison of activities of chimeric genes constructed from CDC25, SDC25 and BUD5 in Saccharomyces cerevisiae. Mol Gen Genet 245, 167-176.

Carvalho, J., Bertram, P.G., Wente, S.R., and Zheng, X.F. (2001). Phosphorylation regulates the interaction between Gln3p and the nuclear import factor Srp1p. J Biol Chem 276, 25359-25365.

Castrejon, F., Gomez, A., Sanz, M., Duran, A., and Roncero, C. (2006). The RIM101 pathway contributes to yeast cell wall assembly and its function becomes essential in the absence of mitogen-activated protein kinase Slt2p. Eukaryot Cell 5, 507-517.

Chen, E.J., and Kaiser, C.A. (2003). LST8 negatively regulates amino acid biosynthesis as a component of the TOR pathway. J Cell Biol 161, 333-347.

Cheng, C., Huang, D., and Roach, P.J. (1997). Yeast PIG genes: PIG1 encodes a putative type 1 phosphatase subunit that interacts with the yeast glycogen synthase Gsy2p. Yeast 13, 1-8.

Cherkasova, V.A., and Hinnebusch, A.G. (2003). Translational control by TOR and TAP42 through dephosphorylation of eIF2alpha kinase GCN2. Genes Dev 17, 859-872.

Cohen, P. (1989). The structure and regulation of protein phosphatases. Annu Rev Biochem 58, 453-508.

Colombo, S., Ma, P., Cauwenberg, L., Winderickx, J., Crauwels, M., Teunissen, A., Nauwelaers, D., de Winde, J.H., Gorwa, M.F., Colavizza, D. (1998). Involvement of distinct G-proteins, Gpa2 and Ras, in glucose- and intracellular acidification-induced cAMP signalling in the yeast Saccharomyces cerevisiae. EMBO J 17, 3326-3341.

Connerly, P.L., Esaki, M., Montegna, E.A., Strongin, D.E., Levi, S., Soderholm, J., and Glick, B.S. (2005). Sec16 is a determinant of transitional ER organization. Curr Biol 15, 1439-1447.

Cooper, T.G. (2002). Transmitting the signal of excess nitrogen in Saccharomyces cerevisiae from the Tor proteins to the GATA factors: connecting the dots. FEMS Microbiol Rev 26, 223-238.

Crauwels, M., Donaton, M.C., Pernambuco, M.B., Winderickx, J., de Winde, J.H., and Thevelein, J.M. (1997). The Sch9 protein kinase in the yeast Saccharomyces cerevisiae controls cAPK activity and is required for nitrogen activation of the fermentable-growth-medium-induced (FGM) pathway. Microbiology 143 (Pt 8), 2627-2637.

Cuesta, R., Hinnebusch, A.G., and Tamame, M. (1998). Identification of GCD14 and GCD15, novel genes required for translational repression of GCN4 mRNA in Saccharomyces cerevisiae. Genetics 148, 1007-1020.

Cui, D.Y., Brown, C.R., and Chiang, H.L. (2004). The type 1 phosphatase Reg1p-Glc7p is required for the glucose-induced degradation of fructose-1,6-bisphosphatase in the vacuole. J Biol Chem 279, 9713-9724.

Cunningham, T.S., Rai, R., and Cooper, T.G. (2000). The level of DAL80 expression down-regulates GATA factor-mediated transcription in Saccharomyces cerevisiae. J Bacteriol 182, 6584-6591.

De Craene, J.O., Soetens, O., and Andre, B. (2001). The Npr1 kinase controls biosynthetic and endocytic sorting of the yeast Gap1 permease. J Biol Chem 276, 43939-43948.

De Silva-Udawatta, M.N., and Cannon, J.F. (2001). Roles of trehalose phosphate synthase in yeast glycogen metabolism and sporulation. Mol Microbiol 40, 1345-1356.

De Virgilio, C., and Loewith, R. (2006). The TOR signalling network from yeast to man. Int J Biochem Cell Biol 38, 1476-1481.

Del Sal, G., Manfioletti, G., and Schneider, C. (1988). A one-tube plasmid DNA mini-preparation suitable for sequencing. Nucleic Acids Res 16, 9878.

Deng, C., and Saunders, W.S. (2001). RIM4 encodes a meiotic activator required for early events of meiosis in Saccharomyces cerevisiae. Mol Genet Genomics 266, 497-504.

Devasahayam, G., Burke, D.J., and Sturgill, T.W. (2007). Golgi manganese transport is required for rapamycin signaling in Saccharomyces cerevisiae. Genetics 177, 231-238.

Devasahayam, G., Ritz, D., Helliwell, S.B., Burke, D.J., and Sturgill, T.W. (2006). Pmr1, a Golgi Ca2+/Mn2+-ATPase, is a regulator of the target of rapamycin (TOR) signaling pathway in yeast. Proc Natl Acad Sci U S A 103, 17840-17845.

Di Como, C.J., and Arndt, K.T. (1996). Nutrients, via the Tor proteins, stimulate the association of Tap42 with type 2A phosphatases. Genes Dev 10, 1904-1916.

Distler, M., Kulkarni, A., Rai, R., and Cooper, T.G. (2001). Green fluorescent protein-Dal80p illuminates up to 16 distinct foci that colocalize with and exhibit the same behavior as chromosomal DNA proceeding through the cell cycle of Saccharomyces cerevisiae. J Bacteriol 183, 4636-4642.

Donaton, M.C., Holsbeeks, I., Lagatie, O., Van Zeebroeck, G., Crauwels, M., Winderickx, J., and Thevelein, J.M. (2003). The Gap1 general amino acid permease acts as an amino acid sensor for activation of protein kinase A targets in the yeast Saccharomyces cerevisiae. Mol Microbiol 50, 911-929.

Doss, S., Schadt, E.E., Drake, T.A., and Lusis, A.J. (2005). Cis-acting expression quantitative trait loci in mice. Genome Res 15, 681-691.

Douville, J., David, J., Lemieux, K.M., Gaudreau, L., and Ramotar, D. (2006). The Saccharomyces cerevisiae phosphatase activator RRD1 is required to modulate gene expression in response to rapamycin exposure. Genetics 172, 1369-1372.

Durnez, P., Pernambuco, M.B., Oris, E., Arguelles, J.C., Mergelsberg, H., and Thevelein, J.M. (1994). Activation of trehalase during growth induction by nitrogen sources in the yeast Saccharomyces cerevisiae depends on the free catalytic subunits of cAMP-dependent protein kinase, but not on functional Ras proteins. Yeast 10, 1049-1064.

Eckert-Boulet, N., Larsson, K., Wu, B., Poulsen, P., Regenberg, B., Nielsen, J., and Kielland-Brandt, M.C. (2006). Deletion of RTS1, encoding a regulatory subunit of protein phosphatase 2A, results in constitutive amino acid signaling via increased Stp1p processing. Eukaryot Cell 5, 174-179.

Eckert-Boulet, N., Nielsen, P.S., Friis, C., dos Santos, M.M., Nielsen, J., Kielland-Brandt, M.C., and Regenberg, B. (2004). Transcriptional profiling of extracellular amino acid sensing in Saccharomyces cerevisiae and the role of Stp1p and Stp2p. Yeast 21, 635-648.

Elbein, A.D., Pan, Y.T., Pastuszak, I., and Carroll, D. (2003). New insights on trehalose: a multifunctional molecule. Glycobiology 13, 17R-27R.

Fabrizio, P., Pozza, F., Pletcher, S.D., Gendron, C.M., and Longo, V.D. (2001). Regulation of longevity and stress resistance by Sch9 in yeast. Science 292, 288-290.

Farkas, I., Hardy, T.A., Goebl, M.G., and Roach, P.J. (1991). Two glycogen synthase isoforms in Saccharomyces cerevisiae are coded by distinct genes that are differentially controlled. J Biol Chem 266, 15602-15607.

Fath, S., Mancias, J.D., Bi, X., and Goldberg, J. (2007). Structure and organization of coat proteins in the COPII cage. Cell 129, 1325-1336.

Favre, B., Zolnierowicz, S., Turowski, P., and Hemmings, B.A. (1994). The catalytic subunit of protein phosphatase 2A is carboxyl-methylated in vivo. J Biol Chem 269, 16311-16317.

Fellner, T., Lackner, D.H., Hombauer, H., Piribauer, P., Mudrak, I., Zaragoza, K., Juno, C., and Ogris, E. (2003a). A novel and essential mechanism determining specificity and activity of protein phosphatase 2A (PP2A) in vivo. Genes Dev 17, 2138-2150.

Fellner, T., Piribauer, P., and Ogris, E. (2003b). Altering the holoenzyme composition and substrate specificity of protein phosphatase 2A. Methods Enzymol 366, 187-203.

Forsberg, H., Hammar, M., Andreasson, C., Moliner, A., and Ljungdahl, P.O. (2001). Suppressors of ssy1 and ptr3 null mutations define novel amino acid sensor-independent genes in Saccharomyces cerevisiae. Genetics 158, 973-988.

Foulkes, J.G., and Cohen, P. (1980). The regulation of glycogen metabolism. Purification and properties of protein phosphatase inhibitor-2 from rabbit skeletal muscle. Eur J Biochem 105, 195-203.

Foury, F. (1997). Human genetic diseases: a cross-talk between man and yeast. Gene 195, 1-10.

Francois, J., and Parrou, J.L. (2001). Reserve carbohydrates metabolism in the yeast Saccharomyces cerevisiae. FEMS Microbiol Rev 25, 125-145.

Frederick, D.L., and Tatchell, K. (1996). The REG2 gene of Saccharomyces cerevisiae encodes a type 1 protein phosphatase-binding protein that functions with Reg1p and the Snf1 protein kinase to regulate growth. Mol Cell Biol 16, 2922-2931.

Fromme, J.C., Orci, L., and Schekman, R. (2008). Coordination of COPII vesicle trafficking by Sec23. Trends Cell Biol 18, 330-336.

Gagiano, M., Bauer, F.F., and Pretorius, I.S. (2002). The sensing of nutritional status and the relationship to filamentous growth in Saccharomyces cerevisiae. FEMS Yeast Res 2, 433-470.

Gallego, M., and Virshup, D.M. (2005). Protein serine/threonine phosphatases: life, death, and sleeping. Curr Opin Cell Biol 17, 197-202.

Gancedo, J.M. (2008). The early steps of glucose signalling in yeast. FEMS Microbiol Rev 32, 673-704.

Gao, M., and Kaiser, C.A. (2006). A conserved GTPase-containing complex is required for intracellular sorting of the general amino-acid permease in yeast. Nat Cell Biol 8, 657-667.

Garcia, A., Cayla, X., Guergnon, J., Dessauge, F., Hospital, V., Rebollo, M.P., Fleischer, A., and Rebollo, A. (2003). Serine/threonine protein phosphatases PP1 and PP2A are key players in apoptosis. Biochimie 85, 721-726.

Garrett, J.M. (2008). Amino acid transport through the Saccharomyces cerevisiae Gap1 permease is controlled by the Ras/cAMP pathway. Int J Biochem Cell Biol 40, 496-502.

Garriz, A., Qiu, H., Dey, M., Seo, E.J., Dever, T.E., and Hinnebusch, A.G. (2009). A network of hydrophobic residues impeding helix alphaC rotation maintains latency of kinase Gcn2, which phosphorylates the alpha subunit of translation initiation factor 2. Mol Cell Biol 29, 1592-1607.

Gentleman, R.C., Carey, V.J., Bates, D.M., Bolstad, B., Dettling, M., Dudoit, S., Ellis, B., Gautier, L., Ge, Y., Gentry, J., Hornik, K., Hothorn, T., Huber, W., Iacus, S., Irizarry, R., Leisch, F., Li, C., Maechler, M., Rossini, A.J., Sawitzki, G., Smith, C., Smyth, G., Tierney, L., Yang, J.Y., and Zhang, J. (2004). Bioconductor: open software development for computational biology and bioinformatics. Genome Biol 5, R80.

Georis, I., Feller, A., Tate, J.J., Cooper, T.G., and Dubois, E. (2009). Nitrogen catabolite repression-sensitive transcription as a readout of Tor pathway regulation: the genetic background, reporter gene and GATA factor assayed determine the outcomes. Genetics 181, 861-874.

Georis, I., Tate, J.J., Cooper, T.G., and Dubois, E. (2008). Tor pathway control of the nitrogen-responsive DAL5 gene bifurcates at the level of Gln3 and Gat1 regulation in Saccharomyces cerevisiae. J Biol Chem 283, 8919-8929.

Geyskens, I. (2004). Molecular characterization of the Sch9 protein kinase and its role in nutrient-induced signaling in the yeast Saccharomyces cerevisiae. KU Leuven.

Giaever, G., Chu, A.M., Ni, L., Connelly, C., Riles, L., Veronneau, S., et al. (2002). Functional profiling of the Saccharomyces cerevisiae genome. Nature 418, 387-391.

Gietz, R.D., Schiestl, R.H., Willems, A.R., and Woods, R.A. (1995). Studies on the transformation of intact yeast cells by the LiAc/SS-DNA/PEG procedure. Yeast 11, 355-360.

Gildor, T., Shemer, R., Atir-Lande, A., and Kornitzer, D. (2005). Coevolution of cyclin Pcl5 and its substrate Gcn4. Eukaryot Cell 4, 310-318.

Gilstring, C.F., Melin-Larsson, M., and Ljungdahl, P.O. (1999). Shr3p mediates specific COPII coatomer-cargo interactions required for the packaging of amino acid permeases into ER-derived transport vesicles. Mol Biol Cell 10, 3549-3565.

Giots, F., Donaton, M.C., and Thevelein, J.M. (2003). Inorganic phosphate is sensed by specific phosphate carriers and acts in concert with glucose as a nutrient signal for activation of the protein kinase A pathway in the yeast Saccharomyces cerevisiae. Mol Microbiol 47, 1163-1181.

Godard, P., Urrestarazu, A., Vissers, S., Kontos, K., Bontempi, G., van Helden, J., and Andre, B. (2007). Effect of 21 different nitrogen sources on global gene expression in the yeast Saccharomyces cerevisiae. Mol Cell Biol 27, 3065-3086.

Gokool, S., Tattersall, D., Reddy, J.V., and Seaman, M.N. (2007). Identification of a conserved motif required for Vps35p/Vps26p interaction and assembly of the retromer complex. Biochem J 408, 287-295.

Gorner, W., Durchschlag, E., Wolf, J., Brown, E.L., Ammerer, G., Ruis, H., and Schuller, C. (2002). Acute glucose starvation activates the nuclear localization signal of a stress-specific yeast transcription factor. EMBO J 21, 135-144.

Graff, J.W., Ettayebi, K., and Hardy, M.E. (2009). Rotavirus NSP1 inhibits NFkappaB activation by inducing proteasome-dependent degradation of beta-TrCP: a novel mechanism of IFN antagonism. PLoS Pathog 5, e1000280.

Grauslund, M., Lopes, J.M., and Ronnow, B. (1999). Expression of GUT1, which encodes glycerol kinase in Saccharomyces cerevisiae, is controlled by the positive regulators Adr1p, Ino2p and Ino4p and the negative regulator Opi1p in a carbon source-dependent fashion. Nucleic Acids Res 27, 4391-4398.

Grenson, M., Hou, C., and Crabeel, M. (1970). Multiplicity of the amino acid permeases in Saccharomyces cerevisiae. IV. Evidence for a general amino acid permease. J Bacteriol 103, 770-777.

Griffioen, G., Anghileri, P., Imre, E., Baroni, M.D., and Ruis, H. (2000). Nutritional control of nucleocytoplasmic localization of cAMP-dependent protein kinase catalytic and regulatory subunits in Saccharomyces cerevisiae. J Biol Chem 275, 1449-1456.

Griffioen, G., Branduardi, P., Ballarini, A., Anghileri, P., Norbeck, J., Baroni, M.D., and Ruis, H. (2001). Nucleocytoplasmic distribution of budding yeast protein kinase A regulatory subunit Bcy1 requires Zds1 and is regulated by Yak1-dependent phosphorylation of its targeting domain. Mol Cell Biol 21, 511-523.

Griffioen, G., Swinnen, S., and Thevelein, J.M. (2003). Feedback inhibition on cell wall integrity signaling by Zds1 involves Gsk3 phosphorylation of a cAMP-dependent protein kinase regulatory subunit. J Biol Chem 278, 23460-23471.

Guo, W., Grant, A., and Novick, P. (1999). Exo84p is an exocyst protein essential for secretion. J Biol Chem 274, 23558-23564.

Hansen, M., Taubert, S., Crawford, D., Libina, N., Lee, S.J., and Kenyon, C. (2007). Lifespan extension by conditions that inhibit translation in Caenorhabditis elegans. Aging Cell 6, 95-110.

Harashima, T., Anderson, S., Yates, J.R., 3rd, and Heitman, J. (2006). The kelch proteins Gpb1 and Gpb2 inhibit Ras activity via association with the yeast RasGAP neurofibromin homologs Ira1 and Ira2. Mol Cell 22, 819-830.

Healy, A.M., Zolnierowicz, S., Stapleton, A.E., Goebl, M., DePaoli-Roach, A.A., and Pringle, J.R. (1991). CDC55, a Saccharomyces cerevisiae gene involved in cellular morphogenesis: identification, characterization, and homology to the B subunit of mammalian type 2A protein phosphatase. Mol Cell Biol 11, 5767-5780.

Hedbacker, K., and Carlson, M. (2008). SNF1/AMPK pathways in yeast. Front Biosci 13, 2408-2420.

Hein, C., and Andre, B. (1997). A C-terminal di-leucine motif and nearby sequences are required for NH4(+)-induced inactivation and degradation of the general amino acid permease, Gap1p, of Saccharomyces cerevisiae. Mol Microbiol 24, 607-616.

Heitman, J., Movva, N.R., Hiestand, P.C., and Hall, M.N. (1991). FK 506-binding protein proline rotamase is a target for the immunosuppressive agent FK 506 in Saccharomyces cerevisiae. Proc Natl Acad Sci U S A 88, 1948-1952.

Helliwell, S.B., Losko, S., and Kaiser, C.A. (2001). Components of a ubiquitin ligase complex specify polyubiquitination and intracellular trafficking of the general amino acid permease. J Cell Biol 153, 649-662.

Heymann, P., Ernst, J.F., and Winkelmann, G. (2000). Identification and substrate specificity of a ferrichrome-type siderophore transporter (Arn1p) in Saccharomyces cerevisiae. FEMS Microbiol Lett 186, 221-227.

Hinnebusch, A.G. (2005). Translational regulation of GCN4 and the general amino acid control of yeast. Annu Rev Microbiol 59, 407-450.

Hinnebusch, A.G., and Natarajan, K. (2002). Gcn4p, a master regulator of gene expression, is controlled at multiple levels by diverse signals of starvation and stress. Eukaryot Cell 1, 22-32.

Hoffman, C.S., and Winston, F. (1987). A ten-minute DNA preparation from yeast efficiently releases autonomous plasmids for transformation of Escherichia coli. Gene 57, 267-272.

Holsbeeks, I. (2004). Involvement of the general amino acid permease, Gap1, in nitrogen sensing in Saccharomyces cerevisiae. KU Leuven.

Holsbeeks, I., Lagatie, O., Van Nuland, A., Van de Velde, S., and Thevelein, J.M. (2004). The eukaryotic plasma membrane as a nutrient-sensing device. Trends Biochem Sci 29, 556-564.

Hombauer, H., Weismann, D., Mudrak, I., Stanzel, C., Fellner, T., Lackner, D.H., and Ogris, E. (2007). Generation of active protein phosphatase 2A is coupled to holoenzyme assembly. PLoS Biol 5, e155.

Hong, G., Trumbly, R.J., Reimann, E.M., and Schlender, K.K. (2000). Sds22p is a subunit of a stable isolatable form of protein phosphatase 1 (Glc7p) from Saccharomyces cerevisiae. Arch Biochem Biophys 376, 288-298.

Hong, S.P., and Carlson, M. (2007). Regulation of snf1 protein kinase in response to environmental stress. J Biol Chem 282, 16838-16845.

Honjoh, S., Yamamoto, T., Uno, M., and Nishida, E. (2009). Signalling through RHEB-1 mediates intermittent fasting-induced longevity in C. elegans. Nature 457, 726-730.

Horak, J. (2003). The role of ubiquitin in down-regulation and intracellular sorting of membrane proteins: insights from yeast. Biochim Biophys Acta 1614, 139-155.

Ikehara, T., Ikehara, S., Imamura, S., Shinjo, F., and Yasumoto, T. (2007). Methylation of the C-terminal leucine residue of the PP2A catalytic subunit is unnecessary for the catalytic activity and the binding of regulatory subunit (PR55/B). Biochem Biophys Res Commun 354, 1052-1057.

Jacinto, E., and Lorberg, A. (2008). TOR regulation of AGC kinases in yeast and mammals. Biochem J 410, 19-37.

Janssens, V., and Goris, J. (2001). Protein phosphatase 2A: a highly regulated family of serine/threonine phosphatases implicated in cell growth and signalling. Biochem J 353, 417-439.

Janssens, V., Goris, J., and Van Hoof, C. (2005). PP2A: the expected tumor suppressor. Curr Opin Genet Dev 15, 34-41.

Janssens, V., Longin, S., and Goris, J. (2008). PP2A holoenzyme assembly: in cauda venenum (the sting is in the tail). Trends Biochem Sci 33, 113-121.

Jauniaux, J.C., and Grenson, M. (1990). GAP1, the general amino acid permease gene of Saccharomyces cerevisiae. Nucleotide sequence, protein similarity with the other bakers yeast amino acid permeases, and nitrogen catabolite repression. Eur J Biochem 190, 39-44.

Jiang, H., Tatchell, K., Liu, S., and Michels, C.A. (2000). Protein phosphatase type-1 regulatory subunits Reg1p and Reg2p act as signal transducers in the glucose-induced inactivation of maltose permease in Saccharomyces cerevisiae. Mol Gen Genet 263, 411-422.

Jiang, Y. (2006). Regulation of the cell cycle by protein phosphatase 2A in Saccharomyces cerevisiae. Microbiol Mol Biol Rev 70, 440-449.

Jiang, Y., and Broach, J.R. (1999). Tor proteins and protein phosphatase 2A reciprocally regulate Tap42 in controlling cell growth in yeast. EMBO J 18, 2782-2792.

Jules, M., Beltran, G., Francois, J., and Parrou, J.L. (2008). New insights into trehalose metabolism by Saccharomyces cerevisiae: NTH2 encodes a functional cytosolic trehalase, and deletion of TPS1 reveals Ath1p-dependent trehalose mobilization. Appl Environ Microbiol 74, 605-614.

Kaeberlein, M., Hu, D., Kerr, E.O., Tsuchiya, M., Westman, E.A., Dang, N., Fields, S., and Kennedy, B.K. (2005a). Increased life span due to calorie restriction in respiratory-deficient yeast. PLoS Genet 1, e69.

Kaeberlein, M., Powers, R.W., 3rd, Steffen, K.K., Westman, E.A., Hu, D., Dang, N., Kerr, E.O., Kirkland, K.T., Fields, S., and Kennedy, B.K. (2005b). Regulation of yeast replicative life span by TOR and Sch9 in response to nutrients. Science 310, 1193-1196.

Kirchhausen, T. (2007). Making COPII coats. Cell 129, 1251-1252.

Kleizen, B., and Braakman, I. (2004). Protein folding and quality control in the endoplasmic reticulum. Curr Opin Cell Biol 16, 343-349.

Kodama, Y., Omura, F., Takahashi, K., Shirahige, K., and Ashikari, T. (2002). Genome-wide expression analysis of genes affected by amino acid sensor Ssy1p in Saccharomyces cerevisiae. Curr Genet 41, 63-72.

Koren, R., Rainis, L., and Kleinberger, T. (2004). The scaffolding A/Tpd3 subunit and high phosphatase activity are dispensable for Cdc55 function in the Saccharomyces cerevisiae spindle checkpoint and in cytokinesis. J Biol Chem 279, 48598-48606.

Kota, J., and Ljungdahl, P.O. (2005). Specialized membrane-localized chaperones prevent aggregation of polytopic proteins in the ER. J Cell Biol 168, 79-88.

Kota, J., Melin-Larsson, M., Ljungdahl, P.O., and Forsberg, H. (2007). Ssh4, Rcr2 and Rcr1 affect plasma membrane transporter activity in Saccharomyces cerevisiae. Genetics 175, 1681-1694.

Kraakman, L., Lemaire, K., Ma, P., Teunissen, A.W., Donaton, M.C., Van Dijck, P., Winderickx, J., de Winde, J.H., and Thevelein, J.M. (1999). A Saccharomyces cerevisiae G-protein coupled receptor, Gpr1, is specifically required for glucose activation of the cAMP pathway during the transition to growth on glucose. Mol Microbiol 32, 1002-1012.

Kushner, D.B., Lindenbach, B.D., Grdzelishvili, V.Z., Noueiry, A.O., Paul, S.M., and Ahlquist, P. (2003). Systematic, genome-wide identification of host genes affecting replication of a positive-strand RNA virus. Proc Natl Acad Sci U S A 100, 15764-15769.

Lahav, R., Gammie, A., Tavazoie, S., and Rose, M.D. (2007). Role of transcription factor Kar4 in regulating downstream events in the Saccharomyces cerevisiae pheromone response pathway. Mol Cell Biol 27, 818-829.

Lakshmanan, J., Mosley, A.L., and Ozcan, S. (2003). Repression of transcription by Rgt1 in the absence of glucose requires Std1 and Mth1. Curr Genet 44, 19-25.

Lauwers, E., and Andre, B. (2006). Association of yeast transporters with detergent-resistant membranes correlates with their cell-surface location. Traffic 7, 1045-1059.

Lauwers, E., Grossmann, G., and Andre, B. (2007). Evidence for coupled biogenesis of yeast Gap1 permease and sphingolipids: essential role in transport activity and normal control by ubiquitination. Mol Biol Cell 18, 3068-3080.

Lauwers, E., Jacob, C., and Andre, B. (2009). K63-linked ubiquitin chains as a specific signal for protein sorting into the multivesicular body pathway. J Cell Biol 185, 493-502.

Lee, C.K., Shibata, Y., Rao, B., Strahl, B.D., and Lieb, J.D. (2004). Evidence for nucleosome depletion at active regulatory regions genome-wide. Nat Genet 36, 900-905.

Leggett, D.S., Hanna, J., Borodovsky, A., Crosas, B., Schmidt, M., Baker, R.T., Walz, T., Ploegh, H., and Finley, D. (2002). Multiple associated proteins regulate proteasome structure and function. Mol Cell 10, 495-507.

Lemaire, K., Van de Velde, S., Van Dijck, P., and Thevelein, J.M. (2004). Glucose and sucrose act as agonist and mannose as antagonist ligands of the G protein-coupled receptor Gpr1 in the yeast Saccharomyces cerevisiae. Mol Cell 16, 293-299.

Leulliot, N., Quevillon-Cheruel, S., Sorel, I., de La Sierra-Gallay, I.L., Collinet, B., Graille, M., Blondeau, K., Bettache, N., Poupon, A., Janin, J. (2004). Structure of protein phosphatase methyltransferase 1 (PPM1), a leucine carboxyl methyltransferase involved in the regulation of protein phosphatase 2A activity. J Biol Chem 279, 8351-8358.

Liu, X., Yang, H., Zhang, X., Liu, L., Lei, M., Zhang, Z., and Bao, X. (2009). Bdf1p deletion affects mitochondrial function and causes apoptotic cell death under salt stress. FEMS Yeast Res 9, 240-246.

Liu, X., and Zheng, X.F. (2007). Endoplasmic reticulum and Golgi localization sequences for mammalian target of rapamycin. Mol Biol Cell 18, 1073-1082.

Ljungdahl, P.O. (2009). Amino-acid-induced signalling via the SPS-sensing pathway in yeast. Biochem Soc Trans 37, 242-247.

Logan, M.R., Nguyen, T., Szapiel, N., Knockleby, J., Por, H., Zadworny, M., Neszt, M., Harrison, P., Bussey, H., Mandato, C.A. (2008). Genetic interaction network of the Saccharomyces cerevisiae type 1 phosphatase Glc7. BMC Genomics 9, 336.

Lu, A., and Hirsch, J.P. (2005). Cyclic AMP-independent regulation of protein kinase A substrate phosphorylation by Kelch repeat proteins. Eukaryot Cell 4, 1794-1800.

Lupashin, V.V., Hamamoto, S., and Schekman, R.W. (1996). Biochemical requirements for the targeting and fusion of ER-derived transport vesicles with purified yeast Golgi membranes. J Cell Biol 132, 277-289.

Ma, D., Zerangue, N., Lin, Y.F., Collins, A., Yu, M., Jan, Y.N., and Jan, L.Y. (2001). Role of ER export signals in controlling surface potassium channel numbers. Science 291, 316-319.

Ma, P., Wera, S., Van Dijck, P., and Thevelein, J.M. (1999). The PDE1-encoded low-affinity phosphodiesterase in the yeast Saccharomyces cerevisiae has a specific function in controlling agonist-induced cAMP signaling. Mol Biol Cell 10, 91-104.

MacKintosh, C., Beattie, K.A., Klumpp, S., Cohen, P., and Codd, G.A. (1990). Cyanobacterial microcystin-LR is a potent and specific inhibitor of protein phosphatases 1 and 2A from both mammals and higher plants. FEBS Lett 264, 187-192.

Magasanik, B., and Kaiser, C.A. (2002). Nitrogen regulation in Saccharomyces cerevisiae. Gene 290, 1-18.

Magazinnik, T., Anand, M., Sattlegger, E., Hinnebusch, A.G., and Kinzy, T.G. (2005). Interplay between GCN2 and GCN4 expression, translation elongation factor 1 mutations and translational fidelity in yeast. Nucleic Acids Res 33, 4584-4592.

Mahmud, S.A., Hirasawa, T., and Shimizu, H. (2010). Differential importance of trehalose accumulation in Saccharomyces cerevisiae in response to various environmental stresses. J Biosci Bioeng 109, 262-266.

Maidan, M.M., De Rop, L., Serneels, J., Exler, S., Rupp, S., Tournu, H., Thevelein, J.M., and Van Dijck, P. (2005). The G protein-coupled receptor Gpr1 and the Galpha protein Gpa2 act through the cAMP-protein kinase A pathway to induce morphogenesis in Candida albicans. Mol Biol Cell 16, 1971-1986.

Malkus, P., Jiang, F., and Schekman, R. (2002). Concentrative sorting of secretory cargo proteins into COPII-coated vesicles. J Cell Biol 159, 915-921.

Mamoun, C.B., Beckerich, J.M., Gaillardin, C., and Kepes, F. (1999). Disruption of YHC8, a member of the TSR1 gene family, reveals its direct involvement in yeast protein translocation. J Biol Chem 274, 11296-11302.

Marbach, I., Licht, R., Frohnmeyer, H., and Engelberg, D. (2001). Gcn2 mediates Gcn4 activation in response to glucose stimulation or UV radiation not via GCN4 translation. J Biol Chem 276, 16944-16951.

Martinez-Pastor, M.T., Marchler, G., Schuller, C., Marchler-Bauer, A., Ruis, H., and Estruch, F. (1996). The Saccharomyces cerevisiae zinc finger proteins Msn2p and Msn4p are required for transcriptional induction through the stress response element (STRE). EMBO J 15, 2227-2235.

Martzen, M.R., McCraith, S.M., Spinelli, S.L., Torres, F.M., Fields, S., Grayhack, E.J., and Phizicky, E.M. (1999). A biochemical genomics approach for identifying genes by the activity of their products. Science 286, 1153-1155.

Marzioch, M., Henthorn, D.C., Herrmann, J.M., Wilson, R., Thomas, D.Y., Bergeron, J.J., Solari, R.C., and Rowley, A. (1999). Erp1p and Erp2p, partners for Emp24p and Erv25p in a yeast p24 complex. Mol Biol Cell 10, 1923-1938.

Mascarenhas, C., Edwards-Ingram, L.C., Zeef, L., Shenton, D., Ashe, M.P., and Grant, C.M. (2008). Gcn4 is required for the response to peroxide stress in the yeast Saccharomyces cerevisiae. Mol Biol Cell 19, 2995-3007.

Matsumoto, K., Uno, I., Ishikawa, T., and Oshima, Y. (1983). Cyclic AMP may not be involved in catabolite repression in Saccharomyces cerevisiae: evidence from mutants unable to synthesize it. J Bacteriol 156, 898-900.

McNew, J.A., Coe, J.G., Sogaard, M., Zemelman, B.V., Wimmer, C., Hong, W., and Sollner, T.H. (1998). Gos1p, a Saccharomyces cerevisiae SNARE protein involved in Golgi transport. FEBS Lett 435, 89-95.

McNew, J.A., Sogaard, M., Lampen, N.M., Machida, S., Ye, R.R., Lacomis, L., Tempst, P., Rothman, J.E., and Sollner, T.H. (1997). Ykt6p, a prenylated SNARE essential for endoplasmic reticulum-Golgi transport. J Biol Chem 272, 17776-17783.

Menant, A., Barbey, R., and Thomas, D. (2006). Substrate-mediated remodeling of methionine transport by multiple ubiquitin-dependent mechanisms in yeast cells. EMBO J 25, 4436-4447.

Millward, T.A., Zolnierowicz, S., and Hemmings, B.A. (1999). Regulation of protein kinase cascades by protein phosphatase 2A. Trends Biochem Sci 24, 186-191.

Mitsuzawa, H. (1993). Responsiveness to exogenous cAMP of a Saccharomyces cerevisiae strain conferred by naturally occurring alleles of PDE1 and PDE2. Genetics 135, 321-326.

Moorhead, G.B., Trinkle-Mulcahy, L., and Ulke-Lemee, A. (2007). Emerging roles of nuclear protein phosphatases. Nat Rev Mol Cell Biol 8, 234-244.

Moskvina, E., Schuller, C., Maurer, C.T., Mager, W.H., and Ruis, H. (1998). A search in the genome of Saccharomyces cerevisiae for genes regulated via stress response elements. Yeast 14, 1041-1050.

Moy, T.I., and Silver, P.A. (1999). Nuclear export of the small ribosomal subunit requires the ran-GTPase cycle and certain nucleoporins. Genes Dev 13, 2118-2133.

Nelson, S.F., McCusker, J.H., Sander, M.A., Kee, Y., Modrich, P., and Brown, P.O. (1993). Genomic mismatch scanning: a new approach to genetic linkage mapping. Nat Genet 4, 11-18.

Nikko, E., and Andre, B. (2007a). Evidence for a direct role of the Doa4 deubiquitinating enzyme in protein sorting into the MVB pathway. Traffic 8, 566-581.

Nikko, E., and Andre, B. (2007b). Split-ubiquitin two-hybrid assay to analyze protein-protein interactions at the endosome: application to Saccharomyces cerevisiae Bro1 interacting with ESCRT complexes, the Doa4 ubiquitin hydrolase, and the Rsp5 ubiquitin ligase. Eukaryot Cell 6, 1266-1277.

Niranjan, T., Guo, X., Victor, J., Lu, A., and Hirsch, J.P. (2007). Kelch repeat protein interacts with the yeast Galpha subunit Gpa2p at a site that couples receptor binding to guanine nucleotide exchange. J Biol Chem 282, 24231-24238.

Nothwehr, S.F., Ha, S.A., and Bruinsma, P. (2000). Sorting of yeast membrane proteins into an endosome-to-Golgi pathway involves direct interaction of their cytosolic domains with Vps35p. J Cell Biol 151, 297-310.

Ogris, E., Du, X., Nelson, K.C., Mak, E.K., Yu, X.X., Lane, W.S., and Pallas, D.C. (1999). A protein phosphatase methylesterase (PME-1) is one of several novel proteins stably associating with two inactive mutants of protein phosphatase 2A. J Biol Chem 274, 14382-14391.

Orlova, M., Barrett, L., and Kuchin, S. (2008). Detection of endogenous Snf1 and its activation state: application to Saccharomyces and Candida species. Yeast 25, 745-754.

Ouyang, Y., Xu, Q., Mitsui, K., Motizuki, M., and Xu, Z. (2009). Human trehalase is a stress responsive protein in Saccharomyces cerevisiae. Biochem Biophys Res Commun 379, 621-625.

Pal, G., Paraz, M.T., and Kellogg, D.R. (2008). Regulation of Mih1/Cdc25 by protein phosphatase 2A and casein kinase 1. J Cell Biol 180, 931-945.

Palmer, D.A., Thompson, J.K., Li, L., Prat, A., and Wang, P. (2006). Gib2, a novel Gbeta-like/RACK1 homolog, functions as a Gbeta subunit in cAMP signaling and is essential in Cryptococcus neoformans. J Biol Chem 281, 32596-32605.

Parlati, F., Varlamov, O., Paz, K., McNew, J.A., Hurtado, D., Sollner, T.H., and Rothman, J.E. (2002). Distinct SNARE complexes mediating membrane fusion in Golgi transport based on combinatorial specificity. Proc Natl Acad Sci U S A 99, 5424-5429.

Parsons, A.B., Geyer, R., Hughes, T.R., and Boone, C. (2003). Yeast genomics and proteomics in drug discovery and target validation. Prog Cell Cycle Res 5, 159-166.

Paumi, C.M., Chuk, M., Snider, J., Stagljar, I., and Michaelis, S. (2009). ABC transporters in Saccharomyces cerevisiae and their interactors: new technology advances the biology of the ABCC (MRP) subfamily. Microbiol Mol Biol Rev 73, 577-593.

Pedelini, L., Marquina, M., Arino, J., Casamayor, A., Sanz, L., Bollen, M., Sanz, P., and Garcia-Gimeno, M.A. (2007). YPI1 and SDS22 proteins regulate the nuclear localization and function of yeast type 1 phosphatase Glc7. J Biol Chem 282, 3282-3292.

Peeters, T., Louwet, W., Gelade, R., Nauwelaers, D., Thevelein, J.M., and Versele, M. (2006). Kelch-repeat proteins interacting with the Galpha protein Gpa2 bypass adenylate cyclase for direct regulation of protein kinase A in yeast. Proc Natl Acad Sci U S A 103, 13034-13039.

Peeters, T., Versele, M., and Thevelein, J.M. (2007). Directly from Galpha to protein kinase A: the kelch repeat protein bypass of adenylate cyclase. Trends Biochem Sci 32, 547-554.

Peggie, M.W., MacKelvie, S.H., Bloecher, A., Knatko, E.V., Tatchell, K., and Stark, M.J. (2002). Essential functions of Sds22p in chromosome stability and nuclear localization of PP1. J Cell Sci 115, 195-206.

Pety de Thozee, C., and Ghislain, M. (2006). ER-associated degradation of membrane proteins in yeast. ScientificWorldJournal 6, 967-983.

Pfund, C., Lopez-Hoyo, N., Ziegelhoffer, T., Schilke, B.A., Lopez-Buesa, P., Walter, W.A., Wiedmann, M., and Craig, E.A. (1998). The molecular chaperone Ssb from Saccharomyces cerevisiae is a component of the ribosome-nascent chain complex. EMBO J 17, 3981-3989.

Pineau, L., Bonifait, L., Berjeaud, J.M., Alimardani-Theuil, P., Berges, T., and Ferreira, T. (2008). A lipid-mediated quality control process in the Golgi apparatus in yeast. Mol Biol Cell 19, 807-821.

Popova, Y., Thayumanavan, P., Lonati, E., Agrochao, M., and Thevelein, J.M. (2010). Transport and signaling through the phosphate-binding site of the yeast Pho84 phosphate transceptor. Proc Natl Acad Sci U S A 107, 2890-2895.

Portela, P., and Moreno, S. (2006). Glucose-dependent activation of protein kinase A activity in Saccharomyces cerevisiae and phosphorylation of its TPK1 catalytic subunit. Cell Signal 18, 1072-1086.

Poulsen, P., Wu, B., Gaber, R.F., and Kielland-Brandt, M.C. (2005). Constitutive signal transduction by mutant Ssy5p and Ptr3p components of the SPS amino acid sensor system in Saccharomyces cerevisiae. Eukaryot Cell 4, 1116-1124.

Ptacek, J., Devgan, G., Michaud, G., Zhu, H., Zhu, X., Fasolo, J., Guo, H., Jona, G., Breitkreutz, A., Sopko, R. (2005). Global analysis of protein phosphorylation in yeast. Nature 438, 679-684.

Ramaswamy, N.T., Li, L., Khalil, M., and Cannon, J.F. (1998). Regulation of yeast glycogen metabolism and sporulation by Glc7p protein phosphatase. Genetics 149, 57-72.

Reddy, J.V., and Seaman, M.N. (2001). Vps26p, a component of retromer, directs the interactions of Vps35p in endosome-to-Golgi retrieval. Mol Biol Cell 12, 3242-3256.

Regenberg, B., and Hansen, J. (2000). GAP1, a novel selection and counter-selection marker for multiple gene disruptions in Saccharomyces cerevisiae. Yeast 16, 1111-1119.

Risinger, A.L., Cain, N.E., Chen, E.J., and Kaiser, C.A. (2006). Activity-dependent reversible inactivation of the general amino acid permease. Mol Biol Cell 17, 4411-4419.

Risinger, A.L., and Kaiser, C.A. (2008). Different ubiquitin signals act at the Golgi and plasma membrane to direct GAP1 trafficking. Mol Biol Cell 19, 2962-2972.

Roberg, K.J., Bickel, S., Rowley, N., and Kaiser, C.A. (1997). Control of amino acid permease sorting in the late secretory pathway of Saccharomyces cerevisiae by SEC13, LST4, LST7 and LST8. Genetics 147, 1569-1584.

Robertson, L.S., Causton, H.C., Young, R.A., and Fink, G.R. (2000). The yeast A kinases differentially regulate iron uptake and respiratory function. Proc Natl Acad Sci U S A 97, 5984-5988.

Robertson, L.S., and Fink, G.R. (1998). The three yeast A kinases have specific signaling functions in pseudohyphal growth. Proc Natl Acad Sci U S A 95, 13783-13787.

Rohde, J.R., Bastidas, R., Puria, R., and Cardenas, M.E. (2008). Nutritional control via Tor signaling in Saccharomyces cerevisiae. Curr Opin Microbiol 11, 153-160.

Rolland, F., De Winde, J.H., Lemaire, K., Boles, E., Thevelein, J.M., and Winderickx, J. (2000). Glucose-induced cAMP signalling in yeast requires both a G-protein coupled receptor system for extracellular glucose detection and a separable hexose kinase-dependent sensing process. Mol Microbiol 38, 348-358.

Rolland, F., Wanke, V., Cauwenberg, L., Ma, P., Boles, E., Vanoni, M., de Winde, J.H., Thevelein, J.M., and Winderickx, J. (2001). The role of hexose transport and phosphorylation in cAMP signalling in the yeast Saccharomyces cerevisiae. FEMS Yeast Res 1, 33-45.

Rolland, F., Winderickx, J., and Thevelein, J.M. (2002). Glucose-sensing and -signalling mechanisms in yeast. FEMS Yeast Res 2, 183-201.

Ronald, J., Brem, R.B., Whittle, J., and Kruglyak, L. (2005). Local regulatory variation in Saccharomyces cerevisiae. PLoS Genet 1, e25.

Rose, M.D., Novick, P., Thomas, J.H., Botstein, D., and Fink, G.R. (1987). A Saccharomyces cerevisiae genomic plasmid bank based on a centromere-containing shuttle vector. Gene 60, 237-243.

Rowen, D.W., Meinke, M., and LaPorte, D.C. (1992). GLC3 and GHA1 of Saccharomyces cerevisiae are allelic and encode the glycogen branching enzyme. Mol Cell Biol 12, 22-29.

Rubenstein, E.M., McCartney, R.R., Zhang, C., Shokat, K.M., Shirra, M.K., Arndt, K.M., and Schmidt, M.C. (2008). Access denied: Snf1 activation loop phosphorylation is controlled by availability of the phosphorylated threonine 210 to the PP1 phosphatase. J Biol Chem 283, 222-230.

Rubio-Texeira, M., and Kaiser, C.A. (2006). Amino acids regulate retrieval of the yeast general amino acid permease from the vacuolar targeting pathway. Mol Biol Cell 17, 3031-3050.

Rubio-Texeira, M., Van Zeebroeck, G., Voordeckers, K., and Thevelein, J.M. (2010). Saccharomyces cerevisiae plasma membrane nutrient sensors and their role in PKA signaling. FEMS Yeast Res 10, 134-149.

Ruis, H., and Schuller, C. (1995). Stress signaling in yeast. Bioessays 17, 959-965.

Salama, N.R., and Schekman, R.W. (1995). The role of coat proteins in the biosynthesis of secretory proteins. Curr Opin Cell Biol 7, 536-543.

Sambrook, J., Frisch, E.F., and Maniatis, T. (1989). Molecular cloning: a laboratory manual. Cold Spring Harbor Laboratory Press, Cold Spring Harbor, NY.

Santoyo, J., Alcalde, J., Mendez, R., Pulido, D., and de Haro, C. (1997). Cloning and characterization of a cDNA encoding a protein synthesis initiation factor-2alpha (eIF-2alpha) kinase from Drosophila melanogaster. Homology To yeast GCN2 protein kinase. J Biol Chem 272, 12544-12550.

Sato, K., and Nakano, A. (2007). Mechanisms of COPII vesicle formation and protein sorting. FEBS Lett 581, 2076-2082.

Schmelzle, T., Beck, T., Martin, D.E., and Hall, M.N. (2004). Activation of the RAS/cyclic AMP pathway suppresses a TOR deficiency in yeast. Mol Cell Biol 24, 338-351.

Schmitt, A.P., and McEntee, K. (1996). Msn2p, a zinc finger DNA-binding protein, is the transcriptional activator of the multistress response in Saccharomyces cerevisiae. Proc Natl Acad Sci U S A 93, 5777-5782.

Schneper, L., Duvel, K., and Broach, J.R. (2004). Sense and sensibility: nutritional response and signal integration in yeast. Curr Opin Microbiol 7, 624-630.

Seaman, M.N. (2004). Cargo-selective endosomal sorting for retrieval to the Golgi requires retromer. J Cell Biol 165, 111-122.

Seaman, M.N. (2006). Endosome sorting: GSE complex minds the Gap. Nat Cell Biol 8, 648-649.

Seaman, M.N. (2008). Endosome protein sorting: motifs and machinery. Cell Mol Life Sci 65, 2842-2858.

Seaman, M.N., McCaffery, J.M., and Emr, S.D. (1998). A membrane coat complex essential for endosome-to-Golgi retrograde transport in yeast. J Cell Biol 142, 665-681.

Segal, S.P., Dunckley, T., and Parker, R. (2006). Sbp1p affects translational repression and decapping in Saccharomyces cerevisiae. Mol Cell Biol 26, 5120-5130.

Segre, A.V., Murray, A.W., and Leu, J.Y. (2006). High-resolution mutation mapping reveals parallel experimental evolution in yeast. PLoS Biol 4, e256.

Shemer, R., Meimoun, A., Holtzman, T., and Kornitzer, D. (2002). Regulation of the transcription factor Gcn4 by Pho85 cyclin PCL5. Mol Cell Biol 22, 5395-5404.

Sherman, F., and Hicks, J. (1991). Micromanipulation and dissection of asci. Methods Enzymol 194, 21-37.

Shi, Y. (2009). Assembly and structure of protein phosphatase 2A. Sci China C Life Sci 52, 135-146.

Shirra, M.K., McCartney, R.R., Zhang, C., Shokat, K.M., Schmidt, M.C., and Arndt, K.M. (2008). A chemical genomics study identifies Snf1 as a repressor of GCN4 translation. J Biol Chem 283, 35889-35898.

Shu, Y., Yang, H., Hallberg, E., and Hallberg, R. (1997). Molecular genetic analysis of Rts1p, a B' regulatory subunit of Saccharomyces cerevisiae protein phosphatase 2A. Mol Cell Biol 17, 3242-3253.

Simola, M., Hanninen, A.L., Stranius, S.M., and Makarow, M. (2000). Trehalose is required for conformational repair of heat-denatured proteins in the yeast endoplasmic reticulum but not for maintenance of membrane traffic functions after severe heat stress. Mol Microbiol 37, 42-53.

Smets, B., De Snijder, P., Engelen, K., Joossens, E., Ghillebert, R., Thevissen, K., Marchal, K., and Winderickx, J. (2008). Genome-wide expression analysis reveals TORC1-dependent and -independent functions of Sch9. FEMS Yeast Res 8, 1276-1288.

Smith, A., Ward, M.P., and Garrett, S. (1998). Yeast PKA represses Msn2p/Msn4p-dependent gene expression to regulate growth, stress response and glycogen accumulation. EMBO J 17, 3556-3564.

Smith, C.L., Horowitz-Scherer, R., Flanagan, J.F., Woodcock, C.L., and Peterson, C.L. (2003). Structural analysis of the yeast SWI/SNF chromatin remodeling complex. Nat Struct Biol 10, 141-145.

Soetens, O., De Craene, J.O., and Andre, B. (2001). Ubiquitin is required for sorting to the vacuole of the yeast general amino acid permease, Gap1. J Biol Chem 276, 43949-43957.

Somers, I. (2006). Sch9 kinase control and glucose-induced stimulation of protein phosphatases in yeast. KU Leuven.

Sood, R., Porter, A.C., Olsen, D.A., Cavener, D.R., and Wek, R.C. (2000). A mammalian homologue of GCN2 protein kinase important for translational control by phosphorylation of eukaryotic initiation factor-2alpha. Genetics 154, 787-801.

Spang, A. (2009). On vesicle formation and tethering in the ER-Golgi shuttle. Curr Opin Cell Biol 21, 531-536.

Spear, E.D., and Ng, D.T. (2003). Stress tolerance of misfolded carboxypeptidase Y requires maintenance of protein trafficking and degradative pathways. Mol Biol Cell 14, 2756-2767.

Springael, J.Y., and Andre, B. (1998). Nitrogen-regulated ubiquitination of the Gap1 permease of Saccharomyces cerevisiae. Mol Biol Cell 9, 1253-1263.

Springer, S., Chen, E., Duden, R., Marzioch, M., Rowley, A., Hamamoto, S., Merchant, S., and Schekman, R. (2000). The p24 proteins are not essential for vesicular transport in Saccharomyces cerevisiae. Proc Natl Acad Sci U S A 97, 4034-4039.

Stanbrough, M., Rowen, D.W., and Magasanik, B. (1995). Role of the GATA factors Gln3p and Nil1p of Saccharomyces cerevisiae in the expression of nitrogen-regulated genes. Proc Natl Acad Sci U S A 92, 9450-9454.

Stanhill, A., Schick, N., and Engelberg, D. (1999). The yeast ras/cyclic AMP pathway induces invasive growth by suppressing the cellular stress response. Mol Cell Biol 19, 7529-7538.

Stark, M.J. (1996). Yeast protein serine/threonine phosphatases: multiple roles and diverse regulation. Yeast 12, 1647-1675.

Staub, O., and Rotin, D. (2006). Role of ubiquitylation in cellular membrane transport. Physiol Rev 86, 669-707.

Steinmetz, L.M., Sinha, H., Richards, D.R., Spiegelman, J.I., Oefner, P.J., McCusker, J.H., and Davis, R.W. (2002). Dissecting the architecture of a quantitative trait locus in yeast. Nature 416, 326-330.

Sturgeon, C.M., Kemmer, D., Anderson, H.J., and Roberge, M. (2006). Yeast as a tool to uncover the cellular targets of drugs. Biotechnol J 1, 289-298.

Sturgill, T.W., Cohen, A., Diefenbacher, M., Trautwein, M., Martin, D.E., and Hall, M.N. (2008). TOR1 and TOR2 have distinct locations in live cells. Eukaryot Cell 7, 1819-1830.

Sugajska, E., Swiatek, W., Zabrocki, P., Geyskens, I., Thevelein, J.M., Zolnierowicz, S., and Wera, S. (2001). Multiple effects of protein phosphatase 2A on nutrient-induced signalling in the yeast Saccharomyces cerevisiae. Mol Microbiol 40, 1020-1026.

Svetlov, V.V., and Cooper, T.G. (1998). The Saccharomyces cerevisiae GATA factors Dal80p and Deh1p can form homo- and heterodimeric complexes. J Bacteriol 180, 5682-5688.

Takahashi, M., Shibata, H., Shimakawa, M., Miyamoto, M., Mukai, H., and Ono, Y. (1999). Characterization of a novel giant scaffolding protein, CG-NAP, that anchors multiple signaling enzymes to centrosome and the golgi apparatus. J Biol Chem 274, 17267-17274.

Tapia, H., and Morano, K.A. (2010). Hsp90 nuclear accumulation in quiescence is linked to chaperone function and spore development in yeast. Mol Biol Cell 21, 63-72.

Tate, J.J., and Cooper, T.G. (2007). Stress-responsive Gln3 localization in Saccharomyces cerevisiae is separable from and can overwhelm nitrogen source regulation. J Biol Chem 282, 18467-18480.

Tate, J.J., Feller, A., Dubois, E., and Cooper, T.G. (2006a). Saccharomyces cerevisiae Sit4 phosphatase is active irrespective of the nitrogen source provided, and Gln3 phosphorylation levels become nitrogen source-responsive in a sit4-deleted strain. J Biol Chem 281, 37980-37992.

Tate, J.J., Georis, I., Feller, A., Dubois, E., and Cooper, T.G. (2009). Rapamycin-induced Gln3 dephosphorylation is insufficient for nuclear localization: Sit4 and PP2A phosphatases are regulated and function differently. J Biol Chem 284, 2522-2534.

Tate, J.J., Rai, R., and Cooper, T.G. (2006b). Ammonia-specific regulation of Gln3 localization in Saccharomyces cerevisiae by protein kinase Npr1. J Biol Chem 281, 28460-28469.

Thevelein, J.M. (1994). Signal transduction in yeast. Yeast 10, 1753-1790.

Thevelein, J.M., Beullens, M., Honshoven, F., Hoebeeck, G., Detremerie, K., Griewel, B., den Hollander, J.A., and Jans, A.W. (1987). Regulation of the cAMP level in the yeast Saccharomyces cerevisiae: the glucose-induced cAMP signal is not mediated by a transient drop in the intracellular pH. J Gen Microbiol 133, 2197-2205.

Thevelein, J.M., Bonini, B.M., Castermans, D., Haesendonckx, S., Kriel, J., Louwet, W., Thayumanavan, P., Popova, Y., Rubio-Texeira, M., Schepers, W. (2008). Novel mechanisms in nutrient activation of the yeast protein kinase A pathway. Acta Microbiol Immunol Hung 55, 75-89.

Thevelein, J.M., Cauwenberg, L., Colombo, S., De Winde, J.H., Donation, M., Dumortier, F., Kraakman, L., Lemaire, K., Ma, P., Nauwelaers, D. (2000). Nutrient-induced signal transduction through the protein kinase A pathway and its role in the control of metabolism, stress resistance, and growth in yeast. Enzyme Microb Technol 26, 819-825.

Thevelein, J.M., and de Winde, J.H. (1999). Novel sensing mechanisms and targets for the cAMP-protein kinase A pathway in the yeast Saccharomyces cerevisiae. Mol Microbiol 33, 904-918.

Thevelein, J.M., Gelade, R., Holsbeeks, I., Lagatie, O., Popova, Y., Rolland, F., Stolz, F., Van de Velde, S., Van Dijck, P., Vandormael, P. (2005). Nutrient sensing systems for rapid activation of the protein kinase A pathway in yeast. Biochem Soc Trans 33, 253-256.

Thevelein, J.M., and Voordeckers, K. (2009). Functioning and evolutionary significance of nutrient transceptors. Mol Biol Evol 26, 2407-2414.

Tirupati, H.K., Shaw, L.C., and Lewin, A.S. (1999). An RNA binding motif in the Cbp2 protein required for protein-stimulated RNA catalysis. J Biol Chem 274, 30393-30401.

Toda, T., Cameron, S., Sass, P., Zoller, M., Scott, J.D., McMullen, B., Hurwitz, M., Krebs, E.G., and Wigler, M. (1987a). Cloning and characterization of BCY1, a locus encoding a regulatory subunit of the cyclic AMP-dependent protein kinase in Saccharomyces cerevisiae. Mol Cell Biol 7, 1371-1377.

Toda, T., Cameron, S., Sass, P., Zoller, M., and Wigler, M. (1987b). Three different genes in S. cerevisiae encode the catalytic subunits of the cAMP-dependent protein kinase. Cell 50, 277-287.

Tokiwa, G., Tyers, M., Volpe, T., and Futcher, B. (1994). Inhibition of G1 cyclin activity by the Ras/cAMP pathway in yeast. Nature 371, 342-345.

Tu, J., Song, W., and Carlson, M. (1996). Protein phosphatase type 1 interacts with proteins required for meiosis and other cellular processes in Saccharomyces cerevisiae. Mol Cell Biol 16, 4199-4206.

Tung, H.Y., Wang, W., and Chan, C.S. (1995). Regulation of chromosome segregation by Glc8p, a structural homolog of mammalian inhibitor 2 that functions as both an activator and an inhibitor of yeast protein phosphatase 1. Mol Cell Biol 15, 6064-6074.

Urban, J., Soulard, A., Huber, A., Lippman, S., Mukhopadhyay, D., Deloche, O., Wanke, V., Anrather, D., Ammerer, G., Riezman, H., Broach, J.R., De Virgilio, C., Hall, M.N. and Loewith, R. (2007). Sch9 is a major target of TORC1 in Saccharomyces cerevisiae. Mol Cell 26, 663-674.

Van de Velde, S., and Thevelein, J.M. (2008). Cyclic AMP-protein kinase A and Snf1 signaling mechanisms underlie the superior potency of sucrose for induction of filamentation in Saccharomyces cerevisiae. Eukaryot Cell 7, 286-293.

Van Dijck, P. (2009). Nutrient sensing G protein-coupled receptors: interesting targets for antifungals? Med Mycol 47, 671-680.

Van Hoof, C., Janssens, V., De Baere, I., Stark, M.J., de Winde, J.H., Winderickx, J., Thevelein, J.M., Merlevede, W., and Goris, J. (2001). The Saccharomyces cerevisiae phosphotyrosyl phosphatase activator proteins are required for a subset of the functions disrupted by protein phosphatase 2A mutations. Exp Cell Res 264, 372-387.

Van Hoof, C., Martens, E., Longin, S., Jordens, J., Stevens, I., Janssens, V., and Goris, J. (2005). Specific interactions of PP2A and PP2A-like phosphatases with the yeast PTPA homologues, Ypa1 and Ypa2. Biochem J 386, 93-102.

Van Nuland, A., Vandormael, P., Donaton, M., Alenquer, M., Lourenco, A., Quintino, E., Versele, M., and Thevelein, J.M. (2006). Ammonium permease-based sensing mechanism for rapid ammonium activation of the protein kinase A pathway in yeast. Mol Microbiol 59, 1485-1505.

Van Zeebroeck, G., Bonini, B.M., Versele, M., and Thevelein, J.M. (2009). Transport and signaling via the amino acid binding site of the yeast Gap1 amino acid transceptor. Nat Chem Biol 5, 45-52.

Varlamov, O., Volchuk, A., Rahimian, V., Doege, C.A., Paumet, F., Eng, W.S., Arango, N., Parlati, F., Ravazzola, M., Orci, L. (2004). i-SNAREs: inhibitory SNAREs that fine-tune the specificity of membrane fusion. J Cell Biol 164, 79-88.

Vattem, K.M., and Wek, R.C. (2004). Reinitiation involving upstream ORFs regulates ATF4 mRNA translation in mammalian cells. Proc Natl Acad Sci U S A 101, 11269-11274.

Versele, M., de Winde, J.H., and Thevelein, J.M. (1999). A novel regulator of G protein signalling in yeast, Rgs2, downregulates glucose-activation of the cAMP pathway through direct inhibition of Gpa2. EMBO J 18, 5577-5591.

Virshup, D.M., and Shenolikar, S. (2009). From promiscuity to precision: protein phosphatases get a makeover. Mol Cell 33, 537-545.

Volchuk, A., Ravazzola, M., Perrelet, A., Eng, W.S., Di Liberto, M., Varlamov, O., Fukasawa, M., Engel, T., Sollner, T.H., Rothman, J.E. (2004). Countercurrent distribution of two distinct SNARE complexes mediating transport within the Golgi stack. Mol Biol Cell 15, 1506-1518.

Walsh, E.P., Lamont, D.J., Beattie, K.A., and Stark, M.J. (2002). Novel interactions of Saccharomyces cerevisiae type 1 protein phosphatase identified by single-step affinity purification and mass spectrometry. Biochemistry 41, 2409-2420.

Walsh, P., Bursac, D., Law, Y.C., Cyr, D., and Lithgow, T. (2004). The J-protein family: modulating protein assembly, disassembly and translocation. EMBO Rep 5, 567-571.

Wang, D., Sung, H.M., Wang, T.Y., Huang, C.J., Yang, P., Chang, T., Wang, Y.C., Tseng, D.L., Wu, J.P., Lee, T.C., Shih, M.C., and Li, W.H. (2007). Expression evolution in yeast genes of single-input modules is mainly due to changes in trans-acting factors. Genome Res 8, 1161-1169.

Wang, H., and Jiang, Y. (2003). The Tap42-protein phosphatase type 2A catalytic subunit complex is required for cell cycle-dependent distribution of actin in yeast. Mol Cell Biol 23, 3116-3125.

Wang, H., Wang, X., and Jiang, Y. (2003). Interaction with Tap42 is required for the essential function of Sit4 and type 2A phosphatases. Mol Biol Cell 14, 4342-4351.

Wang, Y., and Price, M.A. (2008). A unique protection signal in Cubitus interruptus prevents its complete proteasomal degradation. Mol Cell Biol 28, 5555-5568.

Watanabe, R., Castillon, G.A., Meury, A., and Riezman, H. (2008). The presence of an ER exit signal determines the protein sorting upon ER exit in yeast. Biochem J 414, 237-245.

Watanabe, R., and Riezman, H. (2004). Differential ER exit in yeast and mammalian cells. Curr Opin Cell Biol 16, 350-355.

Wei, H., Ashby, D.G., Moreno, C.S., Ogris, E., Yeong, F.M., Corbett, A.H., and Pallas, D.C. (2001). Carboxymethylation of the PP2A catalytic subunit in Saccharomyces cerevisiae is required for efficient interaction with the B-type subunits Cdc55p and Rts1p. J Biol Chem 276, 1570-1577.

Weinberger, A., Kamena, F., Kama, R., Spang, A., and Gerst, J.E. (2005). Control of Golgi morphology and function by Sed5 t-SNARE phosphorylation. Mol Biol Cell 16, 4918-4930.

Wiatrowski, H.A., and Carlson, M. (2001). Identification of a mutant locus by noncomplementation of a transposon insertion library in Saccharomyces cerevisiae. Genetics 158, 1825-1827.

Williams-Hart, T., Wu, X., and Tatchell, K. (2002). Protein phosphatase type 1 regulates ion homeostasis in Saccharomyces cerevisiae. Genetics 160, 1423-1437.

Wilson, W.A., and Roach, P.J. (2002). Nutrient-regulated protein kinases in budding yeast. Cell 111, 155-158.

Wong, K.H., Hynes, M.J., and Davis, M.A. (2008). Recent advances in nitrogen regulation: a comparison between Saccharomyces cerevisiae and filamentous fungi. Eukaryot Cell 7, 917-925.

Wu, J., Tolstykh, T., Lee, J., Boyd, K., Stock, J.B., and Broach, J.R. (2000). Carboxyl methylation of the phosphoprotein phosphatase 2A catalytic subunit promotes its functional association with regulatory subunits in vivo. EMBO J 19, 5672-5681.

Wu, X., Hart, H., Cheng, C., Roach, P.J., and Tatchell, K. (2001). Characterization of Gac1p, a regulatory subunit of protein phosphatase type I involved in glycogen accumulation in Saccharomyces cerevisiae. Mol Genet Genomics 265, 622-635.

Xing, Y., Li, Z., Chen, Y., Stock, J.B., Jeffrey, P.D., and Shi, Y. (2008). Structural mechanism of demethylation and inactivation of protein phosphatase 2A. Cell 133, 154-163.

Yan, G., Shen, X., and Jiang, Y. (2006). Rapamycin activates Tap42-associated phosphatases by abrogating their association with Tor complex 1. EMBO J 25, 3546-3555.

Yang, H., Jiang, W., Gentry, M., and Hallberg, R.L. (2000a). Loss of a protein phosphatase 2A regulatory subunit (Cdc55p) elicits improper regulation of Swe1p degradation. Mol Cell Biol 20, 8143-8156.

Yang, R., Wek, S.A., and Wek, C.A. (2000b). Glucose limitation induces GCN4 translation by activation of Gcn2 protein kinase. Mol Cell Biol 20, 2706-2717.

Yang, J., Roe, S.M., Prickett, T.D., Brautigan, D.L., and Barford, D. (2007). The structure of Tap42/alpha4 reveals a tetratricopeptide repeat-like fold and provides insights into PP2A regulation. Biochemistry 46, 8807-8815.

Yorimitsu, T., Zaman, S., Broach, J.R., and Klionsky, D.J. (2007). Protein kinase A and Sch9 cooperatively regulate induction of autophagy in Saccharomyces cerevisiae. Mol Biol Cell 18, 4180-4189.

Yvert, G., Brem, R.B., Whittle, J., Akey, J.M., Foss, E., Smith, E.N., Mackelprang, R., and Kruglyak, L. (2003). Trans-acting regulatory variation in Saccharomyces cerevisiae and the role of transcription factors. Nat Genet 35, 57-64.

Zabrocki, P., Swiatek, W., Sugajska, E., Thevelein, J.M., Wera, S., and Zolnierowicz, S. (2002a). The Saccharomyces cerevisiae type 2A protein phosphatase Pph22p is biochemically different from mammalian PP2A. Eur J Biochem 269, 3372-3382.

Zabrocki, P., Van Hoof, C., Goris, J., Thevelein, J.M., Winderickx, J., and Wera, S. (2002b). Protein phosphatase 2A on track for nutrient-induced signalling in yeast. Mol Microbiol 43, 835-842.

Zaman, S., Lippman, S.I., Zhao, X., and Broach, J.R. (2008). How Saccharomyces responds to nutrients. Annu Rev Genet 42, 27-81.

Zargari, A., Boban, M., Heessen, S., Andreasson, C., Thyberg, J., and Ljungdahl, P.O. (2007). Inner nuclear membrane proteins Asi1, Asi2, and Asi3 function in concert to maintain the latent properties of transcription factors Stp1 and Stp2. J Biol Chem 282, 594-605.

Zhang, S., Guha, S., and Volkert, F.C. (1995). The Saccharomyces SHP1 gene, which encodes a regulator of phosphoprotein phosphatase 1 with differential effects on glycogen metabolism, meiotic differentiation, and mitotic cell cycle progression. Mol Cell Biol 15, 2037-2050.

Zhao, Y., McIntosh, K.B., Rudra, D., Schawalder, S., Shore, D., and Warner, J.R. (2006). Fine-structure analysis of ribosomal protein gene transcription. Mol Cell Biol 26, 4853-4862.

Zheng, Y., and Jiang, Y. (2005). The yeast phosphotyrosyl phosphatase activator is part of the Tap42-phosphatase complexes. Mol Biol Cell 16, 2119-2127.

Zu, T., Verna, J., and Ballester, R. (2001). Mutations in WSC genes for putative stress receptors result in sensitivity to multiple stress conditions and impairment of Rlm1-dependent gene expression in Saccharomyces cerevisiae. Mol Genet Genomics 266, 142-155.

Zurita-Martinez, S.A., and Cardenas, M.E. (2005). Tor and cyclic AMP-protein kinase A: two parallel pathways regulating expression of genes required for cell growth. Eukaryot Cell 4, 63-71.

Zurita-Martinez, S.A., Puria, R., Pan, X., Boeke, J.D., and Cardenas, M.E. (2007). Efficient Tor signaling requires a functional class C Vps protein complex in Saccharomyces cerevisiae. Genetics 176, 2139-2150.